Contribution of tumour cell signalling and the microenvironment to the pathogenesis of EBV-associated B cell lymphoma and nasopharyngeal carcinoma

BY

MAHA IBRAHIM

A thesis submitted to
The University of Birmingham
For the degree of
DOCTOR OF PHILOSOPHY

Institute of Cancer and Genomic Sciences
College of Medical and Dental Sciences
University of Birmingham
May 2018

Abstract

In this thesis I have explored different components of the pathogenesis of several related EBV associated cancers. In the first part of the thesis I focus on the microenvironment of two of these cancers, nasopharyngeal carcinoma (NPC) and diffuse large B cell lymphoma (DLBCL). Our group has developed a therapeutic vaccine against EBV which has already been shown to be safe in patients with NPC. Therefore, in the first results chapter (chapter 3), I present a description of the phenotyping of expression of the immune microenvironment including immune checkpoint (ICP) genes and MHC class I and class II genes in NPC tissues. I showed for the first time in NPC tissue samples, two types of PD-L1 expressing tumours: diffuse and marginal. In re-analysis of published data, I found co-expression of immune checkpoint genes and their receptors in EBV positive NPC samples; information which is likely to inform the design of combination immunotherapy in NPC patients. I have shown in my re-analysis of EBV positive NPC that PD-L1 is not up-regulated by LMP-1. In chapter 4, I show the results of studies of the expression of collagen and collagen receptors in DLBCL in which I have identified the over-expression of a potentially novel immune checkpoint receptor, LAIR-1, on the macrophages infiltrating this tumour. In the second part of the thesis I switch my line of inquiry to the tumour cells of EBV-associated cancers, this time focussing on Hodgkin lymphoma (HL), another EBV-associated lymphoma. During the course of the work presented in this chapter I was able to define a role for aberrant sphingosine-1-phosphate (S1P) signalling in driving PI3-K activation mediated through up-regulation of S1PR1 and downregulation of S1PR2 receptors in HL. I also showed that in turn, PI3-K signalling increases the expression of potentially oncogenic downstream transcription factors, such as BATF3 which I have shown to be overexpressed in HL. These data suggest that antagonists of S1P could be considered for the treatment of patients with HL.

Acknowledgment

I would like to thank the following establishments for generously funding my project while giving me the opportunity to pursue my postgraduate studies in such reputable University here in the UK:

- The Egyptian Ministry of Higher Education

- Southern Egypt Cancer Institute, Assiut University

Also, I would like to recognize and thank all the staff members of the University of Birmingham for facilitating/assisting in my research. The specialized EBV Center is definitely a state of the art research center

I would like to sincerely dedicate my special thanks and great gratitude to my principle supervisor Professor Paul Murray for all the sincere effort, his precious generous time he usually gave me and his sincere pieces of advices he has been providing me for the past four years. I would like to thank him for his continuous support, enthusiasm, positivity, patience, and willingness to share with me his great experience and vast knowledge in the field of oncology. He has such an amazing knowledge that is topped with his wonderful so helpful, kind, generous and thoughtful personality. His continuous enthusiasm and devotion have been the main drive for me throughout the entire time of my PHD studies. Professor Paul is not only a great resource for myself, members in PGM group but also has been a great resource for all groups in the Cancer Science Centre. Without him, this work would never succeeded.

Also, I would like to extend my recognition as well as my gratitude to my co-supervisor Dr. Graham Taylor. Dr. Taylor's intellectual, valuable experience, patience was always available to guide me in my study. For certain his meticulousity for details had left a positive impact on my research and academic career.

I am very grateful to Dr. Wenbin Wei as well as Dr. Robert Hollows for all the

support they have provided me with through the bioinformatics work in my thesis. Also, I am greatly thankful to Dr.Abeer Shaaban. Her experience in pathology is remarkable. Thank you Dr. Abeer for sparing the time and effort to help me in my project.

My special gratitude and thanks to all my lovely colleagues in the PGM group.

- Tracey Perry and Lauren Lupino, Navta Massand, Grace Mitchel, thank you for teaching me all the necessary lab skills and technical support to master my PHD work here.

- Ghada Mohamed, Sandra margielewska, Naheema Gordon, Regina Andrijes, Victoria Stavrou and Vera Novitskaia, thank you all for being there for me through all these years. Thank you for making me happy and enjoy work in a friendly smiley warm and fun environment.

I can never forget all the assistance and support I have received from the following research groups:

- Dr. Frank Mussai group; Dr. Caramla De Santo for the vast knowledge in the macrophage work that they shared with me.

- Professor Ben's group; Dr. Neeraj Lal, Dr Galeb Gassous, Chris Bagnall for the Vectra help.

- Professor Hisham Mehanna, Dr. Jill Brookes, Dr. Alex Dowel, Dr William Simmons, Dr Isla Humphreys, Dr. Nicholas Davies and Dr Christopher Dawson for all their enormous help, support and sincere advice.

Also, I would like to show my appreciation and thanks to my family. Especially, my parents: Professor AbdelKalek and my mother Madeha El-Rafei who have been a source of inspiration to me throughout my life. I would like to let them

know that their continuous encouragement and prayers have sustained me that far. Many thanks for all your sacrifices and love. You were behind every step of my work. If it wasn't for my parents, my brothers (Ahmed and Mahmoud) and my sister Shahnaz, I can never forget your support. Thank you all.

Finally, although words can’t adequately express my feelings, I would like to express my deepest gratitude to my husband who showed me a lot of nice feelings and support. He has always been encouraging me to be enthusiastic. Thank you Ahmed El Amir Mohamed.

Maha Ibrahim

CONTENTS

LIST OF FIGURES

LIST OF TABLES

LIST OF COMMON ABBREVIATIONS

ABC	:	Activated B-cell-like
ALK	:	Anaplastic lymphoma kinase
ALNHL	:	Anaplastic large non Hodgkin lymphoma
AML	:	Acute myeloid leukaemia
ATP	:	Adenosine triphosphate
BATF3	:	Basic leucine zipper transcription factor, ATF-like 3
Bcl-2	:	B-cell lymphoma 2
BCL6	:	B-cell lymphoma 6
BCR	:	B cell receptor
BL	:	Burkitt's lymphoma
BLIMP1	:	B lymphocyte induced maturation protein 1
BTLA	:	B and T lymphocyte associated
CARD11	:	Caspase recruitment domain family member 11
c-FLIP	:	Cellular FLICE-inhibitory protein
cHL	:	Classic Hodgkin lymphoma
CIITA	:	MHC-II transactivator
CK	:	Cytokeratin
CNS	:	Central nervous system
COLI	:	Collagen I
COLIII	:	Collagen III
COLIV	:	Collagen IV
COLVI	:	Collagen VI
COO	:	Cell of origin

CPM	:	Counts per million
CTLA4	:	Cytotoxic T-lymphocyte associated protein 4
CTLs	:	Cytotoxic T cells
DDR-1	:	Discoidin domain receptor-1
DDR-2	:	Discoidin domain receptor-2
DHS	:	Delipidated human serum
DLBCL	:	Diffuse large B cell lymphoma
DMS	:	N,N-Dimethylsphingosine
EBNA1	:	Epstein–Barr nuclear antigen 1
EBV	:	Epstein-Barr virus
ECM	:	Extracellular matrix
ECOG	:	Eastern Cooperative Oncology Group
ESMO	:	European Society of Medical Oncology
EZH2	:	Enhancer of zeste 2 polycomb repressive complex 2 subunit
FBS	:	Fetal bovine serum
FDC	:	Follicular dendritic cell
FITC	:	Fluorescein isothiocyanate
FL	:	Follicular lymphoma
FOXP1	:	Forkhead box P1
FOXP3	:	Forkhead box P3
GC	:	Germinal centre
GC B	:	Germinal centre B cells

GCB DLBCL	:	Germinal centre B-cell like DLBCL
GCET1	:	Germinal center B cell-expressed transcript-1
GEO	:	Gene Expression Omnibus
G-MCSF	:	Granulocyte-macrophage colony stimulating factor
GPCR	:	G-protein coupled receptor
H&E	:	Haematoxylin and eosin
HAVCR2	:	Hepatitis A virus cellular receptor 2
HL	:	Hodgkin Lymphoma
Hpf	:	High power field
ICOS	:	Inducible T-Cell Costimulator
ID2	:	Inhibitor of DNA binding 2
IF	:	Immunoflourescence
Ig	:	Immunoglobulin
IHC	:	Immunohistochemistry
IL13	:	Interleukin 13
IL7	:	Interleukin 7
IL9	:	Interleukin 9
IM	:	Infectious mononucleosis
INF-γ	:	Interferon gamma
IPI	:	International Prognostic Index
IRF	:	Interferon regulatory factor
ITAM	:	Immunoreceptor tyrosine-based activation motif

IκBα	:	Nuclear factor of kappa light polypeptide gene enhancer in B-cells inhibitor, alpha
JAK	:	Janus-kinase
KO	:	Knockout
L&H	:	Lymphocytic and histiocytic cells
LAG-3	:	Lymphocyte activating 3
LAIR-1	:	Leukocyte-associated Ig-like receptor-1
LAIR-2	:	Leukocyte-associated Ig-like receptor-2
LCLs	:	Lymphoblastoid cell lines
LMP-1	:	Latent membrane protein -1
LMP-2	:	Latent membrane protein- 2
LRCHL	:	Lymphocyte-rich classical Hodgkin lymphoma
MCCHL	:	Mixed-cellularity classical Hodgkin lymphoma
M-CSF	:	Macrophage colony-stimulating factor
mTOR	:	Mechanistic target of rapamycin
MUM1	:	Melanoma associated antigen
MVD	:	Micro-vessel density
MYC	:	Myelocytomatosis oncogene
Myd88	:	Myeloid differentiation primary response gene 88
NF-κb	:	Nuclear factor κappa-light-chain-enhancer of activated B cells
NHL	:	Non Hodgkin Lymphoma
NK	:	Natural killer
NO	:	Nitric oxide

NPC	:	Nasopharyngeal carcinoma
NSHL	:	Nodular sclerosis Hodgkin Lymphoma
P2RY8	:	Purinergic receptor P2Y8
PAX5	:	Paired box protein Pax-5
PBS	:	Phosphate buffered saline
PD1	:	Programmed cell death 1
PDGFRA	:	Platelet-derived growth factor receptor A
PD-L1	:	Programmed cell death ligand-1
PD-L2	:	Programmed cell death 1 ligand-2
PI3-K	:	PI 3-Kinase indicates phosphatidylinositol-3-kinase
PMLBCL	:	Primary mediastinal B-cell lymphoma
PTL	:	Primary testicular lymphoma
PTPN1	:	Tyrosine-protein phosphatase non-receptor type 1
R-CHOP	:	Rituximab cyclophosphamide doxorubicin hydrochloride vincristine prednisolone
RNAseq	:	RNA sequencing
RPMI	:	Roswell Park Memorial Institute medium
RS	:	Reed-Sternberg
S1P	:	Sphingosine 1-phosphate
S1PR	:	Sphingosine 1-phosphate receptor
SCC	:	Squamous cell carcinoma
SOCS1	:	Suppressor of cytokine signalling 1
SPHK	:	Sphingosine kinase
STAT3	:	Signal transducer and activator of transcription 3

TAMs	:	Tumour-associated macrophages
TBS	:	Tris buffered saline
TCF3	:	Transcription factor 3
TdT	:	Terminal deoxynucleotidyl transferase
THP-1	:	Human monocytic leukaemia cell line
TIE1	:	Tyrosine kinase with immunoglobulin-like and EGF-like domains 1
TILs	:	Tumour infiltrating lymphocytes
TNFR	:	Tumour necrosis factor receptor
TNFα	:	Tumour necrosis factor α
TRKA	:	Tropomyosin receptor kinase A
TRKB	:	Tropomyosin receptor kinase B
VTCN1	:	V-set domain containing T-cell activation inhibitor 1,
WHO	:	World Health Organisation

CHAPTER ONE
INTRODUCTION

The Epstein-Barr virus (EBV) is an oncogenic herpesvirus that is associated with the development of a number of malignancies. Here, I discuss the general features of some of EBV-associated cancers that are relevant to this thesis, before considering the oncogenic functions of EBV and then detailing how this virus might contribute to the pathogenesis of each tumour type. Table 1.1 provides a list of the tumours associated with EBV adapted from Taylor and Steven **(Taylor and Steven, 2016).**

Table 1.1 EBV associated malignancies and their associated EBV related proteins

Tumour type	**Proteins associated with EBV tumours**
Post-transplant lymphoproliferative disease	EBNA1, 2, 3A, 3B, 3C, LP, LMP-1, LMP-2
Hodgkin lymphoma	EBNA1, LMP-1, LMP-2
Diffuse large B lymphoma	EBNA1, 2, 3A, 3B, 3C, LP, LMP-1, LMP-2
Burkitt's lymphoma	EBNA1
Extra-nodal T/NK lymphoma	EBNA1, LMP-2
Nasopharyngeal carcinoma	EBNA1, LMP-1, LMP-2

EBV indicates Epstein-Barr virus, LMP-1 indicates Latent membrane protein 1, LMP-2 indicates Latent membrane protein 2, EBNA-1 indicates Epstein–Barr nuclear antigen-1 and NK indicates Natural killer. Table 1.1 adapted from Taylor and Steven **(Taylor and Steven, 2016).**

1.1 The Epstein-Barr virus

The Epstein-Barr virus (EBV) is a gamma-herpesvirus that colonises the B cell system of its human host, allowing it to persist asymptomatically in the majority of the world's adult population. In most people primary infection goes unnoticed, whereas in a minority of individuals with primary infection results in infectious mononucleosis (IM), a benign condition that almost always resolves after several weeks or months.

1.1.1 EBV is a transforming B lymphotropic virus

If peripheral blood lymphocytes from asymptomatic chronic virus-carriers are cultured *in vitro* then the minor fraction of EBV-infected B cells present can grow out as EBV-transformed, immortalised cell lines, known as lymphoblastoid cell lines (LCLs), but only if T lymphocytes are first depleted or their activity inhibited with drugs such as cyclosporin A **(Rickinson et al., 1984).** Direct infection of resting B lymphocytes with EBV derived from producer B cell lines will also give rise to LCL. Publication in 1984 of the complete genome sequence of the B95.8 strain of EBV provided the opportunity not only to define the genes encoded by EBV, but also to explore how each contributes to the process of *in vitro* B cell transformation **(Baer et al., 1984).** The EBV genes are separated into the 'latent' genes, expressed in a phase of the virus life cycle in which there is no virus replication (known as latency), and the 'lytic' genes which are expressed during the virus replicative cycle ultimately leading to the assembly and release of infectious virions. The latent genes act collectively and in a coordinated fashion to drive *in vitro* B cell transformation. These latent genes include six nuclear antigens (EBNAs 1, 2, 3A, 3B, 3C and EBNA-LP), two latent membrane proteins (LMP-1 and LMP-2), the non-coding Epstein-Barr-

encoded RNA (EBER1 and EBER2), and a number of viral miRNA **(Kerr et al., 1992, Pfeffer et al., 2004).** The use of recombinant EBV technology has confirmed the absolute requirement for EBNA2 and LMP-1 in the *in vitro* transformation of B cells and highlighted important contributions of EBNA-LP, EBNA3A, EBNA3C and LMP-2A **(Young et al., 2016).** The form of latency observed in LCL in which all the latent genes are expressed is known as latency III. A summary of latent genes on the EBV genome are shown in Figure 1.1.

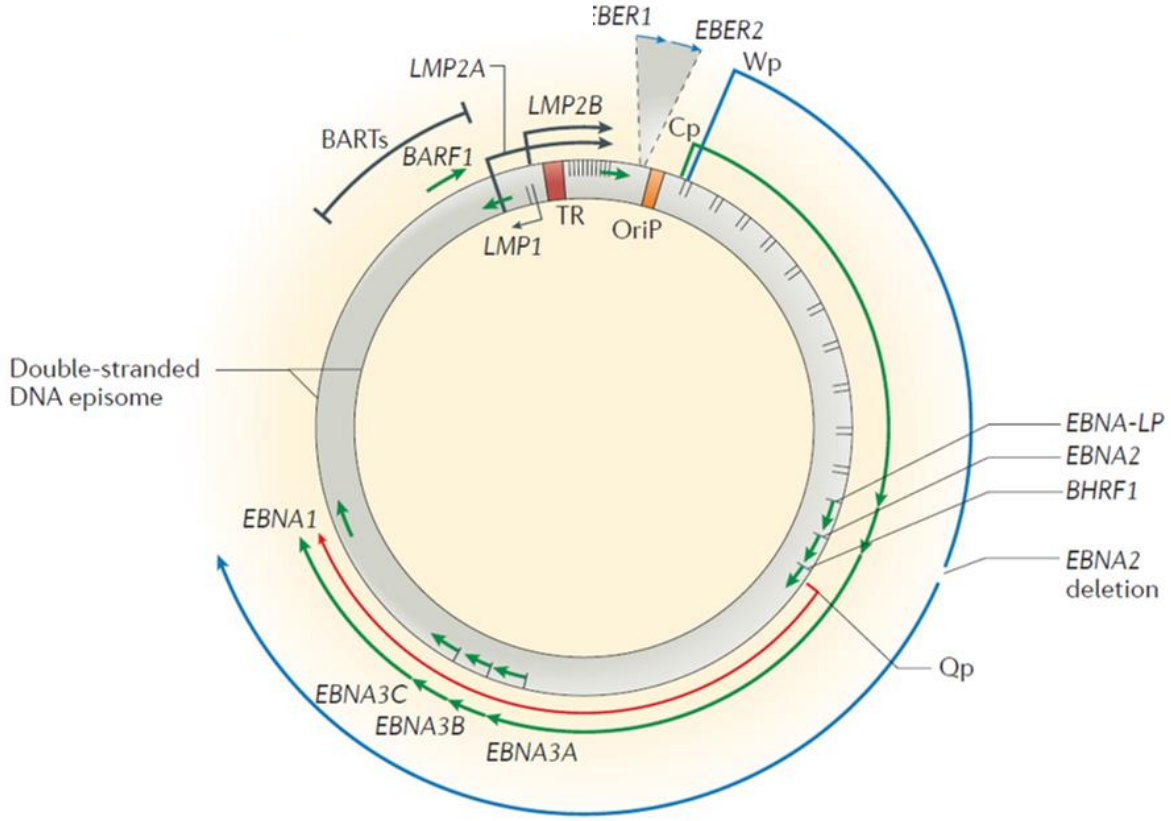

Figure 1.1 Latent genes of EBV genome.
The figure shows position of latent genes in EBV. Epstein-Barr virus encoded latent genes including Epstein–Barr nuclear antigens (EBNAs 1, 2, 3A, 3B and 3C, and EBNA leader protein (EBNA-LP), latent membrane proteins (LMPs 1, 2A and 2B), BamHI fragment H rightward open reading frame (BHRF1) and BamHI-A fragment rightward reading frame (BARF1). The main genome features are highlighted: the origin of replication (OriP) (orange), latent gene exons (short thick green arrows); consistently expressed small non-polyadenylated non-coding RNAs - EBERs 1 and 2 (short blue arrows; splice variants of EBNA (long green and red arrows); LMP-1, LMP-2A and LMP-2B (black arrows) and EBNA1 are expressed in latency type II phase, whilst all the latent genes including EBNAs 2 and 3 are expressed in latency type III phase of viral infection. Figure is adapted from Young et al **(Young et al., 2016)**.

1.1.2 Asymptomatic infection of B cells

Memory B cells are the major site of EBV persistence **(Babcock et al., 1998).** EBV-infected B cells initially express the latency III programme and are the in vivo equivalent of in vitro transformed LCL. By processes yet undefined, these EBV-infected B cells then enter a germinal centre (GC) reaction, and express an alternative form of latency, known as latency II in which there is expression of EBNA1, LMP-1 and LMP-2, but none of the other EBNAs **(Babcock et al., 2000)**. LMP-1 and LMP-2 provide surrogate CD40 and B cell receptor (BCR) signals, respectively, and it is their combined expression which probably mediates the survival of EBV-infected B cells in the GC and their subsequent differentiation **(Gires et al., 1997, Caldwell et al., 1998).** To avoid recognition by the immune system, EBV-infected memory B cells shut down virus gene expression (latency 0), only occasionally switching on EBNA1 expression to promote proliferation (latency I) **(Babcock et al., 2000).** EBV-infected B cells can also differentiate into plasma cells which switches on the lytic cycle ultimately leading to the production of new virions **(Laichalk and Thorley-Lawson, 2005)**.

1.2 Diffuse large B cell lymphoma

Diffuse large B cell lymphoma (DLBCL) is an aggressive tumour, resulting in death within 1 or 2 years if untreated. However, this disease is potentially curable. Around 10% of diffuse large B cell lymphoma is EBV-positive **(Swerdlow et al., 2008)**. Prevalence of EBV infection according to the subtype of DLBCL varies as follows: EBV is consistently positive in certain EBV-related subtypes such as EBV-positive mucocutaneous ulcer, EBV-positive DLBCL NOS and DLBCL associated with chronic inflammation, Lymphomatoid granulomatosis, and Primary effusion lymphoma. EBV infection represents 60-75% of plasmablastic lymphoma

(Swerdlow et al., 2016). Below I discuss the general characteristics of this heterogeneous group of diseases.

1.2.1 Incidence of DLBCL

DLBCL is the most common type of Non Hodgkin Lymphoma (NHL), accounting for 25-30% of adult NHL in western countries and is also the most prevalent NHL in developing countries **(Swerdlow et al., 2008)**. However, DLBCL represents only 5% of paediatric NHL. Although DLBCL is an aggressive tumour, resulting in death within 1 or 2 years in untreated patients, it is potentially curable **(Jaffe et al., 2010).**

1.2.2 Histology of DLBCL

The current sub-classification of DLBCL is important because of distinct biological properties of the different sub-entities **(Chan, 2013)**. However, DLBCL is usually characterized by a complete effacement of the nodal architecture by a diffuse proliferation of neoplastic large B cells. Unlike HL, infiltration of the peri-nodal tissue is frequent and blood vessels are usually positive for tumour infiltration. Some cases are associated with prominent sclerosis, even forming bands and coarse fibres. Necrosis can be seen frequently and sometimes may pose diagnostic challenges if the entire sample is necrotic. There are many histological variants of DLBCL. World health organization (WHO) classification of haematolymphoid malignancies including the old (2008) and the new (2016) classifications of DLBCL are summarized in Tables 1.2 and 1.3, respectively. Some of the DLBCL variants included the following:

The centroblastic (large non cleaved cell) variant is the most common subtype, whereby tumour cells have large rounded nuclei, snake bite nuclear chromatin, multiple nucleoli, with a moderate amount of eosinophilic cytoplasm **(Rosai, 2011)**.

The *immunoblastic variant* is common in elderly men, usually in immunocompromised patients, and sometimes in those infected with HIV. The nuclei of the mitotically active neoplastic cells are sometimes atypical and are larger than those of reactive histiocytes, showing round, indented, or irregularly folded nuclei, simulating mononuclear Hodgkin cells. Sometimes this form shows some plasmacytoid features, with tumour cells having large eccentric nuclei, and peripheral basophilic cytoplasm **(Rosai, 2011)**

Several other morphological variants are worth mentioning in the context of this thesis. They include the *myxoid variant* which can mimic a sarcoma (e.g. myxofibrosarcoma or myxoid chondrosarcoma) because of the presence of abundant myxoid stroma in which the round, spindle, or stellate lymphoma cells are suspended **(Tse et al., 1991)**. In *DLBCL with fibrillary matrix/rosettes there is* an abundant fibrillary matrix, with or without rosette formations simulating schwannian origin tumours. In the *spindle cell variant* the lymphoma cells assume a spindle configuration as a result of passive entrapment in sclerotic stroma or growth in the form of spindle cell fascicles. This type of DLBCL may simulate morphologically undifferentiated pleomorphic sarcoma or other sarcomas. Although mimicking sarcoma, it can be morphologically identified as DLBCL through proper sampling to find a focus of a classic pattern of lymphoma **(Tsang et al., 1992).**

Primary mediastinal B-cell lymphoma (PMLBCL)

Although PMLBCL is a subset of DLBCL, it is a biologically distinct entity with features that overlap with Nodular sclerosis Hodgkin Lymphoma (NSHL). In fact this type of DLBCL can precede nodular sclerosis HL as well as the presentation of composite tumours consisting of PMBCL and NSHL. PMLBCL has a superior prognosis compared to other molecular subtypes of DLBCL. It usually presents as

a mediastinal mass with sheets of neoplastic tumour cells with clear large cells, sometimes with RS (Reed-Sternberg)-like cells delineated by sclerotic stroma. This may be a diagnostic challenge which needs to be differentiated from extra-gonadal germ cell tumours such as germinoma and the clear cell variant of thymoma **(Rosenwald et al., 2003).**

Double hit lymphoma and double expressor lymphoma

DLBCL with translocations of both cMYC and BCL2 (B-cell lymphoma 2) is called double hit lymphoma (DHL) and accounts for about 5% of DLBCL. This entity is important because it is associated with advanced stage, high international prognostic index (IPI) score and decreased overall survival in patients treated with R-CHOP. cMYC and BCL2 genes together collaborate by promoting cellular proliferation and survival, respectively **(Green et al., 2012b)**.

Double expressor lymphoma is considered a new entity recognized by the updated WHO classification 2016 (Table 1.3), and is defined as a lymphoma that expresses both BCL2 and cMYC by IHC. This entity is more frequent than double hit lymphoma (around 20%). In a previous study, immunohistochemistry for cMYC and BCL2 was used to stratify patients and shown to be an additional predictive marker for aggressiveness in DLBCL **(Green et al., 2012b, Smith, 2017)**.

Transformed (secondary) DLBCL

DLBCL may arise either *de novo* or as a consequence of transformation from indolent low grade B cell NHL, including follicular lymphoma (FL), small lymphocytic lymphoma (SLL), lymphoplasmacytic lymphoma (LPL), nodal marginal zone lymphoma (MZL), or lymphoma of the mucosa associated lymphoid tissues (MALT

lymphoma). It can also less commonly arise from T cell lymphoma such as angioimmunoblastic T cell lymphoma **(Montoto and Fitzgibbon, 2011).**

Extra-nodal DLBCL

DLBCL can arise in extra-nodal locations, such as the gastro-intestinal tract, testis, CNS, skin or bone, with some specific types occurring predominantly or exclusively in extra-nodal sites; each having its own distinctive clinical and biological features. These types of lymphoma include plasmablastic lymphoma, lymphomatoid granulomatosis, primary effusion lymphoma, pyrothorax-associated lymphoma, PMLBCL, intravascular large B-cell lymphoma, T-cell/histiocyte-rich large B-cell lymphoma and EBV-positive DLBCL NOS **(Jaffe et al., 2010)**. Some extra-nodal tumours are treated differently. This is especially the case for primary testicular DLBCL (PTL) and primary central nervous system (CNS) lymphoma. The former is usually characterized by aggressive behaviour and CNS dissemination, which necessitates a special treatment strategy. PTL is a highly aggressive type of DLBCL with poor prognosis; it is usually disseminating and commonly recurs either on the ipsilateral or contralateral side **(Zucca et al., 2003).** The standard treatment of localized (stage I to II) PTL is R-CHOP (Rituximab, cyclophosphamide, hydroxydaunocymin (doxorubicin), oncovin (vincristine), and prednisone) with CNS prophylaxis and contralateral testis irradiation **(Vitolo et al., 2011).**

1.2.3 DLBCL in the WHO classifications

Table 1.2 WHO old classification of B cell lymphoma, 2008

Diffuse large B-cell lymphoma NOS
Common morphologic variants
Centroblastic
Immunoblastic
Anaplastic and other rare morphologic variants
Molecular subgroups
GCB
Activated B-cell-like (non-GCB)
Immunohistochemical subgroups
CD5+ DLBCL
Primary DLBCL of the CNS
Primary cutaneous DLBCL, leg type
EBV+ DLBCL of the elderly
Diffuse large B-cell lymphoma subtypes
T-cell/histiocyte-rich large B-cell lymphoma
Primary DLBCL of the CNS
Primary cutaneous DLBCL, leg type
EBV-positive DLBCL of the elderly
Other lymphomas of large B cells
Primary mediastinal (thymic) LBCL
Intravascular large B-cell lymphoma
DLBCL associated with chronic inflammation
Lymphomatoid granulomatosis
ALK-positive LBCL
Plasmablastic lymphoma
Large B-cell lymphoma arising in HHV8-associated multicentric Castleman disease
Primary effusion lymphoma
Borderline cases
B-cell lymphoma, unclassifiable, with features intermediate between DLBCL and Burkitt's lymphoma
B-cell lymphoma, unclassifiable, with features intermediate between DLBCL and classical Hodgkin lymphoma

* CNS indicates central nervous system; DLBCL indicates diffuse large B-cell lymphoma; EBV indicates Epstein-Barr virus; GCB indicates germinal center B cell; ALK indicates anaplastic lymphoma kinase. Table taken from Swerdlow **(Swerdlow et al., 2008)**.

Table 1.3 WHO New classification of B cell lymphoma, 2016

Diffuse large B-cell lymphoma (DLBCL) variants	New modification in WHO classification 2016
Diffuse large B-cell lymphoma (DLBCL), NOS	Immunohistochemistry algorithm for differentiating GCB vs ABC/non-GC type required may affect therapy Double-expressor lymphoma: Co-expression of cMYC and BCL2 markers is currently used for prognosis Mutational landscape better understood but clinical impact remains to be determined
Germinal center B-cell type	
Activated B-cell type	
T-cell/histiocyte-rich large B-cell lymphoma	
Primary DLBCL of the central nervous system (CNS)	
Primary cutaneous DLBCL, leg type	
EBV+ DLBCL, NOS	Previous name was EBV+ DLBCL of the elderly, now modified because can happen in younger patients Does not include EBV+ B-cell lymphomas that can be given a more specific diagnosis
EBV+ mucocutaneous ulcer	New category associated with iatrogenic immunosuppression or age-related immunosenescence
DLBCL associated with chronic inflammation	
Lymphomatoid granulomatosis	
Primary mediastinal (thymic) large B-cell lymphoma	
Intravascular large B-cell lymphoma	
ALK+ large B-cell lymphoma	
Plasmablastic lymphoma	
Primary effusion lymphoma	
HHV8+ DLBCL, NOS*	
High-grade B-cell lymphoma, with cMYC and BCL2 and/or BCL6 rearrangements	New entity for all “double-/triple-hit” lymphomas other than FL or lymphoblastic lymphomas
High-grade B-cell lymphoma, NOS*	Together with the new entity for the “double-/triple-hit” lymphomas, changes the 2008 category of B-cell lymphoma, unclassifiable, with features intermediate between DLBCL and Burkitt’s lymphoma (BCLU). Includes blastoid-appearing large B-cell lymphomas and cases lacking cMYC and BCL2 or BCL6 translocations that would formerly have been called BCLU.
B-cell lymphoma, unclassifiable, with features intermediate between DLBCL and classical Hodgkin lymphoma	

*New modification of 2008 Lymphoma neoplasms classification. Table taken from Swerdlow **(Swerdlow et al., 2016)**.

1.2.4 Cell of origin (COO) Classification of DLBCL

The latest WHO classification of lymphoid neoplasms reported in 2016 includes the cell of origin classification which separates DLBCL into three types: germinal center B cell-like (GCB), activated B-cell-like (ABC) molecular “subgroups” of DLBCL based on gene expression profile (GEP) as well as a group of cases that could not be put into either category (unclassifiable). In a landmark study microarray based gene expression was initially used to sub-classify DLBCL patients into GCB and ABC subtypes. This demonstrated prognostic stratification based on gene expression profiling, finding that patients with the ABC subtype had a poorer clinical outcome than those with the GCB subtype **(Alizadeh et al., 2000, Lenz et al., 2008)**. Remission of DLBCL patients was observed to be approximately 80% in patients with GCB subtype, while remission was observed only in around 50% in ABC subtype **(Pon and Marra, 2016)**. Despite these findings, the treatment of DLBCL patients still depends mainly on stage, age of the patient, and if bulky disease is present. Although the COO classification has implications for prognosis, according to the European Society of Medical Oncology (ESMO) guidelines, it has no impact on patient management at present **(Tilly et al., 2015)**. DLBCL patients are treated with CHOP combination chemotherapy. In cases with bulky or localized tumours, radiotherapy is sometimes indicated **(Chan, 2013)**.

In addition to GCB and ABC subtypes, double-hit lymphomas (approximately 5% to 10% of patients) and double-expressor lymphomas, which overexpress cMYC and BCL2 protein, are described as aggressive DLBCLs also associated with a poor prognosis.

Mutations specific to the ABC subtype involve genes associated with BCR signalling or upstream of nuclear factor- κappa B (NF-κB), leading to constitutive activation in upstream genes; CD79B, CARD11 and MYD88 as a consequence.

In the ABC subtype of DLBCL, mutations affecting genes involved in B-cell receptor signalling, NF-κB signalling causing constitutive activation of this pathway as a consequence of acquired mutations in upstream genes such as those in P2RY8, EZH2 and FOXO1, as well as genes involved in histone modification **(Morin et al., 2011, Manso et al., 2017)**. Recurrent cytogenetic alterations in DLBLC include (14; 18) translocation involving BCL2 which is found in 45% of GCB DLBCL and amplification of *REL* was detected in DLBCLs, but absent in ABC type. On the other hand, chromosomal aberrations involving chromosome 3, are seen exclusively in the ABC subtype and observed in 25% of patients **(Rosenwald et al., 2002)**.

Attempts have been made to use immunohistochemistry (IHC) to sub-classify DLBCL into either GCB or ABC type. A summary of these algorithms is shown in Figure 1.2 **(Gutiérrez-García et al., 2011)**. The Hans criteria uses three markers (CD10, BCL6, and MUM1), while in the Choi algorithm, five immunohistochemical markers (GCET1, CD10, BCL6, MUM1, and FOXP1) are employed **(Choi et al., 2009)**. The Tally algorithm has the strongest correlation with microarray based classification **(Meyer et al., 2010)**.

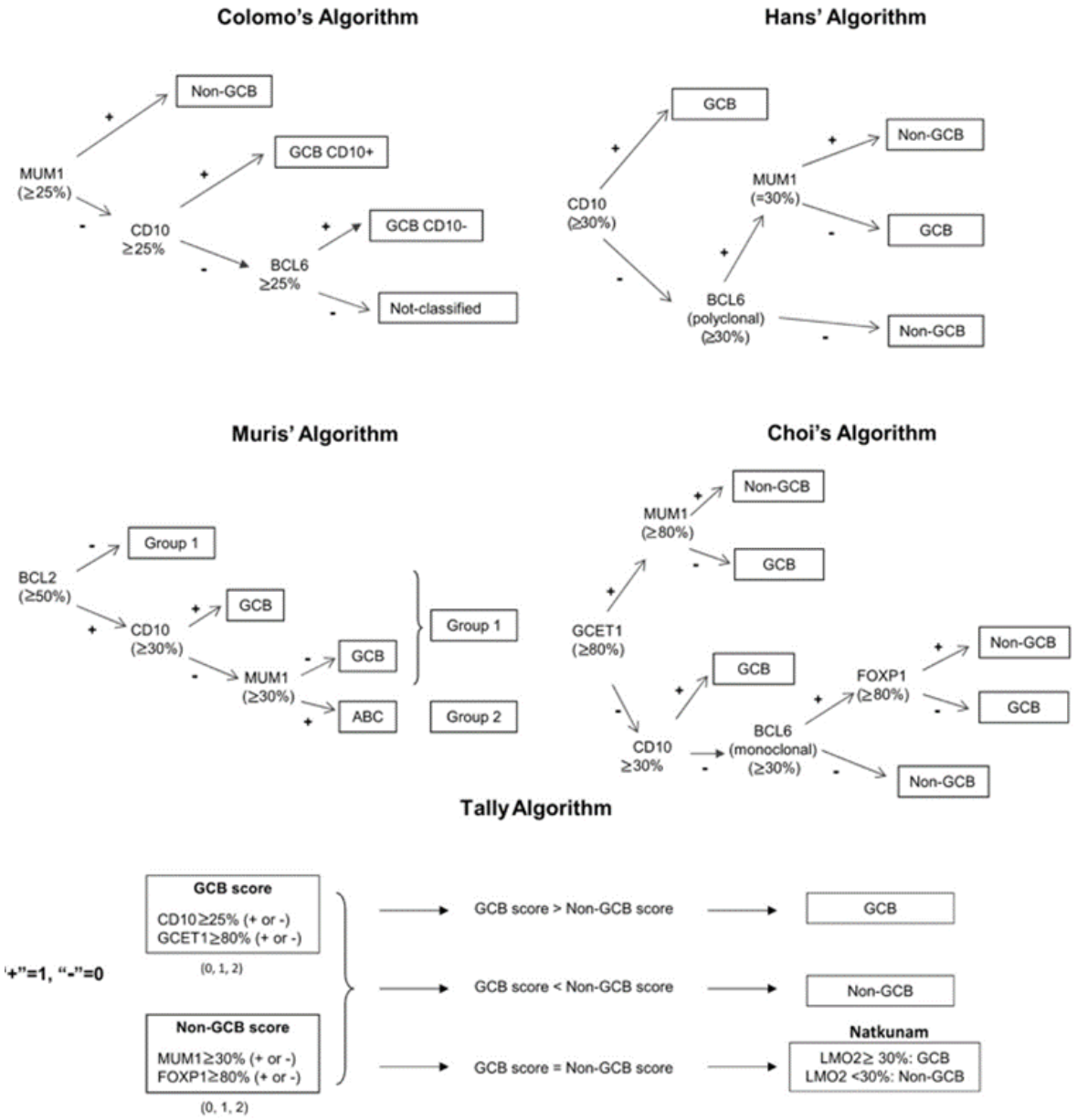

Figure 1.2 IHC based algorithms for classification of DLBCL. Different algorithms using IHC markers expression for classifying DLBCL into two phenotypes; germinal centre and Non-germinal centre phenotype. Colomo's algorithm used (MUM1, CD10, and BCL6 markers), Hans' algorithm used (CD10, BCL6, and MUM1 markers), Muris' (CD10 and MUM1 in addition to BCL2), Choi's algorithm used (GCET1, MUM1, CD10, FOXP1, and BCL6 markers), while Tally algorithm used (CD10, GCET1, MUM1, FOXP1, and LMO2 markers). Cut off for every marker positivity shown for every algorithm. Colomo's algorithm unlike other algorithms identified in its classification unclassified category in addition to the other two phenotypes. Figure taken from *Gutiérrez-García* et al **(Gutiérrez-García et al., 2011)**.

1.2.5 Immuno-phenotyping

Apart from those markers used in the COO described above, the following IHC markers are also helpful in the diagnosis of DLBCL; CD19, CD20, CD22, CD79A, CD45, PAX-5, Vimentin and Ki-67. Ki-67 is a gene which encodes a nuclear non-histone protein expressed in all phases of the cell cycle but not in quiescent cells. In general, there is a good correlation between Ki-67 staining and mitotic count **(Rosai, 2011)**. In a large series reported by He et al, patients with high Ki-67 scores had shorter failure-free survival **(He et al., 2014)**. DLBCL is generally negative for smooth muscle actin (SMA), but it is expressed in the spindle cell variant, which may be misdiagnosed as intra-nodal soft tissue sarcoma. Terminal deoxynucleotidyl transferase (TdT) and cytokeratin (CK) are negative; however CK sometimes is positive in anaplastic variant of DLBCL, which may lead to the misdiagnosis of metastatic carcinoma or anaplastic carcinoma. However, its positivity for CD30 and anaplastic lymphoma kinase (ALK) is usually helpful in the diagnosis. ALK is expressed in ALK-positive DLBCL either in the cytoplasm or in the both the nucleus and cytoplasm depending upon the chromosomal translocation involved **(Rosai, 2011)**. CD43 is a type I transmembrane glycoprotein expressed in different types of hematopoietic cells. DLBCL expresses CD43 in around 25% of cases; these cases respond poorly to therapy **(Ma et al., 2015)**.

1.2.6 Prognostic factors in DLBCL

The International Prognostic Index (IPI) is considered the most useful measure of prognosis for DLBCL patients. The risk factors used to calculate the IPI are:

■ Age >60 years;

■ High stage (III-IV);

■ Elevated serum lactate dehydrogenase;

■ ECOG performance status of 2 – 4;

■>1 Extra-nodal site

Table 1.4 International Prognostic Index (IPI) and Revised International Prognostic Index (R-IPI) with their associated risk and survival outcome

Risk group	Number of prognostic factors	4 years PFS (%) survival	4 years OS (%)
IPI			
Low	0-1	-	-
Low/Intermediate	2	-	-
High/ Intermediate	3	0	23.9
High	4,5	27.8	55.6
Revised IPI			
Low	0	-	-
Intermediate	1,2	-	-
High	3,4,5	16.9	33.3

*OS indicates overall survival, PFS indicates progression free survival. Table taken Wang et al **(Wang et al., 2015)**.

1.3 Hodgkin lymphoma

HL is a common lymphoma in the Western world, with an annual incidence of approximately 3/100,000.

1.3.1 Histology of HL

HL is divided into two major types; classical HL (cHL) and nodular lymphocyte predominant (NLPHL) forms **(Swerdlow et al., 2008)**. cHL is further divided into four histological subtypes: NSCHL, lymphocyte-rich classical Hodgkin lymphoma (LRCHL), mixed-cellularity classical Hodgkin lymphoma (MCCHL), and lymphocyte-depletion classical Hodgkin lymphoma (LDCHL) **(Mani and Jaffe, 2009)**. EBV infection varies in different types of HL, EBV infection is more common in certain histology subtypes of HL (more likely in MCCHL and LDCHL than in other subtypes of classic HL) **(Massini et al., 2009)**. However, recent studies revealed rare cases of non-classic type of HL; NLPHL appeared to be EBV positive, without history of immunosuppression in those patients **(Wang et al., 2014)**.

In all HL cases, the affected lymph nodes show disruption of the tissue architecture containing malignant cells which are in the minority and are surrounded by non-neoplastic cells including T- and B-lymphocytes, as well as extracellular matrix, including collagen. Cross-talk between the tumour cells and the tumour microenvironment is crucial for the growth and survival, as well as the immune escape of the tumour cells **(Aldinucci et al., 2010)**. The tumour cells of NLPHL are known as lymphocytic and histiocytic (L&H) cells. The tumour cells of cHL are the more typical Hodgkin/Reed-Sternberg (HRS) cells **(Küppers, 2009)**. L&H cells express B-cell markers, including CD20 and CD19. In contrast, HRS cells of cHL have lost the B cell phenotype.

1.3.2 Origin of HRS cells of cHL

The cells from which HRS cells are derived were a subject of some debate for many years; early studies suggested HRS cells might be derived from macrophages, dendritic cells or granulocytes. However, Ralf Küppers ' group showed that HRS cells have clonally rearranged immunoglobulin genes, and so it is now accepted that HRS cells derive from mature B lymphocytes **(Küppers et al., 1994)**. What is more, this study showed that the variable region sequences of the immunoglobulin genes in HRS cells were subject to somatic hypermutation. This provided conclusive evidence that HRS cells are derived from cells that have been through a GC reaction **(Küppers et al., 1994, Kanzler et al., 1996, Vockerodt et al., 2008, Marafioti et al., 2000)**. In around quarter of cHL, the rearranged immunoglobulin sequences harbour 'crippling' mutations that encode a non-functional surface immunoglobulin B cell receptor (BCR) **(Kanzler et al., 1996)**. Because signalling through the BCR is important for the survival of germinal centre B cells, we can assume that HRS cells of cHL originate from pre-apoptotic cells that were rescued by a transforming event (either viral, cellular or both) (Figure 1.3) adapted from Kapatai and Murray **(Kapatai and Murray, 2007)**.

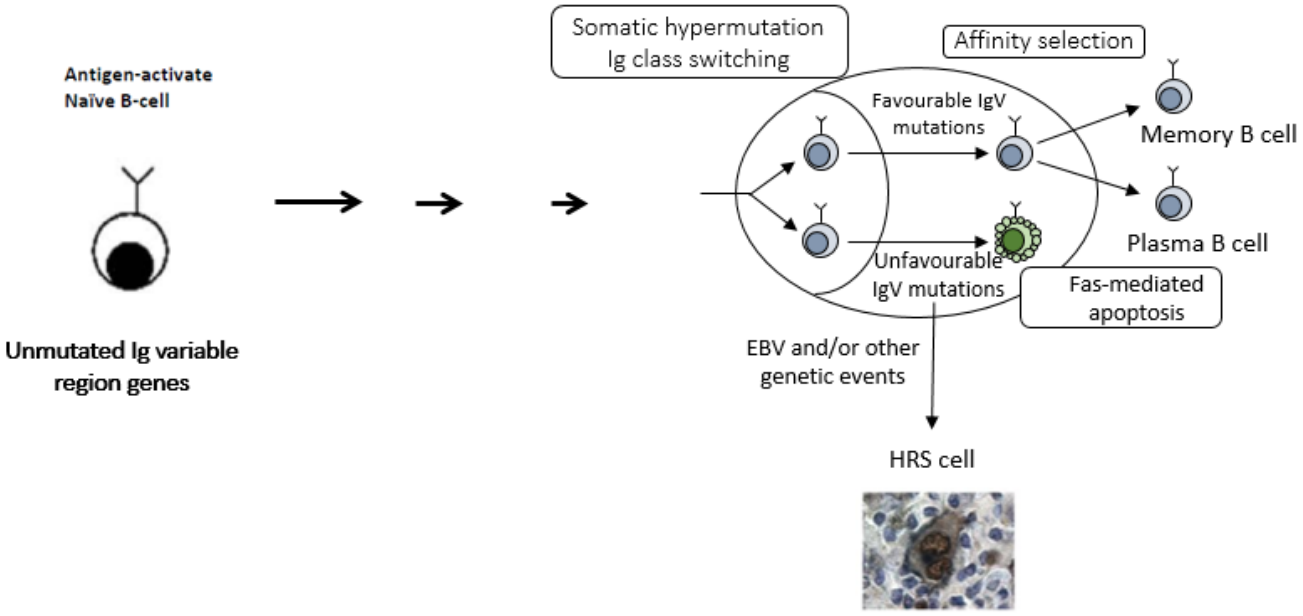

Figure 1.3: Origin of the Hodgkin/Reed-Sternberg (HRS) cell in relation to the germinal centre. A naïve B cells exposed to antigen enter the B-cell follicles, proliferate rapidly and establish germinal centres in form of secondary follicles. Here the B cells undergo somatic hypermutation of the immunoglobulin variable (IgV) region genes within the germinal centre. Only those cells acquiring a BCR with an increased affinity for antigen will survive to exit the GC. B cells with unfavourable BCR mutations will be eliminated by Fas-mediated apoptosis. Those carrying B-cell receptor (BCR) with high affinity for antigen will escape apoptosis and survive, then leave the germinal centre and undergo class switching then differentiate into memory B cells or plasma cells. GC B cells carrying non-functional BCR should undergo apoptosis, but may be rescued by Epstein-Barr virus and/or still unknown genetic alterations. Such cells may be the progenitors of HRS cells, Figure taken from Kapatai and Murray **(Kapatai and Murray, 2007).**

The lack of expression of a functional BCR is a feature of cHL, which can occur as a result of 'crippling' immunoglobulin mutations. However, the expression of immunoglobulin genes can also be downregulated by epigenetic silencing of transcription factors which include BOB-1/POU2AF1, OCT2/POU2F2 and Spi-1/PU.1 **(Re et al., 2001, Jundt et al., 2002b, Torlakovic et al., 2001, Stein et al., 2001)**, as well as the immunoglobulin promoter region itself **(Doerr et al., 2005, Ushmorov et al., 2004)**. Furthermore, mutations in the octamer region of the immunoglobulin promoter can prevent transcription factor binding **(Theil et al., 2001)**. In addition, a number of other components of the BCR, or of its downstream signalling pathway are either absent or expressed at low levels in HRS cells **(Schwering et al., 2003b)**.

1.3.3 Suppression of the B cell phenotype in HRS cells

As discussed above HRS cells show a global downregulation of B-cell lineage genes. This has been shown to be due to loss of transcription factor networks that regulate B cell development; including PAX5, early B-cell factor 1 (EBF1) and TCF3/E2A **(Nutt and Kee, 2007, Bohle et al., 2013)**. EBF1 has been shown to cooperate with TCF3 and PAX5 which leads to the expression of many B-cell genes. EBF1 is a B-cell commitment factor, and its loss also results in the abnormal over-expression of inhibitor of DNA binding 2 (ID2), which inhibits TCF3 to further suppress B-cell lineage gene expression **(Küppers et al., 2003, Renné et al., 2006)**. ID2 amplification occurs in around a half of all HL cases, and results in ID2 over-expression **(Renné et al., 2006)**. HRS cells also aberrantly express ABF1, which further inhibits TCF3 activity **(Mathas et al., 2006)**.

The loss of B cell identity also appears to be due in part to the aberrant expression of genes that are characteristic of other haematopoietic lineage cells such as T-cells, NK-cells (Natural killer) and myeloid cells **(Hertel et al., 2002, Ushmorov et al., 2004, Schwering et al., 2003a, Küppers et al., 2003, Tiacci et al., 2012, Steidl**

et al., 2012). Notch signalling in HRS cells occurs as a result of contact with cells within the tumour microenvironment, including other HRS cells that express the Notch ligand Jagged-1 **(Jundt et al., 2002a, Jundt et al., 2008, Smith et al., 2005, Köchert et al., 2011)**. Aberrant Notch signalling can lead to aberrant expression of T cell-specific genes, as well as suppression of B cell-specific genes, including PAX-5 **(Jundt et al., 2008)**.

1.3.4 Deregulated cellular signalling in classical HL

HRS cells show deregulated activation of multiple cell signalling pathways as shown in Figure 1.4 adapted from Murray and Bell **(Murray and Bell, 2015)**.

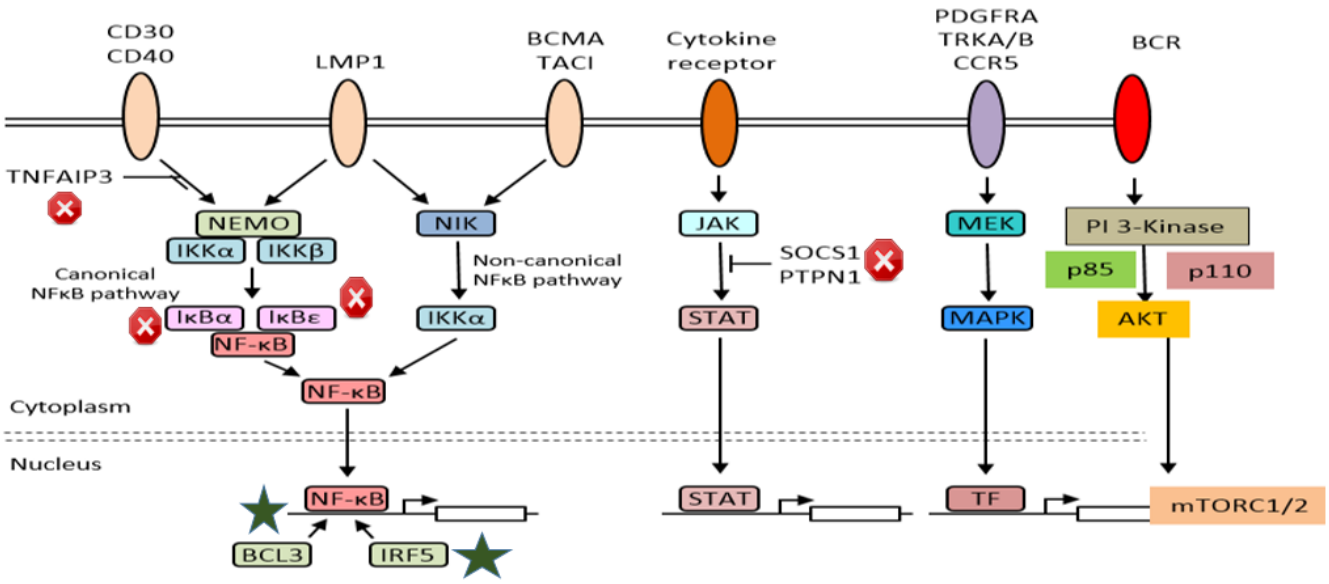

Figure 1.4: Deregulated cell signalling pathways in HRS cells HRS cells constitutively activate canonical and non-canonical NF-κB pathways. Multiple receptors including CD30, CD40 and RANKL activate the canonical pathway through the IKK complex resulting in the degradation of the NF-κB inhibitors IκBα and IκBε, followed by the translocation of active NF-κB complexes to the nucleus where they activate target genes together with other genes as BCL3 and IRF5. c-Rel overexpression can occur in subset of cases resulting in activation of NF-κB. TNFAIP3, negative regulator of NF-κB pathway, mediated through inhibiting the IKK complex. In EBV positive HL, LMP-1 can promote activation of both canonical and non-canonical NF-κB pathways. Another pathway mediated through cytokines produced either by RS cells or cells in the microenvironment, can stimulate cytokine receptors resulting in activation of JAK/STAT signalling pathway. Mutated SOCS1 gene; suppressor of cytokine signalling 1 and the protein tyrosine phosphatase (PTPN1/PTP1B) genes can also promote activation of the JAK/STAT pathway. Several tyrosine kinase receptors such as PDGFA, TRKA, TRKAB and CCR5 are deregulated in HL, resulting in activation of transcription factors. PI3K/Akt signalling pathway is deregulated in HL in constitutive manner resulting in phosphorylation of the downstream oncogenic target Akt and P110, with subsequent effect of cell growth mediated through mTOR1/2. P110 which is important in B and T cell development can activate downstream signalling of G-protein coupled receptors. BCR indicates B-cell receptor; PI3-Kinase indicates phosphatidylinositol-3-kinase. Increased signalling indicated in *green stars;* functional loss by mutations indicated in red signs. Figure modified from Murray and Bell **(Murray and Bell, 2015)**.

HRS cells show constitutive activation of NF-κB transcription factors **(Bargou et al., 1996)**. NF-κB activity is essential for HRS cell survival, because inhibition of this pathway leads to apoptosis in HL cell lines after growth factor withdrawal and also results in reduced tumour formation in severe combined immune deficiency (SCID) mice **(Bargou et al., 1997, Izban et al., 2001)**. HRS cells express different TNF receptors, including CD30, CD40, TACI, BCMA and RANK all of which are able to trigger NF-κB signalling **(Carbone et al., 1995, Fiumara et al., 2001, Horie et al., 2002, Chiu et al., 2007)**. The tumour microenvironment expresses ligands of these receptors and thus can lead to their enhanced activation **(Carbone et al., 1995, Pinto et al., 1997)**. NF-κB signalling is also activated by genomic changes in HRS cells including amplification of the c-REL NF-κB subunit **(Joos et al., 2003, Martín-Subero et al., 2002, Barth et al., 2003)**. Furthermore, approximately 20% of cHL cases also harbour inactivating mutations in the IκB inhibitor proteins, IκB alpha or IκB epsilon **(Cabannes et al., 1999, Emmerich et al., 1999, Jungnickel et al., 2000, Emmerich et al., 2003, Lake et al., 2009)**. In other cases, HRS cells overexpress the co-activator of NF-κB, BCL3 **(Martin-Subero et al., 2006, Mathas et al., 2005)**. Finally, recurrent mutations have been reported in the TNFAIP3/A20 gene, a negative regulator of NF-κB **(Schmitz et al., 2009, Reichel et al., 2015)**.

HRS cells are also characterised by aberrant JAK/STAT signalling, which promotes their proliferation and survival. HRS cells secrete many cytokines, including IL-7, IL-9 and IL-13 **(Kapp et al., 1999, Skinnider et al., 2001, Cattaruzza et al., 2009)** all of which can activate JAK/STAT signalling, the net effect of which is to increase the phosphorylation and activation of the transcription factors STAT3, STAT4 and STAT6 **(Kube et al., 2001, Hinz et al., 2002, Skinnider et al., 2002)**. Many of these cytokines are also secreted by other cells within the tumour microenvironment

(Aldinucci et al., 2002). JAK/STAT signalling is also further activated by genomic changes which include JAK2 amplification as well as inactivating mutations of the negative regulators, SOCS1 and PTPN1/PTPB1 **(Joos et al., 2000, Weniger et al., 2006, Gunawardana et al., 2014)**. Some receptor tyrosine kinases (RTKs), such as PDGFRA, TRKA, TRKB and TIE1 show over activity in HRS cells which can also lead to activation of JAK/STAT signalling **(Renné et al., 2005, Renné et al., 2007)**. The PI3-K/Akt pathway is also constitutively activated in HL-derived cell lines and in HRS cells from primary tumour tissues **(Georgakis et al., 2006, Dutton et al., 2005).** Importantly, the PI3-K/Akt pathway contributes to the survival of HL cell lines *in vitro*. However, the mechanisms responsible for this effect are not known.

1.4 Nasopharyngeal carcinoma

Nasopharyngeal carcinoma (NPC) is a tumour of the epithelial lining of the nasopharynx that is particularly prevalent in South East Asia. This form of NPC is consistently associated with EBV infection and accounts for the majority of cases in so called 'endemic' regions. It is often described as a lymphoepithelioma because of the prominent lymphocytic infiltration.

Histopathological features of NPC

The association of EBV with different histologic variants of NPC has been classified as follows: The majority of undifferentiated NPC are consistently positive for EBV, with the undifferentiated carcinoma constituting the most common subtype **(Barnes, 2005, Thompson, 2006)**.

The WHO classification has divided NPC histopathology into two main subtypes, according to the extent of its differentiation. These include keratinizing squamous-cell carcinoma and non-keratinizing carcinoma. Non-keratinizing carcinoma is further subdivided into non-keratinizing differentiated carcinoma (NKDC) and non-

keratinizing undifferentiated carcinoma (NKUC) **(Shanmugaratnam, 1978)**. Non-keratinizing undifferentiated carcinoma is the most common type and is consistently EBV positive; EBV-positive carcinomas represent almost 97% of endemic NPC cases. This subtype has characteristic morphologic features, with tumours displaying a pronounced lymphoid infiltration. The keratinizing forms are rare, representing approximately 1% of the endemic forms **(Lun et al., 2013)**. Histological variants of NPC differ in their association with EBV. The majority of undifferentiated NPC is consistently positive for EBV, while the keratinizing type is weakly associated with EBV. Although the undifferentiated variant is high grade, it is highly responsive to radiotherapy and five-year survival rates can reach 65%, unlike the more differentiated keratinized form, which has more dismal prognosis, in the form of radio-resistance and survival rates between 20-40% **(Barnes, 2005, Thompson, 2006)**.

Pathogenesis of NPC

The pathogenesis of NPC is complex and involves a persistent EBV infection of progenitor cells exposed to environmental carcinogens in salted fish and cigarette smoke and alcohol. A scheme for the pathogenesis of NPC is presented in Figure 1.5 taken from **(Young et al., 2016).**

Endemic NPC is linked to multiple factors, which include viral infection, genetic factors and dietary or habitual factors **(Lo et al., 2004)**. EBV infects epithelial cells lining the upper respiratory tract, mainly in the oropharynx and possibly the salivary gland **(Young and Dawson, 2014)**. NPC tumours were found to harbour monoclonal EBV genomes, indicating that EBV infection occurred before the expansion of the final malignant clone **(Raab-Traub and Flynn, 1986)**. Furthermore, normal nasopharyngeal epithelium from high-risk patients is EBV

negative, indicating that EBV infection is not an early event in tumorigenesis. The non-polyadenylated EBER RNAs, which are abundantly expressed in latently infected cells, were identified in high-grade lesions including severe dysplasia and carcinoma *in-situ*, yet negative in low-grade lesions and normal nasopharyngeal epithelium. NPC pathogenesis is characterized by multiple genetic alterations. Studies of normal epithelium and the low-grade dysplastic lesions from high risk patients, revealed the presence of genetic alterations such as 3p and 9q deletions in absence of the EBV infection **(Chan et al., 2000, Pathmanathan et al., 1995a)**. As described in Li et al **(Li et al., 2017)** and Young et al **(Young et al., 2016)**, this suggest that cytogenetic changes in the epithelium are required before EBV infection can be established.

Chromosomal deletion of chromosome 3p and 9p are the most frequent aberration in NPC which result in inactivation of tumour suppressor genes (TSGs). TSGs such as RASSF1, RARβ2 and p16, p15, p14, DAP-kinase located at chromosome 3p and 9q respectively, were associated with hypermethylation changes and are shown to be important in NPC pathogenesis **(Lo et al., 2012, Lung et al., 2012)**. Cell susceptibility to latent EBV infection is thought to acquire initial genetic alterations in nasopharyngeal epithelium such as Cyclin D1 overexpression, due to in part to gene amplification. Such genetic changes are thought to predispose cells to the establishment and stabilization of EBV infection, resulting in viral persistence **(Chan et al., 2000)**. Once infection occurs, it is thought that EBV-encoded latent genes and micro RNAs sustain the growth and survival of neoplastic cells by activating a plethora of cell signalling pathways and by superimposing genetic and epigenetic changes **(Young and Dawson, 2014)**.

Most cases of NPC present at a late stage and survival is poor; current treatments for advanced disease are limited to concurrent chemo-radiotherapy and are associated with significant morbidity and poor quality of life **(Hui et al., 2013)**.

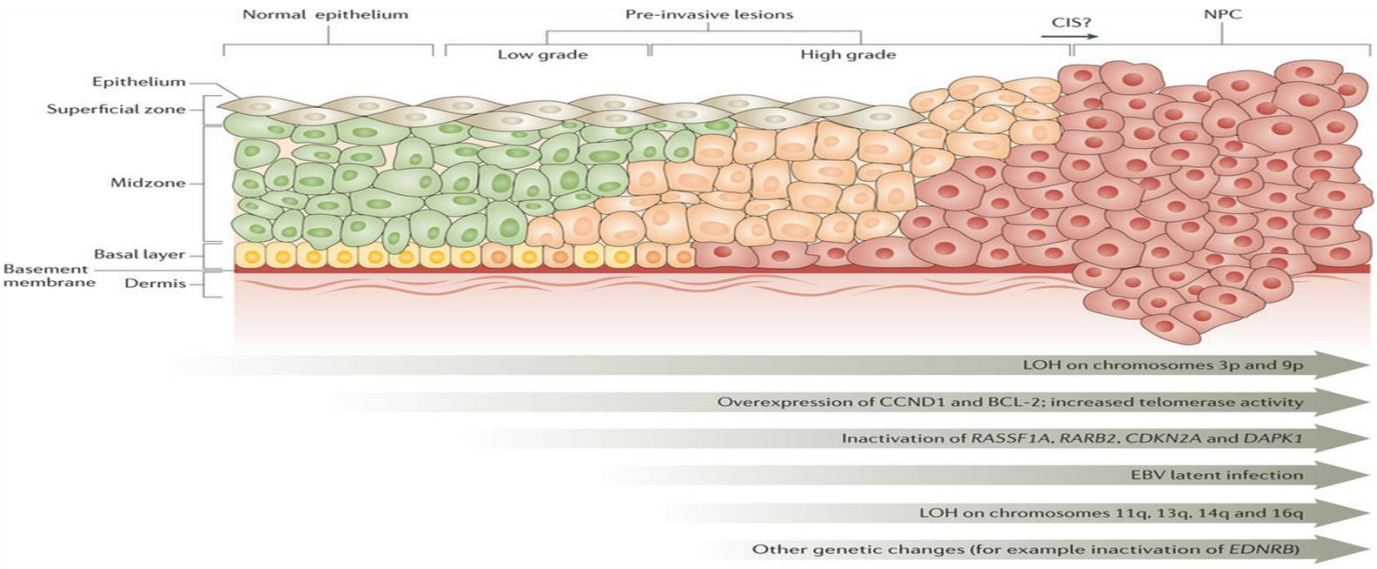

Figure 1.5 Timeline for cancer pathogenesis from molecular and cytogenetic perspective

Tumorigenesis in NPC occur as result of multiple molecular alterations, such as mutations, chromosome deletions, promotor hypermethylation of specific genes, LOH of 3p and 9p chromosomes and EBV infection.

Changes like LOH, cyclin D1 (CCND1) overexpression and CDKN2A, RASSF1A, RARB2 and DAPK1 inactivation are seen in early stages of tumorigenesis. These changes are believed to promote susceptibility to EBV infection and promote expression of EBV latent genes. Therefore, EBV can only be detected in high-grade pre-invasive stages of tumorigenesis, but not in low grade dysplastic lesions.

Figure adapted from Young et al **(Young et al., 2016)**.

1.5 Contribution of EBV to B cell Lymphoma (DLBCL and HL) and NPC

1.5.1 EBV-associated B cell lymphomas

The development of EBV-positive B cell lymphomas might be considered to be in essence a rare accident of EBV's ability to colonise the B cell system. Most EBV-associated B cell lymphomas display somatic hypermutation and therefore originated in cells that have experienced a GC reaction. In some cases one might expect that the differentiation status could in turn dictate the pattern of virus latency found in each tumour. HRS cells in HL express a latency II pattern identical to that found in the GC B cells of asymptomatic carriers and may be suggestive of a GC origin **(Deacon et al., 1993)**. On the other hand, EBV-positive BL cells have a morphology and gene expression profile that is similar to GC B cells and so express a virus latency programme which resembles more closely a memory B cell **(Rowe et al., 2014)**.

1.5.2 Contribution of EBV latent genes to the pathogenesis of lymphomas

In the following sections I focus on the contribution of individual virus genes to the pathogenesis of B cell lymphomas. By virtue of the overwhelming larger literature on cHL, I focus my discussion on this disease, but much of what is discussed almost certainly also applies to DLBCL, at least the ABC type, which shares many features in common with cHL

Epstein-Barr virus nuclear antigen-1

Epstein-Barr virus nuclear antigen-1 (EBNA-1) is necessary for the maintenance of EBV infection as it acts as a viral replication factor and tethers the viral genome to the chromosomes of daughter cells during cell division **(Smith and Sugden, 2013)**. It is expressed in all forms of virus latency, with the exception of Latency 0. In addition to its genome maintenance function, EBNA1 is also a transcription factor

that regulates both viral and cellular gene expression **(Frappier, 2012a, Frappier, 2012b)**, as well as inhibiting TGFβ signalling, at least in part through increasing the turnover of SMAD2 and down-regulating the TGFβ target gene, PTPRK **(Wood et al., 2007, Flavell et al., 2008)**, promoting growth and survival of cHL cells. EBNA1 increases expression of the T cell chemokine CCL20 which may dampen the immune response to HRS cells by recruiting regulatory T cells to the tumour microenvironment **(Baumforth et al., 2008)**.

Latent membrane protein-1

LMP-1 is a member of the tumour necrosis factor receptor (TNFR) superfamily and functions as a constitutively active homologue of the cellular CD40 receptor **(Lam and Sugden, 2003)**. LMP-1 can activate multiple cell signalling pathways that are known to be aberrantly activated in cHL and DLBCL. These include the NF-κB, JAK/STAT, AP-1 and phospatidylinositol-3 kinase (PI3-K)/AKT pathways **(Bargou et al., 1997, Dutton et al., 2005, Heath et al., 2012)**.

The importance of LMP-1 in cHL pathogenesis is further emphasised by the finding that LMP-1 expression in primary GC B cells, the presumed progenitors of cHL, induces many of the changes characteristic of HRS cells. These changes include the down-regulation of B cell transcription factors and BCR signalling components required to maintain B cell identity, and the upregulation of survival genes such as BCL2 and BFL-1 that protect B cells from apoptosis **(Henderson et al., 1991, Vockerodt et al., 2008)**. LMP-1 also induces the expression of FLICE-inhibitory protein (Cellular FLICE-inhibitory protein c-FLIP), a negative regulator of Fas induced apoptosis **(Cahir-McFarland et al., 2004)**, suggesting that one of its major pathogenic roles could be to rescue pre-apoptotic GC B cells from cell death (Figure 1.6). LMP-1 can also regulate cellular gene expression by modifying the H3K27me3

histone mark through poly (ADP-ribose) polymerase 1 (PARP1) activation **(Martin et al., 2016)**. LMP-1 can also affect gene transcription and subsequent B-cell lymphomagensis through the activation of cellular miRNAs, for example by regulating miR-10b, miR-29b, miR-146a, and miR-155 **(Motsch et al., 2007)**. LMP-1 might also contribute to the characteristic morphological features of HRS cells. For example, induced expression of LMP1 down-regulates expression of the shelterin proteins, TRF1, TRF2 and POT1 leading to the formation of multinucleated HRS-like cells **(Lajoie et al., 2015)**.

Latent membrane protein-2

Latent membrane protein-2 (LMP-2) exists as two isoforms, LMP-2A and LMP-2B, which share 8 common coding exons but have different 5′ exons. While the 5′ exon of LMP-2B is non-coding, the unique N-terminus of LMP-2A includes an ITAM motif, which resembles the signalling domain of the BCR. Indeed, in transgenic mice LMP-2A has been shown to function as a BCR mimic, allowing B cell development in the absence of normal signalling through the BCR **(Caldwell et al., 1998, Merchant et al., 2001)**. In doing so LMP-2A engages signalling pathways important for B cell survival, including the RAS/PI3-K/AKT pathway which is implicated in HRS cell survival **(Fukuda and Longnecker, 2007)**. Global gene expression studies show that LMP-2A can suppress expression of numerous B cell transcription factors, including EBF1 and E2A, recapitulating many of the gene expression changes seen in HRS cells **(Portis et al., 2003, Portis and Longnecker, 2004, Vockerodt et al., 2013)**. LMP-2A also activates the Notch pathway, which might contribute to the loss of B cell identity in HRS cells **(Anderson and Longnecker, 2009)**. However, it should be noted that many of the adaptor molecules necessary for both BCR and LMP-2A signalling are absent in HRS cells, and therefore it remains unclear whether

LMP-2A acts as a BCR surrogate in the context of cHL. One possible explanation for this paradox is that LMP-2A provides essential survival signals in the HRS progenitor cells, which retain the downstream BCR signalling molecules, but subsequent transformation events followed by downregulation of B cell specific genes replace some of these critical LMP-2A functions. However, given that EBV-positive cases of cHL are consistently LMP-2A positive, it is likely that LMP-2A also has BCR-independent functions that are important for maintenance of the HRS phenotype.

Whereas LMP-2A has been shown to induce autoimmunity in transgenic mice **(Chang et al., 2012)**, LMP-1 expression in the B cells of transgenic mice can lead to lymphoma development **(Kulwichit et al., 1998, Zhang et al., 2012)**. However, the combined expression of LMP-1 and LMP-2A in transgenic mice resulted in no significant B cell abnormalities **(Vrazo et al., 2012)**, suggesting that LMP-2A might have tumour suppressor functions. Recently it was shown that LMP-1 was dispensable for EBV-induced lymphoma formation in cord blood-humanized mice and that deletion of LMP-2A delayed the onset of lymphoma in this model **(Ma et al., 2017)**. Plasma cell differentiation was inhibited even in the absence of LMP-1 and LMP-2 suggesting that this was important for EBV-induced lymphomagenesis. The apparent contradictory findings from these animal models underscore the need to develop better *in vivo* models of EBV-associated lymphomagenesis.

1.5.3 Suppression of the EBV lytic cycle as a potential pathogenic event in EBV-positive cHL

Productive EBV infection is associated with the temporal expression of immediate early, early and late viral genes leading ultimately to the production of new virus particles. The switch to virus replication from latency is mediated by two distinct mechanisms. The first occurs via plasma cell differentiation, the second through the activation of the BCR. Given that the full replicative cycle of EBV leads to cell death, suppression of both routes to virus replication is probably necessary for transformation.

Plasma cell differentiation is dependent on the temporal expression of transcription factors which co-ordinately induce the transcription of genes required for terminal B-cell differentiation while switching off the germinal centre B-cell program. B lymphocyte induced maturation protein 1 (BLIMP1), which is required for plasma cell differentiation and which can activate the EBV immediate early genes BZLF1 and BRLF1, thus providing a mechanistic link between plasma cell differentiation and EBV reactivation **(Reusch et al., 2015)**. LMP-1 has been shown to suppress plasma cell differentiation by inhibiting BLIMP1α expression. EBV can also induce expression of the dominant negative BLIMP1 isoform, BLIMP1β **(Vrzalikova et al., 2011, Vrzalikova et al., 2012)**. Thus, disruption of the normal functions of BLIMP1α is likely to be important for the pathogenesis of cHL, preventing not only the terminal differentiation of the tumour cell progenitors, but also virus replication. It should be noted that in virus-negative B cell lymphomas, BLIMP1 can be inactivated by other mechanisms, for example by mutation **(Pasqualucci et al., 2006, Mandelbaum et al., 2010)**.The second route to EBV replication occurs via BCR activation. As described earlier EBV-positive HRS cells frequently have non-functional immunoglobulin genes and lack expression of critical downstream molecules of the

BCR signalling pathway. The loss of a functional BCR is likely to be an important event in cHL development because it could also prevent entry into the replicative cycle. Almost all cases of cHL bearing destructive immunoglobulin gene mutations are EBV-positive **(Bräuninger et al., 2006)**. These data suggest that progenitor cells carrying such mutations can only survive if infected with EBV. Further support for this contention is provided by the observation that EBV can immortalise BCR-negative GC B cells *in vitro* **(Mancao et al., 2005, Chaganti et al., 2005, Bechtel et al., 2005)**. Importantly, while LMP-2A can still induce lytic cycle entry in the absence of a functional BCR, it cannot do so when these downstream BCR components are missing **(Vockerodt et al., 2013)**. Thus, the loss of BCR, as well as of BCR signalling components could prevent both BCR- and LMP-2A-induced virus replication. Figure 1.6 summarises the GC model of EBV infection and its role in the pathogenesis of B cell associated EBV lymphomas.

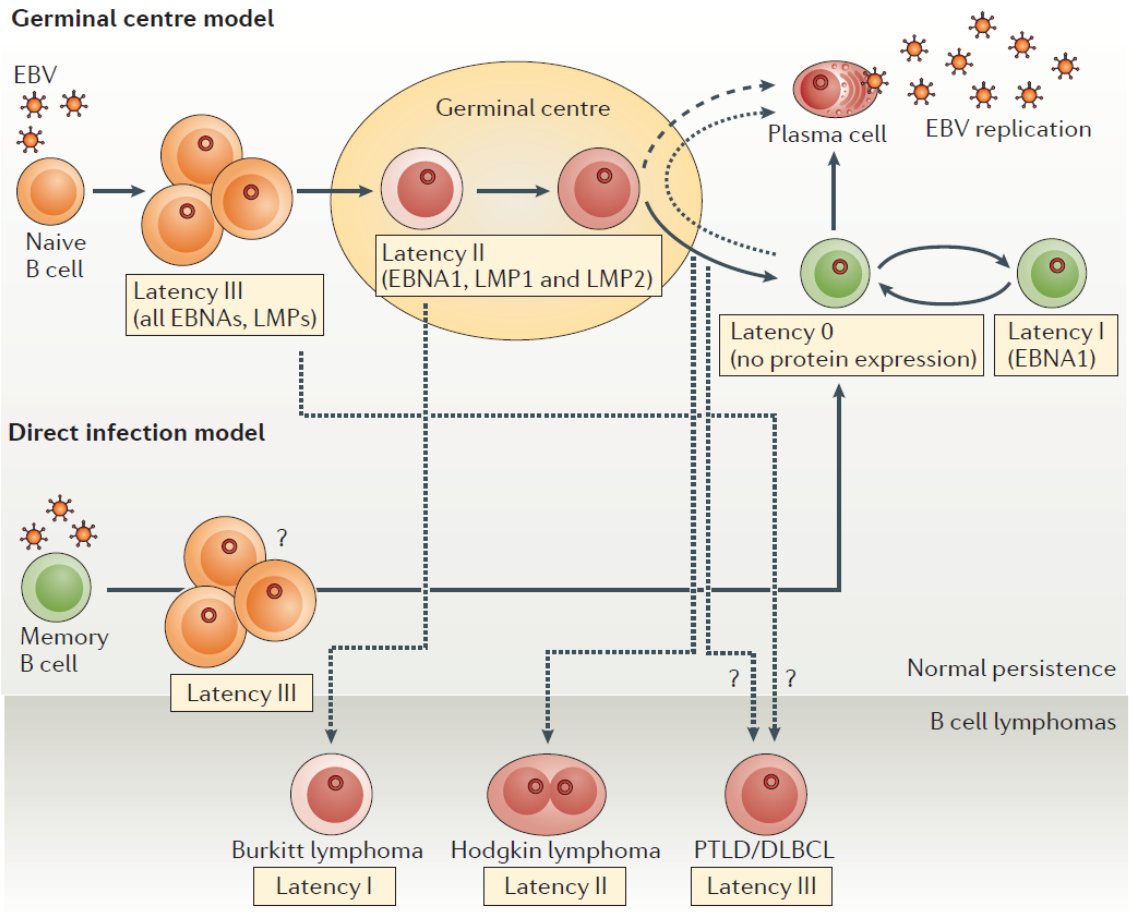

Figure 1.6 EBV infection model in normal lymphoid B cells and its pathogenesis in B cell lymphoma. Top panel shows EBV asymptomatic infection in B cells begins with acquisition of the virus in naïve cells, followed by its proliferation in GC B cells, proceeding establishment of latency III. LMP-1 and LMP-2 latent genes, provide survival benefits in the GC B cells as they function as CD40 receptor and BCR signalling respectively. Infected cells can exit GC as memory cells harbouring the virus, then differentiate to plasma cells with silenced infection, as shown in the black solid arrow. EBV infected plasma cells, can arise directly from GC infected B-cells as well (highlighted with the dash arrow). Another direct infection model shown in the middle panel through direct acquisition of memory cells to the EBV infection, followed by establishment of latency type III. Lower panel of different types of EBV related B cell lymphomas such as post-transplant lymphoproliferative disease (PTLD), diffuse large B cell lymphoma (DLBCL), Hodgkin lymphoma (HL) and Burkitt lymphoma (BL) showed different types of latency, with unsettled exact cell of origin as highlighted by the black dotted lines. Figure taken from Young et al **(Young et al., 2016)**.

1.5.4 EBV and DLBCL; additional remarks

EBV is reported to be more commonly associated with DLBCL in patients who have evidence of immune impairment. For example, EBV-positive DLBCL constitute approximately 30-50% of the later onset lymphomas that arise in patients after transplant and as a consequence of iatrogenic immune suppression. Most EBV-positive DLBCL express either a type II, or more frequently, a type III form of latency. As well as potential roles for LMP-1 and LMP-2 described above for cHL, many DLBCL express EBNA-2 and the EBNA-3 proteins. There is evidence that these proteins could contribute to DLBCL pathogenesis, for example, EBNA-3A and EBNA-3C are potential oncogenes, which together can repress expression of pro-apoptotic and senescence-inducing genes **(Anderton et al., 2008, Skalska et al., 2010, Maruo et al., 2011)**. In contrast, EBNA3B is probably a tumour suppressor gene in DLBCL **(White et al., 2012)**.

It was also reported that EBV-positive DLBCL can occur in older patients without a prior history of immune suppression. This initially led to the designation by WHO, of a new provisional diagnostic entity, referred to as 'EBV-positive diffuse large B cell lymphoma of the elderly **(Oyama et al., 2003, Oyama et al., 2007)**. However, EBV-positive DLBCL was also described in younger patients and in children without any immunodeficiency **(Cohen et al., 2013, Cohen et al., 2017)**. This prompted a revision of the classification in 2016 where EBV-positive DLBCL is now referred to as 'EBV-positive DLBCL NOS'.

1.5.5 EBV association and contribution of EBV genes in NPC

In NPC tumour cells EBV has been reported to display a restricted pattern of virus latency with the expression of EBNA1, LMP-1 and LMP-2A (latency II). Notably, LMP-1 is not expressed in all NPC, and in some positive cases expression is heterogeneous being apparently restricted to a subset of tumour cells **(Khabir et al., 2005)**. LMP-1 has been shown to inhibit epithelial cell differentiation **(Dawson et al., 1990)**. In the context of NPC, LMP-1 can increase tumour cell proliferation and survival via its ability to activate the NF-κB and PI3-K/Akt pathways, as well as regulate growth factor receptors such as EGFR and c-MET **(Dawson et al., 2012)**. LMP-1 can also promote angiogenesis through its ability to increase the expression of hypoxia-inducible factor 1 (HIF) and vascular endothelial growth factor **(Dawson et al., 2012)**. The metastatic potential of NPC cells is increased as a result of LMP-1-induced epithelial-mesenchymal transition. Through activation of its downstream signalling pathways, LMP-1 can also induce the expression of matrix metalloproteinases **(Zhao et al., 2012)**.

In contrast to LMP-1, LMP2-A is constitutively expressed in NPC where it has been shown to promote proliferation of NPC cells, induce epithelial-mesenchymal transition, as well as invasion, and migration. LMP-2A can activate these cellular phenotypes through its ability to stimulate intracellular signalling pathways, notably via Notch, PI3-K/Akt, and Wnt **(Vicari and Trinchieri, 2004)**.

1.5.5.1 Genetic factors in NPC development

Although EBV is probably an early event, pre-existing genetic abnormalities, for example loss of chromosomal material from 3p and 9p are thought to occur before EBV infection and may allow the virus survive in its latent form rather than induce virus replication which is the normal outcome of virus infection of untransformed

epithelial cells **(Chan et al., 2000, Chan et al., 2002, Frappier, 2012c)**. In keeping with this EBV infection is not detectable in normal nasopharyngeal epithelium, but has been detected in *in situ* cancers **(Pathmanathan et al., 1995a, Pathmanathan et al., 1995b)**.

NPC cells display evidence of activating mutations and amplification of components of the PI3-K signalling and receptor tyrosine kinase pathways **(Chou et al., 2009, Chung et al., 2013, Lin et al., 2014)**. Recent global genomic studies have also identified recurrent alterations in genes involved in chromatin remodelling including ARID1A, KMT2D/3 and BAP1 **(Lin et al., 2014)**.

Genomic landscape of NPC

Whole exome and deep sequencing of 128 cases of NPC revealed the presence of 9 frequently mutated genes involved in chromatin remodelling, ERK-MAPK/PI3-K signalling and autophagy **(Lin et al., 2014)**. In a more recent study of more than a 100 micro-dissected primary, recurrent and metastatic NPC samples, obtained from Asian and the USA, whole exome sequencing (WES) revealed the presence of novel molecular mutations believed to be important in the oncogenesis of NPC **(Li et al., 2017)**. The study identified higher rates of somatic mutation in EBV-positive tumours than was previously thought **(Li et al., 2017)**, and contrasted with EBV-negative head and neck squamous cell carcinoma (SCC), where the spectrum of somatic mutations were found to be far fewer in number **(Network, 2015)**. Somatic mutation in negative regulators of the NF-κB pathway was identified as a prominent feature of EBV-positive NPC, with mutation or truncation of CYCLD, TRAF3 and NF-κBIA frequently identified in NPC cases derived from Asian backgrounds **(Li et al., 2017)**. NF-κB has been shown to influence the growth and survival of NPC-derived cell lines *in vitro*, underscoring the importance of pathway dysregulation in NPC

pathogenesis. Somatic alterations in DNA repair and chromatin remodelling genes were also reported, giving rise to additional genetic signatures. In agreement with the earlier study of Lin et al., **(Lin et al., 2014)**, mutations in the PI-3K and Mitogen-activated protein kinase (MAPK) pathways were also identified, with tumours harbouring mutations in PTEN, PIK3CA, ERB3, BRAFL, NF1, FGFR2 and FGFR3 **(Li et al., 2017)**. Inactivation of the tumour suppressor gene, PTEN, can also be induced by LMP-1, through a mechanism involving epigenetic changes and NF-κB activation **(Peng et al., 2016)**. LMP-1 is known to activate the canonical and non-canonical NF-κB signalling pathways **(Soni et al., 2007)**. While LMP-1 protein expression in NPC is variable, in their study, Li and colleagues found that 25.7% of the NPC cases were LMP-1 positive. Interestingly, this study found that LMP-1 positive tumours, unlike their LMP-1 negative counterparts, were found to lack somatic mutations in the NF-κB negative regulators, suggesting that constitutive NF-κB signalling is essential for both LMP-1-dependent and LMP-1-independent NPC pathogenesis. Hariwiyanto and colleagues established that high levels of LMP-1 and LMP-2 were associated with a poorer prognosis and disease-specific survival, suggesting that viral-encoded latent proteins may provide additional stimuli over and above those induced by somatic mutation of the NF-κB pathway **(Hariwiyanto et al., 2010)**. Molecular aberrations in NF-κB, in addition to LMP-1-mediated NF-κB were found to contribute to the unique inflammatory background of NPC **(Li et al., 2017)**. LMP-1 stimulates NF-κB oncogenic pathway mediated through phosphorylation and degradation of IκBα **(Yin et al., 2001)**.

1.5.5.2 Viral and cellular factors influencing tumour immunity

It is well established that certain EBV genes can interfere with the antigen-processing machinery. For example, EBV proteins expressed in the lytic cycle such as BGLF5, BILF1 and BNLF2A are known to interfere through various mechanisms with major antigen presentation through major histocompatibility complex molecules **(Zuo et al., 2009)**. Furthermore, BCRF1 is a functional homologue of IL-10 and can inhibit virus-specific immunity **(Vicari and Trinchieri, 2004)**.

The discovery that PD-L1 and PD1 over-expression is common in EBV-associated NPC indicates that these two immune evasion proteins are important in the tumorigenic process **(Zhang et al., 2015)**. The up-regulation of PD-L1 and PD-L2 was reported in NPC as well as in other EBV-associated malignancies, such as HL may enable the tumour cells to survive the host immune response.

Prevalence of PD-L1 protein expression in NPC

PD-L1 expression on NPC tumours has been reported, albeit to varying extents. This is attributed to the use of different antibodies and different cut-off values used to score tumour cell positivity. It was reported by Chen et al to be positive in 89% (16/18) of cases **(Chen et al., 2013)**, by Fang et al to be 95.0% (132/139) **(Fang et al., 2014)**, by Zhang et al to be 95.0% (132/139) **(Zhang et al., 2015)**, Lee et al to be 25% (26/104) (Lee et al., 2016), by Zhou et al to be 97.0% (128/132) **(Zhou et al., 2017a),** by Zhou et al to be 97.0% (96/99) **(Zhou et al., 2017b)**, by Li et al to be (71%) (85/120) **(Li et al., 2017)**, by Ooft et al to be 60% (55/92) **(Ooft et al., 2017)**, by Zhu et al to be 32.53% (68/209) of NPC samples **(Zhu et al., 2017)** and by Zheng et al to be 73.3% (85/116) **(Zheng et al., 2017)**.

PD-L1 and association with other EBV related malignancies

Viruses and some tumours may utilize the PD1/PD-L1 signalling pathway to avoid detection by the immune system **(Barber et al., 2006) (Iwai et al., 2002)**. Overexpression of PD-L1, in the context of EBV-related malignancies, has been reported. PD-L1 overexpression has been described in EBV associated cancers, which can be mediated through LMP-1 or through PD-L1 amplification **(Network, 2014)**. LMP-1 has also been shown to induce PD-L1 expression through a mechanism involving AP-1 signalling in HL **(Green et al., 2012a)**. PD-L1 over expression has been reported predominantly in EBV-positive post-transplant lymphoproliferative disorders **(Green et al., 2012a)**. EBV positive DLBCL (EBV immunodeficiency related and DLBCL of the elderly) have been reported to be positive in (16/16) 100% of cases examined. Interestingly, however, EBV positive BL were reportedly to be negative in all cases examined **(Chen et al., 2013)**. NK/T cell lymphoma is an aggressive form of lymphoma, which is consistently EBV positive. Higher levels of PD-L1 was shown to be expressed at the protein level in the EBV positive NK cell line (SNK-6), compared to the EBV negative NK cell line (NK-92). A role for LMP-1 in PDL-1 expression was established in these NK cell lines, through activation of the ERK-MAPK/NF-κB pathways **(Bi et al., 2016)**. Studies have revealed the significance of high expression of PD1 in the microenvironment of HL which was associated with poor outcome. In this study, 20% of patients with PD1 density >0.5% cells had disease free survival 61% versus 89% at both 5 and 10 years (p=0.03) **(Greaves et al., 2013)**. T cell effector functions in cHL can be abrogated by the engagement of PD-L1 expressed on HRS cells with its receptor, PD-1, on T cells resulting in functional exhaustion of the T cells **(Muenst et al., 2009, Yamamoto et al., 2008)**. Amplification of the PD-L1 and PD-L2 genes

at 9p24 is common in NSHL **(Green et al., 2012a)**, while the PD-L1 gene can also be deregulated in a proportion of cHL cases as a result of a reciprocal translocation that involves MHC-II transactivator (CIITA) **(Steidl et al., 2011)**. In HL, amplification of PD-L1/PD-L2 is associated with an approximately 90% response rate to Nivolumab. **(Ansell et al., 2015)**. LMP-1 has also been reported to induce PD-L1 expression **(Green et al., 2012a)**. The importance of this pathway in the microenvironment of cHL is exemplified by studies which show that many patients with relapsed or refractory cHL respond to PD1 blockade therapy **(Ansell et al., 2015)** Moreover, recent study have shown PD-L1 expression in HRS highly expressed in cHL (90% in lymphocyte rich HL, 65% in the nodular sclerosis subtype, 67% in the lymphocyte-depleted subtype and 81% in the mixed cellularity subtype), rather than NLPHL (54%). PD-L1 was associated with poor survival rates in EBV negative HL **(Menter et al., 2016).**

PD-L1 and HL

Studies have revealed the significance of high expression of PD1 in the microenvironment of HL which was associated with poor outcome. In this study, 20% of patients with PD1 density >0.5% cells had disease free survival 61% versus 89% at both 5 and 10 years (p=0.03) **(Greaves et al., 2013)**. T cell effector functions in cHL can be abrogated by the engagement of PD-L1 expressed on HRS cells with its receptor, PD-1, on T cells resulting in functional exhaustion of the T cells **(Muenst et al., 2009, Yamamoto et al., 2008)** Amplification of the PD-L1 and PD-L2 genes at 9p24 is common in nodular sclerosis cHL **(Green et al., 2012a)**, while the PD-L1 gene can also be deregulated in a proportion of cHL cases as a result of a reciprocal translocation that involves CIITA **(Steidl et al., 2011)**. In HL, amplification of PD-L1/PD-L2 is associated with an approximately 90% response rate to Nivolumab.

(Ansell et al., 2015). LMP-1 has also been reported to induce PD-L1 expression **(Green et al., 2012a)**. The importance of this pathway in the microenvironment of cHL is exemplified by studies which show that many patients with relapsed or refractory cHL respond to PD1 blockade therapy **(Ansell et al., 2015)**. Moreover, recent study have shown PD-L1 expression in HRS highly expressed in cHL (90% in lymphocyte rich HL, 65% in the nodular sclerosis subtype, 67% in the lymphocyte-depleted subtype and 81% in the mixed cellularity subtype), rather than Nodular lymphocyte predominance HL (54%). PD-L1 was associated with poor survival rates in EBV negative HL **(Menter et al., 2016)**.

The significance of immune checkpoints in these tumours is discussed in section 1.6.

1.5 Tumour microenvironment

A major theme of this thesis is the tumour microenvironment. In this respect, I have focussed on the microenvironment of DLBCL and NPC. I have focussed mainly on the potential contribution of collagen and collagen receptors in DLBCL and the PD-L1 immune checkpoint in NPC.

General introduction of DLBCL Microenvironment

The tumour microenvironment of DLBCL is composed of immune cells, stromal cells, blood vessels and extracellular matrix, which appears to be an important prognostic factor in DLBCL patients **(Scott et al., 2016)**. High density infiltration of tumour associated macrophages (TAMs), specifically M2 macrophages is predictive of poor outcome in several types of cancers **(Condeelis and Pollard, 2006, Qian and Pollard, 2010)**. Macrophage of M2 phenotype numbers are also strongly associated with inferior survival in DLBCL, which is associated with progression of tumour, this was described to be mediated through remodelling of the extracellular matrix **(Shen et al., 2016)**. CD163-expressing macrophages in the

microenvironment of DLBCL was associated with Stage IV and disease progression **(Shen et al., 2016)**. The potential tumour-promoting functions of TAMs may also be explained by their ability to induce angiogenesis mediated by the secretion of soluble pro-angiogenic factors, including vascular endothelial growth factor (VEGF) **(Mantovani et al., 2004)**. Reports have shown that tumour cells secrete cytokines such as chemokine ligand 2 (CCL2) which induce polarization of monocytes to M2 tumour promoting macrophage phenotype upon co-culturing of bone marrow stromal cells with lymphoma cells **(Guilloton et al., 2012)**. Other report indicate that increased density of M2 macrophages (defined as CD68+CD163+ cells), but not M1 macrophages are associated with a poor outcome in R-CHOP treated DLBCL patients **(Wada et al., 2012) (Marchesi et al., 2015)**. Another study showed that a high density of CD163-positive M2 macrophages was a poor prognostic factor in DLBCL **(Shen et al., 2016)**. These findings suggest that the ratio of CD163-positive M2 TAMs correlates positively with disease progression and prognosis in DLBCL. A study that used semi-automated quantitative analysis revealed significance of IHC CD3 and FOXP3 counts as good predictive markers in treated DLBCL patients **(Coutinho et al., 2015)**. The immune microenvironment of DLBCL is characterized by infiltration of mixtures of innate response and adaptive immune cells, including macrophages, APC and NK, dendritic cells and reactive lymphocytes **(Cohen et al., 2017)**. Exhausted T cells, as demonstrated by PD1 positive TILs were reported in DLBCL microenvironment. Chronic antigenic stimulation such as that induced by viral infections results in exhaustion of T cells, with inefficient production of antiviral cytokines **(Wherry and Ahmed, 2004)**. Exhausted T cells can result in lymphoma development **(Bryan and Gordon, 2015)**. PD1 positive cells were shown to be

predominant in EBV positive DLBCL, and associated with decreased cytokine secretion in in vitro studies **(Quan et al., 2015)**.

EBV positive and negative DLBCL are not different in terms of the frequency of T-regs, however, CD8 positive cytotoxic lymphocytes and granzyme expression were predominant in the virus associated DLBCL **(Cohen et al., 2017)**. Lenz et al profiled gene expression in whole DLBCL samples to identify gene expression signatures that correlated with differences in survival following treatment with R-CHOP and showed that the DLBCL microenvironment is an important indicator of outcome. Thus, the two stromal signatures when combined into a single stromal score predicted the survival of DLBCL patients. Importantly, the stromal score was present across both molecular subtypes of GCB and ABC, suggesting that similar tumour microenvironment features can be acquired during the pathogenesis of both of the major forms of DLBCL. High values of the stromal scores were associated with inferior outcomes. Genes defining the stromal-1 signature were enriched for those encoding extracellular matrix components, including collagens and modifiers of collagen synthesis. Also enriched in the stromal-1 signature was a “monocyte” profile, comprising genes that are more highly expressed in CD14+ blood monocytes than in B cells, T cells, or natural killer cells. Recruitment of stromal cells to the tumour microenvironment is recognised to play an important role in tumour progression mediated through changes in the endothelial transcription profile of DLBCL. The stromal-2 signature is reported to be enriched for genes associated with angiogenesis reflected by increased tumour blood-vessel density which predicts poor outcome in DLBCL patients **(Lenz et al., 2008)**.

Reports showed that increased density of M2 macrophages (defined as CD68+CD163+ cells), but not M1 macrophages are associated with a poor outcome

in R-CHOP treated DLBCL patients **(Wada et al., 2012) (Marchesi et al., 2015)**. Another study showed that a high density of CD163-positive M2 macrophages was a poor prognostic factor in DLBCL **(Shen et al., 2016)**. These findings suggest that the ratio of CD163-positive M2 TAMs correlates positively with disease progression and prognosis in DLBCL. Chemo-resistant patients showed more CD68 and tryptase expression, and this was associated with increased microvessel density. CD3 positive T cells in this study showed decreased density with bulky disease, which contributed to the progression and inferior outcome **(Gaudio et al., 2017)**. Microarray studies have shown a distinct cluster related to the microenvironment of DLBCL, named host inflammatory response subtype. Although this signature was associated with prominent host response in the form of T cells and dendritic cells infiltration, however R-CHOP patients in this cluster showed inferior outcome, which indicated an ineffective immune response by inhibited immune cells. This signature was rich in inflammatory related genes, such as components of TCR genes, genes related to NF-κb and IFNγ/STAT1 signalling pathways **(Monti et al., 2005, Abramson and Shipp, 2005)**. Another study examined CD3, PD1 and PD-L1 expression in the microenvironment of DLBCL, and revealed that CD3 T cells were the most frequently identified cell type in the infiltrate, followed by PD-L1 and PD1-positive cells. PD-L1 expression was described to be present more often in the ABC type of DLBCL. PD1 positive T cells in CD3 rich DLBCL, was associated with poor outcome. There is also emerging evidence that the microenvironment can modulate EBV gene functions. Thus, LMP-1 induces expression of the discoidin domain receptor 1 (DDR-1), a potentially oncogenic receptor tyrosine kinase. However, DDR-1 is normally only active in the presence of its ligand, collagen, which is a major constituent of the cHL microenvironment. Notably, ligation of DDR-1 by collagen

promotes the survival of lymphoma cells *in vitro* **(Cader et al., 2013)**. These observations suggest that some of LMP-1's oncogenic effects may be dependent on the tumour microenvironment.

1.6.1 Collagen and collagen receptors

Collagen is a key constituent of the extracellular matrix (ECM) of tumour microenvironments where it may contribute to cancer development and progression. Cross talk between ECM proteins and neoplastic cells has been shown to be important for tumour proliferation, survival and dissemination.

Structure of collagen

Collagen is composed of a triple helical structure, which is formed of repeats of proline, hydroxyl amino acids and glycine (Pro-Hyp-Gly). The three polypeptide chains forming the triple helix collagen, are either similar or different in their repeats, frequently comprised of proline or hydroxyproline amino acid residues in X- and Y-position respectively **(Engel and Bächinger, 2005)**. Hydroxylation of proline occurs due to posttranslational enzymatic action where conversion of the proline at Y position occurs into hydroxyproline. Peptide bonds attaching the amino acids chains are located at the interior side of the triple helical structure of the collagen, conferring resistance to enzymatic action by proteases, however it can be degraded by collagenases enzyme or can be denatured **(Hay, 2013)**. Glycine is located at very third position in the repeating amino acid sequence and is responsible for the folding of the triple helix. The hydroxylation of the proline residues is responsible for the structural stability of collagen and location of hydroxyproline at the Y position adds to this stability. The collagen structure is strengthened by the hydrogen bonds between the backbone of glycine and proline. Formation of collagen fibres starts with cleavage of pro-collagen at the N and C-terminal pro-peptide into tropocollagen

which is formed of three different α chains, followed by microfibril assembly with formation of collagen fibrogenesis, followed by formation of cross links. Collagen can be formed of either continuous fibres or can be interrupted with non-collagenous structures. Straight poly-proline helix per turn is formed of three residues with the glycine facing each other from the inner side **(Shoulders and Raines, 2009)**.

1.6.1.1 Collagen in haematolymphoid neoplasms

Early studies of follicular lymphoma (FL) reported collagen deposition, varying from fine to thick fibres, particularly in high grade cases. In fact, the follicular pattern becomes more obvious with bands of collagen encompassing tumour follicles **(Jaffe et al., 2010)**. Collagen deposition is more common in certain anatomic locations such as retroperitoneum, however it can also occur in other locations such as mediastinal, cervical or other regions **(Rosai, 2011)**. The presence of collagen in inter-follicular regions can be used as an additional helpful feature in differentiating reactive follicular hyperplastic or the most challenging diffuse lymphoid hyperplastic conditions, from FL. The presence of collagen may also be of clinical significance as it was proposed that FL with and without sclerosis are clinically distinct, with findings that the former may be more indolent **(McCurley et al., 1986)**. In FL, it was proposed that the collagen producing cells were fibroblasts or myofibroblasts **(McCurley et al., 1986)**. In other mature B cell neoplasms such as multiple myeloma (MM), 9% of cases were categorized as fibrotic myeloma with extensive collagen deposition. MM with marrow fibrosis is also usually associated with more plasma cell infiltrate and short survival.

As mentioned earlier sclerosis is sometimes seen in other B cell lymphoma such as DLBCL, especially in rare variants of DLBCL like spindle cell and myxoid subtypes,

as well as PMLBCL and grey zone lymphoma which is rare subtypes of DLBCL **(Rosai, 2011)**.

1.6.2 Collagen receptors

There are at least 9 collagen receptor genes; two of these are relevant to this thesis. They are the DDR-1 and LAIR-1.

1.6.2.1 Discoidin domain receptor-1

DDR-1 and DDR-2 are unique among receptor tyrosine kinases in being activated by interaction with the extracellular matrix. Both DDR-1 and DDR-2 are phosphorylated upon binding collagen. DDR-1 was shown to protect lymphoma cells from chemotherapy induced cell death. The EBV latency gene, LMP-1 was shown to upregulate DDR-1 in normal GC B isolated cells. Auto-phosphorylation of DDR-1 induces the activation of downstream signalling pathways, including PI3-K/Akt and NF-κB which are important in the pathogenesis of many cancers and lymphomas, including HL **(Cader et al., 2013)**.

DDR-1 and DDR-2 have emerged as an important subgroup of potentially oncogenic collagen receptors **(Borza and Pozzi, 2014) (Rammal et al., 2016, Valiathan et al., 2012, Villoutreix and Miteva, 2016)**. The DDRs are receptor tyrosine kinases which have a catalytic kinase domain with a distinct extracellular Discoidin (DS) homology domain **(Johnson et al., 1993, Alves et al., 1995)**. Both receptors are activated upon binding to collagen. DDR-1 is activated by various types of collagen including type I, IV, V, VI, and VIII, whereas DDR-2 is only activated by fibrillar collagens, in particular collagens type I, III, and type X **(Vogel et al., 1997, Leitinger, 2003, Shrivastava et al., 1997)**.

DDR-1 expression has already been shown to be an important inducer of several signalling pathways including JAK-STAT, NF-κB and PI3-K **(L'HÔTE et al., 2002,**

Das et al., 2006). DDR-1 also interacts with Notch 1 and induces pro-survival pathways; collagen also increases activated Notch 1 expression **(Kim et al., 2011)**.

1.5.2.2 Leukocyte-associated Ig-like receptor-1

Leukocyte-associated Ig-like receptor (LAIR-1) is a type I transmembrane glycoprotein which is a member of the Ig superfamily. It is expressed on the majority of human PBMCs, including NK cells, T cells, B cells, monocytes, and dendritic cells. Cross-linking of LAIR-1 on human NK cells induces a potent inhibitory signal that is capable of decreasing target cell lysis by both resting and activated NK cells *in vitro.* It also acts as an inhibitory receptor on effector T cells **(Meyaard, 2008)** . LAIR-1 is a known collagen receptor. *In vitro* experiments showed that collagens such as transmembrane collagen XVII, collagen I and III are functional ligands of LAIR-1. These studies showed that LAIR-1 cross linking with collagens I and II can induce suppression of the immune response. Tumours expressing different types of collagens such as collagens I, III, V, VI, XIII, XVII, XVIII, and XXIII were reported to be prognostic markers of tumour aggressiveness **(Parikka et al., 2003, Banyard et al., 2003, Väisänen et al., 2005)**. LAIR-1 may induce immune evasion mediated through tumour cells expressing collagens which interact with LAIR-1 on immune cells **(Lebbink et al., 2006)**. It is proposed that LAIR-1 signalling is regulated via its expression because LAIR-1 levels are generally higher on less differentiated or naive cells, and lower on more activated or differentiated immune cells **(Meyaard, 2008)**. LAIR-1 was recently described as a potineal target in acute myeloid leukaemia (AML), where inhibition of LAIR-1 expressed on surface of AML tumour cells induced cell death. LAIR-1 mediated the action of the apoptosis through the activation of the downstream signalling cAMP response element-binding protein (CREB) pathway through recruitment of SHP phosphatase. LAIR-1 can function

through activation of SHP-1/CAMK1 pathway by phosphorylating downstream transcriptional target gene of LAIR1; CREB and maintain development and growth of AML in *in vitro* experiments. In addition, an *in vivo* study showed that LAIR-1 engrafted tumour cells sustained the growth of AML through stem cell activation **(Kang et al., 2015)**.

1.5.3 PD-L1 immune checkpoint

Immune checkpoints refer to the myriads of pathways involved in inhibitory functions of the immune system that are essential for self-tolerance and modulating the duration of immune responses in tissues, thus protecting them from self-destruction. Recently, these immune-checkpoint pathways have been shown to be important for tumour evasion **(Pardoll, 2012)**. One important checkpoint is that mediated by the engagement of PD-L1 expressed on tumour cells with its receptor, PD1, on T cells resulting in functional exhaustion of the T cells **(Yamamoto et al., 2008)**.

PD1 is also be expressed on other immune cells, including B cells, monocytes, dendritic cells and NK cells, where it mediates its inhibitory effects on other immune functions **(Pardoll, 2012)**.

Mechanisms of PD1/PD-L1 signalling on immune evasion

PD1 PD-L1 pathway inhibits T cell response through the interaction between PD1 and PD-L1, leading to inhibition of TCR which is responsible for influx of calcium, which will be associated with several signalling pathway involved essential for T cell differentiation. Mechanism of T cell inhibition starts with ligation of PD-L1 to PD1 localized on the surface of T cells, followed by phosphorylation of PD1 when SHP1/2 are recruited. This leads to the de-phosphorylation of lymphocyte-specific protein tyrosine kinase (Lck); which is responsible for phosphorylation of intracellular chains in T cells. As a result of Lck dephosphorylation, inactivation of cytoplasmic tyrosine

kinase; Zap-70 results in inhibition of PI3-K/Akt/mTOR and Ras/MAPK/Erk pathways, leading to downregulation of the metabolic activity of T cells. This change in the T cell metabolic reprograming influences T cell differentiation, leading to inhibition of differentiation of effector and memory T cells, while enhancing the differentiation of T regulatory cells and exhausted T cells **(Zhao et al., 2014, Hersey and Gowrishankar, 2015)**.

Although PD1 is expressed on various immune cells, its up-regulation on the surface of T cells, is a sign of exhaustion after persistent antigenic stimulation **(Zou and Chen, 2008)**.

PD1 can be upregulated by various stimuli, such as IFNs **(Massari et al., 2015)**. Inhibition of T cell function and decrease in their number can happen through the high level of expression of PD1 in the microenvironment **(Thompson, 2006, Wang et al., 2014, Blank et al., 2006)**.

PD1 PD-L1 interaction can lead to increased levels of other immune checkpoint molecules such as IDO, which will result in further exhaustion of T cells and enhanced T-reg functions **(Schlößer et al., 2014)**. PD1 PD-L1 axis activation in the tumour microenvironment is not only associated with inhibition of effector T lymphocytes but is also associated with increased T-reg induction and function, thus enhancing the immunosuppressive function of T-regs. This can be enhanced by expression of PD1 on the surface of T-regs, resulting in differentiation to T-regs which express FOXP3, and which eventually will supress Th1 responses **(Momtaz and Postow, 2014)**.

Immune checkpoint inhibitors have been shown to be effective in immunogenic tumours, such as melanoma, renal cell carcinoma, bladder cancer, non-small cell

lung carcinoma, and HL **(Medina and Adams, 2016)**. FDA approved inhibitors include pembrolizumab and Nivolumab **(Topalian et al., 2015)**.

Although PDL-1 expression is important for selecting patients for treatment with PD1 or PDL-1 inhibitors not all PDL-1 positive tumours respond to these inhibitors **(Pardoll, 2012)**. This indicates that more work is required to study the expression of this and other checkpoints in tumours and to relate this to outcome.

Other immune checkpoints molecules

In addition to the PD-L1/PD1 axis, several other immune checkpoint pathways have been identified in NPC. Indoleamine 2, 3-dioxygenase (IDO1), an immunosuppressive enzyme, was reportedly expressed in approximately 28% of NPC cases and shown to inhibit cytolytic T cell function in NPC cell lines. IDO1 negatively influences lymphocyte function in tumours by modulating tryptophan metabolism in both antigen presenting cells and tumour cells, thereby enhancing tumour growth **(Liu et al., 2009)**. Other immune-checkpoint molecules such as hepatitis A virus cellular receptor 2, also known as T cell Immunoglobulin and Mucin domain-3 (TIM3), and Lymphocyte Activation Gene-3 (LAG3) have been shown to be overexpressed in cancers and virus-related pathologies **(Ott and Hodi, 2012)**. TIM3 is broadly expressed on immune cells and is implicated in various diseases such as colitis, HIV and HCV-associated diseases. TIM3 and its ligand, Galectin-9, are expressed on NPC tumour cells, and increased expression is associated with tumour recurrence in NPC. Galectin-9 overexpression is associated with an increase in tumour-associated TIM3 positive lymphocytes and an increase in FOXP3 positive T cells in a subset of recurrent NPC patients. Expression of Galectin-9 on primary NPC tumours is associated with resistance to killing by cytotoxic CD8 T lymphocytes, which are inhibited by the effect of Galectin/TIM3

pathway and the recruitment of additional T-regs in NPC **(Chen et al., 2017)**. LAG3, expressed on T lymphocytes, can inactivate T cells by arresting the cell cycle at S-phase. LAG3 can induce an immunosuppressive microenvironment by enhancing T-reg suppressive functions **(Thaventhiran et al., 2013)**. CTLA-4 is an inhibitory receptor expressed on T lymphocytes which, upon binding PD-L1, down-regulates pathways involved in T cell activation **(Curran et al., 2010, Bour-Jordan et al., 2011, Flies et al., 2011)**. In addition to PD1, other immune inhibitory receptors such as B- and T-lymphocyte attenuator (BTLA) and LAIR-1 are members of the same family of ITIM -immunoreceptor tyrosine-based inhibition motif co-inhibitory receptors. When activated, recruitment of the SHP-1 and SHP-2 phosphatases results in inhibitory signals to downregulate T cell activation **(Thaventhiran et al., 2013)**. Additional PD1 ligand is PD-L2 although its precise role in modulating immune responses is still not verified, and its expression is more restricted compared to PD-L1, thus making it a less obvious target in cancer immunotherapy. PD-L1 is constitutively expressed by a wide variety of immune cells and non-immune cells and most normal tissue cells seem to be able to up-regulate PD-L1 in the presence of strong inflammatory signals. Compared to PD-L1, constitutive basal expression of PD-L2 is low. PD-L2 expression was initially thought to be limited to antigen-presenting cells such as macrophages and dendritic cells (DCs). In recent years however, several studies have shown that PD-L2 expression can be induced broadly on other immune cells and non-immune cells depending on microenvironmental stimuli **(Rozali et al., 2012)**. PD-L1 and PD-L2 are different in their molecular mechanisms of interaction with PD1. Like PD-L1, PD-L2 can induce signalling downstream in T cell, thus modulating T-cell function, but the exact molecular pathway is yet to be elucidated. PD-L2 expression, like PD-L1 expression

may be predictive of response to Pembrolizumab (anti-PD1) immunotherapy **(Rozali et al., 2012)**.

1.6.4 Tumour microenvironment of NPC

The tumour microenvironment comprises tumour cells and non-tumour cells such as fibroblasts, tumour-associated macrophages, eosinophils and lymphocytes **(Schreiber et al., 2011)**. T cells are present within the microenvironment of EBV positive NPC **(Li et al., 2017)**; however, EBV specific T cells are inhibited in the tumour microenvironment. Immunosuppressive T-regs are known to be increased in the peripheral circulation of NPC patients **(Lau et al., 2007)**. Flow cytometric analysis of primary NPC samples, have shown that 11% of T cells exhibited T-reg phenotype (CD4 positive CD25 high FOXP3 positive) **(Lau et al., 2007)**. Another study has shown increased recruitment of FOXP3 positive CD4 T cells in the tumour compartment rather than the stroma as demonstrated by double labelling **(Yip et al., 2009)**. Different phenotypes of TILs have shown different impact on the outcome. The density of CD8 positive TILs showed positive association with lymph node spread while the density of FOXP3 positive TILs have impact on the tumour stage **(Zhang et al., 2010)**. The density of FOXP3 positive TILs was associated with better overall survival and progression free survival, in all patients and in all patients with late stage disease. A low density of CD8 positive TILs or a high ratio of FOXP3 positive TILs to CD8 positive TILs was correlated with better progression free survival in early stage patients **(Yip et al., 2009)**. It is noteworthy that increased levels of FOXP3 positive T-regs were reported to be important prognostic infiltrate in the tumour compartment, associated with inferior survival in many cancers **(Shang et al., 2015)**. The immunoscore seems to be a better prognostic factor than staging in early-stage colorectal cancer **(Pages et al., 2009)**. Immunoscore was

performed based on the evaluation of subpopulations of T cells, especially CD8+ T cells **(Ascierto et al., 2013)**. Immunoscore is a predictive factor as infiltrating CD8+ T lymphocytes are a marker of a pre-existing immunity that can be released from immunosuppression by a PD1/PD-L1 blockade. In melanoma patients treated with anti-PD1 antibody, recruitment of CD8+ T cells was higher at the invasive tumor margin and in the tumor stroma in the pre-treatment samples of responders compared to non-responders **(Tumeh et al., 2014)**.

A recent report compared EBV positive NPC with EBV negative NPC, and identified a distinct microenvironment of EBV positive NPC, characterised by more recruitment of T cells, while CD8-psoitive lymphocytes expressing PD-L1 in virus positive cases showed improved overall survival and disease free survival **(Ooft et al., 2017)**. Hypoxia (hypoxia inducible factor-1α) and anaemia in NPC patients have been shown to be associated with up-regulation of PD-L1 on immune cells **(Zhou et al., 2017a)**. Tumour associated macrophages are important in tumour progression; a study compared the phenotypes of macrophages phenotype in EBV positive and negative NPC, and revealed that EBV positive tumours showed more infiltration of macrophages stained with pan macrophage marker; CD68 and increased FOXP3 T-regs. However macrophages of the M2 phenotype as labelled by CD163 and CD206 were more frequent in EBV negative NPC which reflects distinct viral induced recruitment of the microenvironment populations **(Ooft et al., 2017)**.

1.6.5 MHC class I and II

In addition to immune checkpoints, loss of MHC class I and II can contribute to immune escape. Reduced levels or loss of MHC class I or its accessory proteins is common in NPC Thus, beta-2 microglobulin was shown to be decreased or lost in

48.64% of NPC samples **(Kouvidou et al., 1995)**, this protein play an important role in the assembly of MHC class I, which suggests that with loss of beta-2 microglobulin, will be associated MHC class I loss. In another reports of NPC, it was revealed that 63% of samples have a normal level of expression of MHC class I, while this was reduced in 22% of cases and markedly down-regulated in 15% of cases **(Yao et al., 2000)**. MHC class I downregulation can be of two different types, reversible if it is induced by epigenetic events or genes affecting the regulation of MHC class I or irreversible if it is caused by genetic or chromosomal abnormalities **(Garrido et al., 2017)**. Reversible type have been suggested to benefit from PD1 blockade therapy. Genome wide expression profiling of micro-dissected NPC tumour cells revealed that downregulation of MHC class I genes was associated with expression of EBV genes **(Sengupta et al., 2006)**. Association between specific variants of MHC class I and the risk of NPC development have been reported in various populations **(Li et al., 2009)**. Although MHC-I expression is frequently altered in NPC, reports show that MHC class II is often expressed by NPC tumour cells **(Busson et al., 1988)**. MHC class II expression in NPC was reported to be high in the tumour cells **(Yao et al., 2000)**. Not all NPC cases express MHC class II, however lower levels were observed in 37% of samples analysed; some of these cases also had decreased MHC class I expression. Downregulation of MHC class I on the surface of tumour cells results in immune escape by avoiding being recognized and eliminated by CTLs **(Šmahel, 2017)**. MHC class I gene showed common and significant genetic aberrations in Asian background NPC and these mutational status in MHC class I were associated with poor outcome **(Li et al., 2017)**.

MHC class II expression was shown to be up-regulated in Barrett's oesophagus, a pre-neoplastic process. In addition gain of MHC class II, but loss of MHC class I was observed in the same tumours **(Rajendra et al., 2006)**. MHC class II antigens are not normally positive in most epithelial cells but expressed in several pathological conditions, such as in inflammation, autoimmune and malignant transformation. This gain in MHC class II expression associated with pre-neoplastic changes has been described before associated with loss in MHC class I **(Rajendra et al., 2006)**. MHC class II was observed to be overexpressed in cervical intraepithelial neoplasia, another dysplastic condition **(Cromme et al., 1993)**. CIITA gene have been described in the literature to fuse to PD-L1 can result in PD-L1 gene amplification and overexpression in lymphomas **(Steidl et al., 2011)**. A recent study showed positive association between transcriptional levels of MHC class I locus in malignant melanoma patients and their positive response to PD1 inhibitors. Three predictive markers (PD-L1, granzyme A (GZMA), and MHC class I) distinguished the responders from non-responders to PD1 inhibitors. Tumour cells expressing MHC class II expression can be recognized and efficiently rejected by direct cytotoxic action of CD4+ T cells in melanoma patients, this anti-tumour immune response mediated by CD4 positive cells was shown to be promoted by PD1 blockade **(Yan et al., 2016)**.

MHC class I expressing tumours have good response to PD1 inhibitors, mediated through the pro-tumour activity of IFN-γ, expressed by immune cells, specifically PD-L1 expressing tumour. However combined tumour immunotherapy targeting PD1/PD-L1 axis and IFN-α and IFN-β is still in its early research **(Šmahel, 2017)**. Reports revealed that PD1 blockade in HL reached 87%, while subset of HL patients were known to have downregulated MHC class I, thus speculating that PD1

blockade can be beneficial in HL cases with downregulated MHC-I, which is suggested to be independent from the action of cytotoxic CD8 cells **(Roemer et al., 2016)**. Immune cells other than CD8 cytotoxic cells, for example, macrophages, have been proposed to induce cytotoxic anti-tumour effects, **(Thoreau et al., 2015)**. This effect can be mediated through polarization of M2 to M1 macrophages, which could be cytotoxic even in presence of MHC class I downregulation.

1.6 Sphingolipids

As well as being constitutive parts of the cell membranes of all eukaryotic cells, sphingolipids also have signalling functions. It is these functions which I summarise below, focussing particularly on sphingosine-1-phosphate (S1P). This bioactive lipid has been demonstrated to regulate key cellular processes such as migration, proliferation and survival.

1.7.1 S1P synthesis and degradation

S1P levels are tightly regulated by enzymes that control its synthesis and removal. S1P can be produced by the activity of sphingomyelinase which generates ceramide **(Zhang et al., 1991, Cuvillier et al., 1996)**. Ceramide in turn is converted into sphingosine by ceramidase. S1P is then produced by the phosphorylation of sphingosine mediated by one of two sphingosine kinases (SPHK1 and SPHK2). Removal of S1P can occur by two distinct pathways. The first is by the de-phosphorylation of S1P to sphingosine which is catalysed by one of two S1P phosphatases (SGPP1 and SGPP2). In the second pathway, S1P is degraded by S1P lyase (SGPL1). S1P is transported out of cells by several members of the adenosine triphosphate (ATP)-binding cassette multi-drug resistant transporter family, including ABCC1 and ABCA1 as well by the transporter protein SPNS2 **(Mitra et al., 2006, Sato et al., 2007, Hisano et al., 1999)**. Extracellular S1P can then act upon up to five different G-protein-coupled receptors (GPCRs). This is known as “inside-out” signalling (Figure 1.7).

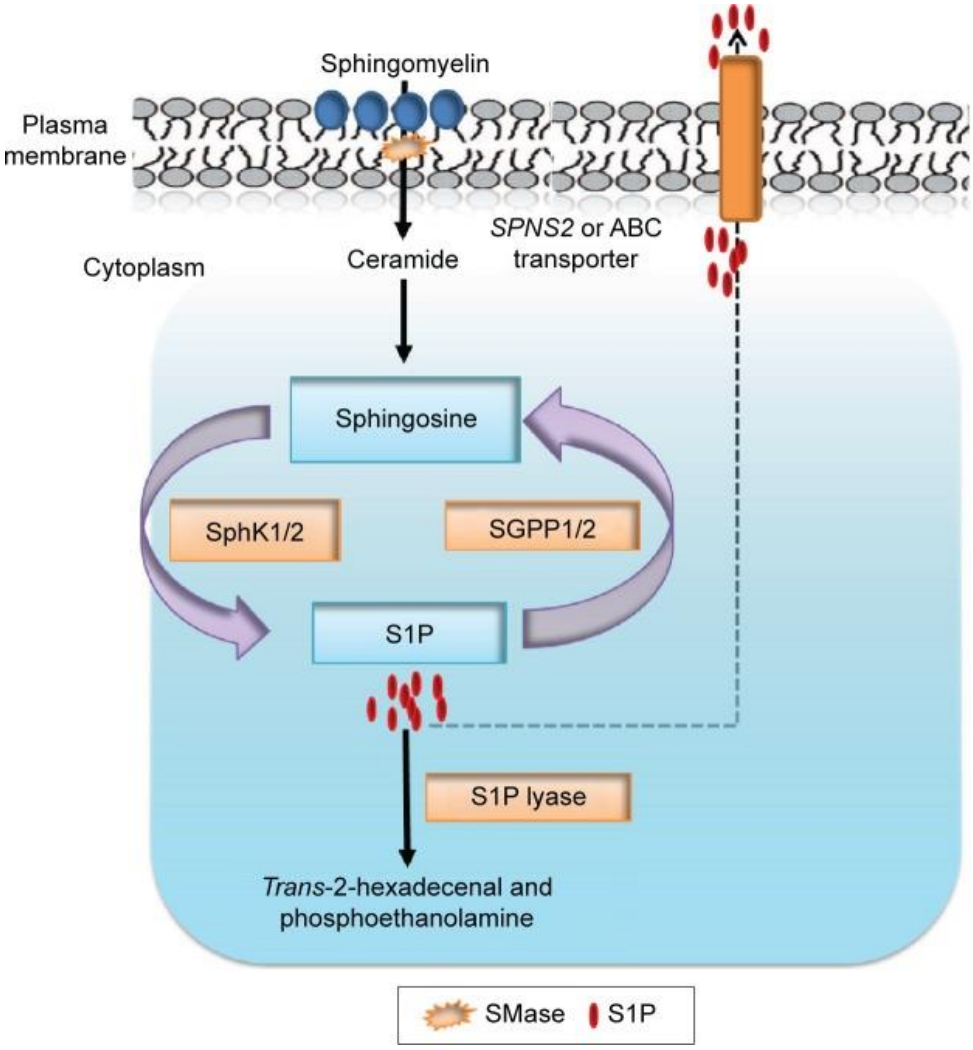

Figure 1.7 S1P signalling pathway
S1P synthesis begins with hydrolysis of sphingomyelin by sphingomyelinase at the plasma membrane. This results in production of ceramide, which is metabolized by ceramidase to produce sphingosine. Consequently, sphingosine is phosphorylated by Sphingosine Kinases 1 and 2 (SPKH1 and 2) and is exported out of the cell by either *SPNS2* or ATP-binding cassette (ABC) transporters. The balance between intracellular concentration of S1P is controlled by its synthesis and degradation: S1P can be converted to sphingosine by phosphatases SGPP1/2 or irreversibly degraded to hexadecenal and phosphoethanolamine by S1P-lyase. Figure adapted from Nema et al **(Nema et al., 2016)**.

1.7.2 The sphingolipid rheostat

S1P has been shown to increase the growth and survival of many different cell types **(Spiegel and Milstien, 2003)**. By contrast, its precursors, ceramide and sphingosine, induce apoptosis and inhibit proliferation **(Zhang et al., 1991, Cuvillier et al., 1996)**. This has led to the concept of the sphingolipid rheostat whereby the balance between S1P on the one hand, and ceramide and sphingosine, on the other, determines cell fate **(Cuvillier et al., 1996)**.

1.7.3 S1P signalling through its receptors

Five S1P receptors (S1PR) are known to exist: These are referred to as S1PR1 (EDG1), S1PR2 (EDG5), S1PR3 (EDG3), S1PR4 (EDG6) and S1PR5 (EDG). Signalling by S1PR mediates both the paracrine and autocrine effects of S1P **(Alvarez et al., 2010)**. The S1P receptors couple to different G proteins (Figure 1.8). S1PR1, S1PR2 and S1PR3 are ubiquitously expressed, whereas S1PR4 and S1PR5 have restricted expression; immune cells and brain **(Brinkmann, 2007, Chun et al., 2010)**. The biological response to S1P is governed by the differential expression of these S1P receptors.

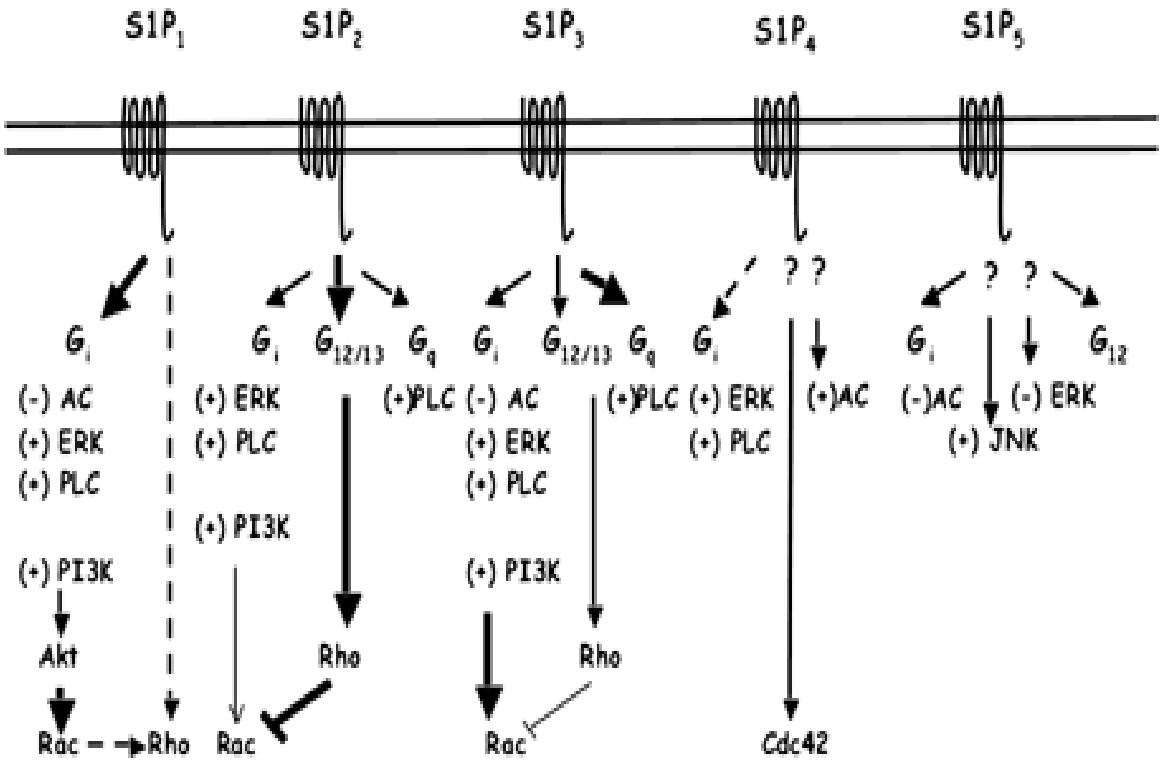

Figure 1.8 S1P receptors family signalling pathways. There are five cell surface S1P receptors (S1PR1-5); each coupling to a different repertoire of G proteins. S1PR1 stimulation results in activation of a range of downstream signalling pathways including the PI3-K, PLC, PI3-K β pathways. S1PR1 activation leads to phosphorylation of AKT with subsequent Rac pathway activation. Activated S1PR1, S1PR3, and S1PR5 can inhibit adenylate cyclase (AC) mediated through Gi, on the contrary, S1PR4 stimulation results in AC activation as well as Cdc42. S1PR2 and S1PR3 inhibits Rac via activation of Rho kinase, that is mediated through binding to G12/13. S1PR1, S1PR2, S1PR3, and S1PR4 can activate ERK and PLC pathways mediated through binding to Gi. In contrast to other S1PR receptors, S1PR5 inhibits ERK activation and activates JNK pathway. Taken from **(Sanchez and Hla, 2004).**

S1PR1

S1PR1 was discovered in 1990 **(Hla and Maciag, 1990)** and has been found to be expressed on many cell types including endothelial cells **(Chun, 2013)**. In the immune system, S1PR1 is expressed on T and B cells, macrophages, dendritic cells and NK cells **(Goetzl et al., 2004) (Chun, 2013)**. S1PR1 exclusively couples to Gi protein which leads to the activation of ERK and PI3-K/Akt signalling, promoting cell survival and proliferation. S1PR1 signalling also leads to the activation of Rac, a Rho family small GTPase which drives cell migration.

S1PR2

S1PR2 couples to Gi, Gq and G12/13 **(Windh et al., 1999, Okamoto et al., 2000, Takuwa, 2002)**. In contrast to S1PR1, signalling through S1PR2 inhibits Rac and downstream cell migration **(Estrada et al., 2008) (Takuwa et al., 2002)**. Furthermore, S1PR2 mediated Rho activation results in the inhibition of Akt signalling, thereby reducing cell survival and inhibiting cell proliferation **(Sanchez et al., 2005, Schüppel et al., 2008)**.

S1PR3

S1PR3 couples to several different G proteins which results in the activation of phospholipase C (PLC) and Ca2+ via Gq and ERK, PI3-K and Rac. The activation of these signalling pathways is context dependent but leads mainly to increased cell survival, proliferation and migration **(Windh et al., 1999, Okamoto et al., 1999)**.

S1PR4

S1PR4 couples with Gi and G12/13 to activate ERK, PLC and Rho as well as Ca2+ mobilisation, cytoskeleton rearrangement and cell migration **(Ishii et al., 2004)**. S1PR4 expression is largely restricted to lymphoid tissues although its function is poorly described.

S1PR5

S1PR5 can couple with Gi and G12/13 and is highly expressed in the brain. It has been suggested to have potential functions in the maturation of oligodendrocytes **(Terai et al., 2003)**.

1.7.4 Over-expression of SPHK1 and cancer

The overexpression of SPHK1 transforms NIH3T3 fibroblasts and enhances tumour formation in mice **(Xia et al., 2000)**. SPHK1 has been shown to be over-expressed in many cancer types. Furthermore, this over-expression has been shown to correlate with increased tumour grade and reduced patient survival **(Ruckhäberle et al., 2008, Pchejetski et al., 2005, Sobue et al., 2008a, Sobue et al., 2008b, Vadas et al., 2008)**.

SPHK1 has been shown to have important anti-apoptotic effects, for example it can protect against death induced by the withdrawal of serum or the addition of TNFα **(Cuvillier et al., 2010)**. This is likely to be due to SPHK1 increasing the levels of the anti-apoptotic proteins, BCL2 and MCL1, whilst at the same time S1P can also increase the expression of pro-apoptotic proteins, BAD BAX **(Sauer et al., 2005, Li et al., 2008) (Avery et al., 2008)**.

The reduced expression of SPHK1 also leads to reduced cell proliferation and can trigger apoptosis in cancer cells arising from the prostate, pancreas, brain and breast **(Akao et al., 2006, Pchejetski et al., 2005) (Guillermet-Guibert et al., 2009, Baran et al., 2007, Kapitonov et al., 2009, Taha et al., 2006)**.

SPHK1 is also implicated in the development of resistance to cancer therapies **(Pchejetski et al., 2005, Baran et al., 2007)**. This is in part because it is well established that many cancer treatments (as renal cell carcinoma) which rely on the generation of ceramide **(Ogretmen and Hannun, 2001)**. For example, in a mouse model of prostate cancer, tumours overexpressing SPHK1 were larger and more

resistant to docetaxel and this was associated with reduced ceramide production **(Pchejetski et al., 2005)**.

1.7.5 Induction of aberrant cell signalling by S1P in cancer cells

Aberrant expression of S1P in B cell lymphomas

One report has shown that SPHK1 is over-expressed in NHL, and was associated with higher clinical grade in 44 tumour samples **(Bayerl et al., 2008)**.

Another study has shown that p53 knockout mice developed thymic lymphoma, associated with increased levels of SPHK1/S1P while ceramide was decreased. Notably, loss of the SPHK1 gene in this model completely abolished the development of thymic lymphomas and improved the survival rates by 30% **(Heffernan-Stroud et al., 2012)**. A number of lines of evidence suggest that aberrant S1P signalling could contribute to the pathogenesis of B cell lymphomas. For example, SPHK1 is over-expressed in NHL and its inhibition can prevent ceramide catabolism and potentiate cell death in a mantle cell lymphoma line **(Webb et al., 2015)**. S1PR1 is also over-expressed in HL and promotes migration the migration of HL cell lines in vitro **(Kluk et al., 2013)**. Conversely, S1PR2 is an inhibitory receptor, is mutated in patients with DLBCL.

S1P is a crucial element for the constitutive activation of STAT3 in tumour cells. For example, in one study it was shown that STAT3 could induce the expression of S1PR1 which was elevated in STAT3 positive tumours. In turn the increased S1PR1 expression further activated STAT3 and upregulated IL6 **(Lee et al., 2010)**. In the ABC form of DLBCL, STAT3 is highly active and is regulated by S1PR1 **(Liu et al., 2012)**.

There is a positive feedback loop between S1PR1 and STAT3, highlighting a crucial role for S1P in the constitutive activation of S1P in tumour cells. Furthermore, in

ABC subtype DLBCL, STAT3 has been found to be highly active and this is due, at least in part, to S1PR1 **(Liu et al., 2012)**.

Aberrant expression of S1P in EBV associated malignancy-NPC

S1P signalling is implicated in the pathogenesis of NPC. EBV infection, or ectopically expressed EBV-encoded latent genes (EBNA1, LMP-1, and LMP2-A) resulted in increased expression of SPKH1. Stimulation of the NPC cell lines by exogenous S1P enhanced the migratory activity of the tumour cells and was mediated through activation of AKT. This migratory activity was inhibited by knockdown of one of the S1P receptors; S1PR3, which was associated with decreased levels of AKT. This feature was clarified by using LY294002; a PI3-K inhibitor which resulted in reduced migration of tumour cells in the presence of S1P. Moreover, S1PR3 receptor was the only S1P receptor which showed differential expression in micro-dissected NPC versus normal nasopharyngeal epithelium **(Lee et al., 2017a)**.

1.7.6 Contribution of SPHK1-S1P signalling to altered cell migration in cancer

The differential expression of S1PR1 and S1PR2 is important for regulating migratory responses. S1PR2, which usually inhibits cell migration and is highly expressed by GC B cells where it plays a critical role in GC B cell positioning and confinement of B cells to the GC; in S1PR2-deficient mice this is disrupted leading to large poorly defined GC **(Cattoretti et al., 2009, Green and Cyster, 2012)**. In contrast, lymphocyte egress is regulated by S1PR1 **(Cyster, 2005)**. This is well demonstrated by the use of FTY720, a functional S1PR1 antagonist which leads to lymphopenia in several animal models and in humans, as a result of lymphocyte egress **(Chiba et al., 1998, Yagi et al., 2000, Mandala et al., 2002)**.

Changes in S1P receptor expression or function could also contribute to cancer development. For example, the S1PR2 –deficient mice described above are prone to develop tumours that resemble DLBCL **(Cattoretti et al., 2009)**. Furthermore, S1PR2 is mutated in around one quarter of patients with DLBCL **(Cattoretti et al., 2009)**.

1.7.7 Therapeutic targeting of S1P or its receptors

There are a variety of therapies against S1P or its receptors that might eventually find application in cancer patients. Below I briefly summarise some of these.

The anti-S1P monoclonal antibody, Sphingomab, sequesters S1P thus preventing its interaction with S1PR **(O'Brien et al., 2009)**. Sphingomab has been shown to reduce tumour progression in murine xenograft models mainly through inhibition of angiogenesis **(Visentin et al., 2006)**. The humanised form of Sphingomab, known as Sonepcizumab has been used in a Phase I clinical trial in cancer patients (ClinicalTrials.gov Identifier: NCT00661414).

S1P receptor antagonists include FTY720 (fingolimod) an analogue of sphingosine **(Sanchez et al., 2003)**. FTY720 once phosphorylated inside cells binds to S1PR1, 3, 4 and 5. FTY720 results in the internalisation and degradation of S1PR1 **(Matloubian et al., 2004)**.

SPHK1 inhibitors act not only to reduce S1P production but also to increase ceramide and sphingosine levels. They include delipidated human serum (DHS) and N,N-Dimethylsphingosine (DMS) both of which can reduce the growth of gastric and lung cancers in mice **(Endo et al., 1991, Okoshi et al., 1991)**. Non-lipid SPHK1 inhibitors (compounds SPHK1 I-V) are non-competitive inhibitors of the Adenosine triphosphate (ATP) binding site and are effective at nanomolar potencies **(French et al., 2003)**.

*Note: Some text within this chapter is taken from our recent book chapter in the series: **(Hudnall and Küppers, 2018)**

1.8 Aims of the Study

The overarching aim of this study was to explore different components of the pathogenesis of three EBV-related cancers

General Aims:

Aim 1) to explore the immune microenvironment of NPC and the potential for tumour cells to be recognized by T cells.

Aim 2) to investigate expression of collagen and collagen receptors in DLBCL

Aim 3) to define the role of aberrant sphingosine-1-phosphate signalling in HL

Specific Aims

Aims of Chapter 3

1) To confirm PD-L1 is overexpressed in NPC
2) To study potential relationship of PD-L1 and LMP-1 expression in NPC
3) To explore immune checkpoint co-expression in NPC, and their potential relationship with LMP-1 expression
4) To investigate the different patterns of PD-L1 expression (marginal or diffuse) which may reflect the underlying molecular mechanism (Inducible or constitutive) of PD-L1 expression in NPC
5) To investigate the frequency and distribution of TILS (CD3) positive cells in relation to PD-L1 and PD1 in NPC
6) To explore the subcellular patterns of PD-L1 protein expression in NPC
7) To explore the prevalence of PD-L1 expression in tumour cells versus immune cells in NPC
8) To investigate correlation of PD-L1 and PD1 expression in the tumour and the microenvironment in NPC

9) To study the frequency and the spatial distribution of lymphocyte immune infiltrate using lymphocyte subpopulation panel in NPC
10) To study immune visibility by evaluating MHC class I and II in NPC by IHC assay

Aims of Chapter 4

1) To explore the expression of collagens and collagen receptors in GC B cells and DLBCL, through the re-analysis of published datasets
2) To investigate the expression of LAIR-1 and DDR-1 collagen ligands in GC B cells and DLBCL using immunohistochemistry
3) To identify cells in the microenvironment expressing LAIR-1 in DLBCL
4) To investigate in vitro the effect of collagen ligation on LAIR-1 expression in macrophages

Aims of Chapter 5

1) To study the expression of S1P receptors focusing mainly on S1PR1 and S1PR2 in normal lymphoid tissue and HL
2) To study the effect of S1P and its receptors on the P13-K pathway using P-AKT signalling as a read out in HL cell lines
3) To identify the transcriptional targets of P13-K signalling pathway in HL and study expression of BATF3 in normal lymphoid tissue and HL
4) To investigate the co-expression of BATF3 and S1PR1 in normal lymphoid tissue and HL
5) To study the effect of BATF3 on S1PR1 expression in HL cell lines

CHAPTER TWO
MATERIALS AND METHODS

2.1 Tissue samples

2.1.1 Nasopharyngeal carcinoma

19 samples were used for MHC class I and MHC class II immunohistochemistry panels, 17 of these cases were available for the Immune checkpoint and T cell subpopulation panels. NPC samples were from UK and provided by Dr Graham Taylor (University of Birmingham, Institute of cancer and genomics). The samples were primary tumour and confirmed to be EBV positive. Clinical and pathological details in Appendix 1.

2.1.2 DLBCL samples

2.1.2.1 Construction of tissue microarray of DLBCL

I selected tumour rich areas using 28 samples H&E sections retrieved from the pathology department, at Queen Elizabeth Hospital, Birmingham (QEHB) based on a cohort of 305 DLBCL patients with full clinical annotation, diagnosed between 1996 and 2008. I used the DLBCL tissue microarray (TMA) to examine the expression of C1q, S1PR1, BATF3 and S1PR2. Cores for the TMA were selected from viable tumour areas in triplicate from different areas. Areas displaying adipose tissue infiltration at the periphery of the lymph node, necrotic or haemorrhagic areas were excluded. Another set of TMA was selected from areas with macrophages or ‘starry-sky’ pattern. TMA recipient blocks were constructed based on pathological assessment in collaboration with Dr Vikki Rand, Northern Institute for Cancer Research, Newcastle University. Controls were used within every set of TMA, as tonsil, large bowel, and renal cortex. Clinical details of these samples are shown in Table 2.1

Table 2.1 Clinical details of DLBCL samples

Factor	Numbers
Gender	M=22 F=6
Immunophenotype	GCB=10 ABC=18
BCL2	Negative=5 Positive=7 Strong positive=3 Not available=3
Stage	1=6 2=7 3=6 4=9
Lactate dehydrogenase (LDH)	Normal=8 >450=12 >1000=5 >5000=3
Revised International Prognostic Index (R-IPI)	1=3 2=14 3=11
B symptoms	No=13 Yes=15
Overall survival (OS)	Alive=14 Deceased=14

***IHC classification was done by IHC using Hans' algorithm (Hans et al., 2004).**

2.1.3 HL samples

A TMA composed of 43 samples were provided by Dr. Elizabeth Soilleux, John Radcliffe Hospital, Oxford, UK. All samples had been reviewed in Oxford and confirmed as primary HL with classification into histological subtypes.

2.2 Immunohistochemistry (IHC)

2.2.1 Positive and negative controls

As controls for all staining, FFPE tonsil blocks were obtained from QEHB, and fresh paediatric tonsils were obtained from Birmingham Children's Hospital under local ethics committee approval (Ref No.06/Q2702/50). Part of these were fixed in 10% v/v formaldehyde (Sigma-Aldrich Ltd., Gillingham) and sectioned by the Histopathology Department at the Royal Orthopaedic Hospital, Birmingham (ROH). The remainder were processed in our lab for other experiments.

2.2.2 Sectioning of tissues

Before sectioning, FFPE blocks were chilled for approximately 20 minutes on ice. FFPE blocks were cut to 4µm in thickness. Sections were floated in a heated water bath at 40°C. Sections were then immediately positioned onto positively charged adhesive-coated slides (Vectabonded, Surgipath™). This was performed in our lab, by HBRC at the University of Birmingham, or by the histopathology department at the ROH. Slides were kept at 4°C for long term storage.

2.2.3 Haematoxylin and eosin (H&E) protocol

For staining, de-paraffinisation of the section was performed by placing in histoclear for 10 min, followed by hydration through decreasing concentrations of ethanol baths (100%, 90%, and 70%) and then washes with water for 2 min. Sections were stained in haematoxylin for 5 minutes, followed by a wash in running tap water for 2 minutes in hot water then for 2 minutes in cold water. This was followed by staining

in Eosin Y for 30 seconds. Dehydration in increasing concentration of ethanol for 3 minutes was followed by 100 % ethanol for 3 minutes. Histoclear washes, then followed by mounting in DPX media (Table 2.2)

2.3 Optimisation of antibodies

Each new antibody was tested on tissue that was identified to express that antigen according to the Human Protein Atlas (available online at: www.proteinatlas.org). The dilution provided by the company was used only as an indication of dilution range. The optimum concentration of each antibody was determined by testing different antibody dilutions on control tissue using positive and negative control sections. Antibodies previously validated by members of our group using HEK293 cell lines (University of Birmingham) included: S1PR2, S1PR1, LAIR-1 and DDR-1. Other antibodies were validated by Dr Vrzalikova using knockdown experiments by western blots or immunofluorescence staining; these antibodies included those against BATF3.

2.4 IHC

For IHC, sections of paraffin-embedded tissue biopsies were initially de-waxed using histoclear solutions (National Diagnostics), for 10 minutes. Rehydration was performed by immersing the slides in IMS for 2x5 minutes, followed by washing under running tap water for 5 minutes. Blocking was done with 0.3% hydrogen peroxide (Sigma-Aldrich Ltd., Gillingham) for 15 minutes to inactivate any endogenous peroxidase, followed by a further wash under running tap water for 5 minutes. Different methods of antigen retrieval were optimised to individual antibodies.

2.4.1 Citrate Antigen Retrieval

Citrate-Antigen retrieval method was used to expose antigens. To prepare antigen retrieval buffer, 1.26g of sodium citrate (VWR) and 0.25g citric acid (VWR) were added to 1 litre of distilled water, and the pH adjusted to between 5.9-6.1 using 0.1M sodium hydroxide. The citrate buffer was heated in a microwave at full power for 10 min. The slides were immersed into the buffer and heated at medium and low power for 10 minutes each. Slides were then cooled for 15 minutes at 4°C then washed in running tap water for 5 minutes. Prior to staining, a hydrophobic barrier was drawn around tissue sections using a Pap pen (Sigma-Aldrich) and conditioned with Tris-buffered saline with 0.1% Tween-20 (TBS-T) for 10 minutes. Tissue sections were blocked with 5X casein (Vector Labs) diluted in distilled water for 10 minutes to prevent non-specific background staining. The primary antibodies were added to the tissue and incubated at room temperature for 1 hour or 18 hours at 4°C as required (Tables 2.2 and Table 2.3). The slides were washed with PBST to remove the primary antibody. Anti-rabbit/anti-mouse secondary universal antibody (Vector Labs) was added to the tissue, and incubated for 30 minutes at room temperature. Slides were washed with PBST 3x 5 minutes each. Diaminobenzidine (DAB) (about 100 µl per section) was added and slides incubated for 5 minutes, followed by rinsing in tap water for 5 minutes. The slides were counterstained by immersing in Mayer's haematoxylin (Sigma-Aldrich Ltd), for 5 minutes, rinsed under running water and then sequentially dehydrated through 70% ethanol (Sigma-Aldrich Ltd., Gillingham), 100% ethanol and histoclear for 10 minutes each, before being mounted with a coverslip using a drop of Omnimount mounting media (National Diagnostics). A bright field microscope was used to visualise the slides.

Agitated low temperature epitope retrieval (ALTER)

Slides were loaded in a rack and placed in a 1.5 litre glass beaker containing 100 mls of EDTA buffer Tween-20 pH8 and 900 ml distilled water. The beaker was covered with foil and placed on a hotplate stirrer (Jenway) 600 rpm at 65°C for 18 hours. The solution was then cooled by placing the beaker under running water for 5 minutes, followed by blocking and antibody incubation as described above.

2.4.2 Cytospins preparation for IHC/IF

Cultured cells were washed in serum-free Roswell Park Memorial Institute medium RPMI-1640 and re-suspended at a concentration of $2x10^6$ cells/ml in serum-free RPMI-1640 with 10% v/v formaldehyde (Sigma-Aldrich Ltd.). Cells were placed on X-tra positive charged Adhesive glass slides (Surgipath Europe) using the Cytospin cytocentrifuge (Shandon, Runcorn, Cytofunnel® disposable sample chambers, and filter cards and Cytoclips™ (ThermoFisher). 100µl of cultured cells (i.e. $2x10^5$ cells) were added to each sample chamber and centrifuged at 1000 rpm for 5 minutes. Cytospins were fixed in 10% neutral buffered formalin for 10 minutes, then rinsed in water, then left to air dry for 30 minutes and stored at -20°C. Before staining, slides were thawed and the endogenous peroxidase activity was blocked by immersing the slides for 10 minutes in 0.3% hydrogen peroxide (Sigma-Aldrich), following which slides were rinsed in running tap water, then subjected to IHC or IF. Cytospins from HL cell lines (L591, L428, L1236 and KMH2) were used in experiments performed in Chapter 5.

2.5 A20 syngeneic xenograft mouse model of DLBCL

A20 tumour cells were injected at 3 x 10^6 cells/mouse intravenously and subcutaneously into 6-9 week old female BALB/c mice (Charles River) (this experiment was performed by Tracey Perry, University of Birmingham) (Home office ethical approval, project no. PPL70_8280). At day 28, mice were killed by cervical dislocation and the lymphomas from spleen and subcutaneous tissue were collected in RPMI-1640, and were analysed by flow cytometry (performed by Tracey Perry, University of Birmingham). A portion of the tumour was preserved for FACS and the rest for embedding in paraffin after fixing in 10% neutral buffered formalin (Surgipath, Leica Microsystems, Milton Keynes). After a minimum of 24 hours, the tissues were embedded in paraffin wax. Paraffin sectioning and H&E staining were performed by the services at the ROH.

2.6 Immunofluorescence (IF)

2.6.1 Detection of antigen by singleplex/multiplex immunofluorescence (IF) using Opal staining method

Opal™ immunostaining, enables multi-labelling in-situ in formalin-fixed, paraffin-embedded (FFPE) tissue or cells using fluorescent dyes and primary antibodies raised in different species. The initial simple multi-labelling method using the tyramide signal amplification (TSA) as was described before **(Toth and Mezey, 2007)**.The newer Opal method uses labelling by fluorophores that bind in a covalent bond to the antigen. After labelling with the dye, removal of the marker by heating process will not affect the TSA signal. This facilitates next sequential binding of second or third antibody to be visualized and labelled and avoiding the issue of the overlapping (PerkinElmer Assay development guide booklet). The Opal kit by PerkinElmer was used according to manufacturer's protocol.

Opal Staining Protocol

Sections were immersed in Xylene 3x10 min, and re-hydrated by immersing the slides in 100%, 95% and 70% ethanol for 10 minutes each, followed by a 2 minute wash in distilled water and 5 minute wash with TBST wash. Incubation in 0.3% hydrogen peroxide as above for 15 minutes was done, and then slides washed again in distilled water for 5 minutes. Antigen retrieval was done using Citrate buffer as described above (Section 2.4), then washed with distilled water and reconditioned by TBST. For blocking, antibody diluent background reducing reagent (S3022, Dako) was used. The antibody was incubated overnight for 18 hours at 4°C or 1 hour at room temperature (Table 2.2 and Table 2.3). To optimise primary antibody as recommended by PerkinElmer Opal protocol (Figure 2.1 provided from PerkinElmer guide booklet), staining was performed initially using conventional IHC at several dilutions: the same dilution as used for IHC and the antibody was diluted 3 times and 5 times the dilution used in standard IHC, because this IF technique is considered to be more sensitive. After primary antibody incubation, slides were washed in TBST. Anti-rabbit/anti-mouse secondary universal antibody was applied to the sections for 30 minutes. Slides were rinsed with TBST 3x 5 minutes each. Signal amplification was carried out with various dyes from the Opal™ Fluorophore kit. Opal dyes were optimally diluted in amplification diluent (FP1135), (range dilution 1:50-1:200) and incubated on slides for 10 minutes. A second round of microwave treatment (MWT in Figure 2.1) with citrate buffer (pH 6) solution was performed for 15 minutes on low heat setting to strip the antigen-antibody complex. This allows for multiplexing of different targets on the same section. A second run of antibody incubations was performed as above starting from the blocking step after

MWT (step 4 in figure 2.1), using different fluorophores for different targets. Stripping was optimised by checking for co-localization of antibodies in the same section, where antibody was omitted. If cross-reactivity was visualized then stripping time was increased (30 minutes of heating in citrate buffer). Another method of avoiding the cross reactivity was changing in the order in which antibodies were applied. DAPI (ThermoFisher) at dilution of (1:1000) was added to sections and incubated for 5 minutes, followed by a wash in TBST for 5 minutes and slides mounted using Vectashield mounting media (H-1400, Vector laboratories). Cells were visualized using a Nikon E600 UV microscope. To account for autofluorescence, an unstained slide was used from the same tissue-type, prepared using the steps above but no antibody/ fluorophore was applied.

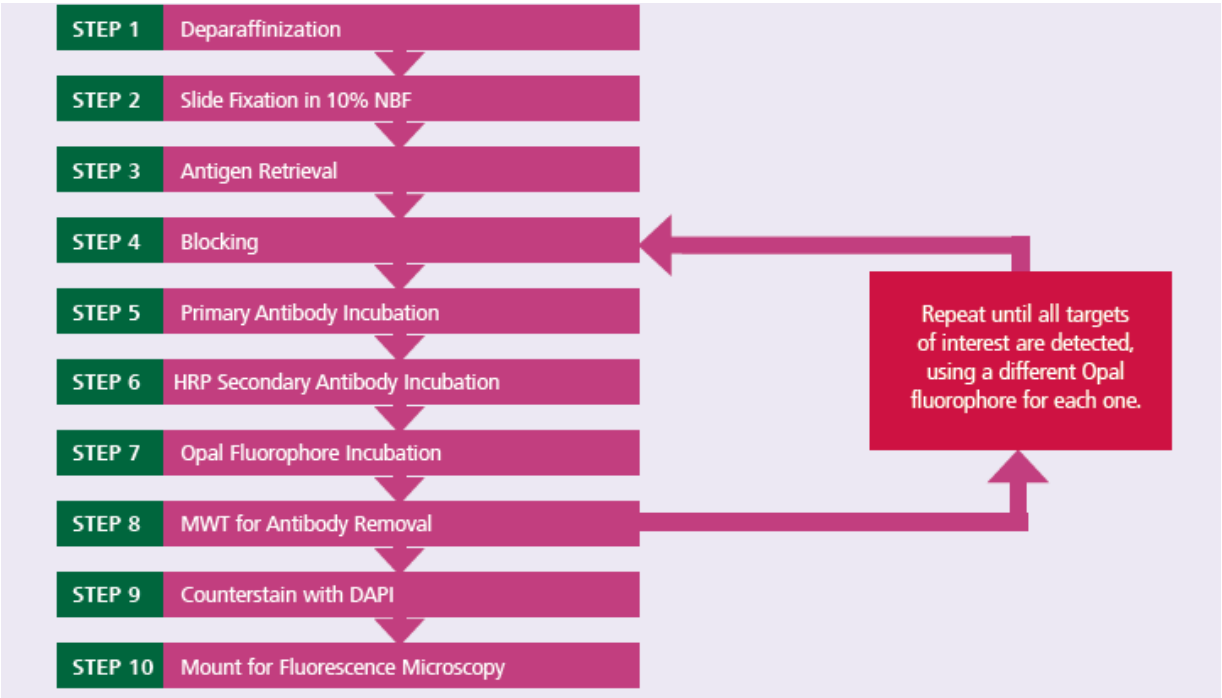

Figure 2.1 Multiplex IF protocol (Chart provided taken from PerkinElmer Assay development guide booklet).

Table 2.2. Reagents and kits used in IHC

Kit/Reagent	Vendor	Catalogue number	Conditions
Diaminobenzidine (DAB)	Vector laboratories	SK-4105	1:1000 substrate for 5 min
P-xylene-bis-pyridinium bromide (DPX)	Invitrogen	X1525	Ready to use
Casein	Vector laboratories	SP-5020	Diluted in 5x Distilled water
Mayer's hematoxylin	Sigma	MHS128-4L	5 min
PAP-PEN	Agilent Technologies	S200230-2	Ready to use
Rb anti-Sheep IgG (H+L) Secondary antibody	ThermoFisher	31480	1:100 for 30 minutes
RAT secondary antibody	Agilent Technologies	P0450	1:200 TBS for 10 min
Sodium citrate tribasic dihydrate ACS reagent	Sigma	S4641-1KG	Section 2.4
DAB	Agilent Technologies	K346711	Apply for 5 minutes
HRP secondary antibody	Vector laboratories labs	ImmPRESS™ Universal Antibody Kit Anti-Rabbit/Mouse Ig (MP-7500)	Ready to use
Ethylenediaminetetraacetic acid (EDTA)	REF 1C100X	(Binding Site., Birmingham, UK)	Section 2.4

Tables 2.3 Markers used in IHC and IF

Target protein	Vendor	Antibody Clone	Dilution IHC	Dilution IF
Lymphoid markers				
CD4	Leica	4B12	N/A	Automated Bond RX by (Chris Bagnall)
CD8	Leica	4B11	N/A	Automated Bond RX by (Chris Bagnall)
FOXP3	Abcam	Ab20034	N/A	Automated Bond RX by (Chris Bagnall)
CD3	Agilent Technologies	IR503	ready to use (tissue)	ready to use (tissue)
CD3	Leica	NCL-L-CD3-565	N/A (tissue)	Performed by Dr Alex Dowell
CD20	Agilent Technologies	IR604	ready to use (tissue)	ready to use (tissue)
CD20	Leica	L26	N/A	Automated Bond RX by (Chris Bagnall)
CD30	Agilent Technologies	Ber-H2	ready to use (tissue)	ready to use (tissue)
BCL6 (PG-B6p)	Agilent Technologies	GA625	ready to use (tissue)	ready to use (tissue)
EBV related markers				
LMP-1	Gift of Professor Martin Rowe	CS-1-4;	NA	1:100 (tissue) 1:80 (cytospins)

Collagen markers				
Collagen 4	Abcam	M0785 (Clone CIV 22)	N/A	1:200
Collagen 3	Abcam	ab7778	1:100 (tissue)	1:600 (tissue)
Collagen 6	LSBio	LS-B696	1:200 (tissue)	1:600 (tissue)
Collagen 1	Abcam	ab34710	1:400 (tissue)	N/A
Collagen 4	Abcam	ab21294 (M0785 Clone CIV 22)	1:200 (tissue)	1:400 (tissue)
Collagen receptors markers				
DDR-1	Cell Signaling	D1G6) XP®	1:80 (tissue)	1:250 (tissue)
LAIR-1	Sigma	HPA011155	1:200 (tissue)	1:600 (tissue) 1:400 (Cytospins)
LAIR-2	Abcam	ab183145, rabbit	1:50 (tissue)	1:100 (tissue)
C1Q	Agilent Technologies	F0254	N/A	1: 80 (tissue)

Neo-vascularization markers				
CD31	Agilent Technologies	IR610	1:50 (tissue)	1:100 (tissue)

Immune checkpoint markers				
PD-L1	Cell Signaling technology	(E1L3N) XP Rabbit monoclonal antibody	N/A	1:800 (tissue) (Performed by Dr Alex Dowell)
PD1	Abcam	N/AT105	N/A	1:200 (tissue) (Performed by Dr Alex Dowell)

Macrophages/monocytes markers				
CD163	Leica	NovocastraTM Lyophilized	1:100 (tissue)	1:600 (tissue)
MRC-1	Sigma	AMAB90746	1:200 (tissue)	1:600 (tissue)

CD68 (PG-M1)	Agilent Technologies	GA613	1:200 (tissue)	1:1200 (tissue)

Dendritic cell (DC) markers				
CD123 (BR4MS)	Leica	NCL-L-CD123	1:80 (tissue)	1:200 (tissue)
CD23 (DAK-CD23)	Agilent Technologies	GA781	1:200 (tissue)	1:400 (tissue)

Lipid related antibodies markers				
S1PR1 (H-60)	Santa Cruz	SC-25489	1:500 (tissue)	1:1200 (tissue) 1:600 (cytospins)
S1PR2	Sigma	HPA014307	1:200 (tissue)	1:200 (tissue) 1:80 (cytospins)

Tag antibodies				
HA tag (Y-11)	Santa Cruz	sc-805	N/A	1:100 (cytospins)
V5 tag (SV5-Pk1)	Abcam	SV5-Pk1 ab27671	N/A	1:200 (cytospins)

Miscellaneous				
C-MYC (Y69)	Abcam	ab23072	1:1000 (tissue)	1:2800 (cytospins)
Phospho-Akt (Ser473)	Cell Signaling	9271	N/A	1:100 (cytospins)
MHC class I (Anti-HLA Class 1 ABC) [EMR8-5]	Abcam	ab70328	Automated Bond RX by (Chris Bagnall)	NA
MHC class II (Anti-HLA DR + DP + DQ) [CR3/43]	Abcam	ab17101	Automated Bond RX by (Chris Bagnall)	NA
Ki-67	Abcam	ab6526	ready to use (tissue)	ready to use (tissue)

BATF3	R&D systems	AF7437	1:1200 (tissue) 1:400 (cytospins)	1:2200 (tissue) 1:800 (cytospins)

Table 2.4 Reagents and kits used in multi-labelling IF

Kit/Reagent	Vendor	Catalogue number	Conditions
OPAL 7-color Kit	PerkinElmer	NEL797001KT	Section 2.6
Opal™ 3-Plex Kit	PerkinElmer	NEL791001KT	Section 2.6
Antibody Diluent, Background Reducing	Agilent Technologies	S3022	ready to use applied for 10 minutes
VECTASHIELD hardSet Mounting Medium	Vector laboratories labs	H-1400	ready to use
Antigen Retrieval Citra Plus Solution	Biogenex	HK081-20K	10x, ready to use
Anti-rabbit IgG (goat)HRP Secondary antibody	PerkinElmer	NEF812001EA	1:200 in PBS 10 min
Anti-mouse IgG (Goat) HRP Secondary antibody	PerkinElmer	NEF822001EA	1:200 in PBS 10 min
DAPI	ThermoFisher	D21490	1:1000 in PBS 10 min

2.6.2 Automated IHC and multiplex staining

Automated IHC staining for MHC class I and II and multiplex labelling using the lymphocyte population panel was performed by Chris Bagnall, optimized in collaboration with Perkin Elmer using Leica Bond RX. IHC slides scanning was performed by Chris Bagnall at HBRC, University of Birmingham. Antibodies details used in those 2 panels are shown in Table 2.3.

2.6.3 Digital semi-automated quantitative scoring using Vectra scanner and Inform software

The multiplex immunofluorescence labelling was performed for the following reasons:

1. Simultaneous detection of multiple tissue biomarkers; confirm single cell co-expression for several biomarkers in one tissue section e.g. characterization of the functional status of immune cells e.g.exhausted dysfunctional T cells, expressing PD-1/PD-L1 (PD1-CD3/PD-L1-CD3 double positive cells)
2. Retain spatial cellular distribution, that can't be visualized by other multilabelling techniques such as flow cytometry. For example, identification of tumour cells versus microenvironment.
3. To obtain results for more markers when tissue is precious, and not enough sections remaining.
4. Allow quantitative analysis of protein levels in cell lines and tissues for defined phenotypes as well as cellular location (e.g nuclei, cytoplasm or membrane)

Recent studies have shown it is possible to multilabel up to 12 biomarkers in lymphoid and myeloid panels, which allowed visualization of 14 different immune

cell populations in-situ in a formalin-fixed paraffin-embedded tissue section. This enabled immunological classification of patients who responded according to high and low myeloid densities of immune cells, which enabled prediction of the response to neoadjuvant GVAX A GM-CSF tumour vaccine therapy used in pancreatic ductal adenocarcinoma. The immunosuppressive cluster was associated with inferior survival **(Tsujikawa et al., 2017)**.

2.6.3.1 Vectra Slide Scanning System

The Vectra imaging system provided by PerkinElmer is designed for scanning of tissues labelled with immunofluorescent markers. It is able to distinguish different fluorophores without overlap and discounts autoflourescence, facilitating the accurate quantification of each marker signal. Separation of all of the fluorescence signals within the sample is essential for quantitative measurement (PerkinElmer Assay development guide booklet). Vectra system version 3.0.3 software, provided by PerkinElmer in the HBRC, University of Birmingham was used for multispectral imaging. The scanning protocol was created as recommended by PerkinElmer using all filters available on the Olympus microscope. The multispectral camera is able to capture wavelengths between 420—720 nm, therefore the following fluorophores were used for staining: Cyanine 3, Cyanine 3.5, Cyanine 5, Cyanine 5.5, Flourescin, Texas red, Opal 520, Opal 540, Opal 570, Opal 620, Opal 650, Opal 670, Opal 690 and DAPI. Antibodies were optimized with recommended exposure time set between 100-150 milliseconds. The images were taken using an Olympus BX-51WI microscope using 10X, 20X and 40X magnifications which captured the multispectral images for further analysis using Inform image analysis software (PerkinElmer). Following whole slide scan, phenochart 1.0.4 (PerkinElmer) was used (Figure 2.1) for manual selection of representative areas of interest of the

tumour or tumour stroma or overlying epithelium. For tissue sections, at least 4 HPF (20x) and for cytospins, 3 HPF (20X) were used for quantification. Scanning of these fields using the high power protocol was applied on selected areas. Areas of crushing, necrosis, and haemorrhage were avoided.

2.6.3.2 Analysis by Inform software

Inform Tissue Finder (Version 2.2.0, PerkinElmer) is software that allows the analysis of multi-labelled image within different or same cellular compartment per single cell with a resultant intensity of the marker in every cellular compartment. The software is semi-automated, whereby it needs repeated steps of training and algorithm development, which allows easy usage of the same protocol on different tissue sections for phenotyping. The algorithm constitutes steps of training for different tissue regions such as tumour, stroma or vessels. This will give results of counts per phenotype in every anatomical location after tissue segmentation is performed. In addition, it allows spatial distribution for every phenotype to be provided. Moreover, the software is user-friendly for a pathologist to assess, who is used to bright-field evaluation, so the fluorescent image can be converted into pseudo-haematoxylin and brown staining mimicking DAB (Perkin Elmer assay development booklet guide). Multispectral images were acquired using Inform software which allowed spectral un-mixing of the image by selecting the specific fluorophores.

Training included creation of a new project and a new algorithm using a spectral library, selecting the reference controls for every fluorophore and use of autofluorescence slides for every tissue or cell line. The tissue segmentation step was used to classify different tissue regions within sections (e.g stroma, tumour and background). This segmentation was performed by the manual drawing tool which

is available in the software and which uses different coloured annotations to differentiate the tumour, the stroma and background (non-cellular areas/empty areas). Cell segmentation was done by adjusting cytoplasmic, membranous and nuclear compartment sizes. Following segmentation, cell phenotyping was done (Figure 2.2 and Figure 2.3). It is hard or sometimes impossible to differentiate overlapping markers in multispectral images. The available options of spectral un-mixing and assessment of every marker singly or coupled with any other marker stained, facilitated evaluation of the multiple stained proteins localized within the same cells. Positivity of markers were based on visual assessment of the author to the intensity scores. An illustration of a sample multi-labelled with PD-L1 (green), CD3 (red) and DAPI is shown Figure 2.4.

Training was performed on every batch using a maximum 8-9 total multispectral images, because variability in tumour areas within different tumours confused the software, and made training more difficult. After visual based morphological serial tissue classification, the software could easily differentiate tumour cells from stroma cells in NPC. In lymphoid malignancies (DLBCL), markers like CD20 were helpful in differentiating tumour cells from stromal cells/mature lymphocytes, DAPI was used to identify tumour cells as large nuclei, while stromal cells were either spindle or rounded if lymphocytes.

2.6.3.3 Exporting the data

Data output of the software included a separate file, for every field, with per-cell and per-cellular-compartment mean intensity and total intensity values for the entire cell and separately for the cytoplasm, membrane and nucleus. Tissue segmentation, cell segmentation, and phenotyping map were also included in the exported data.

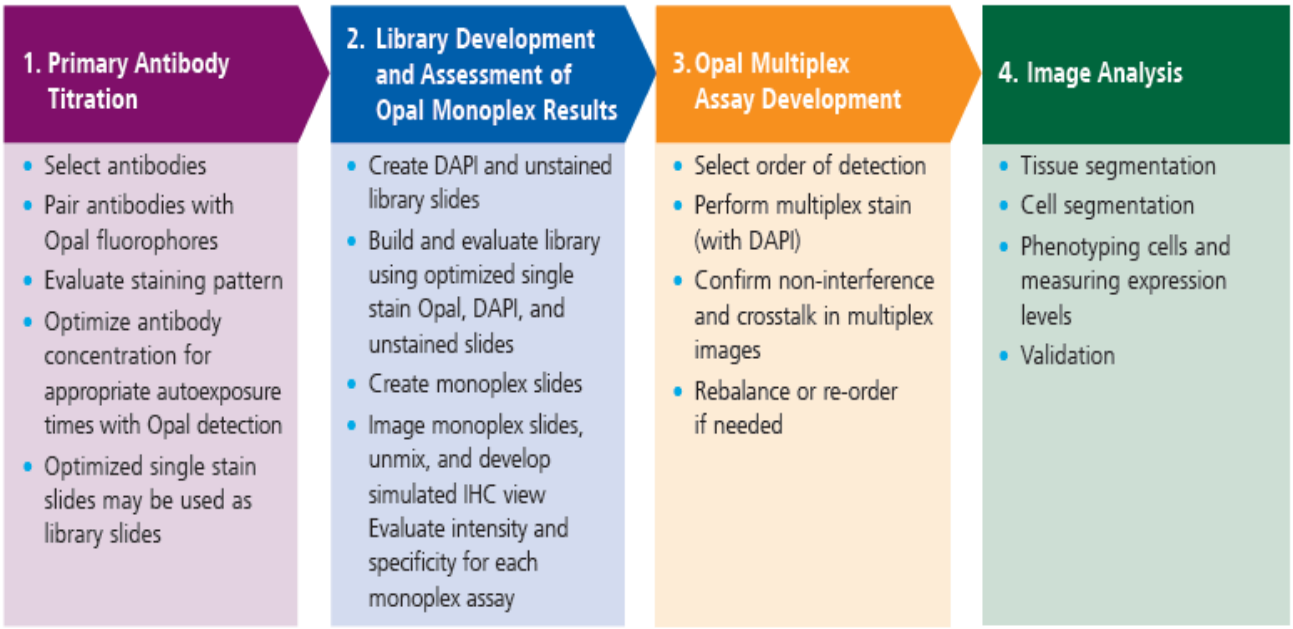

Figure 2.2 Multi-labelling using OPAL, Vectra system and Inform software (Chart provided in PerkinElmer Assay development guide booklet).

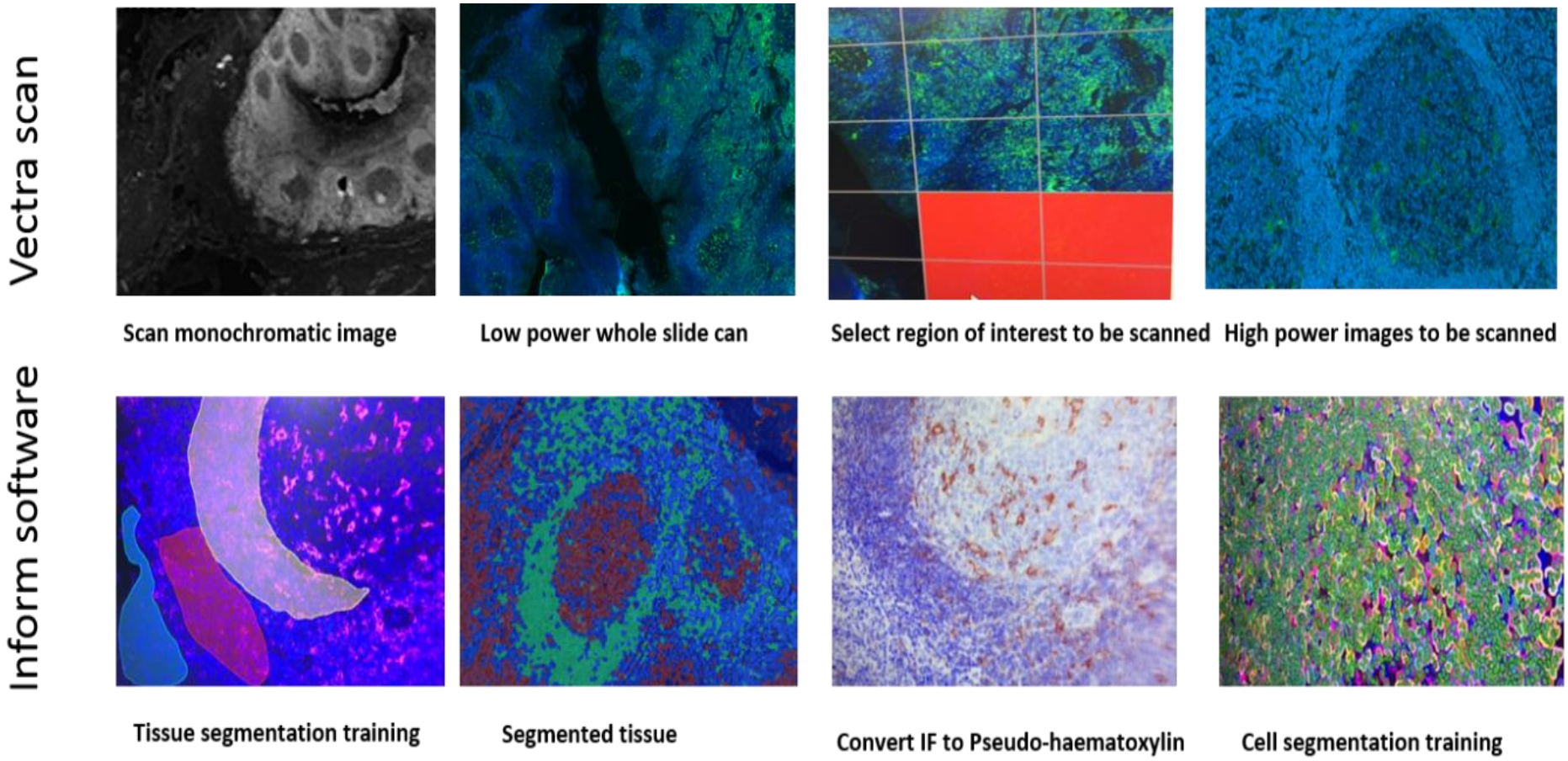

Figure 2.3 Steps of scanning using Vectra and image analysis using Inform software in an Opal stained section of tonsil (LAIR-1; green).

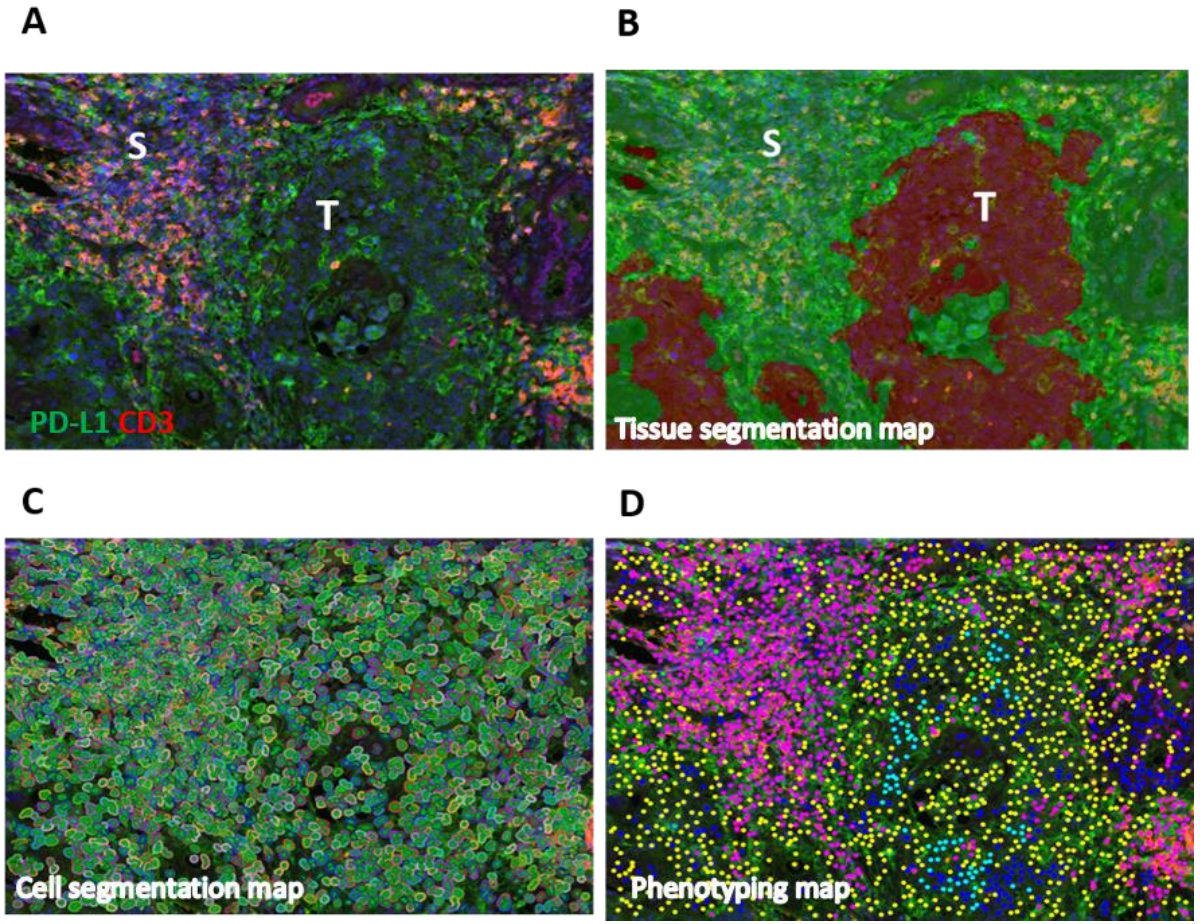

Figure 2.4 Steps of training for tissue/cell segmentation and scoring using tissue, cell segmentation and cell phenotyping

A) Tumour stained with PD-L1 (green) and CD3 (red), B) Tissue segmentation map with tumour (red) and stroma (green), C) Cell segmentation map with nuclear segmentation (green) and cellular segmentation (coloured), D) Phenotyping map, where PD-L1 positive phenotype is represented by green dots, negative cells were labelled as blue, yellow as double positive for PD-L1 and CD3, pink is CD3 single phenotype, (T) indicates tumour and (S) indicates stroma, 20X magnification.

2.6.3.4 Examples of cell phenotyping using Inform

BATF3-S1PR1-CD30 phenotyping in HL using Inform:

I classified tumours that were triple stained with BATF3-S1PR1-CD30.

The following phenotypes were measured:

1) S1PR1 single positive cells S1PR1 staining was identified in tumour cells, blood vessels and reactive lymphocytes.
2) BATF3 single positive cells
3) CD30 single positive cells.
4) S1PR1+ve-CD30+ve cells (but negative for BATF3).
5) BATF3+ve CD30+ve cells (but negative for S1PR1).
6) BATF3+ve-S1PR1+ve-CD30+ve cells.
7) BATF3-ve-S1PR1-ve-CD30-ve cells.

.**BATF3-S1PR1-PAKT phenotyping in HL cell lines**

I classified samples which were triple stained with BATF3-S1PR1-AKT in 4 HL cell lines (L591, L428, L1236 and KMH2) using Inform.

The following phenotypes were measured:

1) S1PR1 single positive cells.
2) BATF3 single positive cells
3) P-AKT single positive cells.
4) S1PR1+ve-P-AKT+ve cells (but negative for BATF3).
5) BATF3+ve P-AKT +ve cells (but negative for S1PR1).
6) BATF3+ve-S1PR1+ve-P-AKT+ve cells.
7) BATF3-ve-S1PR1-ve-P-AKT-ve cells.

Thresholds for these markers were subjective and based on morphological examination of the localisation of the stain and the intensity. The following markers

were considered to be specific if they were localized in the following subcellular localizations: BATF3 (nuclear), S1PR1 (membranous), AKT (membranous), and CD30 (membranous).These cells were screened for protein expression of BATF3, S1PR1, S1PR2, and pAKT by IHC once, in all HL cell lines experiments to validate expression performed by Q-PCR and western blot. *In vitro* studies including transfection and stimulation experiments of chapter 5 were performed by Dr Vrzalikova; University of Birmingham **(Vrzalikova et al., 2018)**.

Immune checkpoint T-cell panel phenotyping in NPC using Inform

NPC cases were stained with CD3/cy3, PD1/FITC, PD-L1/cy5. Whole slide scanning of the cases was carried out using the Vectra, 5 HPF (20X) were selected using phenochart 2.0.4. Areas that contained tumour and stroma areas were selected.

The following phenotypes were measured:

1) PD-L1 single positive cells.
2) CD3 single positive cells.
3) PD1 single positive cells
4) PD-L1+ve-CD3+ve cells.
5) CD3-ve-PD-L1-ve-PD1-ve cells.

The following markers were considered to be specific if they were localized in the following subcellular localizations: CD3 (membranous), PD-L1 (membranous +/- cytoplasmic) and PD1 (membranous). This scoring was done in the tumour and stroma compartments. After analysis, threshold used for considering PD-L1 as positive was equal or more than 5% as clinically used in malignant melanoma and others. The threshold for PD1 positivity was if >5% of TILs were positive, as described by Zhou et al **(Zhou et al., 2017b)**. An example of the phenotyping map and various phenotypes for immune checkpoint T-cell panel is shown in Figure 2.1.

2.7 Semi quantitative scoring

Semi-quantitative scoring in HL, DLBCL and NPC will is described below.

Semi-quantitative scoring for BATF3 and S1PR1 HL

The threshold to score S1PR1 as tumour positive was previously described by Kluk et al **(Kluk et al., 2013)**, whereby a case was considered positive if S1PR1 was present in ⩾25% of tumour cells. For consistency, I applied the same cut-off when assessing the expression of BATF3 and all other S1P receptors (S1PR1 and S1PR2) markers.

Semi-quantitative scoring of MHC class I and class II in NPC

Whole slide scanning of the 19 NPC cases stained for MHC class I and MHC class II was carried out using the digital scanner, HBRC SCN400 Leica, by Chris Bagnall. The slides were analysed digitally with the whole section screened at low power (10X) and high power (60X). First the presence of overlying epithelium was evaluated, and if present, was evaluated for atypia. Staining was evaluated in the epithelium, using H-score, for MHC class I. The epithelium should be positive, so this was used as an internal positive control. Immunostaining was considered positive for MHC class I or MHC class II if it was membranous +/- cytoplasmic. For MHC class I and II lymphocytes were used as positive internal controls. For evaluating tumour downregulation, of MHC class I or MHC class II, comparison with the lymphocytes was used. H-score was calculated for each case using the following formula: [% of cells with intensity 0 x 0] + [% of cells with intensity 1 x 1] + [% of cells with intensity 2 x 2] + [% of cells with intensity 3 x 3] **(McCarty et al., 1985)**. Intensity of markers were classified into weak (+), moderate (++) or strong (+++). Intensity scores were subjective and were based on comparison with the positive internal control intensity, for example MHC class II intensity was compared with

lymphocytes, which were consistently positive with strong intensity (Figure 2.5). Scoring by the author was revised in 8 out of 19 random cases of immuno-stained MHC class I and class II by second senior pathologist; Dr Abeer Shaaban (Queen Elizabeth hospital, University of Birmingham). Disagreement in scoring of 2 cases were mentioned, these were re-evaluated.

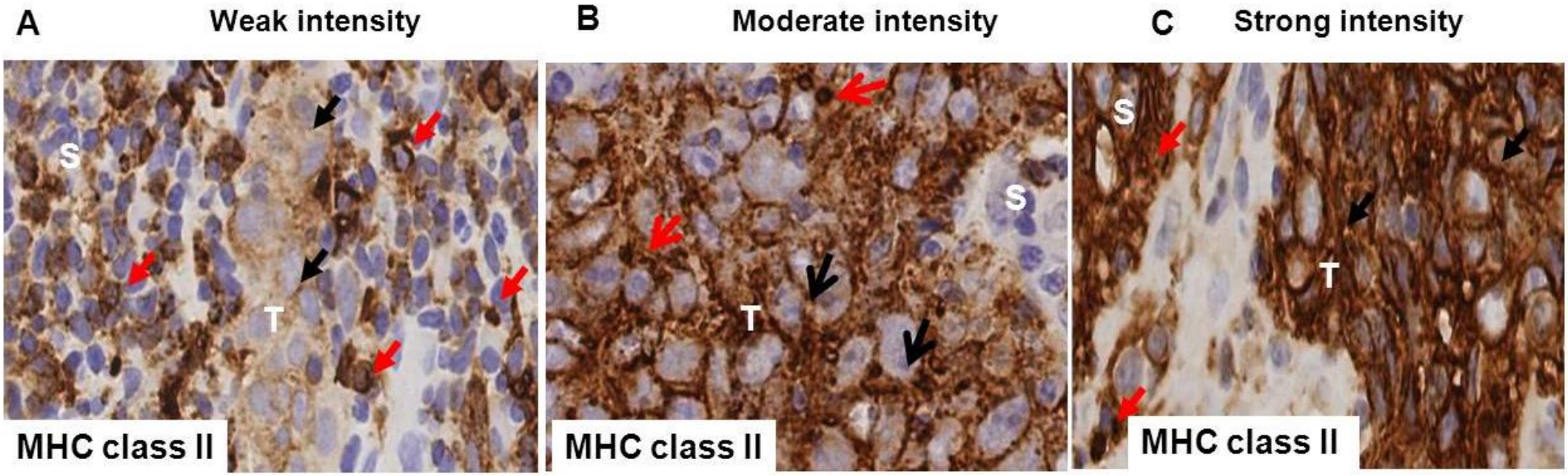

Figure 2.5 Illustration of different intensity of IHC MHC class II in NPC
Tumour cells are stained to MHC Class II (white arrows), displaying weak A), moderate B) and strong C) intensity, while adjacent lymphocytes strong intensity of staining served a positive internal control, (red arrows).

2.8 Digital quantification using Image J software

Image J software (NIH) was used to analyse 6 DLBCL samples. Image J was used to count the morphologically identifiable tumour cells (by haematoxylin) in direct or in close contact with the collagen-positive stromal fibres of stained cells in 10 HPF of tumour (40X) for each case. An average was taken for analysis. Non-viable tumour cells were excluded.

2.9 Statistical analysis

Student's t test was used to determine statistical significance in parametric data, using two tailed t-test. Mann–Whitney U test was used to determine statistical significance in non-parametric data. Comparisons of proportions of phenotypes quantified by H-score or using Inform were done using the Chi-squared test. When plotting markers for correlation, Pearson rank test was used. For correlation matrix analyses (performed by Dr Graham Taylor) of histopathological scoring performed by the author, Spearman's rank test was used. A p-value of < 0.05 was considered to be statistically significant. Statistical analysis of data was performed using Microsoft Excel 2007 and GraphPad Prism 7 software.

2.10 Re-analysis of published gene expression data

The re-analysis of the raw data (published and unpublished) of microarrays and RNA-seq data was performed by Dr Wenbin Wei and Dr Robert Hollows at the University of Birmingham. Microarray data (lymphoma and NPC), were downloaded from the Gene Expression Omnibus website (GEO) website. Probe-level quantile normalization plus robust multi-array (RMA) average normalization of raw CEL files was performed, using the affy package in R. Differential expression analysis was performed using the Limma package in R. Differential expression criteria used was of absolute fold change 1.5 and p value<0.05 were used.

Dr Reuben Tooze, provided data from the meta-analysis of eleven different DLBCL gene expression datasets including more than 2000 cases of whole tumour primary DLBCL microarrays which was published **(Care et al., 2015)** and the analysis was performed in collaboration with the University of Leeds, pathology department. **(Care et al., 2015)**. The resultant p values and correlations for each gene from all datasets were merged by taking the median values. The author used the genes identified in this analysis that were either positively or negatively correlated with LAIR1 and examined the overlap with all known collagen genes or collagen receptor genes, or a published macrophage gene expression signature **(Doig et al., 2013)**. The author tested the significance of the overlap using Chi square test.

RNA-seq data from **(Morin et al., 2011, Béguelin et al., 2013)** were downloaded from the GEO website (GSE45982, GSM1129344, GSM1129345, GSM1129346 and GSM1129347) for DLBCL samples and GC B cells were aligned to the hg19 human genome using Rsubread aligner **(Liao et al., 2013)** and assigned to individual genes using the feature Counts function. Read counts were then normalized between samples and converted to counts-per-million reads for each gene using the edge R package **(Robinson et al., 2010)**. For RNA-seq analysis, only genes which had counts-per-million of greater than 1 in at least four samples were considered.

The author performed all the enrichment analysis and statistical tests such as chi square in results chapter 3, 4 and 5. To investigate the biological functions of genes of interest from the microarray/RNA-seq analysis, 6.7 DAVID ontology tool (http://david.abcc.ncifcrf.gov/home.jsp) was used. For this gene lists were submitted using human NCBI reference identifier **(Dennis et al., 2003)**.

Heat maps of NPC biomarker data were prepared by Dr Robert Hollows using the gplots package in R. Hierarchical clustering for the heat maps used average linkage between samples/markers, based on 1 – correlation as the distance measure. All markers including PD-L1, PD1, MHC class I, MHC class II, CD3, CD8 and FOXP3 were scored on a scale from 0 to 100.

2.11 Details of individual datasets

Lymphoma data from Brune dataset **(Brune et al., 2008)**

Microarray data were downloaded from GEO (GSE12453) for 11 DLBCL samples, 5 NLPHL samples, 4 T cell rich B cell lymphoma (TCRBL) samples, 5 FL samples and 5 Burkitt's lymphoma (BL). In addition, 4 HL samples were downloaded from GSE14829. Tumour samples were compared with normal/control; 5 samples, also downloaded from GSE12450. Each of B cell subsets from tonsil GC B cells (centrocytes and centroblasts), plasma cells and from the peripheral blood (naïve B cells and memory cells) were used as a control for differential expression analysis. I used GC B cells (centrocytes and centroblasts) control samples in the differential gene expression analysis.

Lymphoma data from Morin dataset **(Morin et al., 2011)**

Data were downloaded from NIH database of genotypes and phenotypes (dbGap;http://www.ncbi.nlm.nih.gov/gap) accession code: phs000532-v5.p2 and comprised of RNA-seq of total 104 DLBCL cases: 32 ABC DLBCL (3 EBV positive), 54 GCB and 18 others DLBCL (1 EBV positive). Control samples were 4 tonsillar GC B cell (centroblasts and centrocytes) samples B**é**guelin et al, by **(Béguelin et al., 2013)**, separately downloaded from the GEO at http://www.ncbi.nlm.nih.gov/geo/) (accession GSE45982), they included GSM1129344, GSM1129345, GSM1129346 and GSM1129347. I used in the analysis a total of 86 cases of GCB and ABC-DLBCL and four controls.

***Lymphoma data from Steidl dataset* (Steidl et al., 2012)**

Microarray data were downloaded from GEO (GSE39133) **(Steidl et al., 2012)** for 29 micro-dissected HL and 5 micro-dissected GCB control samples, with known EBV status in subset of the samples.

***NPC RNA-seq data from Dong H dataset* (Dong H, 2016)**

RNA-seq data of whole NPC identified by **(Dong H, 2016)** were downloaded from GEO (GSE68799) and included 42 EBV (LMP-1) positive Chinese NPC and 4 control samples formed of non-neoplastic nasopharyngeal tissue (1 control was LMP-1 positive and the remaining 3 LMP-1 controls were negative). Differentially expressed genes were identified using edge R with $p < 0.001$ and read CPM >1 in at least half of the samples. Data is available at NCBI website: https://www.ncbi.nlm.nih.gov/geo/query/acc.cgi?acc=GSE68799

***Micro-dissected NPC microarray data from Hsu dataset* (Hsu et al., 2012)**

NPC microarray dataset GSE12452 included gene expression from 31 NPC and 10 micro-dissected controls; non-neoplastic nasopharynx. Criteria used to identify differentially expressed genes. Fold change and p value as previously mentioned.

***Whole NPC tumour microarray data from Bose dataset* (Bose et al., 2009)**

NPC microarray dataset GSE13597 included 32 NPC samples of whole tumour sections, with undifferentiated nasopharyngeal carcinoma histology. Genes differentially expressed between LMP-1 positive and LMP-1 negative NPC were evaluated in this array using, LMP-1 status and levels were determined using Q-PCR, fluidigm and IHC. Controls were three samples of non-malignant nasopharyngeal tissue.

2.12 Cell culture

2.12.1 Monocytes Isolation of monocytes from PBMCs using Miltenyl CD14+ magnetic beads

Human PBMCs were isolated from leukocyte buffy coats from healthy donors. A total of 20 mls of whole blood were provided in each cone from one donor. Blood was added to serum free RPMI1640 and layered on the top of Lymphoprep (Axis-Shield) and subjected to density gradient centrifugation 1400 RPM for 30 min. The buffy layer of white blood cells was then washed and suspended in sterile MACs buffer (Miltenyi Biotech).

2.12.2 Cell culture counting

Cell density was calculated using a Neubauer haemocytometer (Marienfeld,Harsewinkel). Dead cells were identified by Trypan Blue (Sigma-Aldrich Ltd., Gillingham) and excluded from counting. Live cells were counted using an Olympus CK30 inverted light microscope in four regions, and then an average of the total number was calculated. This number was then multiplied by 10^4 and the dilution factor of the Trypan Blue to get the number of cells per ml of culture.

2.12.3 CD14+ cells isolation from PBMCs

Isolation of human CD14+ monocytes was performed using Miltenyi magnetic bead separation kit according to manufacturer's protocol. Resulting CD14+ monocytes were checked for purity by flow cytometry staining using CD14-FITC (ThermoFisher) before proceeding to differentiation process with the assistance of Tracey Perry (University of Birmingham).

2.12.4 Polarisation of monocytes into M1 and M2 subtypes

Polarization of monocytes to M1 and M2 macrophages with Granulocyte-macrophage colony stimulating factor (G-MCSF) and Macrophage colony-stimulating factor (M-CSF) was performed. The buffy coat layer of leukocytes was collected and placed into a fresh 50 ml conical tube. CD14+ monocytes were plated in RPMI-1640+10% FBS+1% glutamax (Invitrogen) for M0, and with the addition of 5ng/ml of G-MCSF (Peprotech) for M1 or 25ng/ml of M-CSF (Peprotech) for M2. After 10 days of differentiation, attached cells were collected and washed with sterile PBS, then re-suspended in density $2x10^6$ cells/ml in complete medium.

2.12.5 Collagen stimulation pre-differentiation

Collagen type I at concentration 10 microgrammes/ml, prepared fresh in cold sterile PBS was used for coating plastic 6-well tissue-culture plates. 1-2 mls of diluted collagen solution per well was used. The plates were incubated at 4 °C for 2 hours, then collagen was removed by washing carefully with 2mls of PBS. Monocytes were cultured on 6-well plates at a density of 1 $x10^6$ /ml, together with either collagen, vehicle (acetic acid) or left untreated as a control.

2.12.6 Collagen stimulation post-differentiation

Soluble collagen was added directly to cells using 100ug/ml soluble type I collagen (Millipore), vehicle (acetic acid) and PBS for untreated cells, for 30 minutes, 1, 2, 4, 24, 48, and 72h. After these time points, cells were harvested, stained and analysed by flow cytometry for LAIR-1 and macrophage markers (Table 2.5).

2.12.7 Preparation of Human acute monocytic leukaemia cells

Human acute monocytic leukaemia (THP-1) cell line, provided by Dr Carmela De Santo, University of Birmingham was cultured in RPMI 1640 (Gibco, Life Technologies Ltd) supplemented with 10% v/v FBS (Sigma), 1 mM pyruvate (Gibco) and 1% penicillin-streptomycin (Sigma-Aldrich).

2.12.8 Maintenance of monocytes/macrophages and THP1 in culture

Cells were incubated at 37°C in a humidified atmosphere rich in 5% carbon dioxide (Galaxy R CO_2 Incubator; RS Biotech). Cell viability and counting was evaluated with an inverted microscope. THP-1 cells were passaged to prevent overgrowth.

2.12.9 Flow cytometry staining with flurophore-conjugated antibodies

After harvesting the monocytes or macrophages, the expression of different markers was evaluated by staining with 3µl of each of the following antibodies: LAIR-1, CD163 and CD14 (Table 2.5). A minimum of $1x10^6$ cells were used for each panel of antibodies. For THP-1 cells before staining, frozen cells were thawed to 37°C and diluted in 10 ml of cold PBS or DMEM with 10% FCS, followed by centrifugation of cells at 1,100 RPM for 10 minutes. The cells were washed once more and finally re-suspended in 1ml of PBS or DMEM with 10% FCS.

Table 2.5 Summary of the antibodies used for FACS analysis

Antibody	Species	Clone	Company	Fluorophore	Catalogue number
CD14	Human	61D3	ebioscience	FITC	11-0149-42
CD163	Human	GH/61	ebioscience	APC	17-1639-41
LAIR-1	Human	342219	R&D	PE	FAB2664P

2.12.10 FACS analysis

In vitro polarised macrophages were stained with panel of fluorescently conjugated antibodies. Cells with high side scatter and low forward scatter were excluded from analysis. Gated population was then analysed for CD14 expression. The CD14+ve cells were then further analysed for M1 and M2 phenotypes. M1 phenotype was defined CD163-ve/+ve ^{low}. M2 phenotype was defined CD163+ve. Then LAIR-1 expression was assessed in the M1 and M2 populations. Flow cytometry analysis was performed under the supervision of Tracey Perry, University of Birmingham.

CHAPTER THREE

CHARACTERISATION OF THE IMMUNE-MICROENVIRONMENT AND MHC EXPRESSION IN NASOPHARYNGEAL CARCINOMA

3.1 INTRODUCTION

Nasopharyngeal carcinoma (NPC) is a tumour which arises in the lining of the nasopharyngeal epithelium and which is particularly prevalent in South East Asia. NPC is driven by a persistent Epstein-Barr virus (EBV) infection of target cells following exposure to environmental carcinogens in salted fish and cigarette smoke. Most NPC cases present at a late stage **(Omar et al., 2006)** and survival is poor; current treatments for advanced disease are limited to concurrent chemo-radiotherapy and are associated with significant morbidity and poor quality of life **(Busson, 2013)**. Therefore, innovation in the therapeutic approach is required, not only to improve cure rates, but also to de-intensify conventional treatments and reduce long-term toxicities.

PD-L1, an immune checkpoint molecule, is expressed in 89-95% of NPC **(Chen et al., 2013)**. A role for PD-L1 and its receptor, PD1 in NPC was shown by clinical trials with clinical responses as reduction in tumour size in a proportion of NPC patients receiving the humanized monoclonal antibody, pembrolizumab, which blocks PD1 **(Hsu et al., 2015)**. NPC patients over-expressing PD-L1 measured by IHC have inferior outcomes in contrast to patients with lower IHC expression scores **(Zhang et al., 2015, Fang et al., 2014, Zhou et al., 2017b)**. In contrast, one report describes a positive correlation between PD-L1 expression by IHC and survival in patients with non-metastatic NPC **(Lee et al., 2016)**.

The molecular mechanisms which underpin the frequent expression of PD-L1 in NPC are unclear. One possibility is that PD-L1 overexpression occurs in response to inflammatory cytokines released by infiltrating anti-tumour lymphocytes **(Fang et al., 2014)**. This mechanism of tumour escape from immune-cell mediated response

is called adaptive immune resistance, and may indicate a possible mechanism to target by PD1 blockade.

Intrinsic immune resistance is an alternate scenario, whereby PD-L1 is constitutively expressed because of underlying dysregulated signalling pathways in the tumour cell or possibly by genetic mechanisms such as amplification; expression in such cases does not indicate the presence of an active immune response (inducible type) **(Taube et al., 2012)**. However, another recent study has shown that both these mechanisms are not necessarily mutually exclusive, whereby PD-L1 can be secondarily expressed due to a superimposed Interferon-gamma (INF-γ) effect overlapping an existing constitutive mechanism **(Topalian et al., 2016)**. In order to develop the necessary immunotherapeutic agents for NPC patients, it is important to know if PDL-1 overexpression is of the constitutive or inducible type.

Recent reports indicate that EBV-LMP-1 could also regulate PD-L1 expression. Thus, EBV negative NPC cell lines transfected with LMP-1 show elevated levels of PD-L1 expression when treated with INF-γ, however in this study IFN-γ alone was able to independently increase PD-L1 expression in NPC cell lines. In EBV positive NPC, LMP-1 up-regulates not only PI3-K, but also AP-1, STAT3 and NF-κB pathways, and this is proposed to sustain the over-expression of PD-L1 **(Chen et al., 2013, Fang et al., 2014)**. In addition, NPC was reported to show decreased or loss of expression of MHC class I, which could contribute to tumour escape of NPC cells **(Sengupta et al., 2006, Kouvidou et al., 1995, Yao et al., 2000)**. Microarray analysis of micro-dissected NPC has shown that the downregulation of MHC class I was associated with EBV gene expression **(Sengupta et al., 2006)**. Other studies show alterations at the protein level of MHC class I. Thus, beta-2 microglobulin (B2M) expression was reduced or absent in

18/37 NPC cases **(Kouvidou et al., 1995)**. As B2M is essential for the formation of MHC class I molecules **(Springer, 2015)**, this suggests impairment in antigen processing and presentation functions in NPC.

Unexpectedly, MHC class II has been reported to be upregulated in NPC **(Busson et al., 1988)**. MHC-DR is up-regulated in 55% of NPC cases **(Li et al., 2007)**.and in some cases MHC class II may be expressed more frequently in the tumour compared with the tumour stroma **(Yao et al., 2000)**. Not all NPC cases express MHC class II, however, with lower levels observed in 37% of samples analysed; some of these cases also had decreased MHC class I expression **(Yao et al., 2000)**.

To summarize, the presence of significant variability in the heterogeneous microenvironment of NPC, with its distinctive exuberant lymphocytic infiltration, suggests that use of targeted therapy against immunomodulatory functions might be beneficial. I focussed on the PDL-1/PD1 pathway in this chapter because this is the only checkpoint (apart from the combination with anti-CTLA4 drugs) which has so far been investigated clinically in NPC patients. The aim of this chapter is to comprehensively characterize the immune microenvironment of EBV-associated NPC and to study the potential role of LMP-1. In turn, this knowledge might help to refine therapies against immune checkpoints for patients with this disease.

3.2 RESULTS

3.2.1 PD-L1 is an immune signature gene that is up-regulated in NPC tumour cells compared to normal nasopharyngeal epithelium

In the first series of analyses I wanted to compare the global expression of immune-related genes in NPC tumour cells with that in normal tissues. The initial premise being to confirm the over-expression of PD-L1 in these tumours. To do this I made use of the following three datasets:

- Dataset (1) a published microarray study; GSE12452 **(Hsu et al., 2012)** that had described gene expression in micro-dissected NPC tumour cells and in non-neoplastic/normal nasopharyngeal epithelium and which were re-analysed by Drs Wei and Hollows **(Hsu et al., 2012)**.
- Dataset (2) a comprehensive list of immune checkpoint genes (ICP) compiled by Grace Mitchell in our laboratory (Appendix 2).
- Dataset (3) a list of extended immune signature genes termed the Co-ordinate Immune Response Cluster (CIRC) by Lal et al comprising a 61 gene cluster of inhibitory molecules which influences the immune infiltration **(Lal et al., 2015)** (Appendix 3).

Figure 3.1 and Tables 3.1 and 3.2 show that there was no significant enrichment or depletion of ICP signature genes (Dataset 2) among those genes either up- or down-regulated in micro-dissected NPC compared to normal nasopharyngeal epithelium. However, Figure 3.2 and Tables 3.3 and 3.4 show that CIRC genes (Dataset 3) were significantly enriched among those genes up-regulated in NPC and depleted among those genes down-regulated in NPC. Genes up-regulated in NPC and present in both ICP and CIRC signatures were TNFSF4, ICOS, PD-L1 and CTLA4.

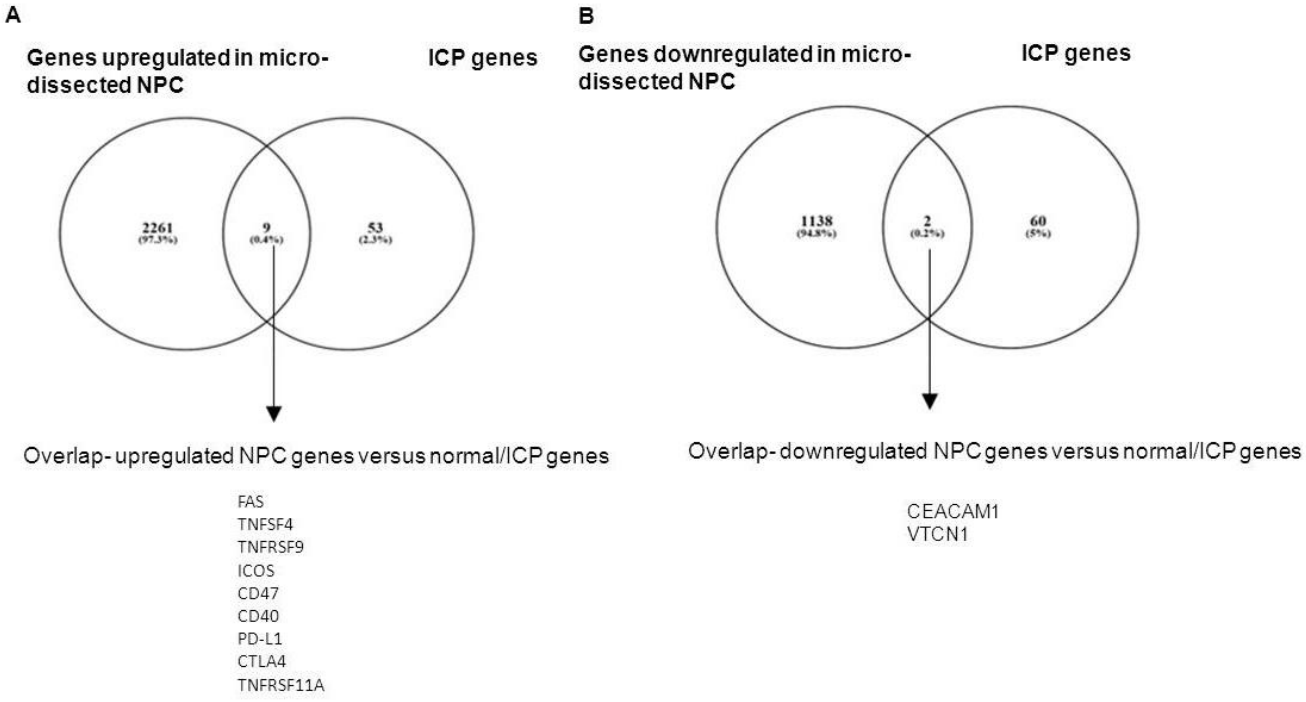

Figure 3.1 PD-L1 is among the ICP genes upregulated in micro-dissected NPC tumour cells compared to the normal nasopharyngeal tissue
A and B; Venn diagrams show the overlap between ICP genes and those either up- or down-regulated in NPC compared to normal nasopharyngeal epithelium.

Table 3.1: Number of genes upregulated and downregulated in micro-dissected NPC versus normal epithelium and present in the immune checkpoint signature

Genes of the arrays	Total number	Number of genes used in the enrichment analysis (present on both Immune checkpoint related genes and NPC array=20219)
Immune checkpoint genes	65	62
Upregulated genes in micro-dissected NPC versus normal epithelium	2270	2270
Downregulated genes micro-dissected NPC versus normal epithelium	1140	1140

Table 3.2: Chi-squared test of the overlap between genes differentially expressed in micro-dissected NPC versus normal epithelium and ICP genes

Genes of the array	Observed (0)	Expected (E)	0-E	Chi square	Odds Ratio	p-value
Immune checkpoint genes and upregulated genes in micro-dissected NPC versus normal epithelium	9	6.960435213	2.0392205	0.597407	1.343395	0.4396
Immune checkpoint genes and genes downregulated in micro-dissected NPC versus normal epithelium	2	3.495721846	-1.4957218	0.639978	0.55703	0.4237

Tables 3.1 and 3.2 summarises the results of statistical test performed for these analyses.

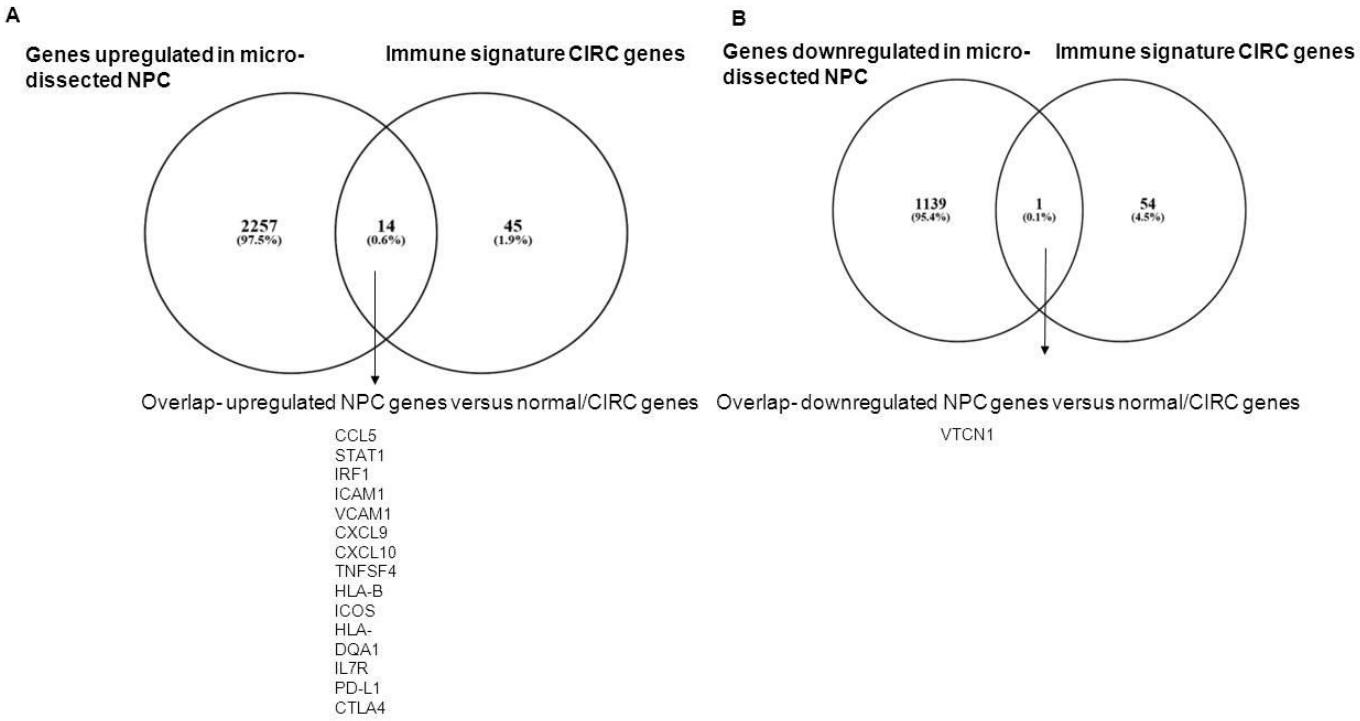

Figure 3.2 PD-L1 is among the CIRC genes upregulated in micro-dissected NPC tumour cells compared to the normal nasopharyngeal tissue
A and B Venn diagrams show the overlap between CIRC genes and those either up- or down-regulated in NPC compared to normal nasopharyngeal epithelium.

Table 3.3: Number of genes upregulated and downregulated in micro-dissected NPC versus normal epithelium and present in CIRC signature

Genes of the arrays	Total number	Number of genes used in the enrichment analysis (present on Immune signature CIRC genes and NPC array=20219)
Immune signature CIRC	59	55
Upregulated genes in micro-dissected NPC versus normal epithelium	2270	2270
Downregulated genes micro-dissected NPC versus normal epithelium	1140	1140

Table 3.4: Chi-squared test of the overlap between genes differentially expressed in micro-dissected NPC versus normal epithelium and present in CIRC genes

Genes of the arrays	Observed (0)	Expected (E)	0-E	Chi square	Odds Ratio	P-value
Immune signature CIRC genes and upregulated genes in micro-dissected NPC versus normal epithelium	14	6.174885009	7.825115	9.916367	2.708398	0.0016
Immune signature CIRC genes and genes downregulated in micro-dissected NPC versus normal epithelium	1	3.101043573	-2.1010436	1.423516	0.309303	0.2328

Tables 3.3 and 3.4 summarises the results of statistical test performed for these analyses

3.2.2 PD-L1 expression and LMP-1 status in NPC

Having confirmed the over-expression of several immune inhibitory molecules, including PD-L1 in NPC, and because it was previously reported that LMP-1 can up-regulate PD-L1 in NPC cell lines **(Fang et al., 2014)**, I next wanted to determine if the expression of these genes varied by LMP-1 status. LMP-1 status was known for 42 tumours reported in the re-analysis of micro-dissected NPC described above; (GSE68799) by Dong H **(Dong H, 2016)** (Dataset 5). Only two ICP genes, CD276 and GZMB, were up-regulated in LMP-1-positive NPC versus LMP-1-negative NPC, and no ICP genes were down-regulated in LMP-1-positive compared with LMP1-negative micro-dissected NPC (Figure 3.3, Tables 3.5 and 3.6). Only 5 CIRC genes, CCL5, CD276, CXCL9, CXCL10 and GZMB were upregulated in LMP-1-positive compared with LMP-1-negative micro-dissected NPC (Figure 3.4, Tables 3.7 and 3.8). These data suggest that other factors, possibly cellular in origin, might up-regulate PD-L1 when LMP-1 is not expressed. These data are also consistent with a recent study that showed that PD-L1 IHC expression scores in patient samples were not correlated with the EBV DNA load **(Zhou et al., 2017b)**. To further study if LMP-1 status had any impact on expression of ICP genes and CIRC genes, I took advantage of a further dataset; GSE13597, by Bose et al **(Bose et al., 2009)** (re-analysed by Drs Wei and Hollows), referred to here as Dataset (4), a microarray analysis that had compared gene expression in whole NPC tissues (i.e. including non-tumour components) versus that in whole normal nasopharyngeal tissue **(Bose et al., 2009)**. Analysis of ICP genes in Dataset 4 **(Bose et al., 2009)** is shown in Figure 3.5 and Tables 3.9 and 3.10 and revealed only the up-regulation of ICOS (Inducible T-Cell Costimulator) (among ICP genes) in LMP-1-positive versus LMP-1-negative whole NPC. Analysis of the CIRC genes revealed the upregulation of

HLA-DPB1, ICAM1, HLA-DOB, IL7R, ICOS and HLA-DPA1 (Figure 3.6 and Tables 3.11 and 3.12).

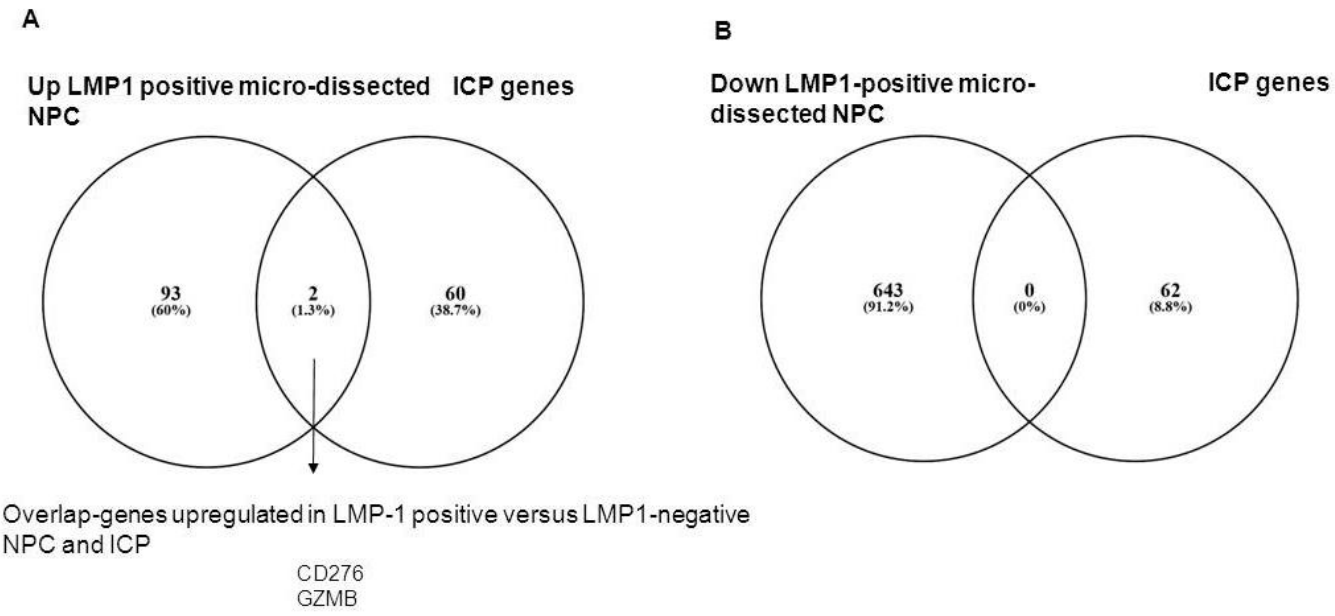

Figure 3.3 PD-L1 is not present among genes up-regulated in LMP-1-positive micro-dissected compared to LMP-1-negative micro-dissected NPC and ICP genes, Venn diagrams show the overlap between ICP genes and those genes either up- or down-regulated in LMP-1-positive vs LMP-1-negative micro-dissected NPC.

Table 3.5: Number of genes upregulated and downregulated in LMP-1 positive micro-dissected NPC versus LMP-1-negative micro-dissected NPC and present in ICP signature

Genes of the arrays	Total number	Number of genes used in the enrichment analysis (present on both Immune checkpoint related genes and NPC array=20219)
Immune checkpoint related genes	65	62
Upregulated genes in LMP-1 positive versus LMP-1 negative micro-dissected NPC	96	95
Downregulated genes in LMP-1 positive versus LMP-1 negative micro-dissected NPC	643	643

Table 3.6: Chi-squared test of the overlap between genes upregulated and downregulated in LMP-1 positive micro-dissected NPC versus LMP1-negative micro-dissected NPC and present in ICP signature

Genes of the arrays	Observed (0)	Expected (E)	0-E	Chi square	Odds Ratio	P-value
Immune checkpoint genes and genes upregulated in LMP-1 positive versus LMP-1 negative micro-dissected NPC	2	0.291295747	1.7087043	10.02304	7.191039	0.0015
Immune checkpoint genes and genes downregulated in LMP-1 positive versus LMP-1 negative micro-dissected NPC	0	1.971612265	-1.9716123	1.971612	0	0.1603

Tables 3.5 and 3.6 summarises the results of statistical test performed for these analyses.

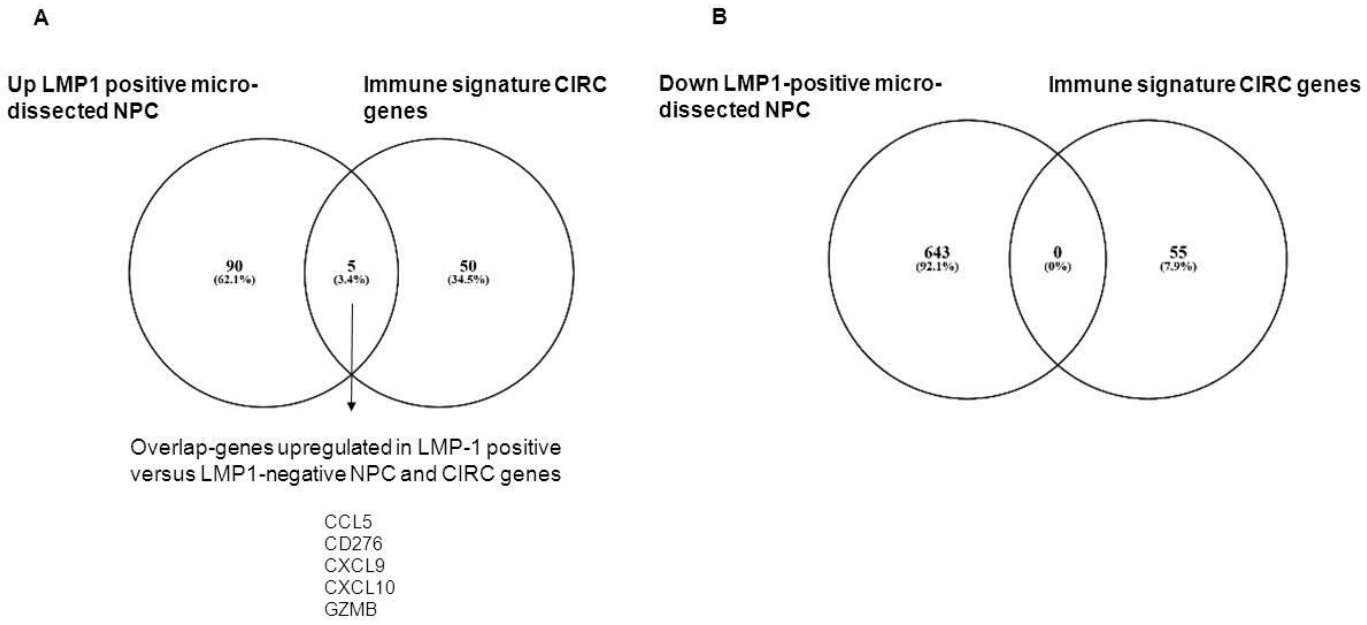

Figure 3.4 PD-L1 is not present among those genes up-regulated in LMP-1-positive micro-dissected compared to LMP1-negative micro-dissected NPC and CIRC genes. A and B; Venn diagrams show the overlap between CIRC genes and those genes either up- or down-regulated in LMP-1-positive vs LMP-1-negative micro-dissected NPC.

Table 3.7: Number of genes upregulated and downregulated in LMP1 positive micro-dissected NPC versus LMP-1-negative micro-dissected NPC and present in CIRC signature

Genes of the arrays	Total number	Number of genes used in the enrichment analysis (present on both Immune checkpoint related genes and NPC array=20219)
Immune signature CIRC	59	55
Upregulated genes in LMP-1 positive versus LMP1 negative micro-dissected NPC	96	95
Downregulated genes in LMP-1 positive versus LMP-1 negative micro-dissected NPC	643	643

Table 3.8: Chi-squared test of the overlap between genes upregulated and downregulated in LMP-1 positive micro-dissected NPC versus LMP-1-negative micro-dissected NPC and present in CIRC signature

Genes of the arrays	Observed (0)	Expected (E)	0-E	Chi square	Odds Ratio	P-value
CIRC signature genes and genes upregulated in LMP-1 positive versus LMP-1 negative micro-dissected NPC	5	0.258407517	4.7415925	87.004819	22.3	<0.0001
CIRC signature genes and genes downregulated in LMP-1 positive versus LMP-1 negative micro-dissected NPC	0	1.74901088	-1.7490109	1.74901088	0	0.186

Tables 3.7 and 3.8 summarises the results of statistical test performed for these analyses

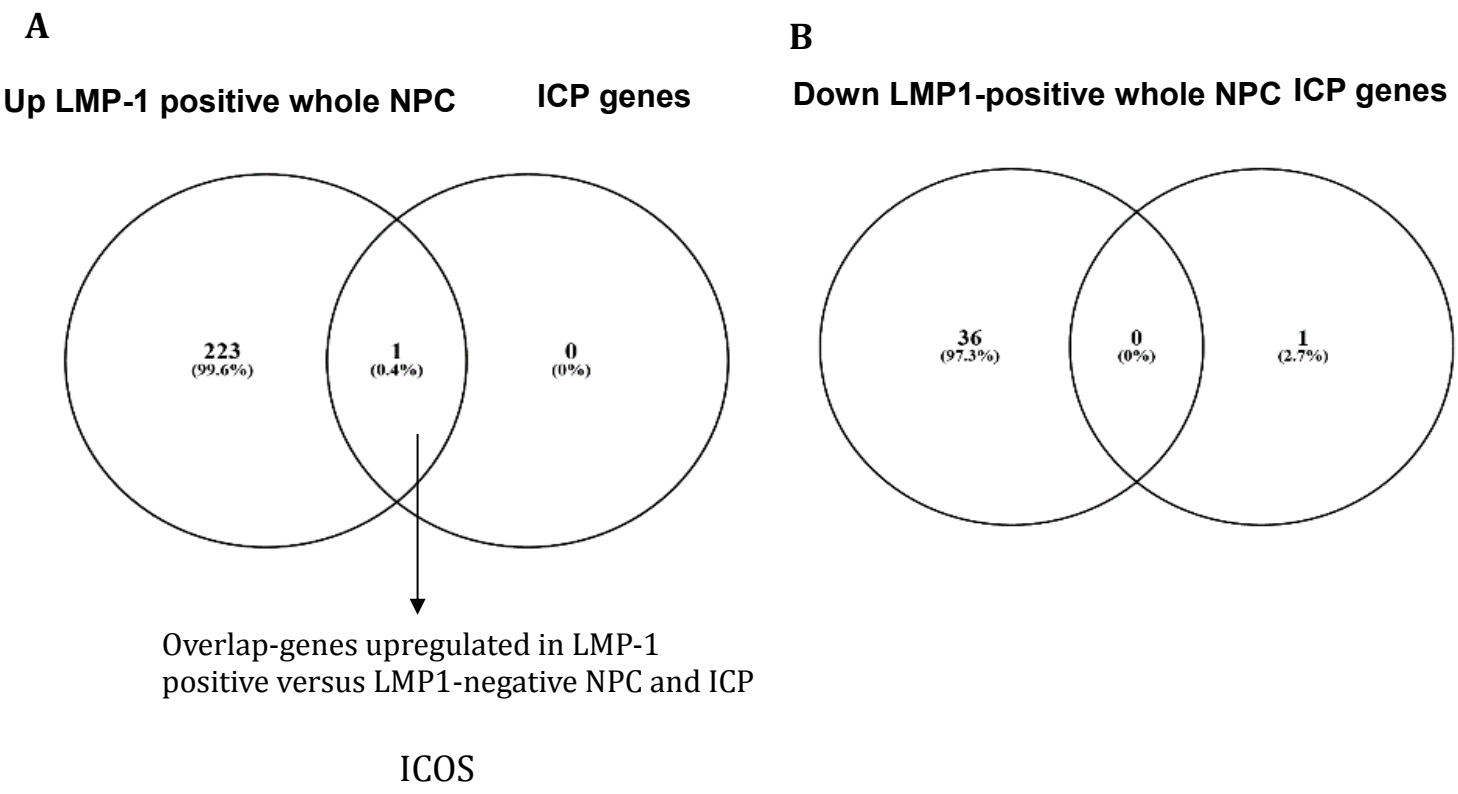

Figure 3.5 PD-L1 is not present among those genes up-regulated in LMP-1-positive compared to LMP-1-negative whole tumour NPC and ICP genes. A and B; Venn diagrams show the overlap between ICP genes and those genes either up- or down-regulated in LMP1-positive versus LMP1-negative whole tumour NPC.

Table 3.9: Number of genes upregulated and downregulated in LMP-1 positive whole tumour NPC versus LMP-1-negative whole tumour NPC and present in ICP signature

Genes of the arrays	Total number	Number of genes used in the enrichment analysis (present on both Immune checkpoint related genes and NPC array=12823
Immune checkpoint related genes	65	1
Upregulated genes in LMP-1 positive versus LMP-1 negative whole NPC	402	224
Downregulated genes in LMP-1 positive versus LMP-1 negative whole tumour NPC	57	36

Table 3.10: Chi-squared test of the overlap between genes upregulated and downregulated in LMP-1 positive whole tumour NPC versus LMP-1-negative whole tumour NPC and present in ICP signature

Genes of the arrays	Observed (0)	Expected (E)	0-E	Chi square	Odds Ratio	P-value
Immune checkpoint genes and genes upregulated in LMP-1 positive versus LMP-1 negative whole NPC	1	0.017468611	0.9825314	55.263	NA	<0.0001
Immune checkpoint genes and genes downregulated in LMP-1 positive versus LMP-1 negative whole NPC	0	0.002807455	-0.0028075	0.002807	0	0.9577

Tables 3.9 and 3.10 summarises the results of statistical test performed for these analyses.

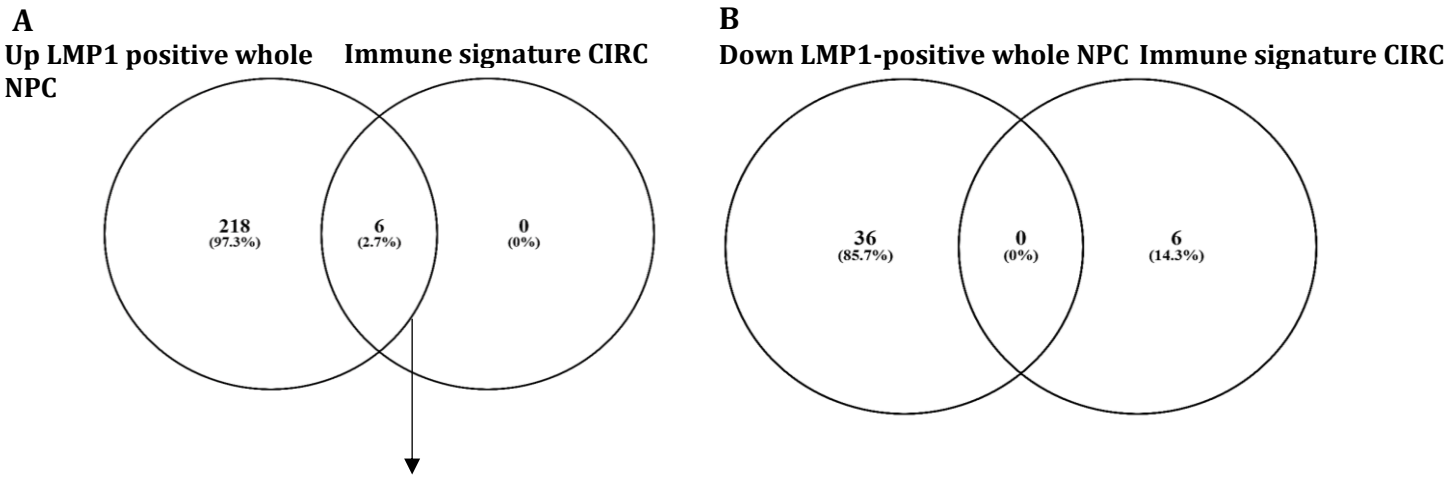

Overlap-genes upregulated in LMP-1 positive versus LMP1-negative NPC and CIRC genes

HLA-DPB1
ICAM1
HLA-DOB
IL7R
ICOS
HLA-DPA1

Figure 3.6 PD-L1 is not present among those genes up-regulated in LMP-1-positive compared to LMP1-negative whole tumour NPC and CIRC genes
A and B; Venn diagrams show the overlap between Immune signature CIRC genes and those genes either up- or down-regulated in LMP-1-positive versus LMP-1-negative whole tumour NPC.

Table 3.11: Number of genes upregulated and downregulated in LMP1 positive whole NPC versus LMP-1-negative whole NPC and present in Immune signature CIRC signature

Genes of the arrays	Total number	Number of genes used in the enrichment analysis (present on both and Immune signature CIRC NPC array=12823)
Immune signature CIRC	59	6
Upregulated genes in LMP1 positive versus LMP1 negative whole NPC	402	224
Downregulated genes in LMP1 positive versus LMP1 negative whole NPC	57	36

Table 3.12: Chi-squared test of the overlap between genes upregulated and downregulated in LMP-1 positive NPC versus LMP-1-negative whole NPC and present in Immune signature CIRC signature

Genes of the arrays	Observed (0)	Expected (E)	0-E	Chi square	Odds Ratio	P-value
Immune signature CIRC and genes upregulated in LMP-1 positive versus LMP-1 negative whole NPC	6	224	5.9555486	797.9181356	NA	<.0001
Immune signature CIRC and genes downregulated in LMP-1 positive versus LMP-1 whole NPC	0	36	-0.0168447	0.016845	0	0.8967

Tables 3.11 and 3.12 summarises the results of statistical test performed for these analyses.

3.2.3 Co-expression of PD-L1 with other immune checkpoints in NPC

The co-expression of immune checkpoints has not been investigated in NPC. Such knowledge is likely to be important for future trials which will probably employ checkpoint inhibitors in combination. Therefore, I used Dataset (5); GSE68799 by Dong H et al (Dong H et al, 2016) which constituted of RNA-seq data of NPC, re-analyzed from EBV Chinese 42 NPC samples, to perform an evaluation of the correlation between PD-L1 expression and that of other relevant checkpoint molecules, especially important here were PD1 and PD-L1, but I also included B and T lymphocyte associated (BTLA), hepatitis A virus cellular receptor 2 (HAVCR2), cytotoxic T-lymphocyte associated protein 4 (CTLA-4), adenosine A2a receptor (ADORA2A), V-set domain containing T-cell activation inhibitor 1 (VTCN1), indoleamine 2,3-dioxygenase 1 (IDO1) and lymphocyte activating 3 (LAG-3). I observed that PD-L1 is positively correlated with the following immune checkpoint genes in order of decreasing R value: PD-L2, hepatitis A virus cellular receptor 2 (HAVCR2), LAG3, ADORA2A, CTLA4, IDO1, BTLA followed by PD1. PD1 is positively correlated with the following immune checkpoint genes in order of decreasing R value: ADORA2A, BTLA, LAG3, CTLA4, HAVCR2, PD-L2, PD-L1, VTCN1 followed by IDO1 (Figure 3.7 and Table 3.13).

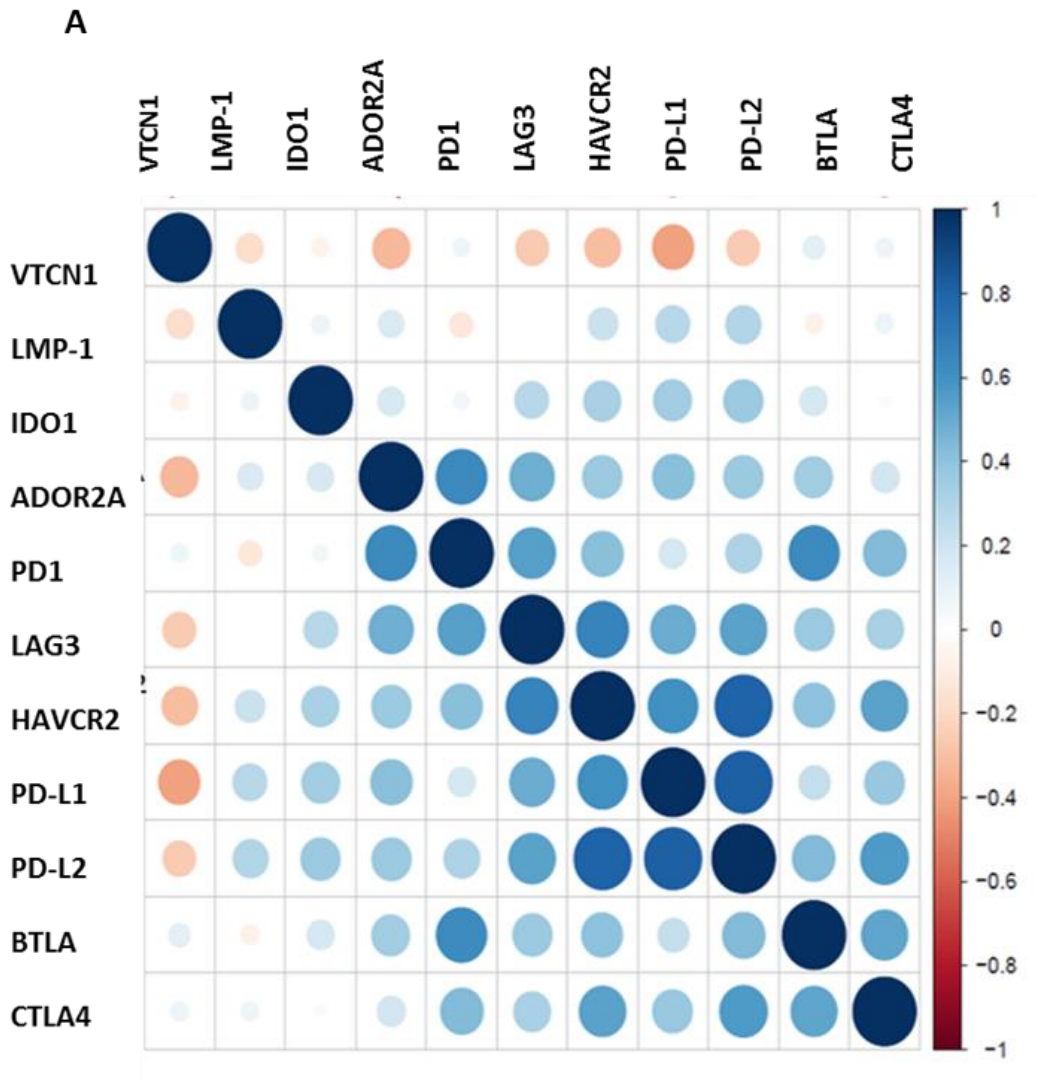

Figure 3.7 Correlation between the expression of immune checkpoint genes in primary EBV positive NPC

PD-L1 expression is positive correlated with PD-L2, HAVCR2, LAG3, ADORA2A, CTLA4, IDO1, BTLA followed by PD1. The plots are based on the 42 tumour Chinese NPC samples. BTLA indicates B and T lymphocyte associated, HAVCR2 indicates hepatitis A virus cellular receptor 2, CTLA-4 indicates cytotoxic T-lymphocyte associated protein 4, ADORA2A indicates adenosine A2a receptor, VTCN1 indicates V-set domain containing T-cell activation inhibitor 1, IDO1 indicates indoleamine 2,3-dioxygenase 1 and LAG-3 indicates lymphocyte activating 3.

Table 3.13 Correlation coefficients for the co-expression analysis of Immune checkpoints in NPC

Immune checkpoint genes	VTCN1	LMP-1	IDO1	ADORA2A	PDCD1	LAG3	HAVCR2	PD-L1	PD-L2	BTLA	CTLA4
VTCN1	1.000	-0.177	-0.068	-0.329	0.067	-0.258	-0.305	-0.403	-0.256	0.111	0.073
LMP-1	-0.177	1.000	0.072	0.152	-0.127	0.005	0.213	0.276	0.296	-0.075	0.073
IDO1	-0.068	0.072	1.000	0.170	0.056	0.272	0.327	0.343	0.367	0.175	-0.025
ADORA2A	-0.329	0.152	0.170	1.000	0.631	0.487	0.369	0.411	0.370	0.341	0.189
PD1	0.067	-0.127	0.056	0.631	1.000	0.543	0.415	0.179	0.308	0.627	0.433
LAG3	-0.258	0.005	0.272	0.487	0.543	1.000	0.662	0.492	0.536	0.367	0.321
HAVCR2	-0.305	0.213	0.327	0.369	0.415	0.662	1.000	0.608	0.808	0.401	0.535
PD-L1	-0.403	0.276	0.343	0.411	0.179	0.492	0.608	1.000	0.811	0.232	0.379
PD-L2	-0.256	0.296	0.367	0.370	0.308	0.536	0.808	0.811	1.000	0.430	0.561
BTLA	0.111	-0.075	0.175	0.341	0.627	0.367	0.401	0.232	0.430	1.000	0.526
CTLA4	0.073	0.073	-0.025	0.189	0.433	0.321	0.535	0.379	0.561	0.526	1.000

Tables 3.13 summarises the results of statistical test performed for these analyses.

3.2.4 Protein expression of PD-L1 in primary NPC

Before embarking on an analysis of the protein expression of PD-L1 and PD1 in primary NPC, I first optimised conditions for immunohistochemistry of these markers and the T cell marker CD3 (Figure 3.8). PD-L1 staining in tonsil was positive in the superficial layers of the squamous epithelium lining the crypt. PD1 was positive in a membranous pattern in scattered activated lymphocytes within the GC, a few lymphocytes within the mantle zone, and on other non-lymphoid populations in the interfollicular region where it was localized in the cytoplasm as well as the membrane. CD3 was positive in the reactive T cells. Multiplex IF for CD3, PD-L1 and PD1 was also optimized (hereafter referred to as the 'immune checkpoint-T cell panel; Figure 3.9).

Next, I investigated the expression of PD-L1 in NPC samples. PD-L1 was positive in tumour cells in 16/17 (94.11%) NPC samples when using a cut off ≥ 5% of PD-L1 positive cells as published by Heeren et al **(Heeren et al., 2016)** and Fang et al **(Fang et al., 2014)**. An example of PD-L1 staining in tumour cells illustrating that the tumour is positive for PD-L1 at the periphery is shown in Figure 3.10 A. I also performed a semi-automated analysis of PD-L1 expression using Inform software. I found that the two methods of scoring were significantly positively correlated ($r=0.6418$ and $p< 0.00001$; Figure 3.10 B and Table 3.14).

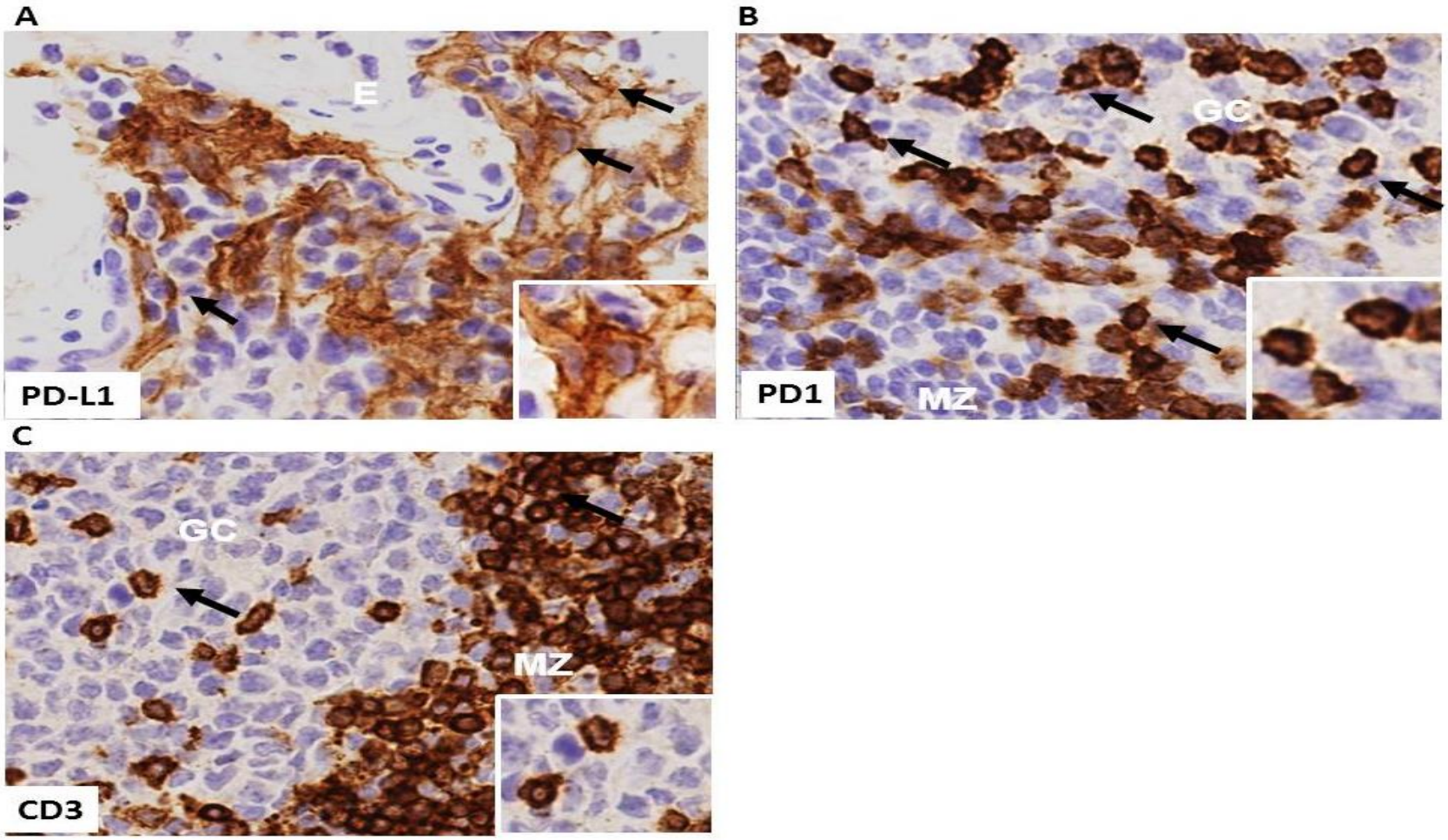

Figure 3.8 IHC of tonsil used as a positive control for the immune checkpoint-T cell panel, A) PD-L1 is expressed by the tonsil crypt squamous epithelium at the black arrows (40X). B) PD1 is expressed by many reactive lymphocytes in the germinal centre (GC), few in mantle zone at black arrows (40X). C) CD3 is positive in the follicular and mantle zone T cells (40X) at black arrows. (E) indicates epithelium, (GC) indicates germinal centre, (MZ) indicates mantle zone.

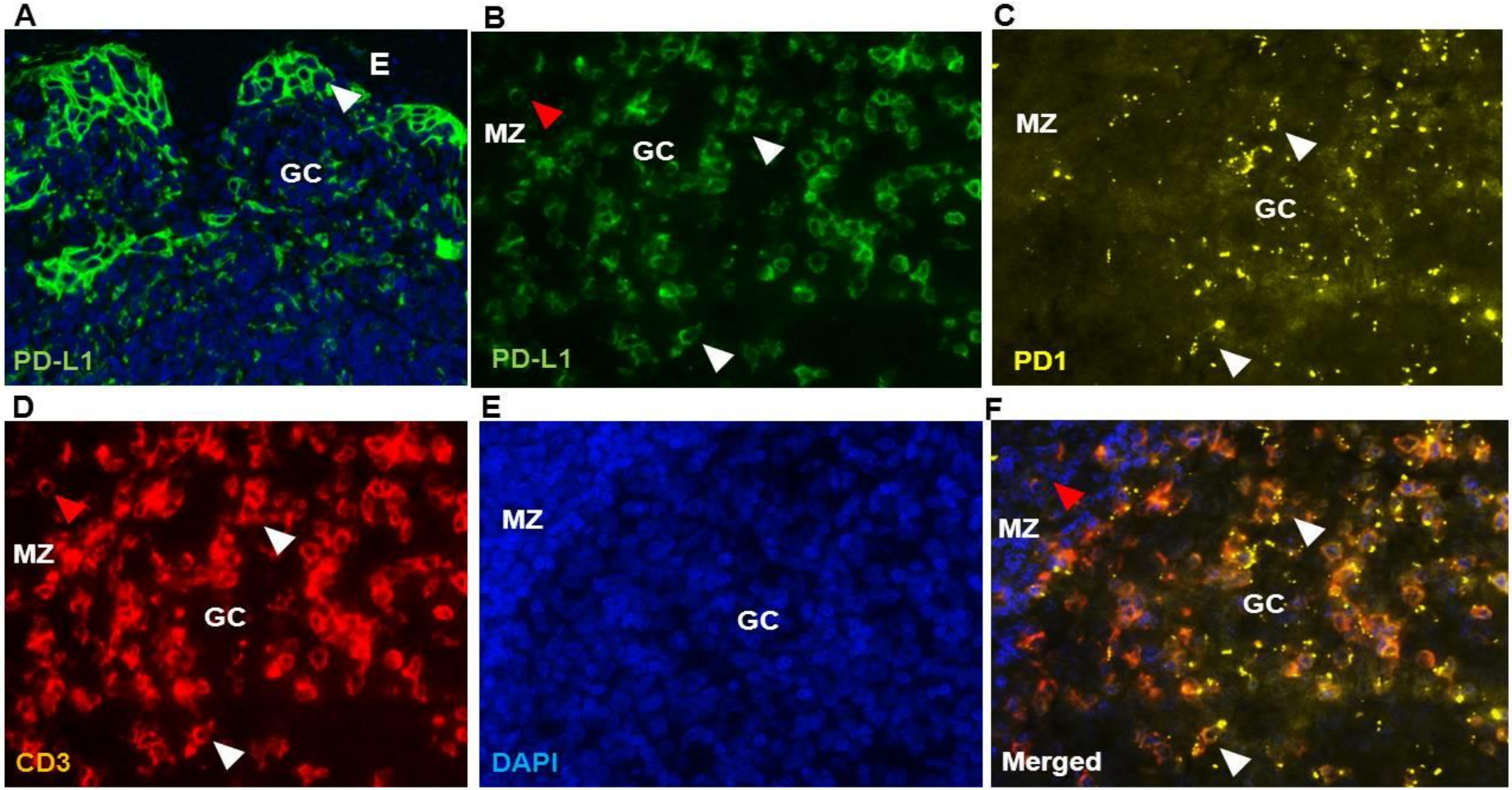

Figure 3.9 Example of optimized multiplex IF for the Immune checkpoint-T cell panel
A) PD-L1 (green) is positive in tonsillar squamous epithelium (arrow head) and present in the GC, B) PD-L1 (green) is present in the GC cells (white arrow head) and T cells in mantle zone (red arrow head), C) PD1 (yellow) is expressed by the reactive lymphocytes in GC, D) CD3 (red) is expressed by the reactive T cells, E) DAPI staining the nuclei (blue) F) overlay of the four multispectral images, (20X), (GC) indicates germinal centre, (MZ) indicates mantle zone, (E) indicates epithelium.

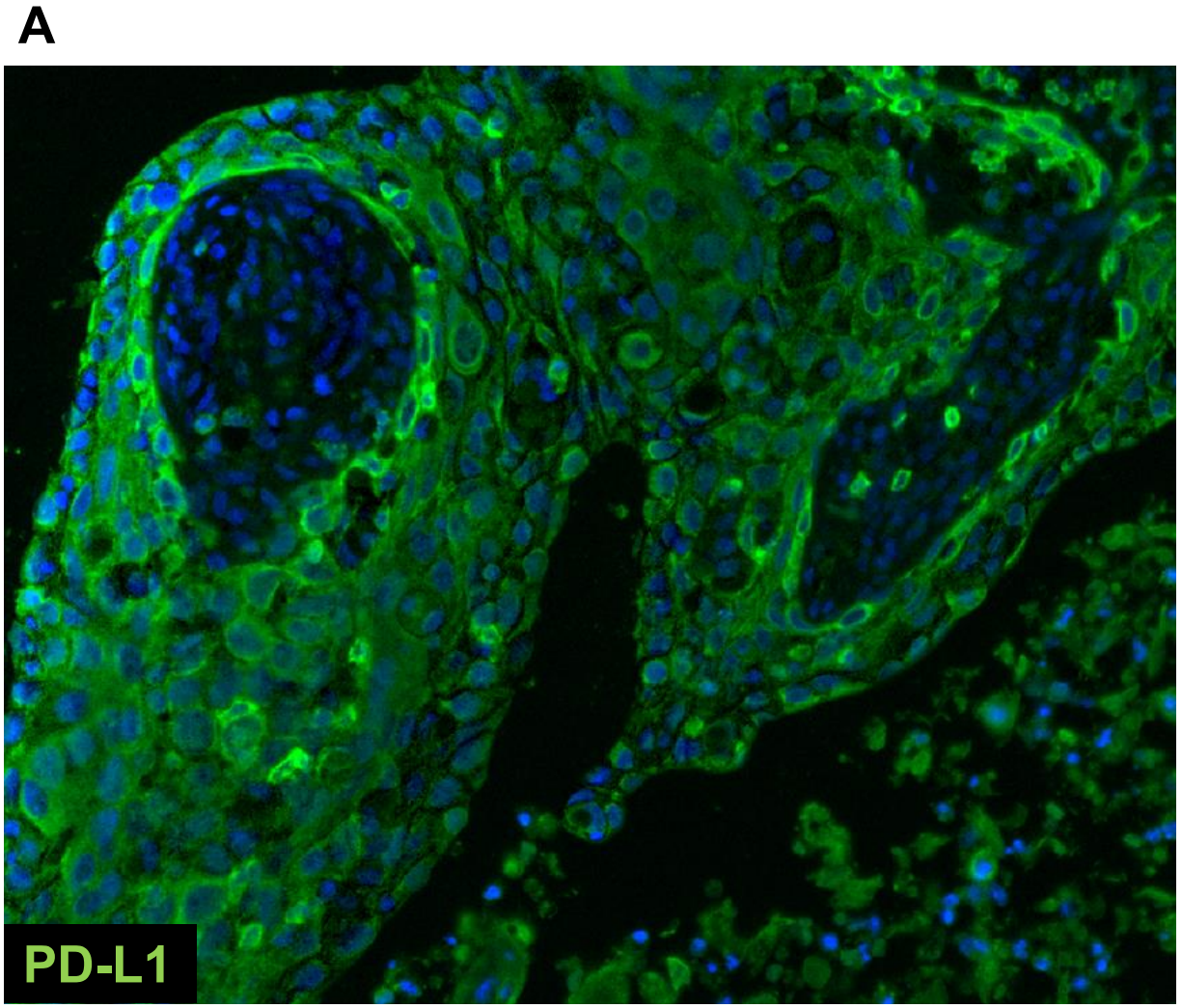

Figure 3.10 Expression of PD-L1 in NPC

A) Representative example of NPC that has PD-L1 (green) expression mainly on the periphery in a membranous pattern, 20X

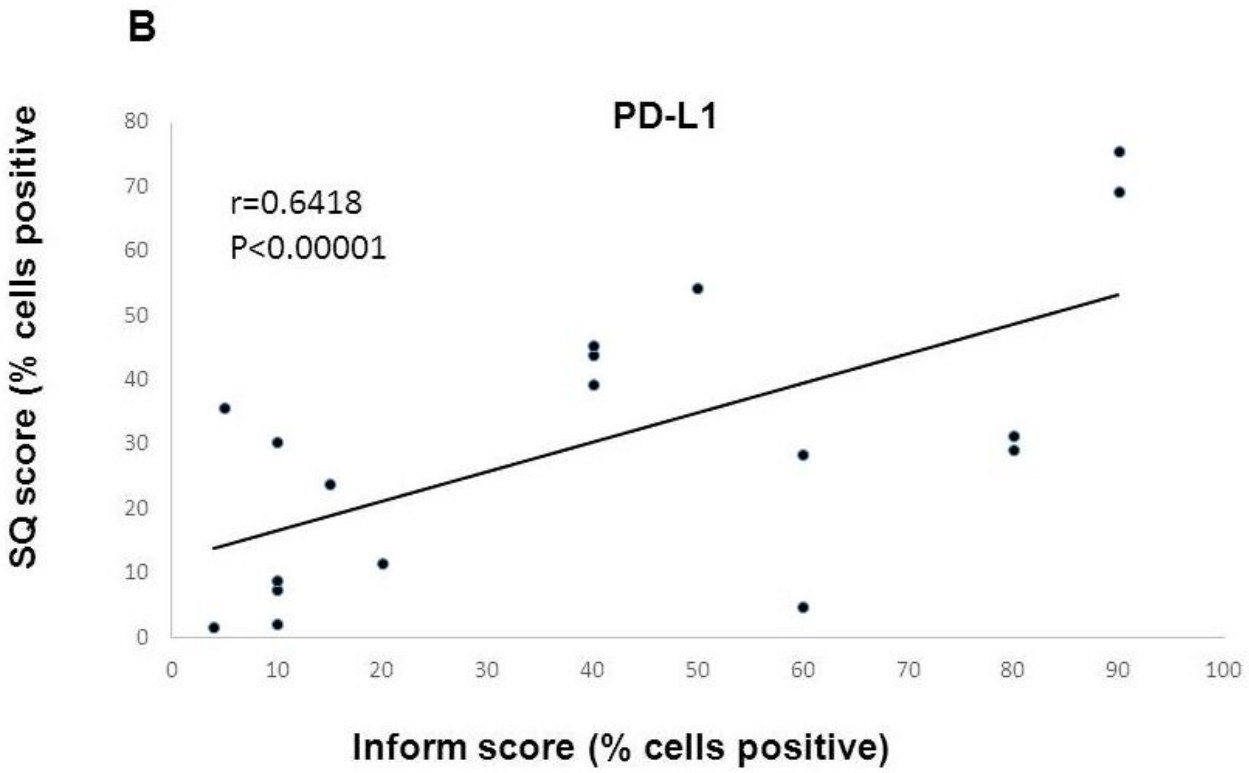

B) Positive correlation between PD-L1 scored using either semi-automated Inform scoring or semi-quantitative scoring of percentage of tumour cells.

3.2.5 Expression of PD-L1 protein in overlying epithelium and NPC

To confirm the over-expression of PD-L1 in NPC and to describe the expression of PD-L1 in the non-neoplastic epithelium of NPC biopsies (the latter is not yet reported), I analysed PD-L1 expression in the non-neoplastic epithelium which was present in 7/17 NPC biopsies. One of these samples contained normal looking epithelium, while the remaining 6 cases had atypical changes, but it was not possible to grade them based on immunofluorescence stained slides. PD-L1 was expressed in non-neoplastic or pre-invasive epithelium in 2/7 samples. Comparison of H-scores for tumour versus the non-neoplastic epithelium, showed a significant increase in PD-L1 expression in the tumour (Figure 3.11, Table 3.14; p=0.0001).

A

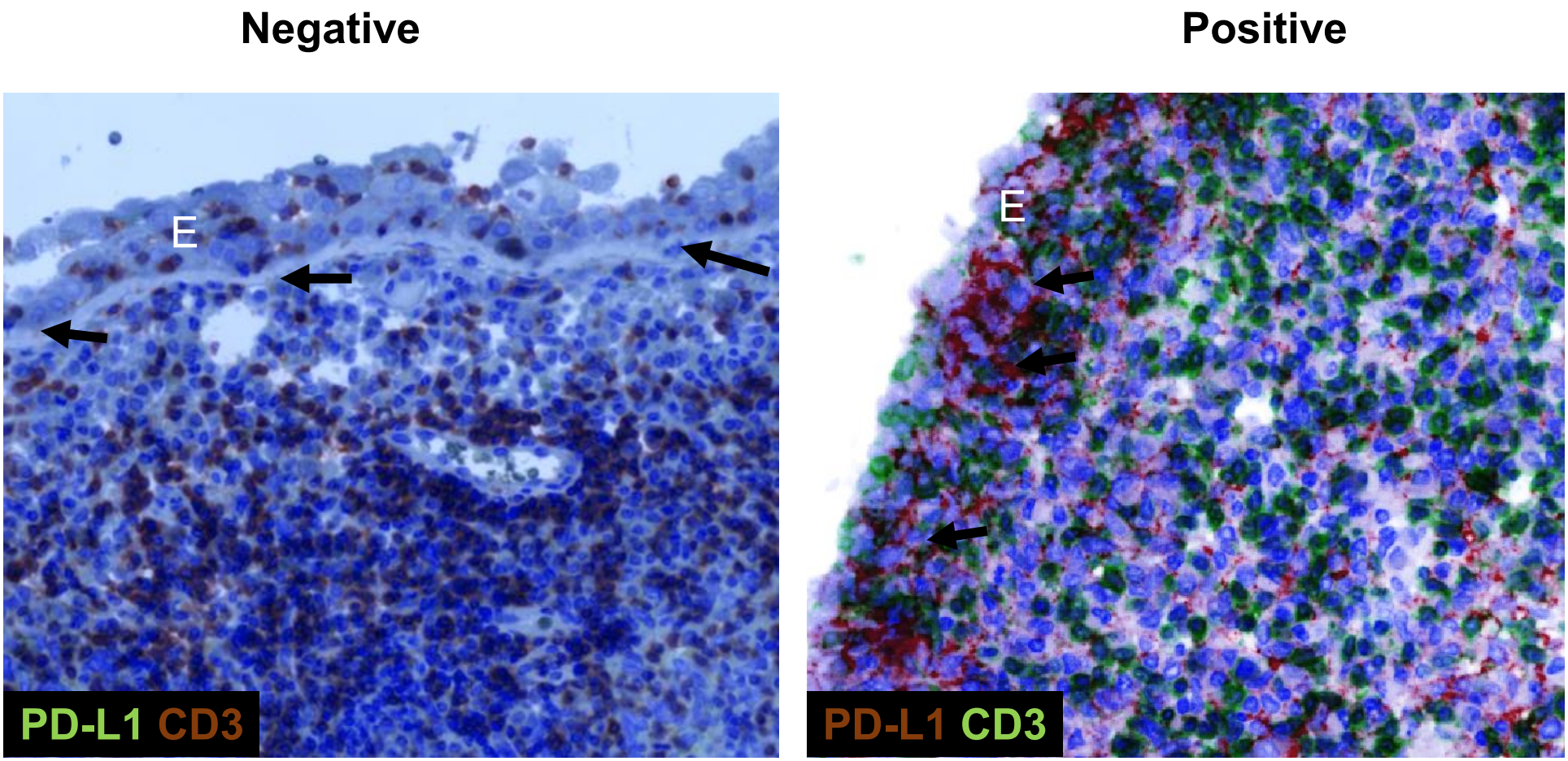

Figure 3.11 Expression of PD-L1 in non-neoplastic tissue in NPC biopsies
A) Shown are representative cases of the staining of PD-L1 in non-neoplastic epithelium from NPC biopsies, image was converted to bright-field to allow evaluation of the dysplasia. Left panel, the overlying epithelium was negative for PD-L1 (black arrows). Scattered reactive CD3 (brown) positive T cells are seen in the tumour stroma. Right panel, PD-L1 was seen positive in parts of the epithelium (black arrows).

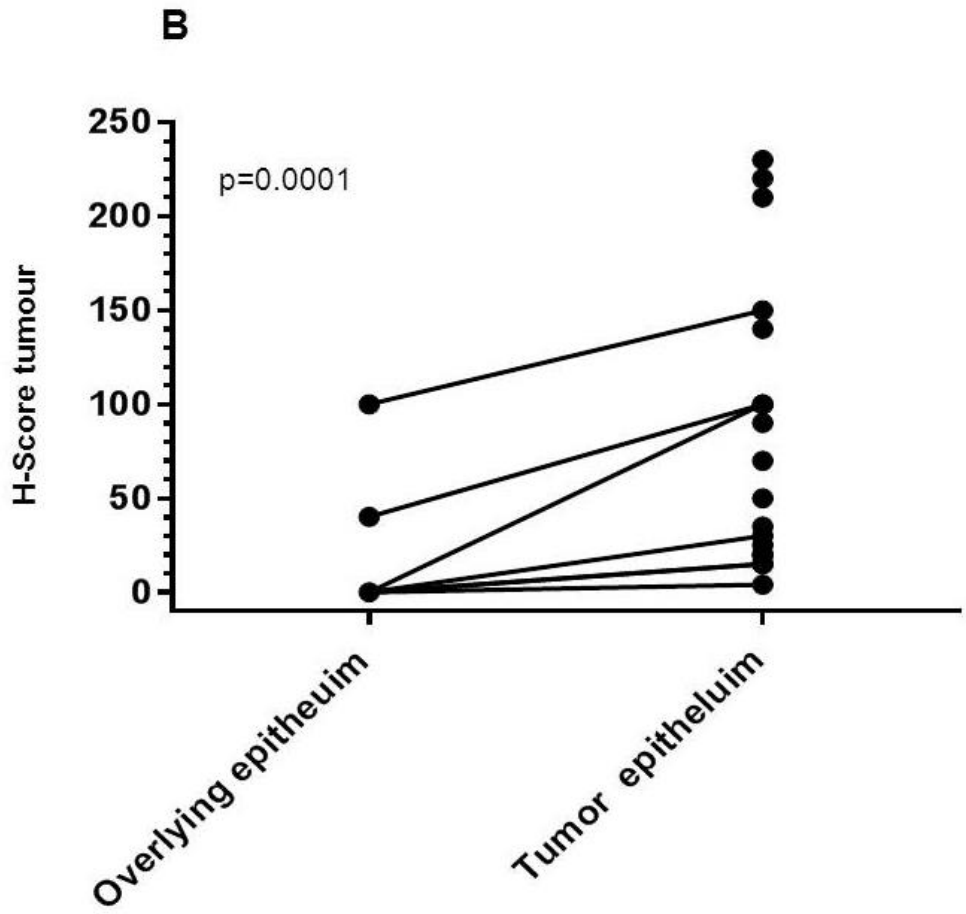

B) Graphical representation shows significantly higher H-scores for PD-L1 expression in tumour compared to non-neoplastic epithelium (p=0.0001), H-score indicates histoscore.

Table 3.14 PD-L1 expression in NPC and non-neoplastic epithelium

Case number	Overlying epithelium	Epithelium status	PD-L1 status overlying epithelium	PD-L1 status tumour epithelium	H-score overlying epithelium	H-score Tumour epithelium
1	Absent	-	-	Positive	-	90
2	Present	Atypical	Negative	Positive	0	220
4	Present	Atypical	Positive	Positive	100	150
7	Absent	-	-	Positive	-	50
8	Present	Atypical	Negative	Negative	0	4
9	Absent	-	-	Positive	-	210
10	Present	Atypical	Positive	Positive	40	100
11	Absent	-	-	Positive	-	140
12	Present	Atypical	Negative	Positive	0	15
14	Absent	-	-	Positive	-	230
15	Present	Normal	Negative	Positive	0	100
16	Present	Atypical	Negative	Positive	0	15
17	Absent	-	-	Positive	-	20
18	Absent	-	-	Positive	-	25
20	Absent	-	-	Positive	-	70
21	Absent	-	-	Positive	-	35
22	Absent	-	-	Positive	-	20

3.2.6 Patterns of PD-L1 expression in NPC

The pattern of PD-L1 expression has not been described in NPC, i.e. whether it is inducible or constitutive. This is important because the expression of these distinct patterns may have prognostic implications. For example, better disease free survival and disease specific survival has been reported for patients with the marginal type rather than the diffuse type of PD-L1 expression in cervical SCC **(Heeren et al., 2016)**. In this study, the scoring system for PD-L1 was as reported by Heeren et al which defined the diffuse pattern as one which may reflect a constitutive mechanism of intrinsic tumour resistance related to molecular alterations and showing the presence of PD-L1 positive tumour cells in the whole tumour **(Heeren et al., 2016)**. The marginal expression of PD-L1 is likely to represent the inducible type, where cytokines released by effector T cells induce PD-L1 expression, I found that 8/16 NPC tumours were of diffuse type. An example of diffuse expression is shown in Figure 3.12. I found that 8/16 cases were of the marginal type. Figure 3.13 shows that the marginal type existed as two variants, either focal when PDL-1 was present in peripheral foci, and circumferential when PD-L1 expression was found through the whole outer portion of the tumour cluster. Figure 3.14 shows IF images converted to bright-field for better visualisation of these different patterns. Figure 3.15 shows that tumours with a diffuse pattern of expression have, as expected, significantly higher levels of PD-L1 protein expression than marginal type tumours

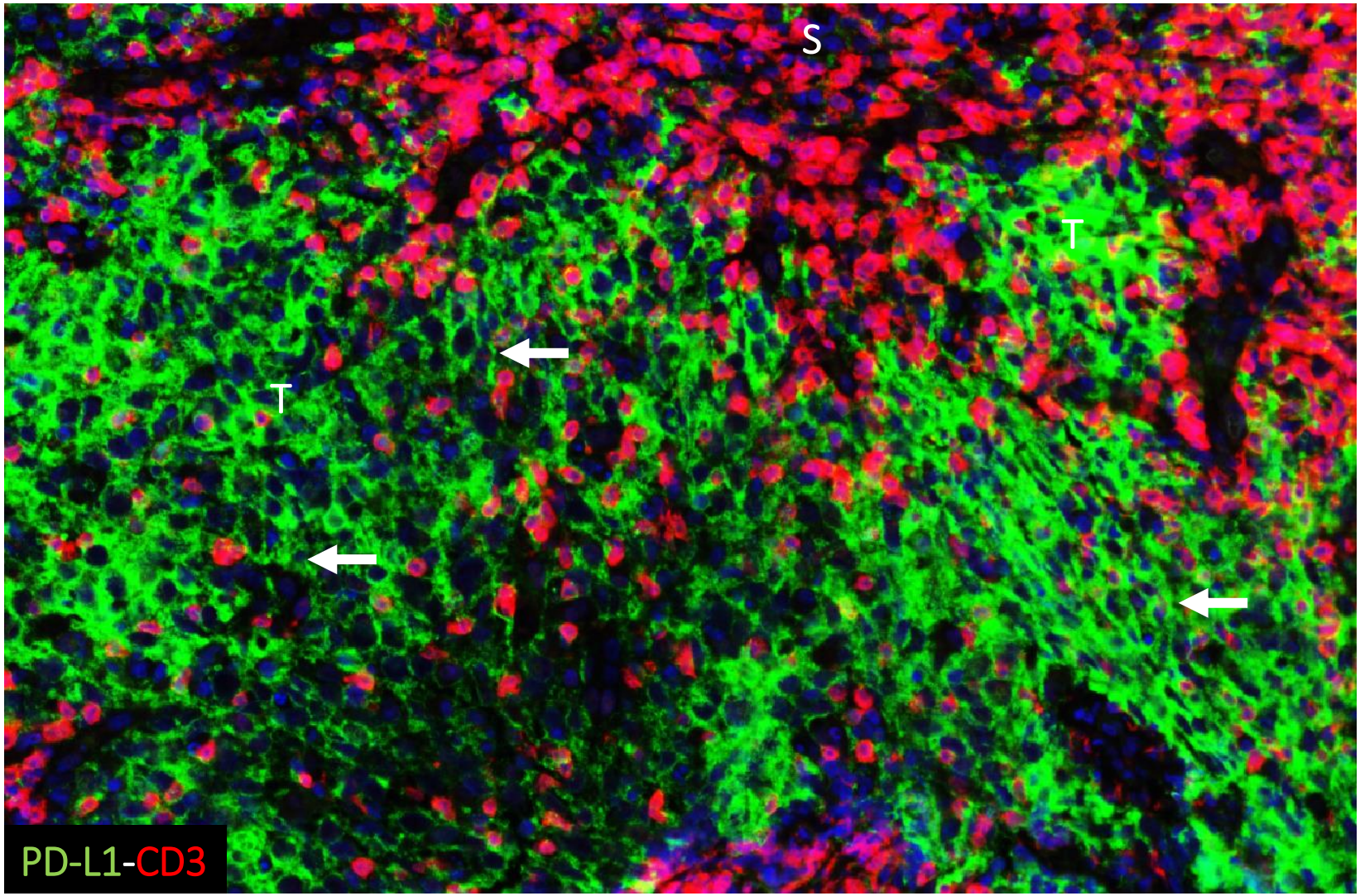

Figure 3.12 Example of diffuse pattern of PD-L1 expression in NPC PD-L1 (green) is diffusely positive in the tumour cells, amongst the tumour groups, with strong intensity. Numerous CD3 positive T cells (red) in close/direct relation to PD-L1 positive tumour cells, 20X (T) indicates tumour, (S) indicates stroma.

A

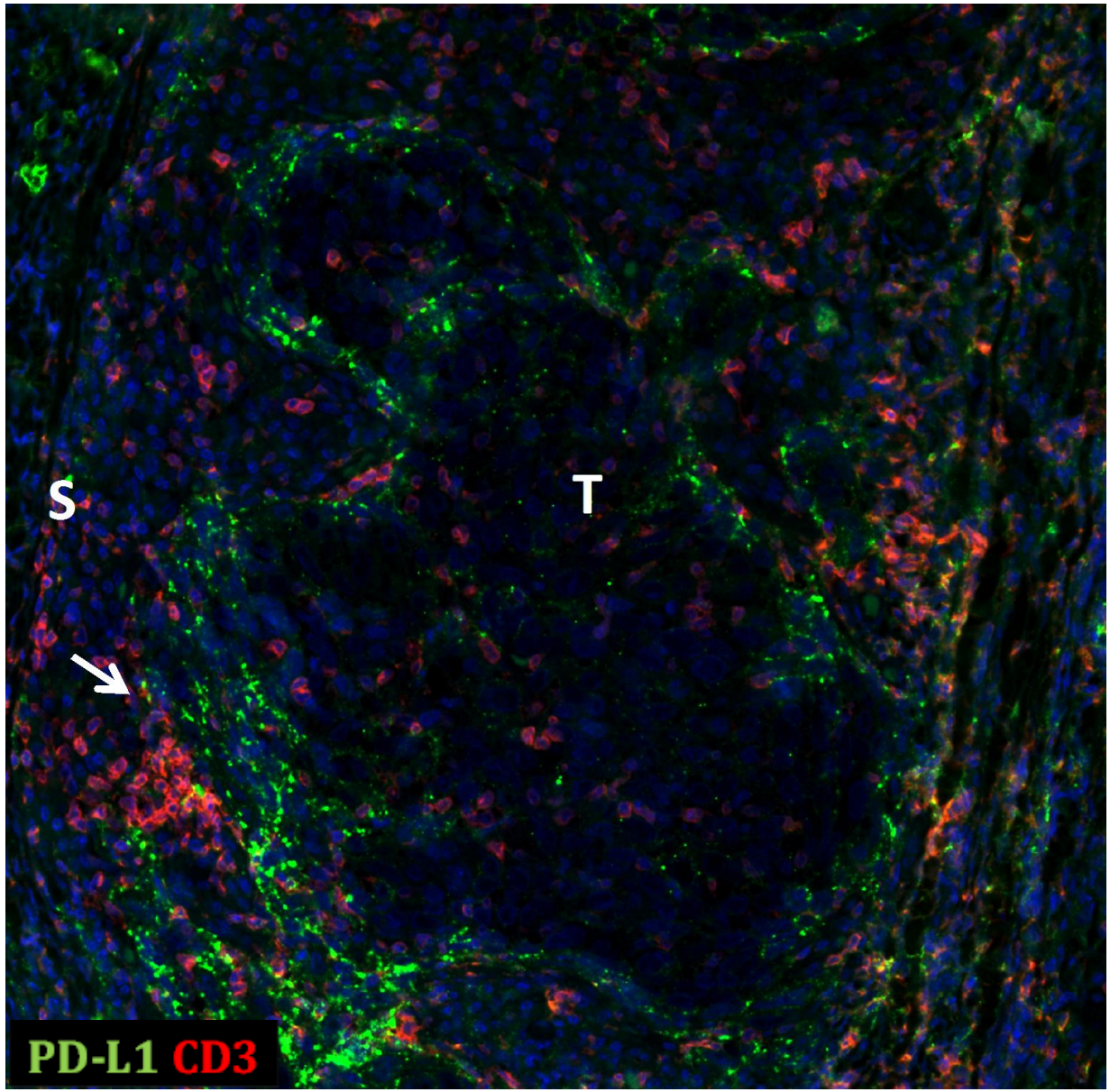

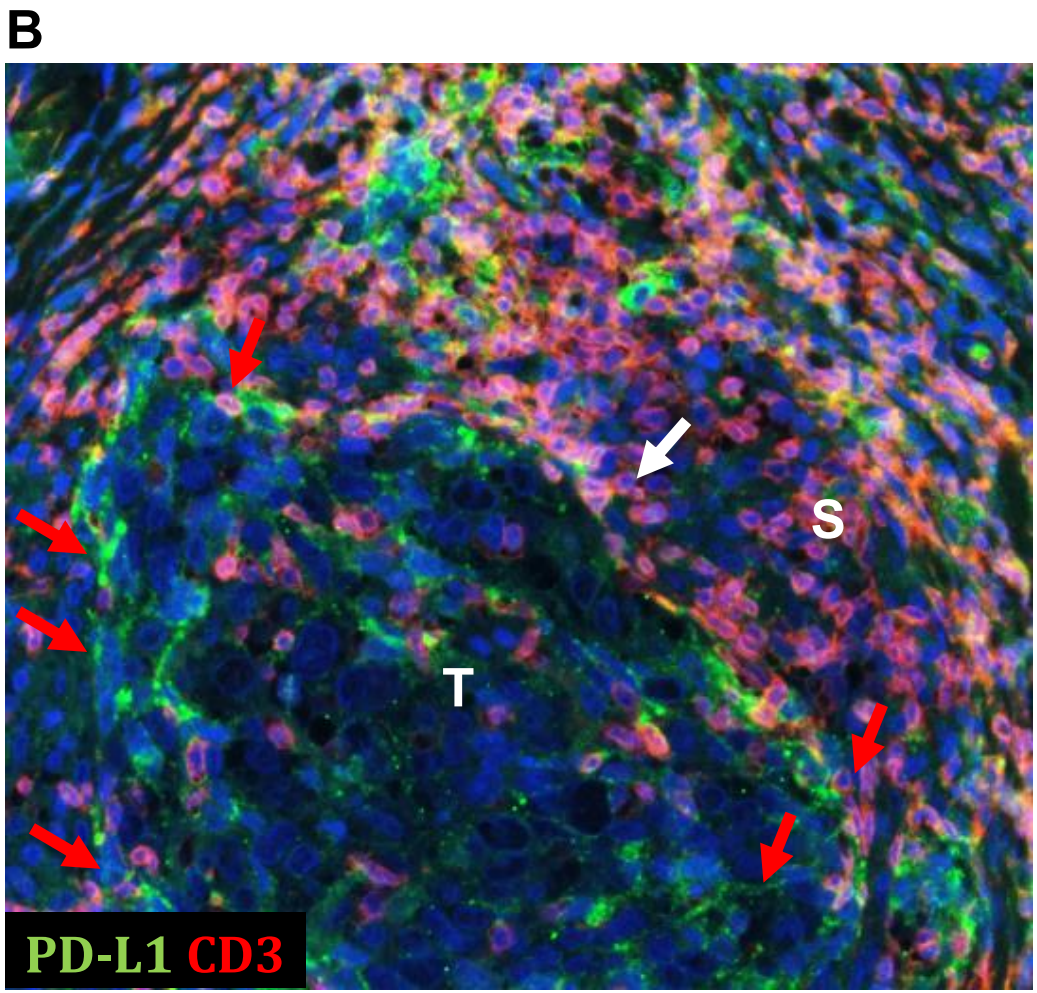

Figure 3.13 Examples of the marginal pattern of PD-L1 expression in NPC
A) and B) Tumour cells are PD-L1 (green) positive only at the periphery (red arrows), circumferentially. Numerous CD3 positive T cells (red) (white arrows) are in close/direct relation to PD-L1 positive tumour cells, 20X. (T) indicates tumour, (S) indicates stroma

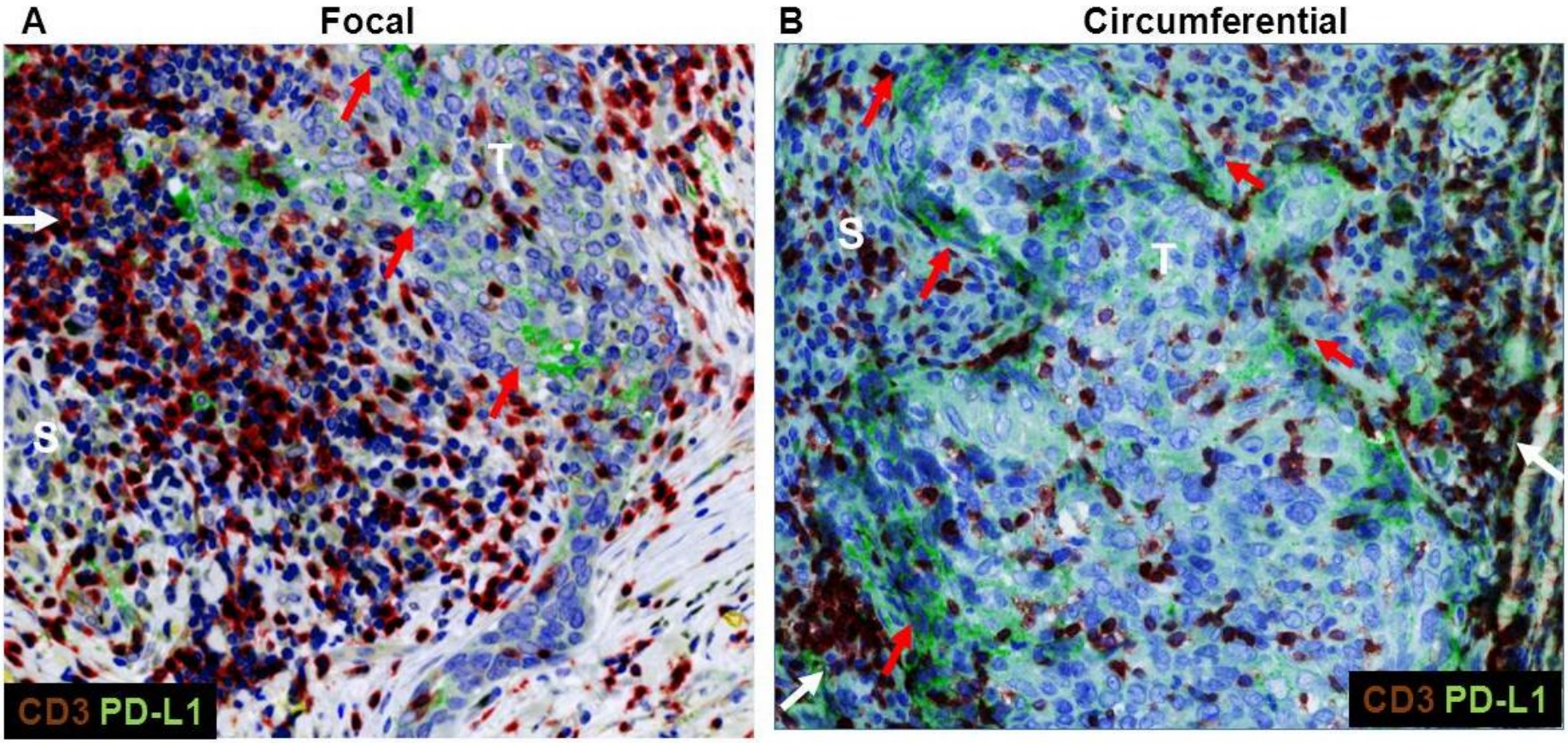

Figure 3.14 Multiplex IF converted to bright-field image, showing variants of marginal pattern of expression of PD-L1 in tumour cells
Both examples are merged images and show groups of tumour cells positive for PD-L1 (green) at the tumour-stroma interphase in focal (left panel), and circumferential (right panel) patterns. Many PD-L1 positive tumour cells in green (red arrows) at the tumour-stroma interface, were in direct contact with scattered CD3 positive T cells in brown at the white arrows, in a clustered non uniform pattern (20X). (T) indicates tumour, (s) indicates stroma.

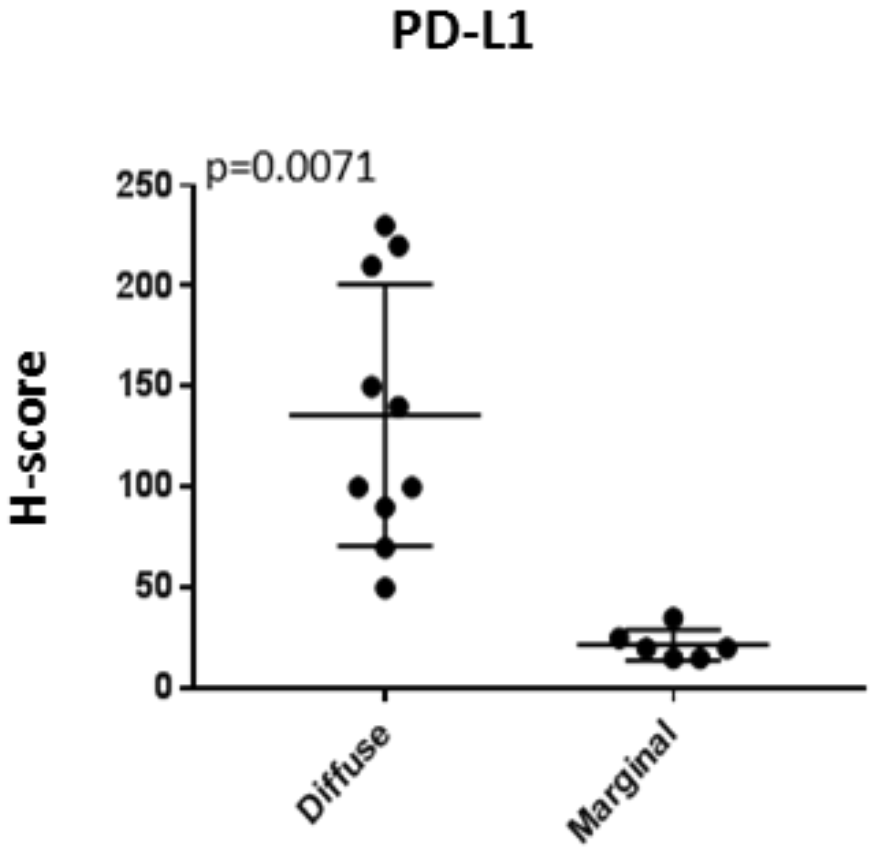

Figure 3.15 Significantly higher PD-L1 expression in diffuse type NPC, H-scores for PD-L1 expression in diffuse versus marginal type NPC.

3.2.7 The frequency and distribution of T cells in PD-L1 expressing NPC

Although the frequency of CD3 positive cells was reported to be not significantly different between PD-L1-positive and PD-L1-negative head and neck SCC **(Kim et al., 2016)**, the relationship between PD-L1 expression types and the frequency and distribution of CD3 positive cells has rarely been explored in NPC. Therefore, I studied the distribution of CD3-expressing cells in relation to PD-L1 expression in tumour cells in the series of 17 NPC cases that were co-stained by IF. I found that in all marginal type cases, T cells were in contact with tumour cells at the tumour-stroma interface, with a high density of T cells in 7/8 cases; most cases also showed a non-uniform distribution of T cells with focal clustering of a high density of CD3 positive T cells (Figure 3.16 A-C; Table 3.15). Next, I examined the distribution of CD3 positive cells in samples with diffuse expression of PD-L1. The density of CD3 positive T lymphocytes in the diffuse/constitutive type was variable among cases but uniform, with no clustering in any case (Figure 3.16 D).

Next, I wanted to examine if CD3 expression was correlated with PD-L1 expression in NPC. To do this I initially took advantage of the re-analysis of Dataset 5 described above (Dong H., 2016). Figure 3.17 A shows a strong positive correlation between CD3 and PD-L1 mRNA expression in NPC ($r=0.97$; $p=<0.0001$). I also correlated H-scores for PD-L1 with CD3 counts in both the intra-tumour and stromal compartments. Surprisingly, I found no significant correlation between PD-L1 expression and CD3 counts in either the intra-tumour or the stroma (Figure 3.17 B). Furthermore, I observed no significant difference in the frequency of intra- tumour or stromal CD3 density with PD-L1 scores using Inform and H-scores as shown in Figure 3.17 C and stromal CD3 positive cells between NPC tumours displaying either the marginal or diffuse patterns of PD-L1 expression.

A

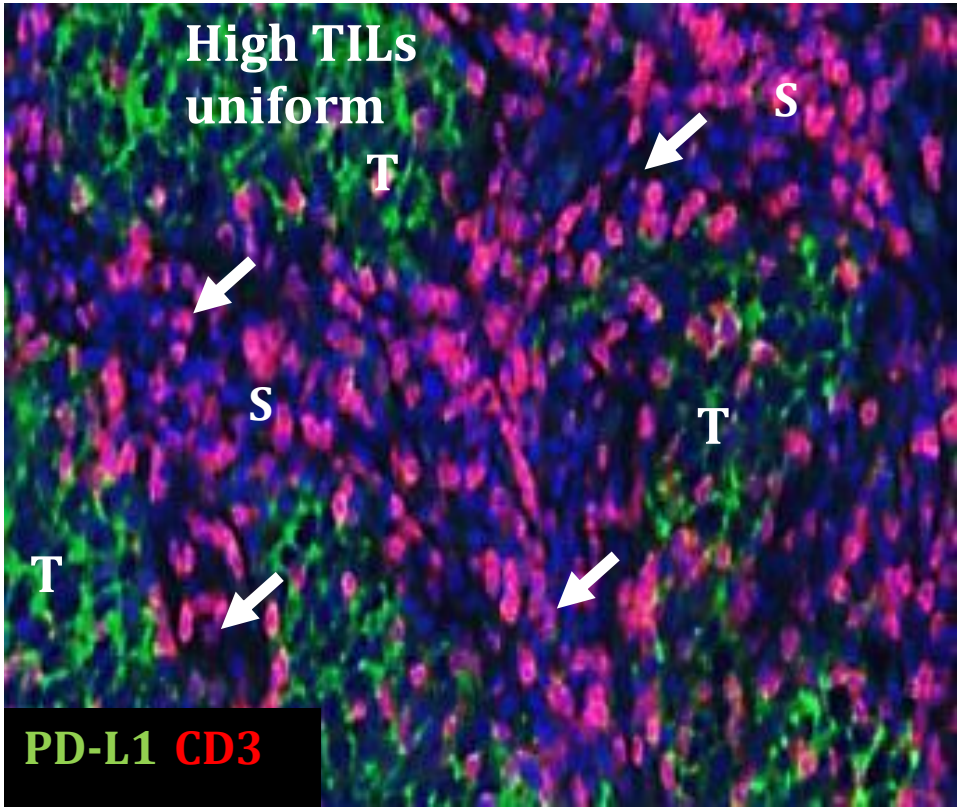
High TILs
uniform
T
S
S
T
T
PD-L1 CD3

B

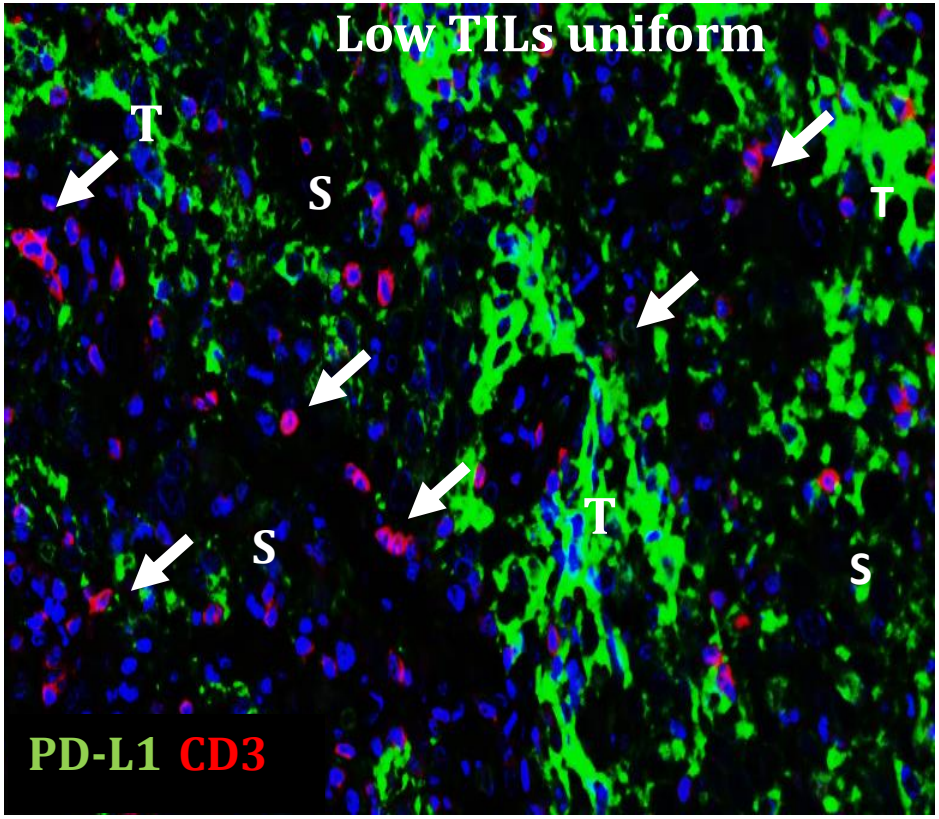
Low TILs uniform
T
S
T
T
S
S
PD-L1 CD3

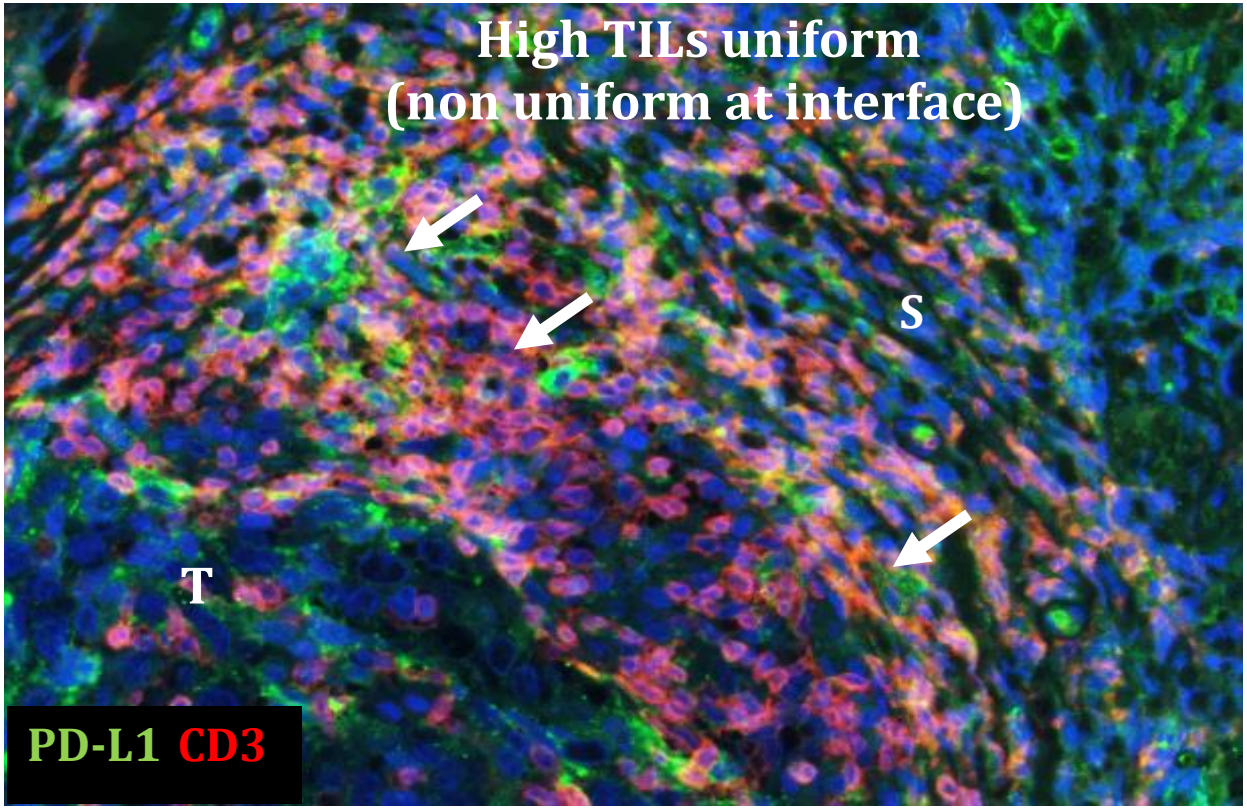

Figure 3.16 Multiplex IF and graphical representation of CD3 distribution and correlative analysis of CD3 with PD-L1 in constitutive and marginal type of PD-L1 expression NPC A) Diffuse type of PD-L1 positive NPC stained with CD3 (red), and PD-L1 (green). PD-L1 is observed diffusely in the tumour cells. Tumour sample is uniformly highly populated with CD3 in both the tumour and stromal compartments (white arrows). B) Example of diffuse type which displayed low levels of CD3 (red) positive cells in both tumour and stroma compartments (white arrows), C) An example of marginal type, with non-uniform aggregation of CD3 (red) at the white arrow around the peripheral PD-L1 (green) positivity in the tumour at the red arrow.

Table 3.15 Topographic description of CD3 in relation to marginal type of PD-L1 positive tumours

Case number	CD3 at contact of PD-L1 +ve tumour cells	CD3 density at the PD-L1 positive tumour interface with the stroma	CD3 distribution at the PD-L1 positive tumour interface with the stroma
2	Present	High	uniform
7	Present	Low	uniform
10	Present	High	Non-uniform
12	Present	high	uniform
16	Present	low	uniform
17	Present	high	Non uniform
18	Present	high	Non uniform
22	Present	high	Non uniform

Table 3.17 summarises the topographic distribution of CD3 in relation of PD-L1 tumour positive cells.

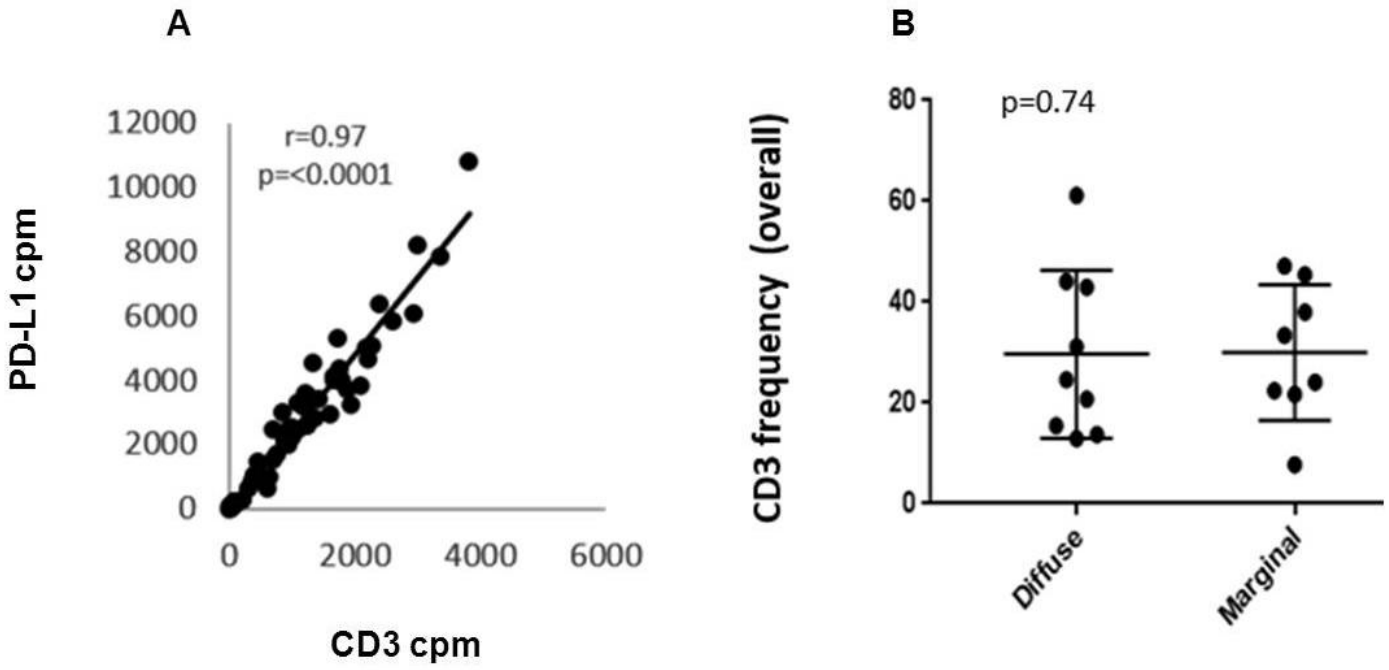

Figure 3.17 Correlation between CD3 and PD-L1 expression in NPC
A) Graphs show a strong positive correlation between CD3 and PD-L1 mRNA expression in NPC (r= 0.97; p<0.0001), B) Graph shows that the frequency of CD3-positive cells was not significantly different between NPC displaying either a diffuse or marginal pattern of PD-L1 expression, p=0.74.

C

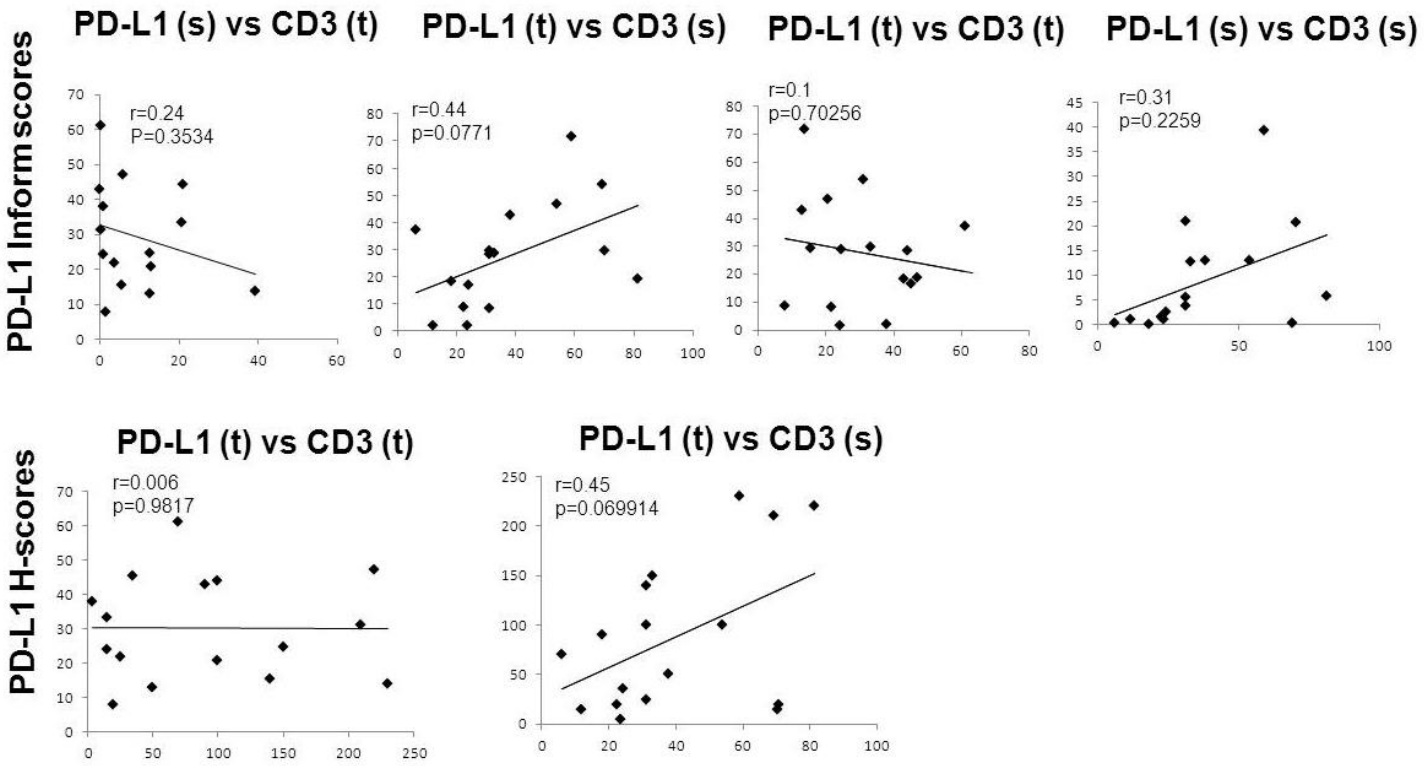

C) Graphs show that the frequency of CD3-positive cells in the intra-tumour compartment is not correlated with PD-L1 scores.

3.2.8 Subcellular localization of PD-L1 in NPC

A different sub-cellular localization of PD-L1 staining i.e. cytoplasmic, or membranous (either complete or incomplete) has been reported in different solid and hematological tumours using the FDA-approved PD-L1 antibody **(Scognamiglio et al., 2016)**. However, a detailed description of the sub-cellular localization of PD-L1 has been rarely reported in NPC. PD-L1 expression was described by Zheng et al in NPC, with the most commonly cytoplasm-mainly tumors represents 65.9% of patients, while mixed cytoplasmic and membranous pattern of PD-L1 positivity were described in 24.7% of patients. Membrane mainly tumour were the least frequent representing 9.4% **(Zheng et al., 2017)**. High expression of cytomembranous pattern was associated with inferior outcome in loco-regional advanced NPC **(Zheng et al., 2017)**. I found that all PD-L1 positive tumours showed incomplete membranous staining, complete membranous in 12/16 cases, and cytoplasmic in 11/16 cases. In total 14/16 NPC showed mixed patterns of PD-L1 localization (Table 3.16). Incomplete was observed as partial membrane staining and complete as circumferential membrane staining. An illustration of these different patterns in a diffuse type of PD-L1- expressing tumour is shown in Figure 3.18.

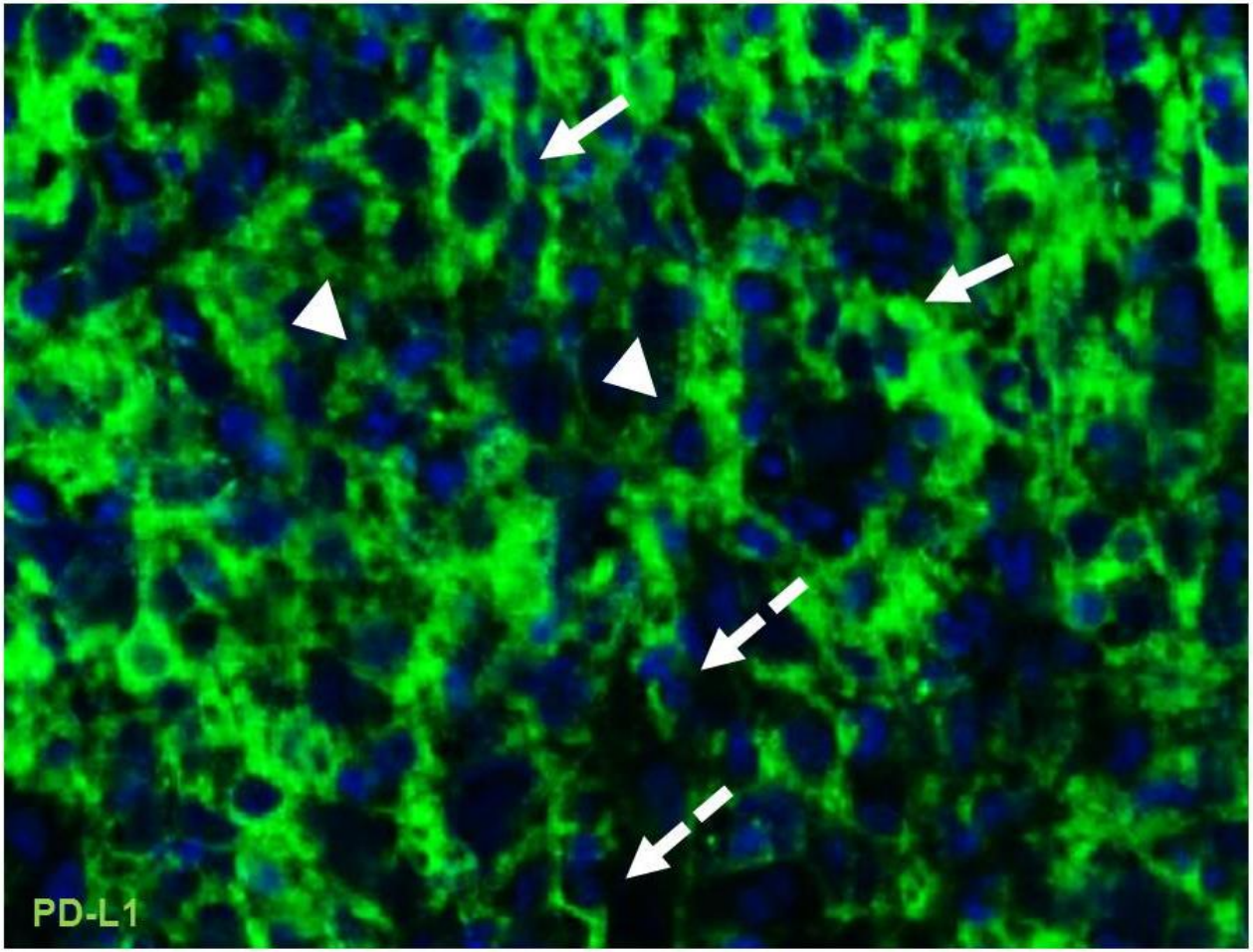

Figure 3.18 show different patterns of the sub-cellular localization of PD-L1 expression in NPC. An example of diffuse type of PD-L1 (green) expression in NPC, with membranous complete (white arrow), membranous incomplete (white broken arrow) in addition to cytoplasmic staining (head white arrow head), (20X).

Table 3.16 indicates presence of either membranous (complete or incomplete), cytoplasmic or mixed staining.

Case number	Membranous		Cytoplasmic	Mixed (Either membranous complete, membranous incomplete +/- cytoplasmic)
	Complete	Incomplete		
1	+	+	+	+
2	+	+	-	+
4	+	+	+	+
7	+	+	+	+
8	-	-	-	-
9	+	+	+	+
10	-	+	+	+
11	+	+	+	+
12	+	+	-	+
14	+	+	+	+
15	+	+	+	+
16	-	+	-	-
17	-	+	-	-
18	+	+	-	+
20	+	+	+	+
21	+	+	+	+
22	-	+	+	+
Total	12	16	11	14

3.2.9 Classification of PD-L1 expression into tumour predominant and immune predominant types

I next classified the NPC samples into immune predominant or tumour predominant, based on the cell phenotype in which PD-L1 is most highly expressed. Tumour predominant was defined as PD-L1 expressing cells are observed more in the tumour cells than the immune cells (TILs or others), while immune predominant was defined as PD-L1 expressing cells are dominantly immune cells (TILs or other) more than the positivity observed in the tumour cells. This was based on a recent study of head and neck SCC that classified PD-L1 phenotypes into immune predominant or tumour predominant. This is important because in these tumours the immune predominant form confers a better survival independently of other clinical parameters, including HPV status and stage **(Heeren et al., 2016)**. I found that 14/16 cases were of tumour predominant type, and only 2 were of immune phenotype type (Table 3.17). Examples of both types are shown in Figure 3.19.

PD-L1 positive, tumour predominant

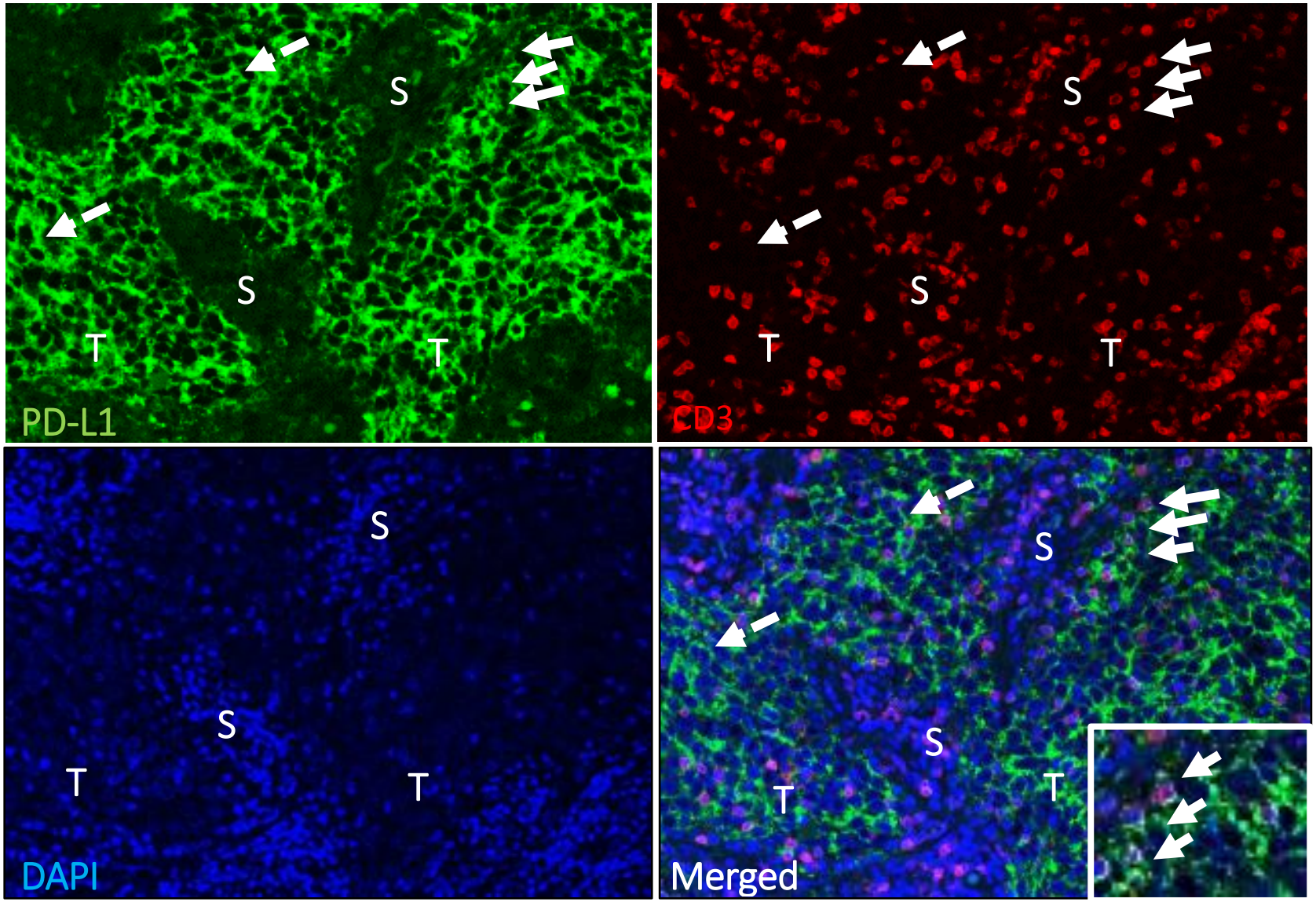

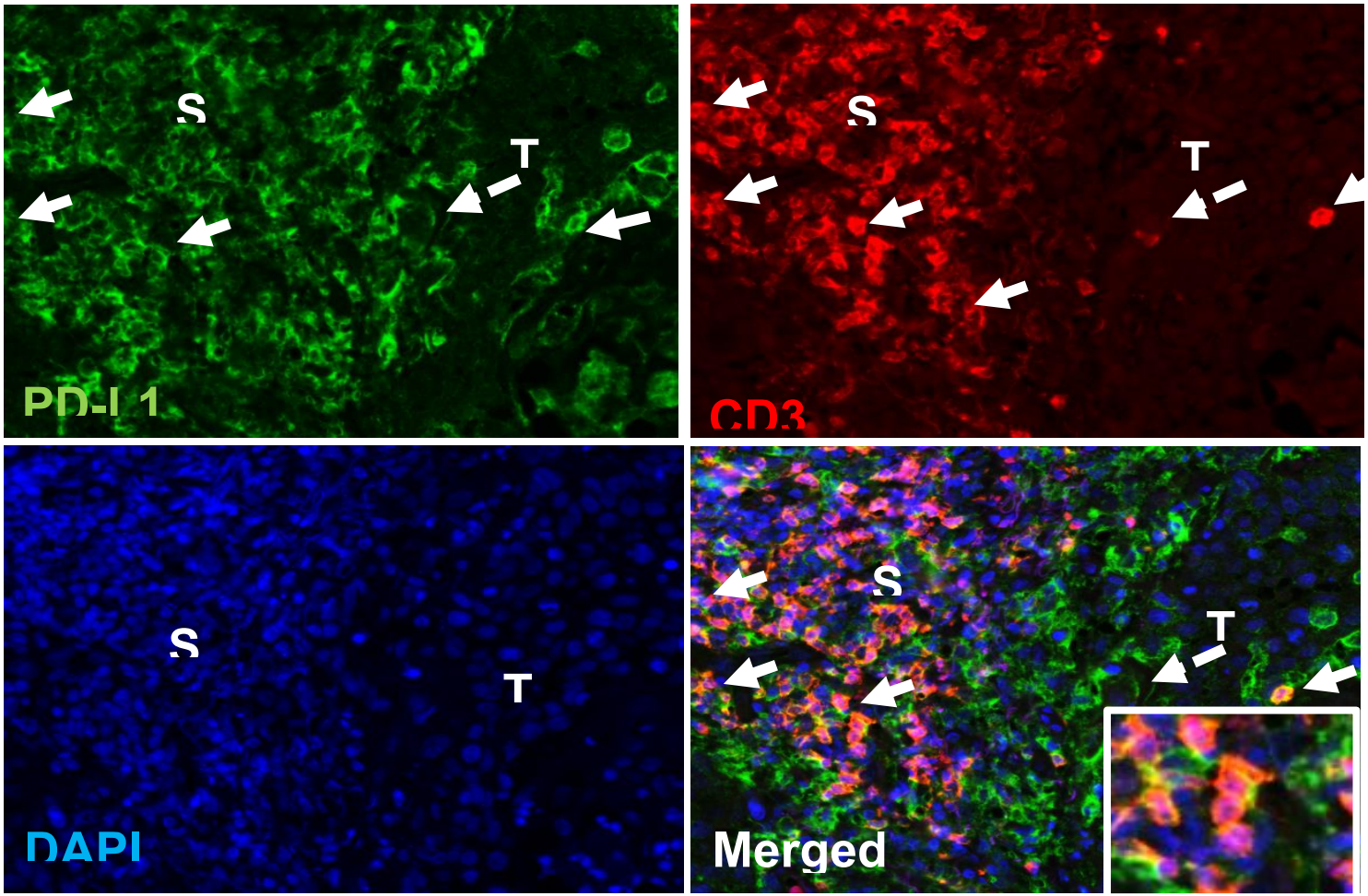

Figure 3.19 Classification of PD-L1 expression into tumour predominant and immune predominant subtypes, Top panel, Tumour predominant type: PD-L1 expression (green) is predominantly present in the tumour (broken white arrows) and in few CD3 T cells expressing PD-L1 (white arrows). Bottom panel, Immune predominant type: PD-L1 is expressed mainly by immune cells, such as CD3 cells (white arrows) and in few tumour cells (broken white arrows) 20X.

Table 3.17 summarizes PD-L1 expression patterns in NPC

Case number	Tumour predominant (TP) versus immune predominant (IP)	PD-L1 positive intra-tumour assessment		PD-L1 positive stroma assessment
		PD-L1 expression by tumour	PD-L1 +ve CD3 T cells	PD-L1 +ve CD3 T cells
1	TP	Diffuse	Present (low)	Present (low)
2	TP	Marginal (circumferential)	Present (low)	Present (low)
4	TP	Diffuse	Absent	Present (low)
7	TP	Diffuse	Present (low)	Present (low)
8	Negative	Negative	Negative	Negative
9	TP	Diffuse	Present (low)	Present (low)
10	TP	Marginal (focal)	Present (low)	Present (low)
11	TP	Diffuse	Present (high)	Present (low)
12	IP	Marginal (focal)	Present (low)	Present (high)
14	TP	Diffuse	Present (low)	Present (low)
15	TP	Diffuse	Present (low)	Present (low)
16	TP	Marginal (focal)	Present (low)	Present (low)
17	IP	Marginal (focal)	Present (low)	Present (low)
18	TP	Marginal (circumferential)	Present (low)	Present (high)
20	TP	Diffuse	Present (low)	Present (low)
21	TP	Marginal (focal)	Present (low)	Present (high)
22	TP	Marginal (focal)	Present (low)	Absent

3.2.10 T cells expressing PD1 are in direct contact with PD-L1 positive NPC tumour cells

PD-L1 was only expressed on immune cells, and not on tumour cells. PD1-positive T cells were in direct contact with PD-L1 positive tumour cells (Figure 3.20 A-E). Next, I examined the correlation between PD1 and PD-L1 frequency in the tumour versus stroma. Figure 3.21 F, is an illustration of scatter plotting of all cases, for PD-L1 versus PD1 frequency in the intra-tumour compartment and Figure 3.20 G plot for PD-L1 and PD1 in the stroma. I found no significant correlation between PD-L1 and PD1 expression in the intra-tumour compartment ($r= 0.1494$ and $p=0.592$), while I found a significant correlation using Pearson correlation between PD1 and PD-L1 expression in the stroma ($r= 0.74$ and $p=0.000683$). PD1 correlates with the PD-L1 expression in the stroma but not in tumour. This can be explained by higher level of expression of PD-L1 (tumour) more than PD1 (tumour), mean of scores were 27.98% and 13.6%, respectively. This can be explained by the presence of half of the samples were PD-L1 expressing -diffuse type. In addition, PD-L1 was present more in the tumour (27.98%) not the stroma (9.69%), respectively, this is matching with tumour predominant and immune predominant classification seen in figure 3.19.

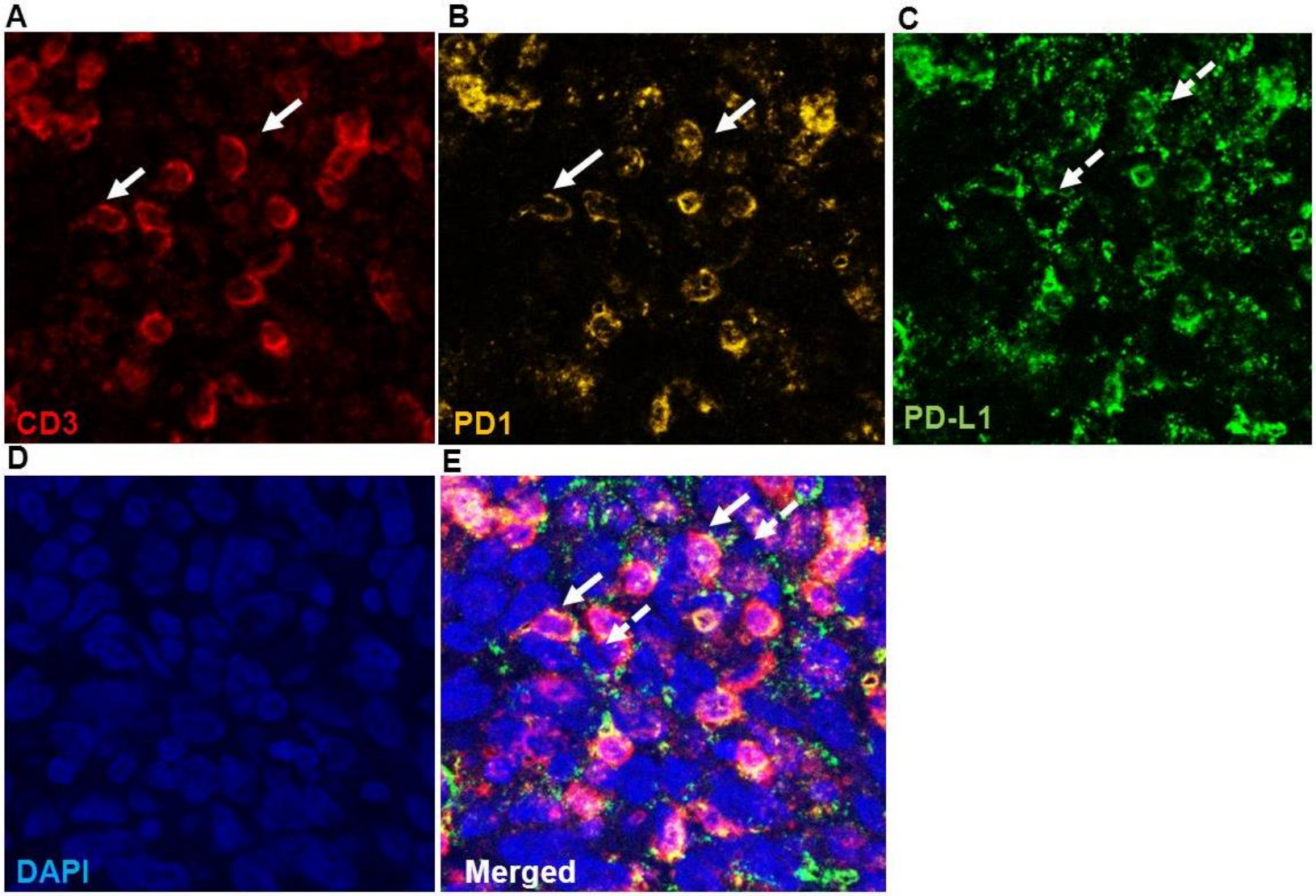

Figure 3.20 Multiplex co-staining for PDL-1-PD1-CD3 expression in NPC A-B) PD1 (yellow) is expressed in CD3-positive cells (red) at white arrows, C) show that these cells are in direct contact with PD-L1 (green) positive tumour cells (broken white arrows), D) DAPI staining the nuclei (blue), E) Merged of all channels (20X), (T) indicates tumour, (S) indicates stroma.

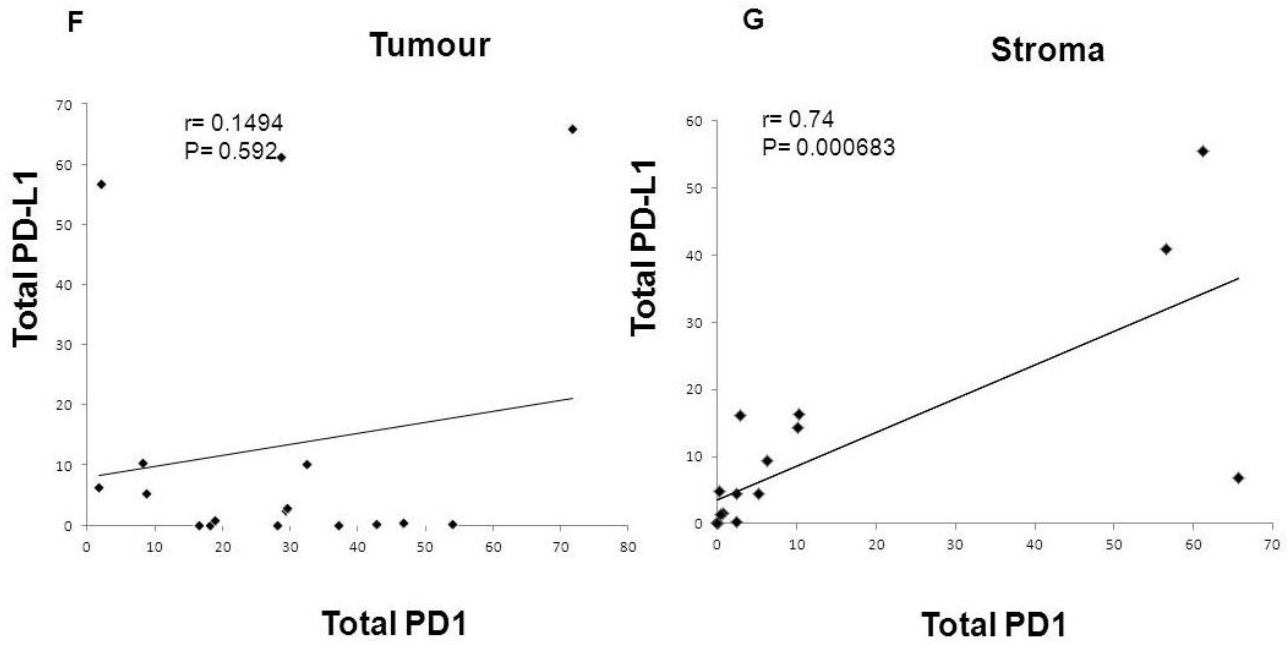

F-G) Plot show a significant positive correlation between the frequency of PD-L1 and PD1 positive cells in the stroma but not in the tumour compartment.

3.2.11 T cell expression of PD-L1 in NPC

14/17 cases showed PD-L1 expression on CD3-positive T cells. PD-L1 expressing T cells were predominantly in the intra-tumour compartment as opposed to the stroma (mean PDL-1 positive/all CD3+=17.64 versus 6.6, respectively; p=0.01; Figure 3.21 and Figure 3.22). There was no significant difference in the frequency (percentage of positive cells) of PD-L1 expression in T cells between diffuse and marginal type NPC.

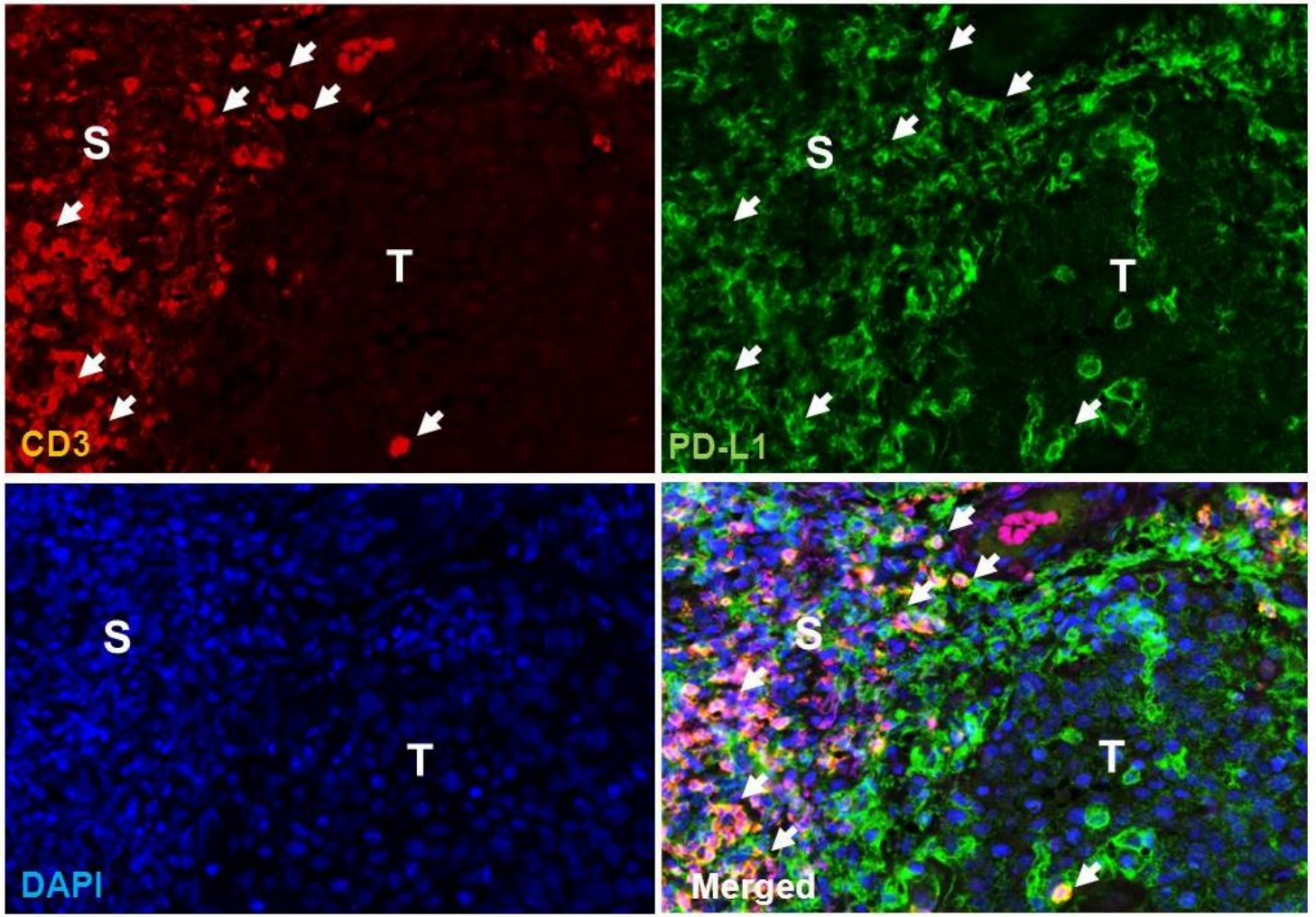

Figure 3.21 Expression of PD-L1 in CD3 positive cells in NPC Four panels, showing tumour and stromal compartments showing scattered T cells highlighted with CD3 (red) are seen expressing PD-L1 at the white arrow, 20X. (T) indicates tumour, (S) indicates stroma.

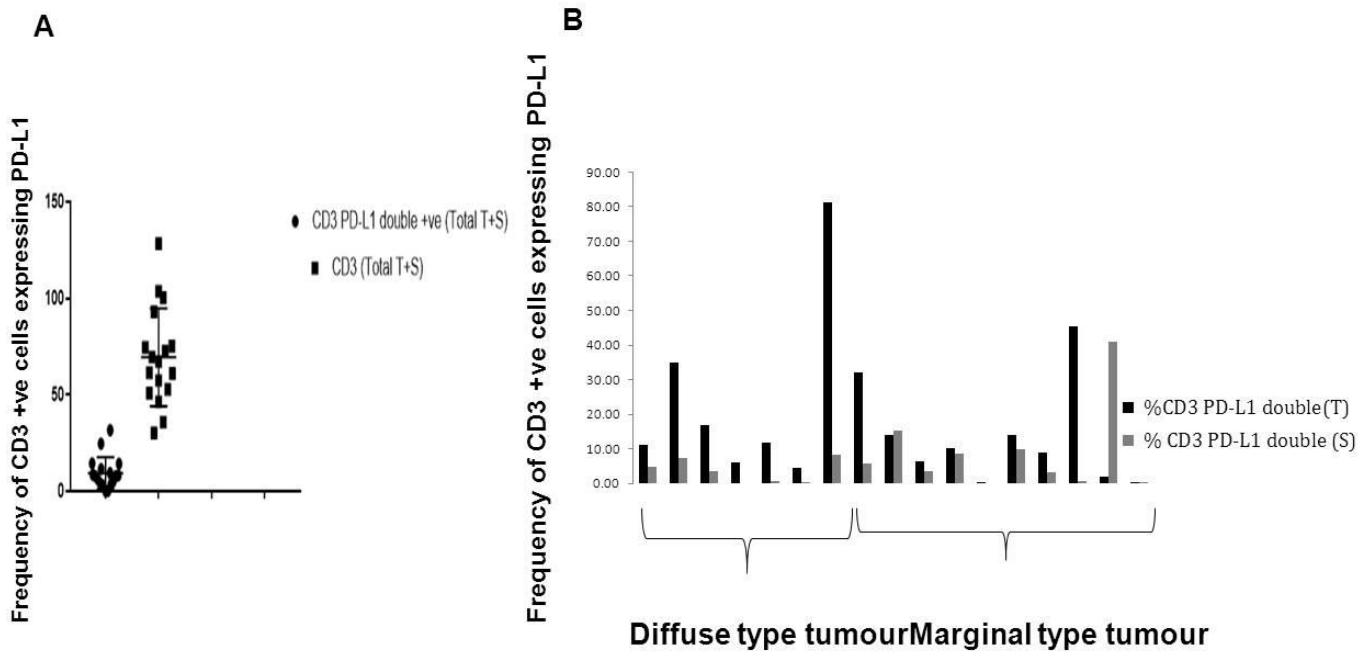

Figure 3.22 Significant enrichment of CD3 expressing PD-L1 as represented by CD3-PD-L1 double phenotype, in intra-tumour and stroma

A) The graph shows the proportion of CD3 expressing PD-L1 with significant difference between PD-L1 double positive CD3 distributed in tumour or stroma, ($p= 0.01$), B) however, there were no significant difference between CD3 expressing PD-L1 in marginal and diffuse types.

In summary the data on PD-L1 expression in NPC shows that it:

- is higher in NPC compared to normal epithelium
- is not correlated with LMP-1 expression in primary NPC
- is correlated with the expression of other immune checkpoints, particularly PD-L2
- is correlated with PD1 expression in the stroma
- can be either diffuse or marginal
- can be expressed on T cells particularly in the intra-tumour compartment.

3.3 RESULTS PART TWO: Frequency of cells expressing FOXP3, CD4, CD8 and CD20 in NPC

In the following section, I focus my description of the microenvironment of NPC on an analysis of the phenotype of T cells, and the presence of B cells.

3.3.1 Optimizing a lymphocyte subpopulation panel in tonsil

First, I tested the staining for the following markers: CD8, FOXP3 and CD20 (hereafter referred to as the 'lymphocyte subpopulation panel'). CD20 stains the GCB cells and the mantle zone B cells, while for T cell subsets, CD8 was positive in numerous extra-follicular T cells and FOXP3 was shown to be positive in the nuclei of T lymphocytes in the GC and in the inter-follicular regions (Figure 3.23).

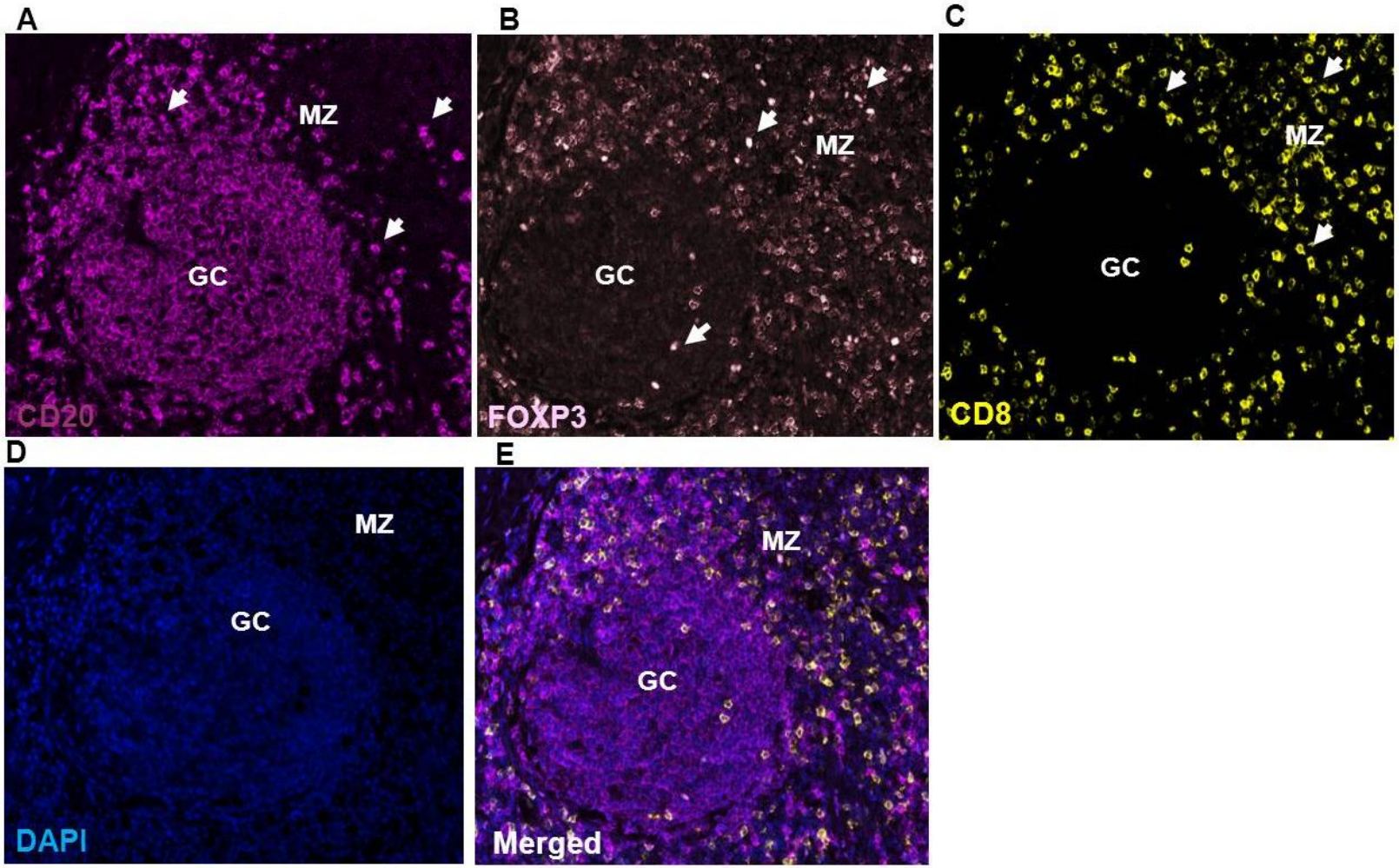

Figure 3.23 Multiplex IF for the 'lymphocyte subpopulation panel'
CD8 (yellow) stains mainly within the T cell zone (white arrows), FOXP3 (pink) is expressed by scattered lymphocytes, inside and many of the cells outside the GC (white arrows), CD20 (magenta) is expressed in GC and mantle zone naïve B cells (white arrows), left lower panel DAPI staining the nuclei (blue), (20X). (GC) indicates germinal centre, (MZ) indicates mantle zone.

3.3.2 Frequency of T and B cells in NPC

Next, I measured the frequency of the sub-population of cells stained with the 'lymphocyte subpopulation panel' (Table 3.18). There were no significant differences in the frequency of cells positive for CD8, FOXP3 and CD20, in the tumour compared with the stroma (Figure 3.24).

Table 3.18 Summary of quantification of frequency of CD8, CD20 and FOXP3 positive cells distributed in the tumour and stroma using the lymphocyte multiplex panel

Case ID	% of CD8 +ve cells		% of FOXP3 +ve cells		% of CD20 +ve cells	
	Tumour	Stroma	Tumour	Stroma	Tumour	Stroma
1	4.1	4.9	2.1	1	4	3.3
2	11	18.1	2.8	3.4	13.7	21.2
4	33.4	25.5	31	10.4	1.1	9.5
7	2.7	3.3	1.3	1.5	6.6	15.9
8	7.3	2.5	7	4.2	1.8	7.1
9	15.4	27	7.5	11.2	3.9	19.8
10	43.6	22.5	16.5	4	5.4	3.3
11	9.8	9.4	4.3	13.4	7.7	3
12	11	10.8	73.9	44.1	3	9.4
14	21	10.4	8.2	2	1.9	2
15	3.9	2.7	0.1	0.4	31.3	25.2
16	4.6	2.8	2.4	1.2	1.1	1.4
17	4.3	7.5	0.9	0.9	4.1	0.5
18	5.2	14.7	4.5	4.8	4.9	3.4
20	13.6	8.8	10.6	7.8	24.5	14.3
21	16.8	11	1.9	2.8	8.4	9.3
22	17.2	46.6	9.5	19.2	1.7	1.5
Median	10.4	9.9	5.8	4.1	4.5	8.2
SD	11	11.1	17.4	10.4	9.1	7.6

SD indicates standard deviation, +ve indicates positive.

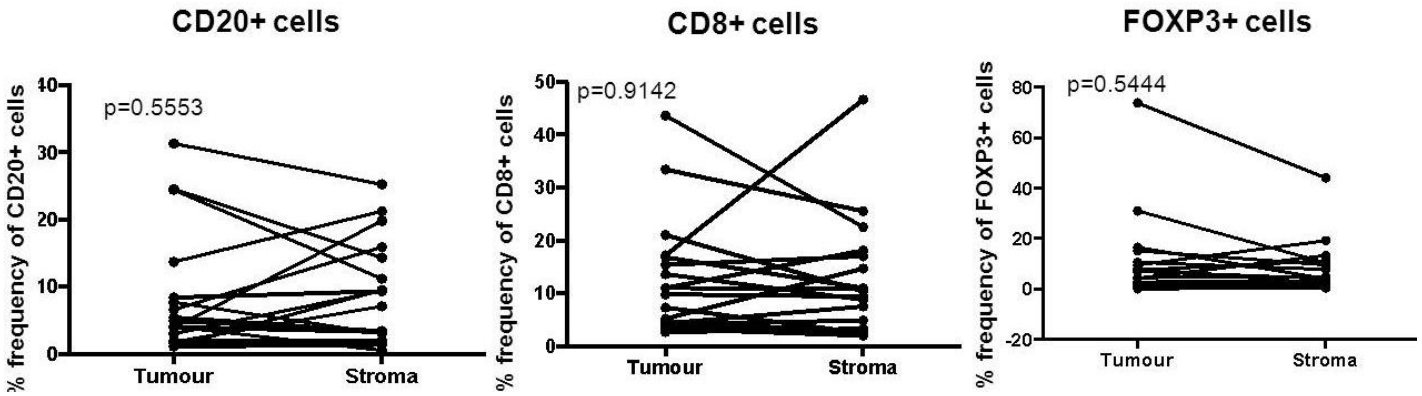

Figure 3.24 Frequency of CD8, FOXP3 and CD20-positive cells in stroma and tumour of NPC

There were no significant differences in the frequency of cells positive for CD8, FOXP3 and CD20, in the tumour compared with the stroma.

3.3.3 FOXP3 is present in the majority of CD3-positive and CD4-positive but rare in CD8 positive T cells in NPC

I co-stained a subset (8 cases) of NPC tumours for CD4, CD3, CD8 and FOXP3. I found that most FOXP3 expressing cells were CD3 and CD4-positive, whereas only a minority were CD8-positive (Figure 3.25).

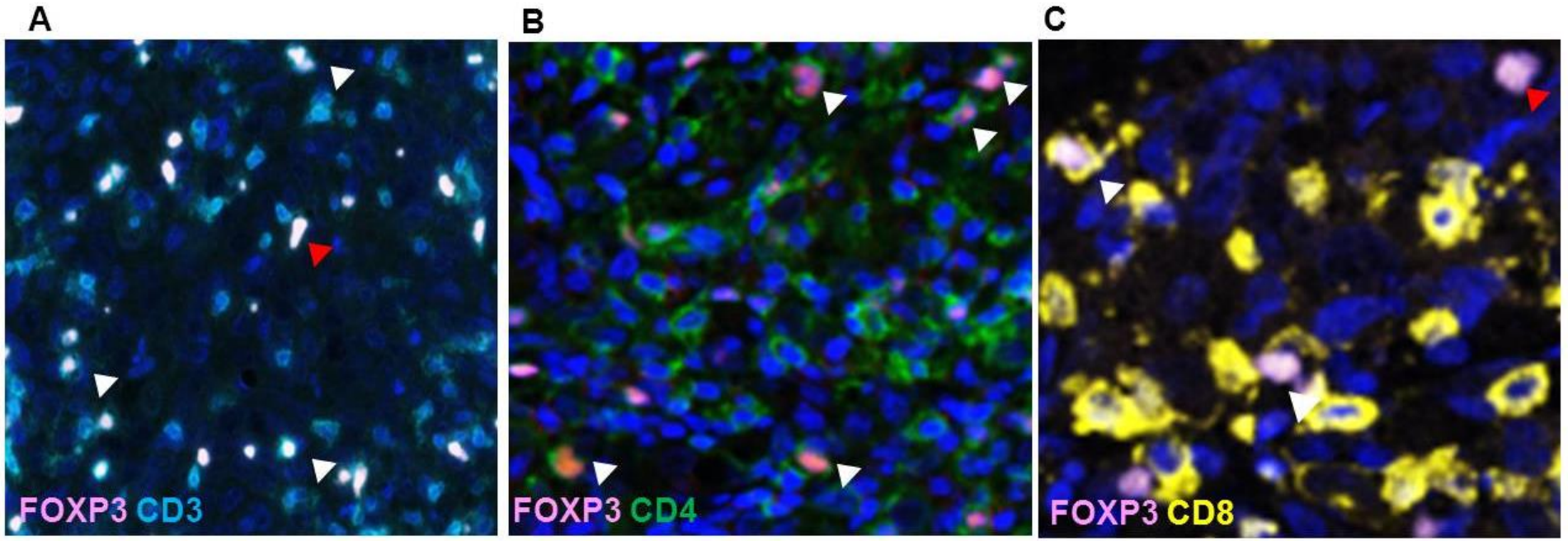

Figure 3.25 Phenotypic analyses of FOXP3 positive cells in NPC
FOXP3 is present in the majority of CD3/CD4-positive T cells but rare in CD8 positive T cells in NPC. A) FOXP3 (pink) is in the nuclei of scattered CD3 positive T cells (cyan) at the white arrows head. Occasional FOXP3 positive cells are negative for CD3 at the red arrow. B) FOXP3 (pink) is positive in the nuclei of scattered CD4 (green)-positive cells (white arrows head). C) FOXP3 (pink) is positive in the nuclei of immune cells (red arrow), and occasional nuclei of CD8 positive T cells (yellow) at the white arrow (20X), (T) indicates tumour, (S) indicates stroma.

3.4 RESULTS PART THREE: MHC class I and MHC class II expression in NPC

In the final section, I describe the results of IHC for MHC class I and class II expression in NPC.

3.4.1 MHC class I protein expression in NPC

MHC class I expression was measured by H-score in tumour and adjacent epithelium. Immune cells were used as a positive internal control. MHC class I was negative in 1/19 NPC. In 18/18 cases tumour cells were heterogeneously positive. 12/18 patients had a tumour MHC class I H-score lower than the median of the normal epithelium (Figure 3.26 and Table 3.19). MHC class I expression patterns in tumour were as follows: MHC class I was strongly expressed in tumour cells in a diffuse pattern (constitutively high) Figure 3.27 A, while other tumours showed decreased expression of MHC class I with some groups of tumour cells positively stained, while others were negative (beneath the positive covering epithelium) (Figure 3.27 B).

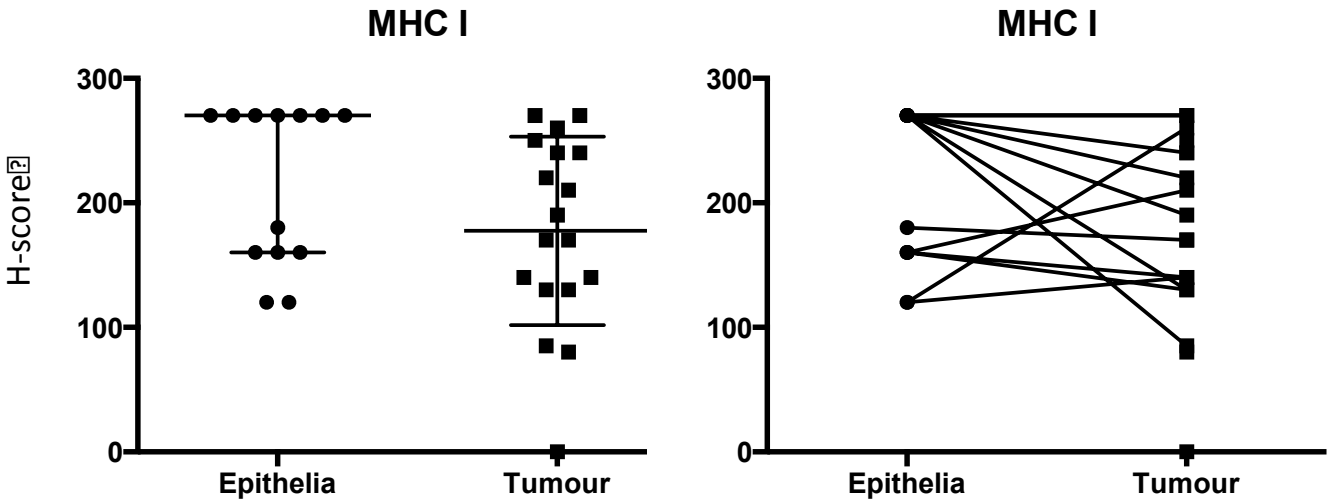

Figure 3.26 MHC class I IHC H-scores in NPC tumour cells compared with the covering epithelium

MHC class I was negative in 1/19 NPC. In 18/18 cases tumour cells were heterogeneously positive for MHC class I but in 12/18 cases expression was lower than the median of that in covering epithelium (Table 3.19)

Table 3.19 Results of MHC class I IHC expression in tumour and covering epithelium

Case number	Tumour H-score	MHC class I status of stromal cells	Covering epithelium H-score
1	140	Positive	160
2	260	Positive	120
4	130	Positive	160
6	270	Positive	270
7	85	Positive	270
8	190	Positive	270
9	170	Positive	180
10	80	Positive	NA
11	170	Positive	160
12	210	Positive	270
14	270	Positive	120
15	140	Positive	270
16	130	Positive	NA
17	250	Positive	270
18	220	Positive	NA
20	0	Positive	270
21	240	Positive	270
22	240	Positive	270
Median	180		270
Mean	177.5		218.6
SD	75.5		63.5

SD indicates standard deviation, +ve indicates positive, NA indicates non available.

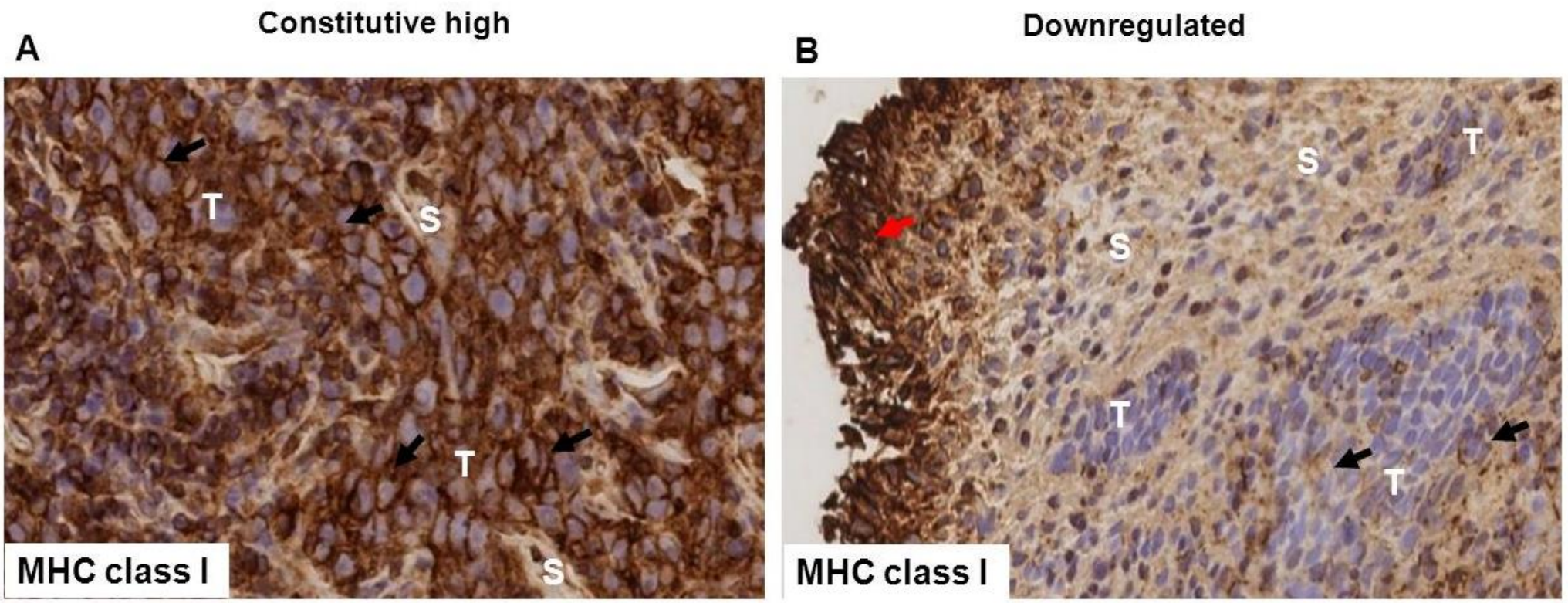

Figure 3.27 MHC class I expression in NPC

A) MHC class I is strongly positive in tumour cells (black arrows), 20X, B) Tumour cells are focally positive for MHC class I (black arrows), with some tumour clusters negative. Covering epithelium is strongly positive (red arrow), 20X, (T) indicates tumour, (S) indicates stroma.

3.4.2 MHC class II protein expression in NPC

MHC class II was absent in 1/19 cases. 18/19 cases were positive but heterogeneously. 10/18 patients had a tumour MHC class II H-score lower than the median of the covering epithelium (Figure 3.28 and Table 3.23). I found that thirteen NPC patients had MHC class II positive stromal cells. Two patients had scattered MHC class II positive TILs. Two patients had few MHC class II positive TILs. These stromal cells may include tumour-associated macrophages and TILs, but to distinguish and confirm this will require extra-stains. (Figures 3.29-3.31).

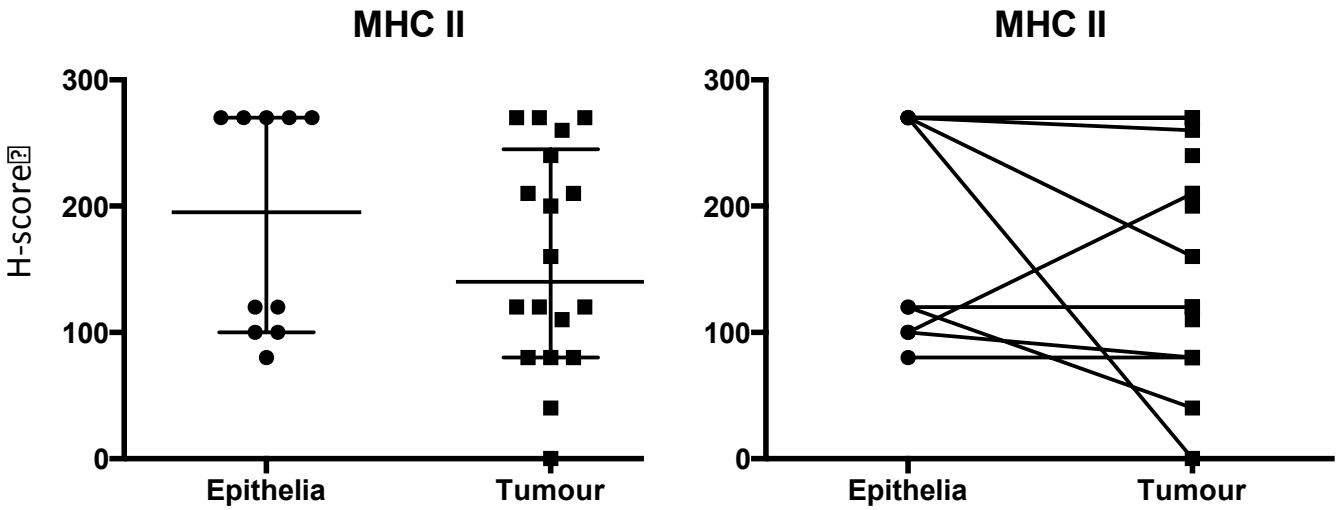

Figure 3.28 MHC class II H-scores in the NPC tumour cells and the covering epithelium

MHC class II was absent in 1/19 cases, which was strongly stained for MHC class I. 18/19 cases were positive for MHC class II but heterogeneously. 10/18 patients had a tumour MHC class II H-score lower than the median of the covering epithelium.

Table 3.20 Results of MHC class II IHC expression in tumour and covering epithelium

Case number	Tumour H-score	MHC II status of stromal cells	Covering epithelium H-score
1	270	Positive	270
2	260	Positive	270
4	210	Positive	100
6	80	Positive	100
7	120	Positive	NA
8	160	Positive	270
9	270	Positive	270
10	40	Positive	120
11	240	Positive	NA
12	80	Positive	80
14	270	Positive	NA
15	120	Positive	NA
16	0	Positive	NA
17	110	Positive	NA
18	120	Positive	120
20	80	Positive	NA
21	200	Positive	NA
22	210	Positive	NA
Median	10.4		195
Mean	157.8		187
SD	86		88.2

SD indicates standard deviation, +ve indicates positive, NA indicates non available.

A

Constitutively off

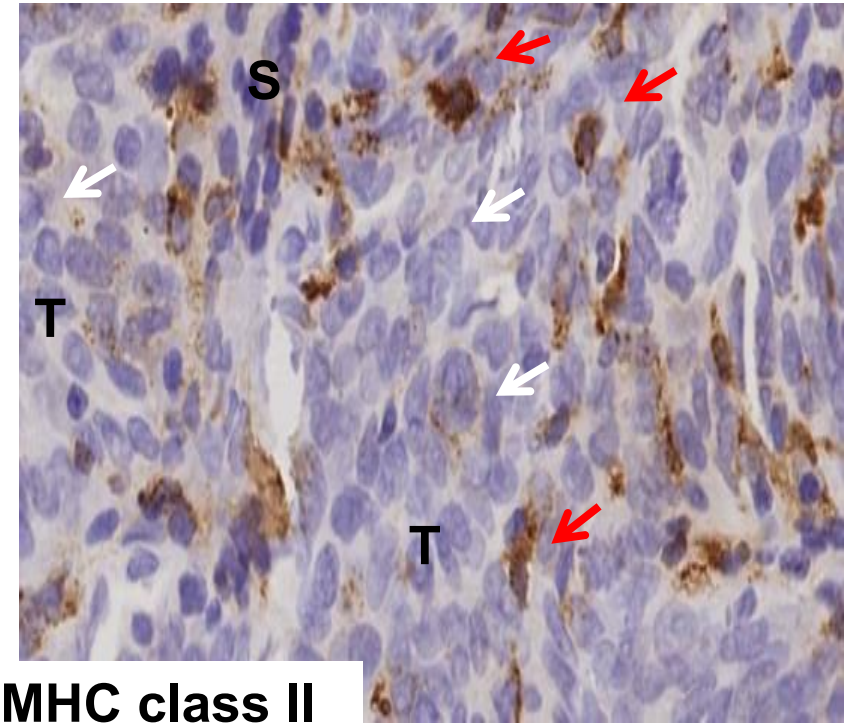

MHC class II

B

Downregulated

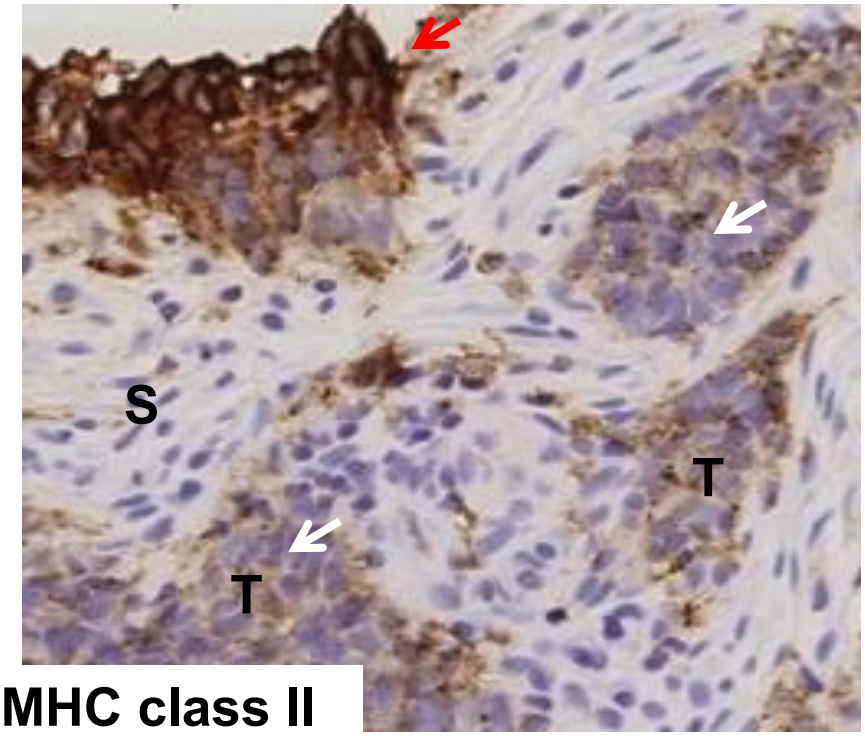

MHC class II

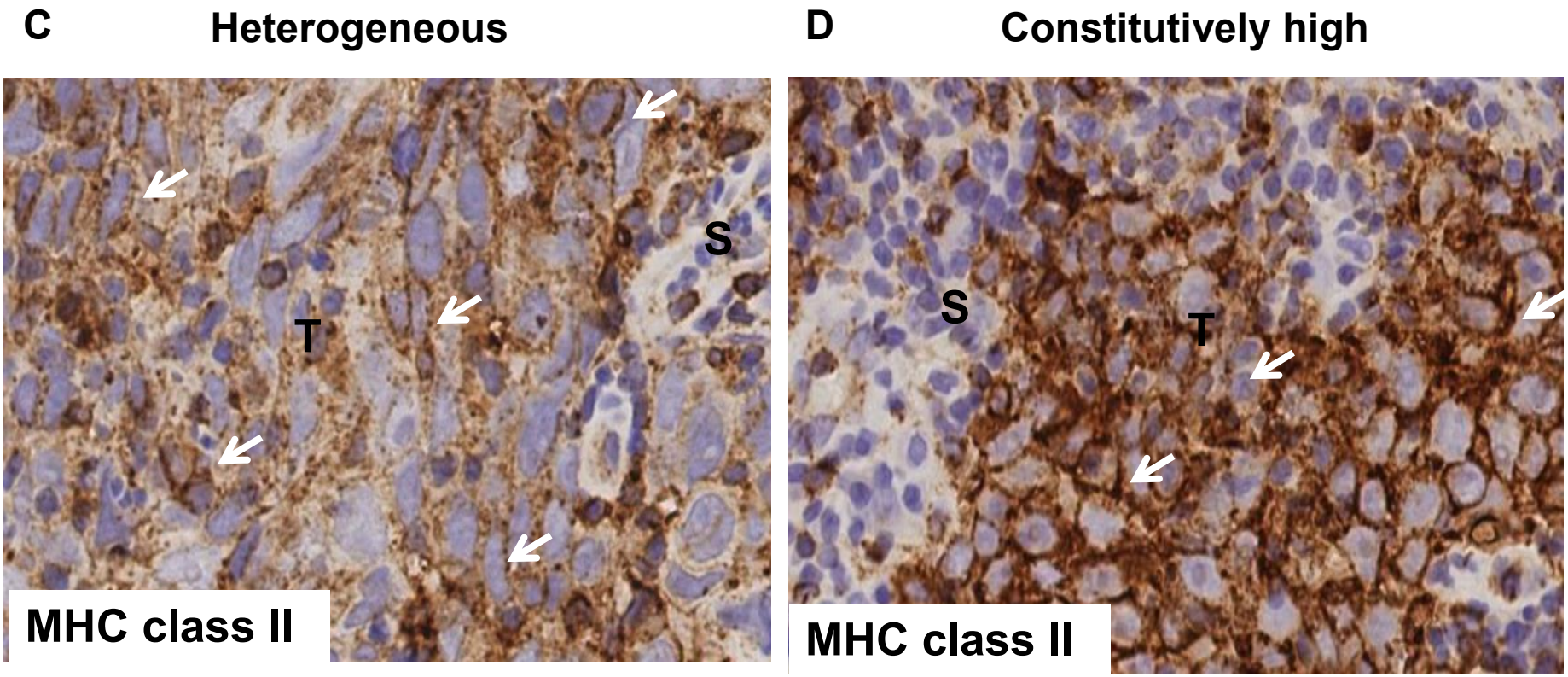

Figure 3.29 MHC class II expression in NPC A) MHC class II was strongly positive in stromal cells (red arrows), but negative in the tumour cells (white arrows) 20X, B) Tumour cells are focally positive (white arrows), while the covering epithelium is strongly positive (red arrows), 20X, C) Tumour cells showing heterogeneous pattern, some tumour cells are weakly positive while others are moderately stained (white arrows) 20X, D) MHC class II diffuse strong positive in tumour cells (white arrows) 20X, (T) indicates tumour, (S) indicates stroma.

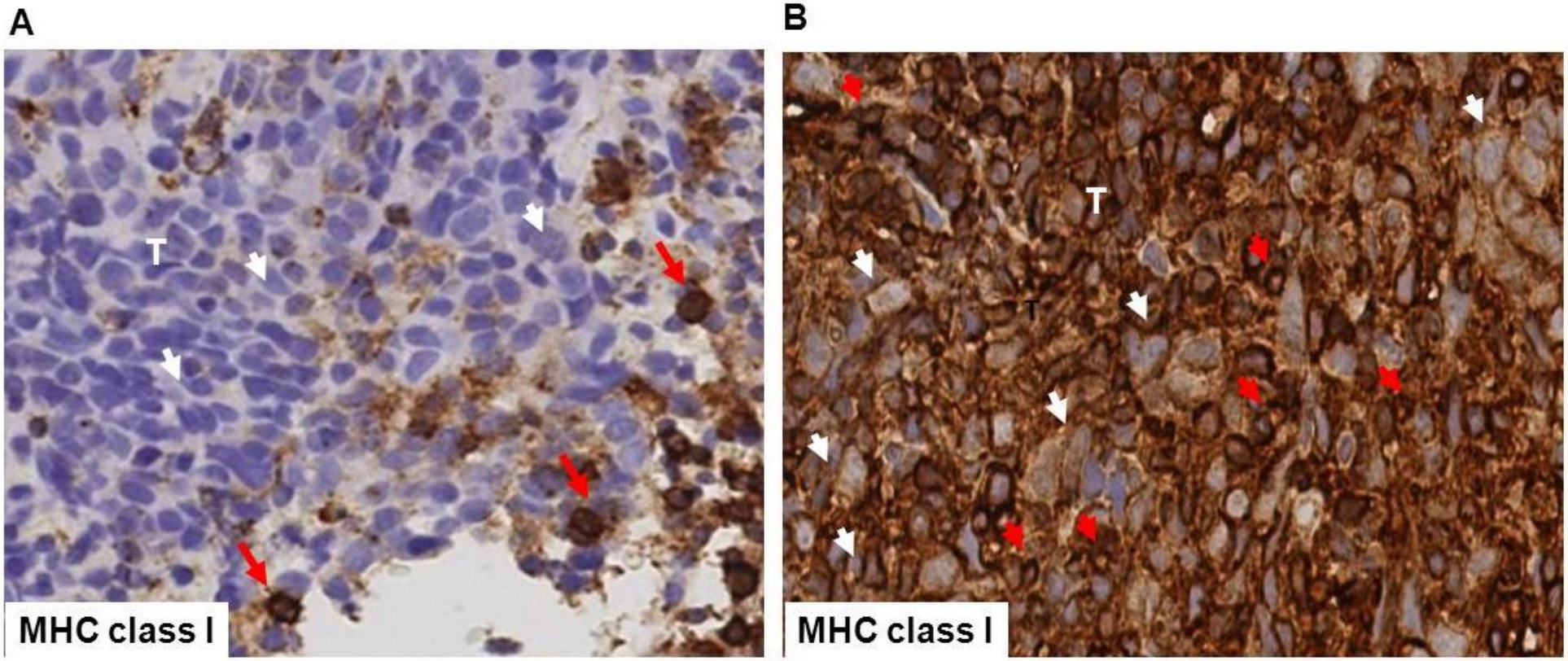

Figure 3.30 MHC class II expression in TILs of NPCA) MHC class II negative case (white arrows), with sparse TILs that are positive for MHC class II (red arrows), 20X B) 20X, Tumour is diffusely positive (white arrows) with scattered positive TILs within the tumour (red arrows) TILs indicates Tumour infiltrating lymphocytes.

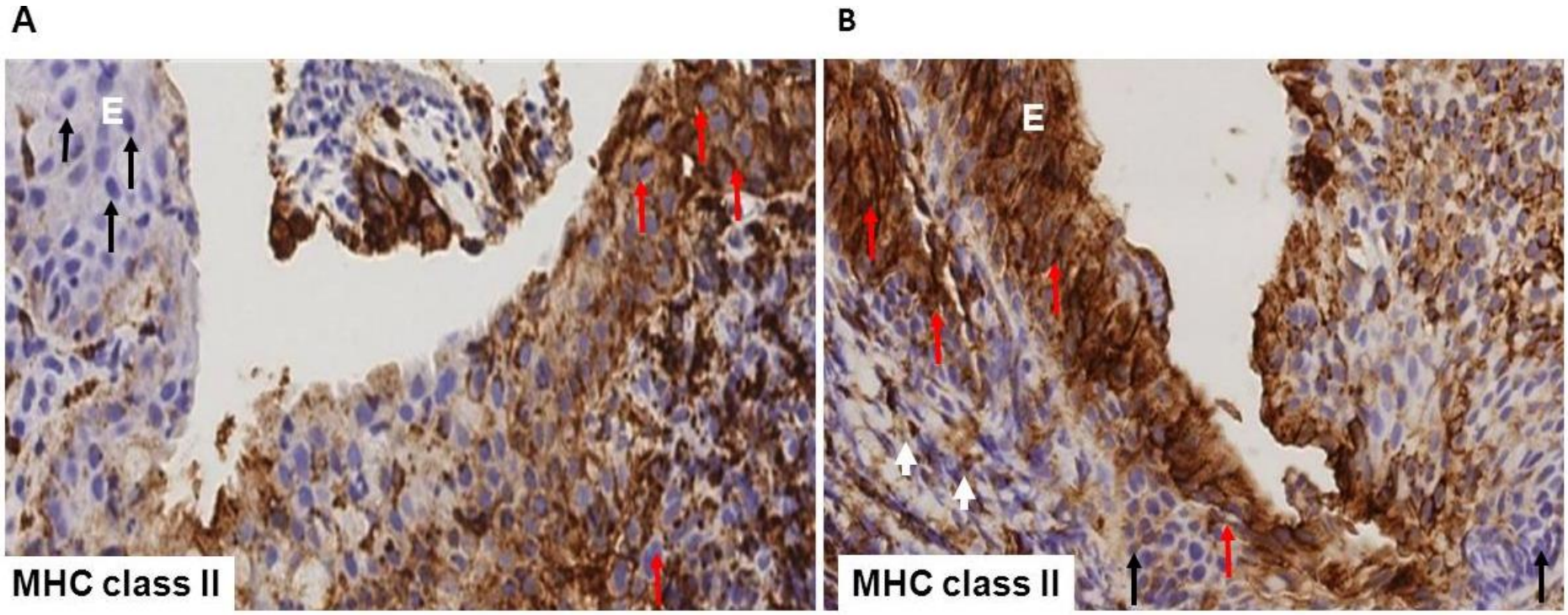

Figure 3.31 MHC class II expression in overlying epithelium
A) MHC class II was positive partially in the dysplastic epithelium (red arrows), while the adjacent normal looking epithelium was negative (black arrows) 20X B) Another example showing covering epithelium positive in the upper two thirds of the epithelium (red arrows), negative is labelled at the white arrows. The underlying stromal cells are also positive (white arrows), D) 20X.

3.4.3 MHC class I and class II expression in NPC

Next, I explored if MHC class I and MHC class II were co-expressed or downregulated in the same sections. I identified three patterns: A) Tumours with high H-scores for both markers, B) tumours with high H-scores for MHC class I but lower MHC class II scores or C) vice versa. Low and high MHC class I and II scores were defined based on the value of the median of the H-score, in the case of MHC class I the median was 170, while for MHC class II, the median was 160. (Figure 3.32 and table 3.21.

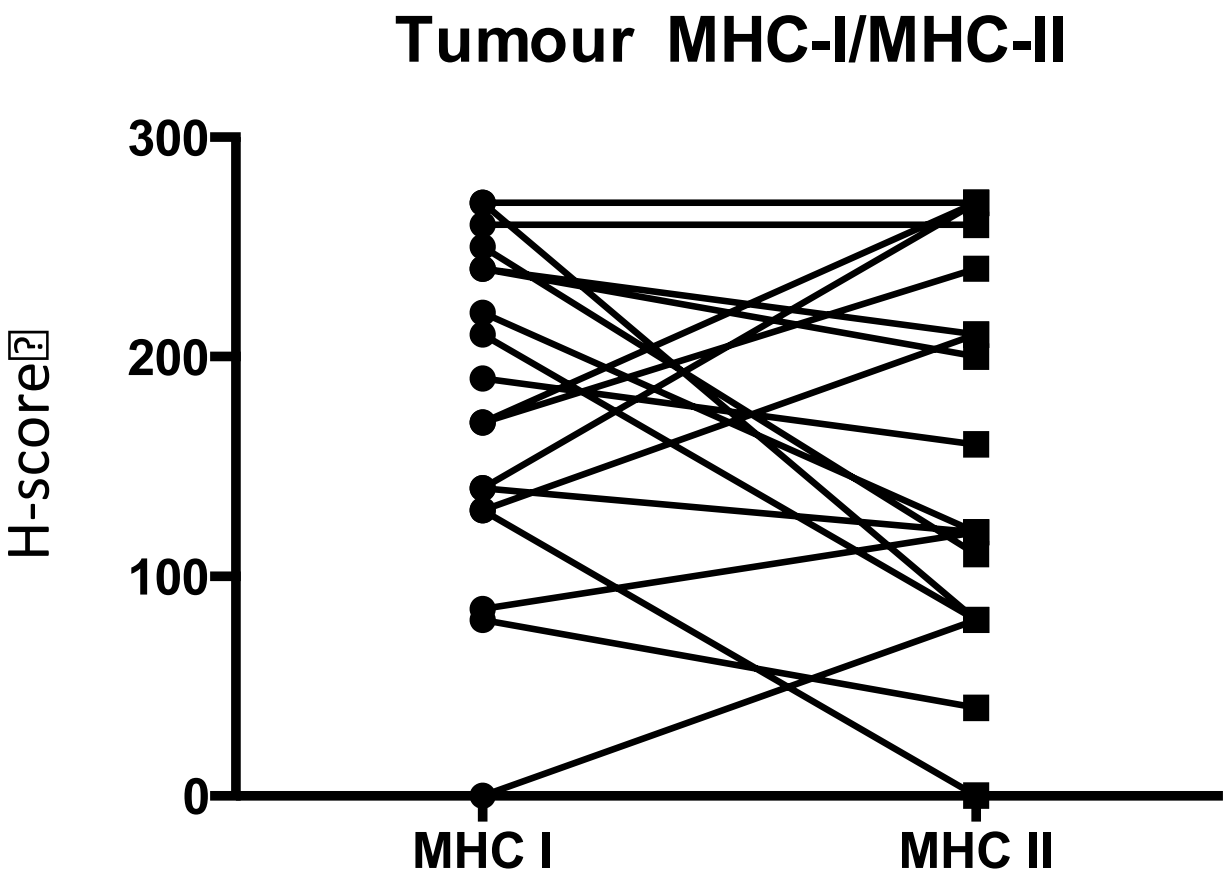

Figure 3.32 MHC class I and MHC class II IHC expression H-scores by tumour cells

H-scores of MHC class I and MHC class II expression for each patient are shown.

Table 3.21 An illustration of MHC class I and class II scores in matched NPC cases

MHC-I and-II score classification	Number of cases
Tumours with low both MHC class I and-II	5
Tumours with high H-scores for both markers	6
Tumours with high H-scores for MHC class I but lower MHC class II scores	3
Tumour with absent MHC class I and low MHC class II	1
Tumour with absent MHC class I and low MHC class II	1
Tumours with high H-scores for MHC class II but lower MHC class I scores	2
Total number of cases	18

3.4.4 Correlation of NPC IHC data

Finally, I was interested to explore the possible correlation between all of the markers I had stained on a whole cohort basis. To do this a correlation matrix was created in which each marker was compared to all the others (Figure 3.33). This analysis revealed several interesting correlations. First, it showed a correlation between; MHC class I expression and PD1-positive immune cells in the tumour (r=0.43), MHC class I and MHC class II expression and CD3+ cells in the stroma (r=0.43 and 0.45 respectively); and MHC class II expression on the tumour cells and PD-L1 expression on the tumour cells (r=0.61). These results might have been expected since MHC expression would be required for the presentation of viral or cellular neo-epitopes to T cells.

This analysis also revealed a correlation between CD3+ cells and CD8+ cells in the tumour and stroma (r=0.35 and r=0.53, respectively), as well as FOXP3+ cells in the tumour (r=0.35). There was also a strong correlation between CD8+ cells in the tumour or stroma and FOXP3+ cells in tumour or stroma (r=0.57-0.77), this correlation between T-reg and CD8+ cells may indicate active immune response, recruiting T-reg, suggesting that high numbers of CD8+ cells may be functionally inhibited by T-regs. T-regs infiltration was reported to be associated with immunosuppression and tumour development in various cancers **(Szylberg et al., 2016)**. Positive correlation of stromal CD3+ cells, CD8+ cells with stromal PD-L1+ cells and PD1+ cells may implicate the presence of anti-tumour immune response which may induce PD-L1 overexpression. On the contrast to the aforementioned findings in the stroma, intra-tumoural CD3+ cells was negatively correlated with PD1+ and PD-L1+ cells in the tumour. This can be interesting, because previous report in colorectal immunoscore showed that low tumoural CD3 density was associated with inferior outcome **(Zhu et al., 2017)**. No correlation was observed between CD3 expression in the tumour and stromal compartments, which could be

explained by local inhibitory mechanisms within the tumour microenvironment which exclude T cells from the tumour (i.e. T cells remain preferentially localised within the stroma). Only weak correlation observed between PD-L1 expression within the tumour (T) and stromal (S) compartments, probably reflecting the different mechanisms controlling expression. For half of the cases (8/16) PD-L1 tumour expression was described as diffuse (intrinsic), which may result from tumour-specific changes such as increased NF-κB signalling, AKT-mTOR pathway activation, loss of PTEN etc. Marginal PD-L1 expressing tumour may be up-regulated by extrinsic mechanisms, such as induction by IFNγ or other inflammatory cytokines which will also act via the PI3K-Akt-mTOR pathway. A positive correlation was observed between stromal CD3+ cells and tumour and stromal PD-L1+ cells. As previously noted, PD-L1 expression may be induced by inflammatory cytokines, such as IFNγ, produced by T cells. The observed tumour PD-L1+ cells expression patterns include both marginal and diffuse; marginal is most often described as cytokine-induced, but diffuse (intrinsic) expression may still be increased by extrinsic mechanisms such as inflammatory cytokines. This is in broad agreement with the analysis of individual samples (Fig. 3.17 C), where a weak positive correlation was shown between CD3+ cells stroma and both PD-L1+ cells in the tumour and stroma. No or only weak correlation (positive or negative) observed between all of the lymphocyte subsets analysed (CD3, CD8, FOXP3, CD20) and PD1 which raises the question as to which cells are expressing PD1 as non T cells, such as NK cells or possibly macrophages or dendritic cells, as reported in other cancers that PD1 can be presented on non T cells, which needs to be further determined.

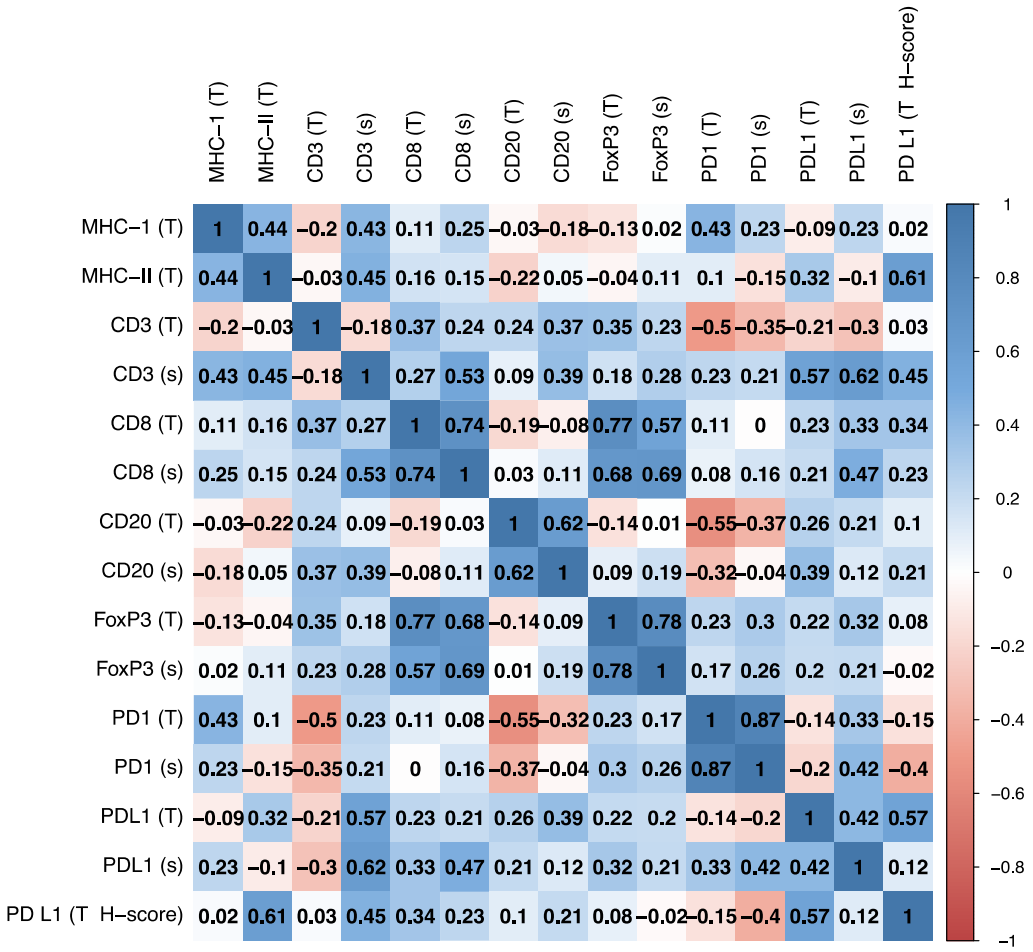

Figure 3.33 Correlation matrix of IHC protein expression levels determined by Inform/H-score for each marker used in this study Correlation matrix for 15 cases of NPC using Spearman's test for each marker. Apart from MHC class I and MHC class II (H-scores were used), all parameters are the frequency of cells positive for the marker in the tumour or stroma compartment. T indicates tumour, s indicates stroma.

3.5 DISCUSSION

In this study, I have described in detail the phenotypic characteristics of the tumour immune microenvironment of NPC, focussing on T cell phenotypes and especially on the expression of the T cell immune checkpoint mediated by PD-L1/PD1. There is currently much interest in using PD-L1/PD1 inhibitors against virus-associated cancers, such as NPC **(Hsu et al., 2015)**.

Results from current clinical trials using FDA approved PD1 inhibitors have been reported. One trial employed Pembrolizumab in patients with recurrent metastatic NPC and showed an overall response rate of 25.9% (27 patients: 1 CR, 6 PR, and 14 stable disease), in addition to other promising results in the form of reduction in target lesion size. In this trial, progression free survival (PFS) was reported to be 49.7% after 6 months and 28.9% after 12 months; the median duration of response was 10.8 months **(Hsu et al., 2017)**. Another phase II study using Nivolumab monotherapy, which has recruited 43 patients with recurrent and metastatic NPC is currently in progress. This study has reported an overall response rate of 19%, suggesting effectiveness of PD1 blockade in endemic non keratinizing NPC patients (NCT02339558) **(Ma et al., 2017)**.

I have confirmed previous studies that report the over-expression of PD-L1 in NPC. Perhaps somewhat surprisingly, I was not able to show that PD-L1 expression was significantly higher in cases that were LMP1-positive, given that LMP-1 has been shown to induce PD-L1 expression in cell lines. This is presumably because non-viral mechanisms to induce PD-L1 expression are operational in cases of LMP-1-negative NPC. In a recent study of the mutational landscape of NPC, it was shown that LMP-1 expression and mutations affecting negative regulators of NF-κB

expression (found in 41% of cases) are mutually exclusive in NPC, both pathways can lead to PD-L1 expression **(Li et al., 2017)**. This can point to the non LMP1-pathway mediated through NF-κB and could explain why I did not observe a correlation between PD-L1 and LMP-1 in my study. PD-L1 has also been shown to be upregulated by INF-γ in malignant melanoma cell lines **(Gowrishankar et al., 2015)**. This was mediated through activation of NF-κB and this mechanism was restricted to the inducible type of PD-L1 expression, however the underlying mechanism of constitutive type of PD-L1 in NPC is still unresolved **(Gowrishankar et al., 2015)**. Co-expression of immune checkpoint genes (PD-L1 and IDO1) were reported in a transcriptome analysis performed on muscle invasive bladder cancers, by re-analysis of the Cancer Genome Atlas (TCGA) and these immune checkpoint genes were identified in an immune genes cluster associated with an aggressive phenotype and d with poor outcome **(Ren et al., 2017)**. Recent data showed promising response to combined immune checkpoint inhibitors, of PD1 (Nivolumab) and CTLA4 (Ipilimumab), in late stage malignant melanoma, with response to treatment reaching 60% **(Larkin et al., 2015)**. The combination of CTLA-4 and PD1 blockade has been the most successful of all combinations currently tested, and is approved for the treatment of advanced melanoma **(Callahan et al., 2016)**. PD1 and CTLA-4 blockade in melanoma patients showed an increased rate of objective tumour responses as compared to blocking either checkpoint alone, supporting the notion that combinatorial checkpoint blockade may result in increased clinical benefit, with response rates of 40% across all dose levels examined **(Wolchok et al., 2013)**. One striking feature of this combination was the relatively high rate of complete responses or near-complete responses, however relatively high rate of toxicities were also observed **(Callahan, 2016)**. Currently, there is an ongoing

Phase II clinical trial recruiting 35 patients with advanced stage NPC, to assess responses to both Ipilimumab and Nivolumab (NCT03097939) **(Van Waes and Musbahi, 2017)**.

I found in the re-analysis of RNA-seq data from LMP-1 positive NPC patients that there was a significant positive correlation between the expression of PD-L1 with other immune checkpoints (PD-L2, HAVCR2, LAG3, ADORA2A, CTLA4, IDO1, BTLA followed by PD1). Importantly, apart from IDO1, these immune checkpoints have so far not been shown in NPC and need further investigation for potential future combinational therapy. For example, LAG3 and PD1 were shown to be co-expressed in TILs infiltrating murine ovarian cancer. This co-expression showed synergistic inhibitory action on T lymphocytes and inhibited the growth of the ovarian cancer, this was the observed with combined LAG3 and PD1 inhibition **(Huang et al., 2015)**. In my study, I found significant positive correlation between PD1 and LAG3 in NPC, similar to that described in a study of colorectal cancer **(Lal et al., 2015)**.

Importantly, PD-L1 was observed in both the tumour cells and the cells of the stroma, suggesting a contribution to this checkpoint from non-tumour cell populations. Regarding the distribution of PD-L1, almost half of patients had a diffuse pattern of PD-L1 staining in their tumours, a pattern which may reflect an intrinsic underlying mechanism, such as amplification as described in other tumours as head and neck SCC. Compared to the marginal type of PD-L1 expression, this constitutive/diffuse pattern was recently described to be associated with poor outcomes in patients with head and neck SCC **(Heeren et al., 2016)**

PTEN loss was reported to induce up-regulation of PD-L1 in colorectal cancer and to be associated with aggressive phenotype and associated with high potentiality

for metastasis **(Song et al., 2013)**. Whether mutations in PTEN in NPC impact on PD-L1 expression has not yet been explored. However, recent studies have shown that recurrent mutations involving the PI3-K pathway with involvement of mutations in PTEN gene, was not commonly observed in NPC **(Li et al., 2017)**. PTEN loss was shown in different types of cancer such as in glioma, breast and prostate and can increase PD-L1 expression mediated through activation of the AKT–mTOR pathway **(Parsa et al., 2007)**.

Clearly, studies assessing the impact of the pattern of PD-L1 expression on patient outcomes are warranted in NPC. The description in the present study, of the existence of focal and circumferential forms of marginal expression is novel and will also require future studies, both laboratory and clinical-based, in order to determine the significance of this finding.

I also observed a high density of PD1 expressing T cells in some NPC, which is in accordance with previous studies on NPC which showed high infiltration of PD1 positive immune cells **(Zhou et al., 2017b, Zhang et al., 2015)**. The co-expression of PD1 and PD-L1 is reported to be associated with decreased disease free survival in NPC patients **(Zhang et al., 2015)**. . However, overall I observed a weak negative correlation between PD1 and PD-L1 in the patient cohort studied. In passing I note that one patient with a particularly high frequency of PD-L1-positive cells also had a high frequency of PD1-positive cells.

I have also seen that NPC tumours can recruit FOXP3-expressing cells and these were present both within the tumour and the stroma, although more of them were present in the tumour areas. These results are broadly in agreement with data reported by Yip et al **(Yip et al., 2009).** Many of these FOXP3-expressing cells were CD4-positive, rather than CD8-positive T cells. In addition to regulatory T cells, the

presence of B cells in the microenvironment could also suppress the function of CD8 cells and also potentially convert effector T cells to T-reg **(Schwartz et al., 2016)**. Moreover, B cells were reported to have good or bad prognosis in different disease settings **(Schwartz et al., 2016)**. If infiltrating B-cells in the NPC microenvironment are suppressive then they may represent a therapeutic opportunity given the availability of B-cell depleting monoclonal antibodies such as Rituximab.

Given the critical role of MHC class I in target cell recognition by cytotoxic T-cells, it is unsurprising that MHC class I downregulation is a common feature of many cancers, including NPC **(Yao et al., 2000)**. My results are similar to previous reports. Thus, we observed patients with normal MHC class I levels and other patients with reduced MHC class I on the tumour cells. PD-L1 was reported to be mutually exclusive with MHC class I expression in ovarian surface epithelial serous tumours **(Aust et al., 2017)** and represents two different evasive mechanisms, however I reported different features in NPC tumours, MHC class I was down-regulated in one case, but PD-L1 expression was preserved in the tumour and vice versa, which suggest the simultaneous involvement of two different evasive mechanisms in NPC tumours, unlike ovarian serous tumours which display two mutually exclusive immune escape mechanisms.

I also observed MHC class II expression on the NPC tumour cells, again a range of expression levels was noted across the patient cohort as has been described by previous work **(Yao et al., 2000)** . The expression of MHC class II by the tumour cells could render them visible to CD4+ T-cells which are increasingly being shown to act as direct effectors in the context of human malignancy **(Perez-Diez et al., 2007, Quezada et al., 2010)**. We note that the tumour of four out of seven patients had reduced MHC class I expression (H-score < median H-score of 180) but these

tumours had levels of MHC class II expression that exceeded the median MHC class II H-score. This result suggests that boosting an effective EBNA1- T-cell response (which is primarily mediated through MHC class II) could potentially be a good method to overcome the MHC class I down-regulation that frequently occurs in NPC.

CHAPTER FOUR

EXPRESSION OF COLLAGENS AND COLLAGEN RECEPTORS IN DIFFUSE LARGE B CELL LYMPHOMA

4.2 INTRODUCTION

DLBCL is a tumour derived from the malignant transformation of B cells undergoing clonal expansion in the GC. The pathogenesis of this tumour is complex; with a common histology underpinned by a unique biology that explains an observed difference in clinical outcome **(Pasqualucci and Dalla-Favera, 2015)**. Gene expression profiling has identified two major DLBCL subgroups, referred to as the GCB and ABC forms, which are believed to originate from distinct stages of B cell differentiation **(Alizadeh et al., 2000)**. Thus, GCB DLBCL is characterised by the expression of typical GC markers such as BCL6 and CD10, whereas ABC DLBCL expresses markers of a later stage of B cell differentiation, such as IRF4 **(Meyer et al., 2010)**. These two subgroups of DLBCL are also characterised by distinct molecular abnormalities **(Swerdlow et al., 2016)**. For example, GCB DLBCL may be defined by translocations leading to BCL2 over-expression, mutations of the histone methyltransferase EZH2, and deletions of PTEN, all of which are rarely encountered in ABC DLBCL **(Testoni et al., 2015)**. In contrast, ABC DLBCL is associated with chronic active B cell receptor (BCR) signalling and NF-κB deregulation **(Bohers et al., 2014)**. The clinical significance of this COO is evident in R-CHOP-treated patients, whereby ABC DLBCL has a substantially inferior outcome **(Alizadeh et al., 2000)** . In light of these clinical implications, the new WHO classification recognizes these DLBCL subtypes as separate diagnostic entities **(Swerdlow et al., 2016)**.

Other studies suggest that the DLBCL microenvironment is an important indicator of outcome. Lenz, et al. defined two stromal signatures which, when combined into a single stromal score, predicted the survival of DLBCL patients **(Lenz et al., 2008)**. Importantly, the stromal score was present across both the GCB and ABC subtypes, suggesting that similar tumour microenvironment features could be acquired during

the pathogenesis of both of the major forms of DLBCL **(Lenz et al., 2008)**. Genes defining the stromal-1 signature were enriched for those encoding extracellular matrix components, including collagens such as DDR-2 and collagens (e.g COL1A2, COL1A1 and COL5A1, COL5A2, COL6A2, COL6A3, COL8A2) , modifiers of collagen synthesis and genes which are initiators of fibrogensis **(Lenz et al., 2008)**. Also enriched in the stromal-1 signature was a "monocyte" profile, comprising of genes that were more highly expressed in CD14+ blood monocytes than in B cells, T cells, or natural killer cells. It included genes related to macrophages such as colony stimulating factor 2 receptor, alpha, low-affinity (granulocyte-macrophage) (CSF2RA), which is growth factor receptor important in macrophages. Furthermore positive correlation between the expression of collagen and monocyte genes was found **(Lenz et al., 2008)**.

Many tumour types are characterised by increased fibrosis commonly involving the deposition of collagens I and III **(Kauppila et al., 1998) (Santala et al., 1999)**. Furthermore, there is a growing recognition of the importance of collagens, not simply as structural components of the extracellular matrix, but also as ligands which can influence signalling in both tumour and stromal cell compartments. At least thirteen different collagen receptors are encoded by the human genome, many of which are implicated in cancer-related processes; including cell proliferation, survival, migration and evasion of immune response **(Multhaupt et al., 2016)**.

In this study I have explored the expression of collagens and collagen receptors in DLBCL, focussing mainly on two collagen receptors: LAIR-1, DDR-1, and their respective ligands.

4.3 RESULTS

4.2.1 Over-expression of collagens and collagen receptor genes in DLBCL

As a first step to investigate the potential contribution of collagen signalling to the pathogenesis of DLBCL, the expression of known collagen and collagen receptor genes was initially analyzed in two published datasets, one of which used RNAseq to measure global gene expression in 86 cases of DLBCL by Morin et al **(Morin et al., 2011)**, and the other, gene expression in normal GC B cells (centroblasts and centrocytes) from four donors by B**é**guelin et al **(Béguelin et al., 2013)**. I found that genes encoding collagen subunits and collagen receptors were significantly enriched (both $p<0.0001$) among genes up-regulated, but not among genes down-regulated, in both GCB- and ABC-DLBCL compared to normal GC B cells (Figure 4.1A).

4.2.2 Over-expression of LAIR-1 in DLBCL

I chose initially to focus on the collagen receptor, LAIR-1, which has been reported to have immune inhibitory functions **(Meyaard et al., 1997, Meyaard, 1999)**. Figure 4.1B and Figure 4.1C show that the mRNA expression of LAIR-1 and that of the genes that encode its known ligands, collagen I (COL1A1, COL1A2) and collagen III (COL3A1), respectively using re-analysis of Morin et al dataset **(Morin et al., 2011)** was significantly higher in both subtypes of DLBCL compared with normal GC B cells. Figure 4.1D shows that the re-analysis of a separate gene expression dataset by Brune et al (GSE12453) **(Brune et al., 2008)** also revealed significantly higher expression of LAIR-1 in DLBCL compared with normal GC B cells.

A

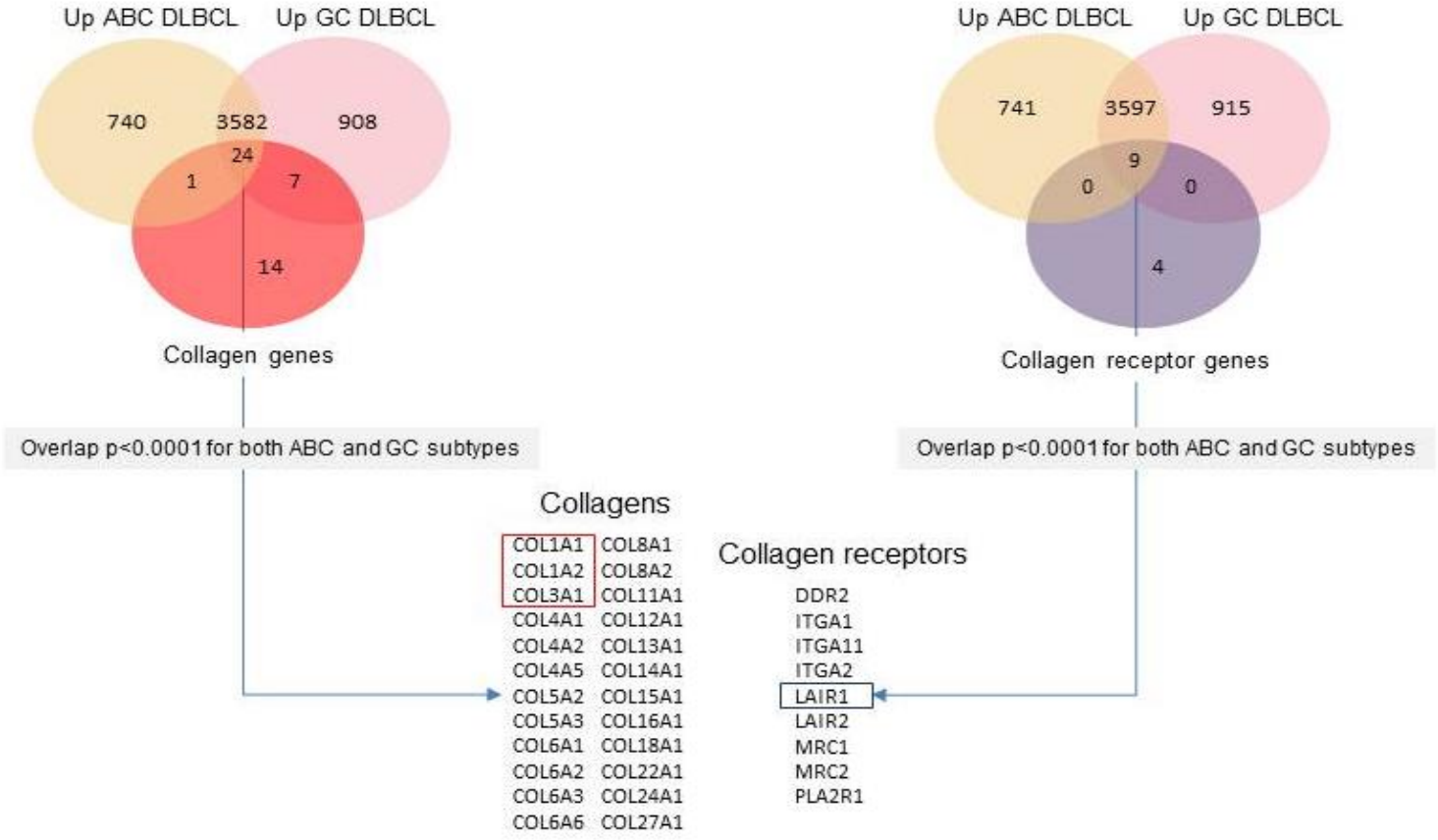
Up ABC DLBCL
Up GC DLBCL
740
3582
908
24
1
7
14
Collagen genes
Up ABC DLBCL
Up GC DLBCL
741
3597
915
9
0
0
4
Collagen receptor genes
Overlap p<0.0001 for both ABC and GC subtypes
Overlap p<0.0001 for both ABC and GC subtypes
Collagens
COL1A1
COL1A2
COL3A1
COL4A1
COL4A2
COL4A5
COL5A2
COL5A3
COL6A1
COL6A2
COL6A3
COL6A6
COL8A1
COL8A2
COL11A1
COL12A1
COL13A1
COL14A1
COL15A1
COL16A1
COL18A1
COL22A1
COL24A1
COL27A1
Collagen receptors
DDR2
ITGA1
ITGA11
ITGA2
LAIR1
LAIR2
MRC1
MRC2
PLA2R1

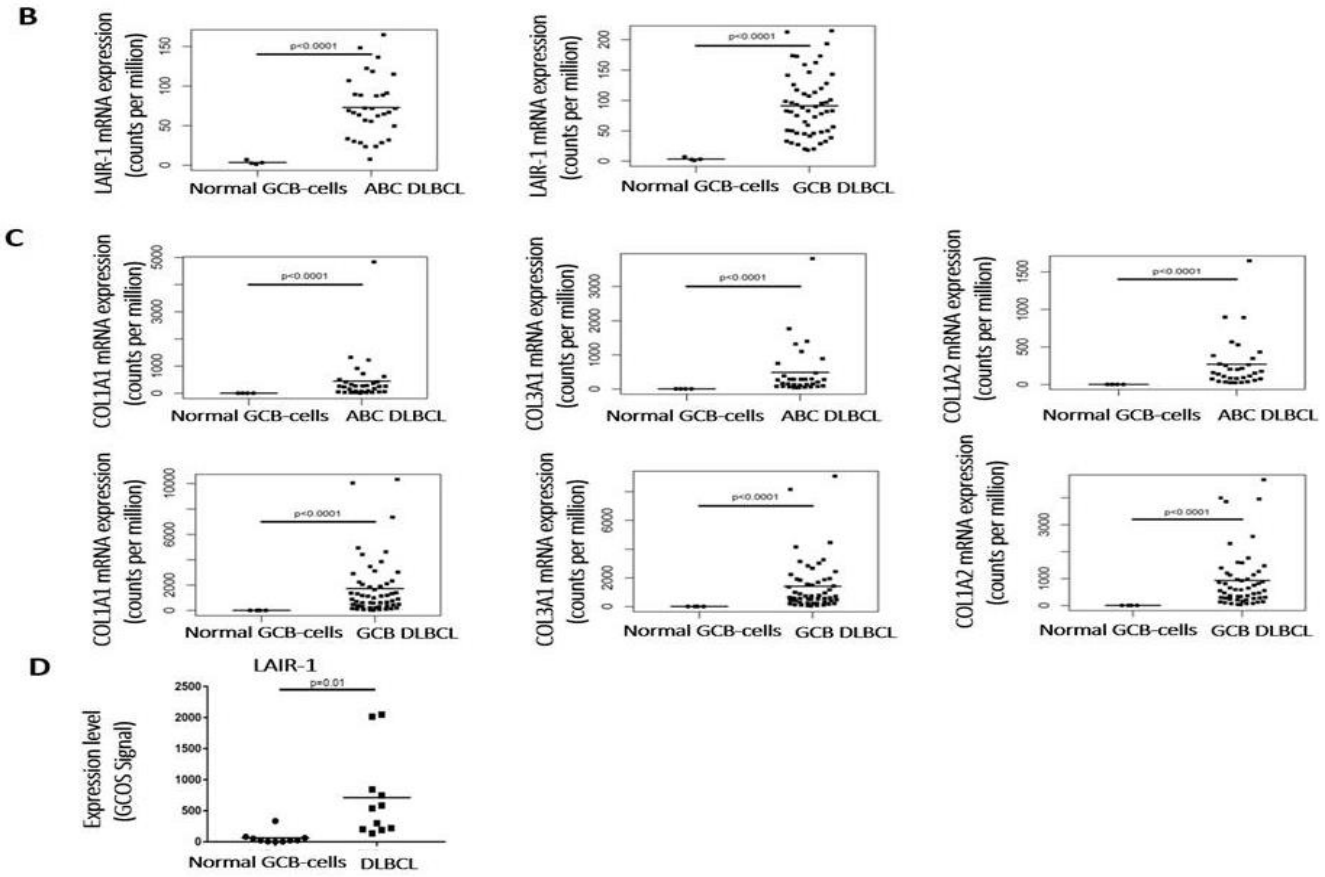

Figure 4.1: Over-expression of collagens and collagen receptor genes in diffuse large B cell lymphoma A) Venn diagrams showing that genes encoding collagen subunits (left panel) and collagen receptors (right panel) were significantly enriched among genes up-regulated ($p<0.0001$), but not among genes down-regulated (not shown), in GC and ABC DLBCL compared to normal germinal centre (GC) B cells, B) The mRNA expression of LAIR-1 was significantly higher in both subtypes of DLBCL compared with normal GC B cells, C) The mRNA expression of the known LAIR-1 ligands, collagen I (COL1A1, COL1A2) and collagen III (COL3A1), was also significantly higher in both subtypes of DLBCL compared with normal GC B cells, D) shows that the re-analysis of a separate gene expression dataset **(Brune et al., 2008)** also revealed significantly higher expression of LAIR-1 in diffuse large B cell lymphoma compared with normal GCB-cells.

4.2.3 The expression of LAIR-1 and its ligands are correlated in DLBCL

Next, I studied the relationship between the expression of LAIR-1 and its collagen ligands in primary DLBCL. A meta-analysis of eleven different DLBCL datasets by Care et al, **(Care et al., 2015)**, excluding the dataset used above **(Morin et al., 2011)**, revealed that genes positively correlated with LAIR-1 in primary DLBCL were significantly enriched (odds ratio= 2.09, p=0.044), and those negatively correlated with LAIR-1 in primary DLBCL, significantly depleted (odds ratio=0, p=0.016) for collagen genes (Figure 4.2A). Collagen genes positively correlated with LAIR-1 in DLBCL included COL1A1 and COL3A1.

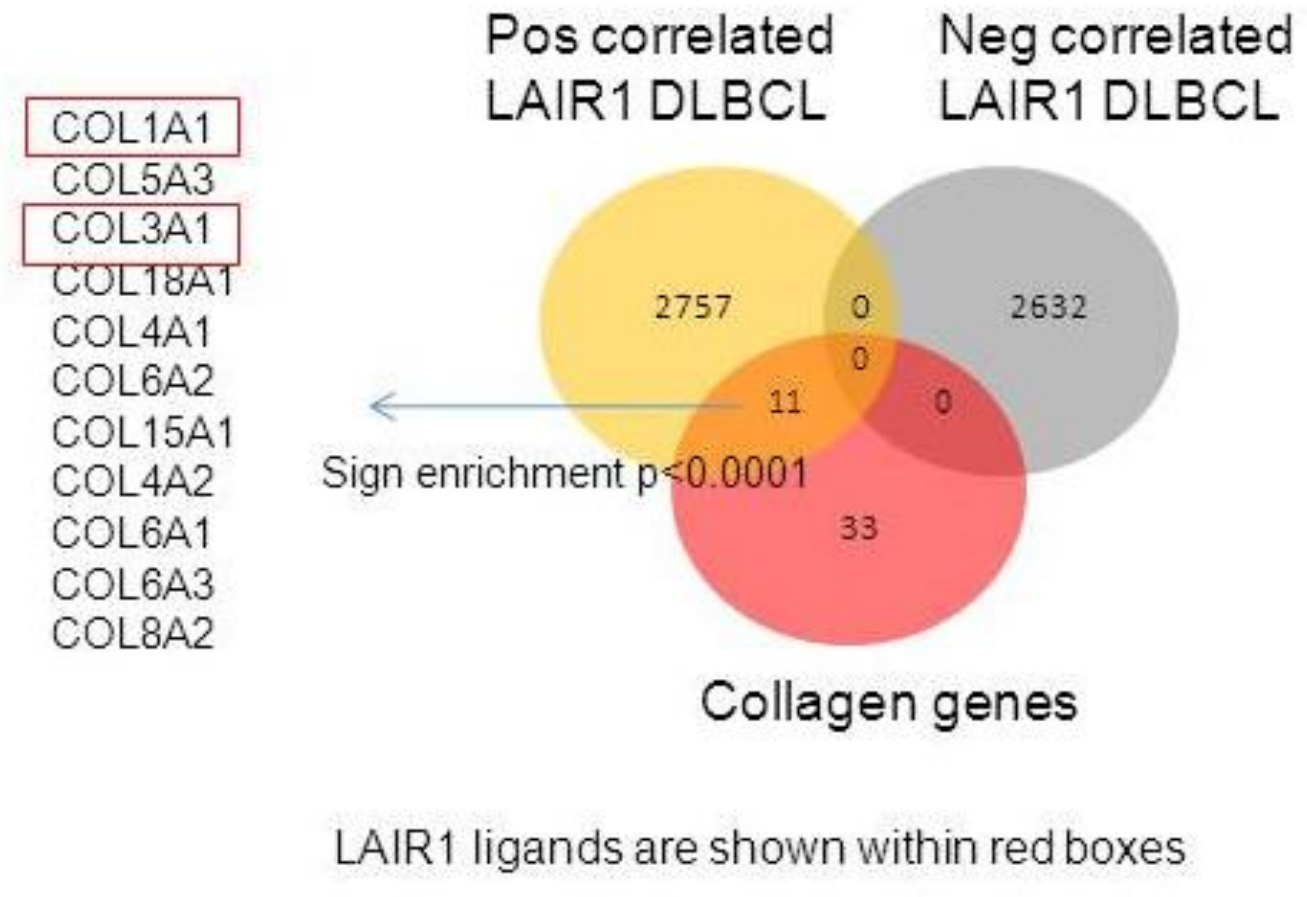

Figure 4.2: The expression of LAIR-1 and its ligands are correlated in diffuse large B cell lymphoma
Results of a meta-analysis of eleven different DLBCL datasets revealed that genes positively correlated with LAIR-1 in primary DLBCL were significantly enriched (odds ratio=2.09, p=0.044), and those negatively correlated with LAIR-1 in primary DLBCL, significantly depleted (odds ratio=0, p=0.016) for collagen genes.

4.2.4 Genes positively correlated with LAIR-1 expression in DLBCL are enriched for macrophage functions

An ontology analysis of the genes that were positively correlated with LAIR-1 in the meta-analysis described above **(Care et al., 2015)**, revealed, a significant enrichment of macrophage functions (Figure 4.3A). To confirm this observation, I compared the genes positively correlated with LAIR-1 with those comprising a published tumour macrophage gene signature generated from a DLBCL gene expression dataset and shown to be conserved across multiple un-related human cancer types (Doig et al., 2013) I found that genes positively correlated with LAIR-1 in primary DLBCL were significantly enriched (odds ratio=93.64, $p<0.0001$), and those negatively correlated with LAIR-1 in primary DLBCL significantly depleted (odds ratio= 0, $p<0.0001$) for macrophage signature genes (Figure 4.3B).

A

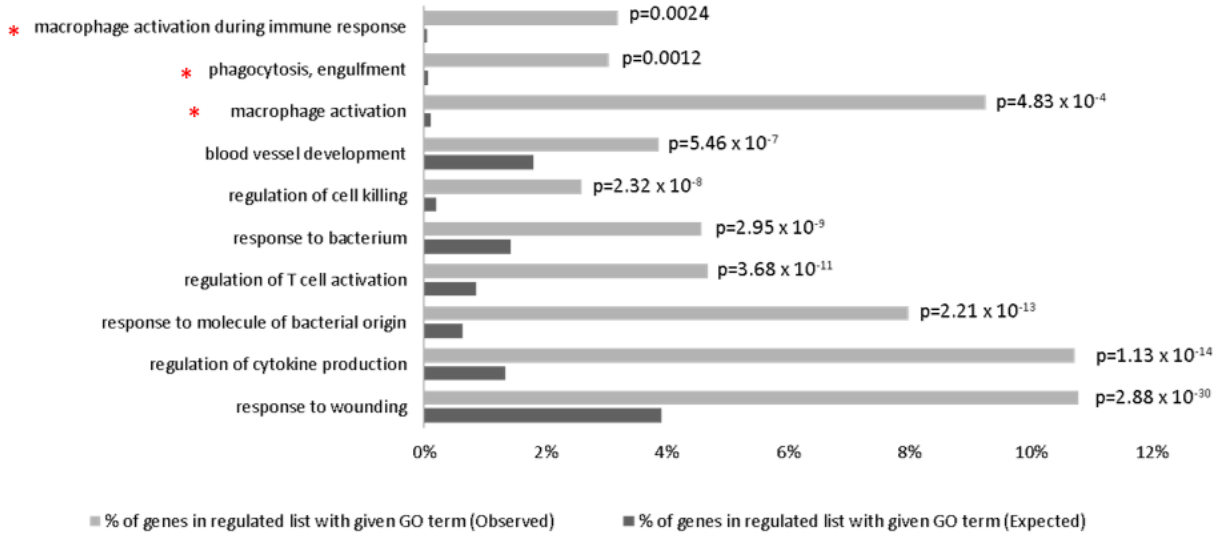
* macrophage activation during immune response
* phagocytosis, engulfment
* macrophage activation
blood vessel development
regulation of cell killing
response to bacterium
regulation of T cell activation
response to molecule of bacterial origin
regulation of cytokine production
response to wounding
p=0.0024
p=0.0012
p=4.83 x 10-4
p=5.46 x 10-7
p=2.32 x 10-8
p=2.95 x 10-9
p=3.68 x 10-11
p=2.21 x 10-13
p=1.13 x 10-14
p=2.88 x 10-30
0%
2%
4%
6%
8%
10%
12%
% of genes in regulated list with given GO term (Observed)
% of genes in regulated list with given GO term (Expected)

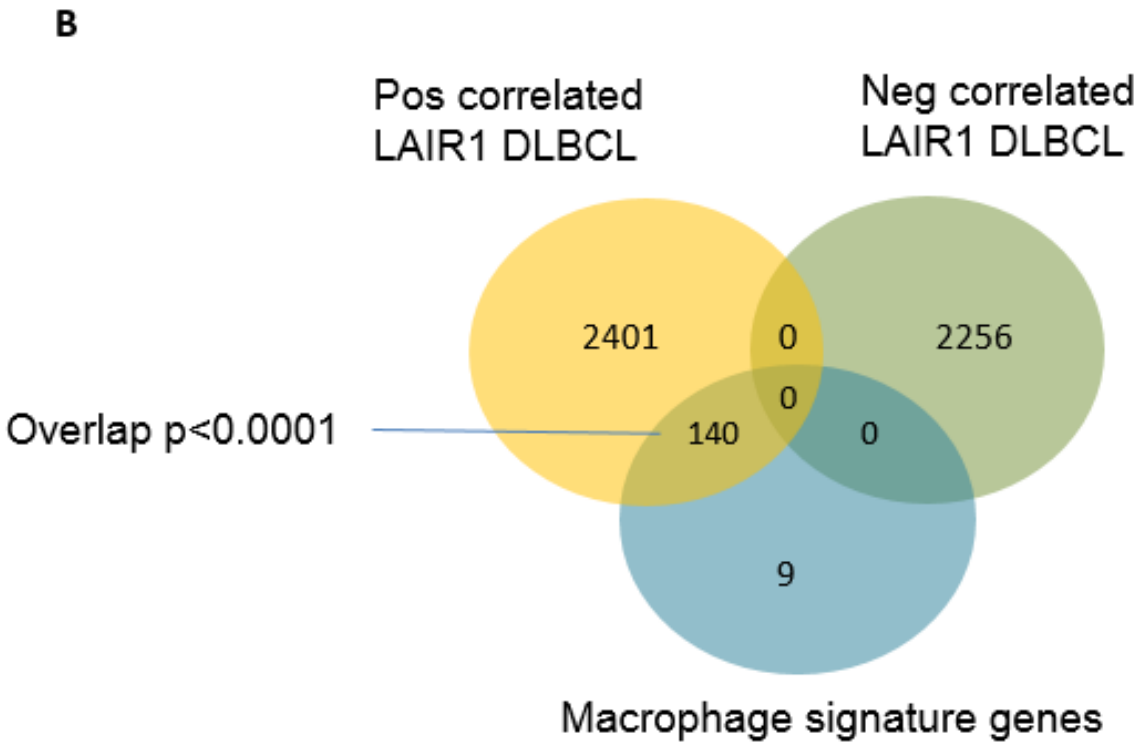

Figure 4.3: Genes positively correlated with LAIR-1 expression in DLBCL are enriched for macrophage functions
A) Gene ontology analysis reveals a significant enrichment of macrophage functions. Light grey bars show the observed percentage, and dark grey bars the expected percentage, of genes in each GO category. B) Genes positively correlated with LAIR-1 in primary DLBCL were significantly enriched (odds ratio=93.64, p<0.0001), and those negatively correlated with LAIR-1 in primary DLBCL significantly depleted (odds ratio= 0, p<0.0001) for macrophage signature genes, GO indicates gene ontology.

4.2.5 LAIR-1 is predominately expressed by M2 macrophages in the microenvironment of DLBCL

To confirm these observations and to directly identify the cell types expressing LAIR-1, I used immunohistochemistry. In normal lymphoid tissues I observed strong LAIR-1 positivity mainly within CD68-positive macrophages, including those present within the GC (Figure 4.4A) which was confirmed by multiplex IF using CD68 (Figure 4.4B). GCB-cells expressing either BCL6 (Figure 4.4C) or Ki67 (Figure 4.4D) were not stained with the LAIR-1 antibody confirming that GC B cells lack detectable LAIR-1 expression. 50 cases of DLBCL were also stained for LAIR-1. All cases showed positive staining for LAIR-1 in macrophages and not in tumour cells (Figure 4.4E). The absence of LAIR-1 in tumour cells but its abundant expression by macrophages in DLBCL was confirmed in 10 representative cases by dual IHC (Figure 4F-I).This was confirmed by the quantification of a representative DLBCL sample using Inform analysis which showed that most CD163 positive cells also expressed LAIR-1 (p<0.0001). With regard to the potential future analysis of *in vivo* models of DLBCL, it is noteworthy that I also observed the expression of LAIR-1 on mouse macrophages infiltrating A20 tumours *in vivo* (Figure 4.4J); A20 is a well-established syngeneic mouse model of human DLBCL. I also showed that in most cases LAIR-1 was expressed in macrophages in the absence of LAIR-2, a negative regulator of LAIR-1 (Figure 4.4K).

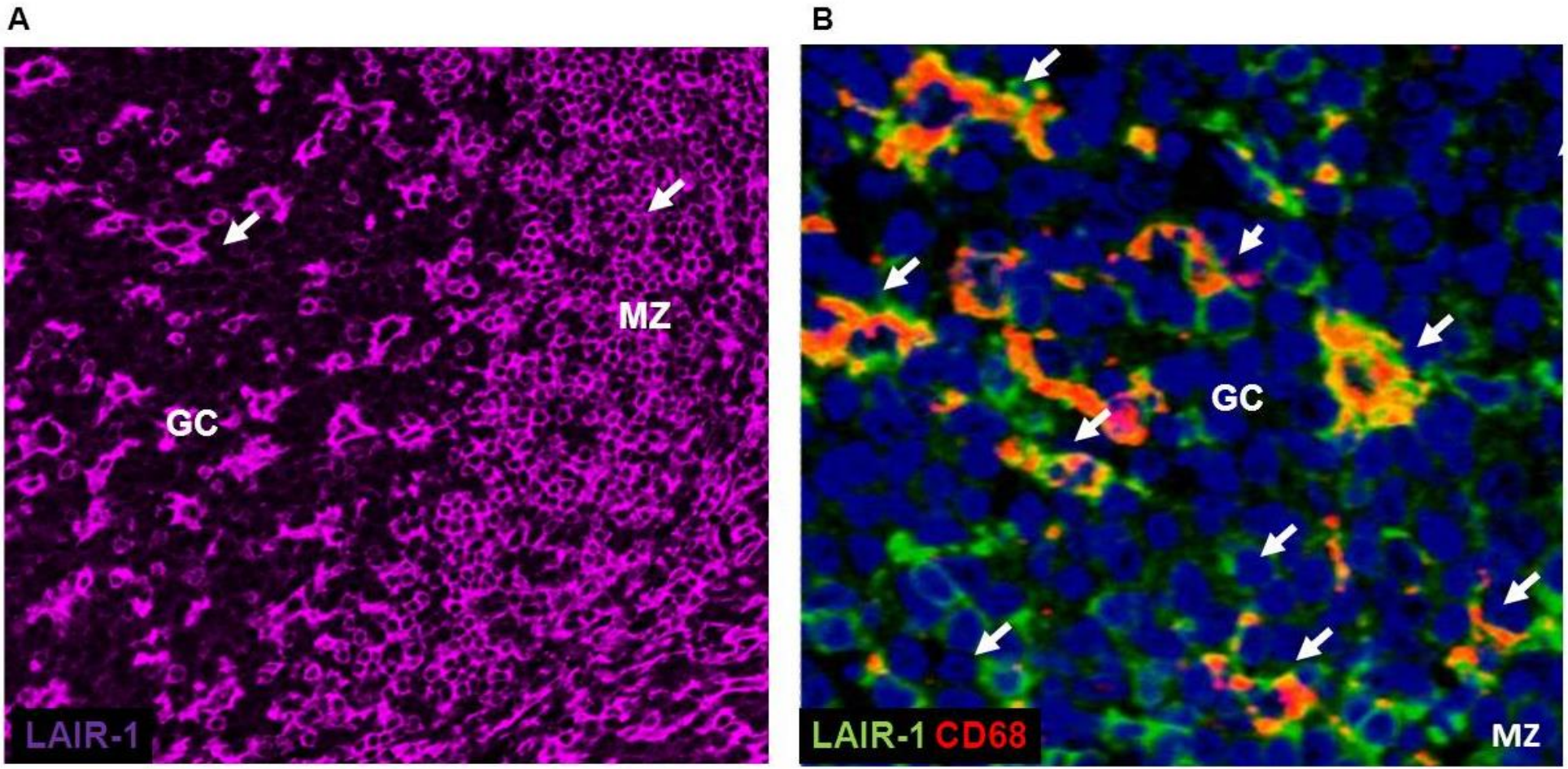
A
MZ
GC
LAIR-1
B
GC
LAIR-1 CD68
MZ

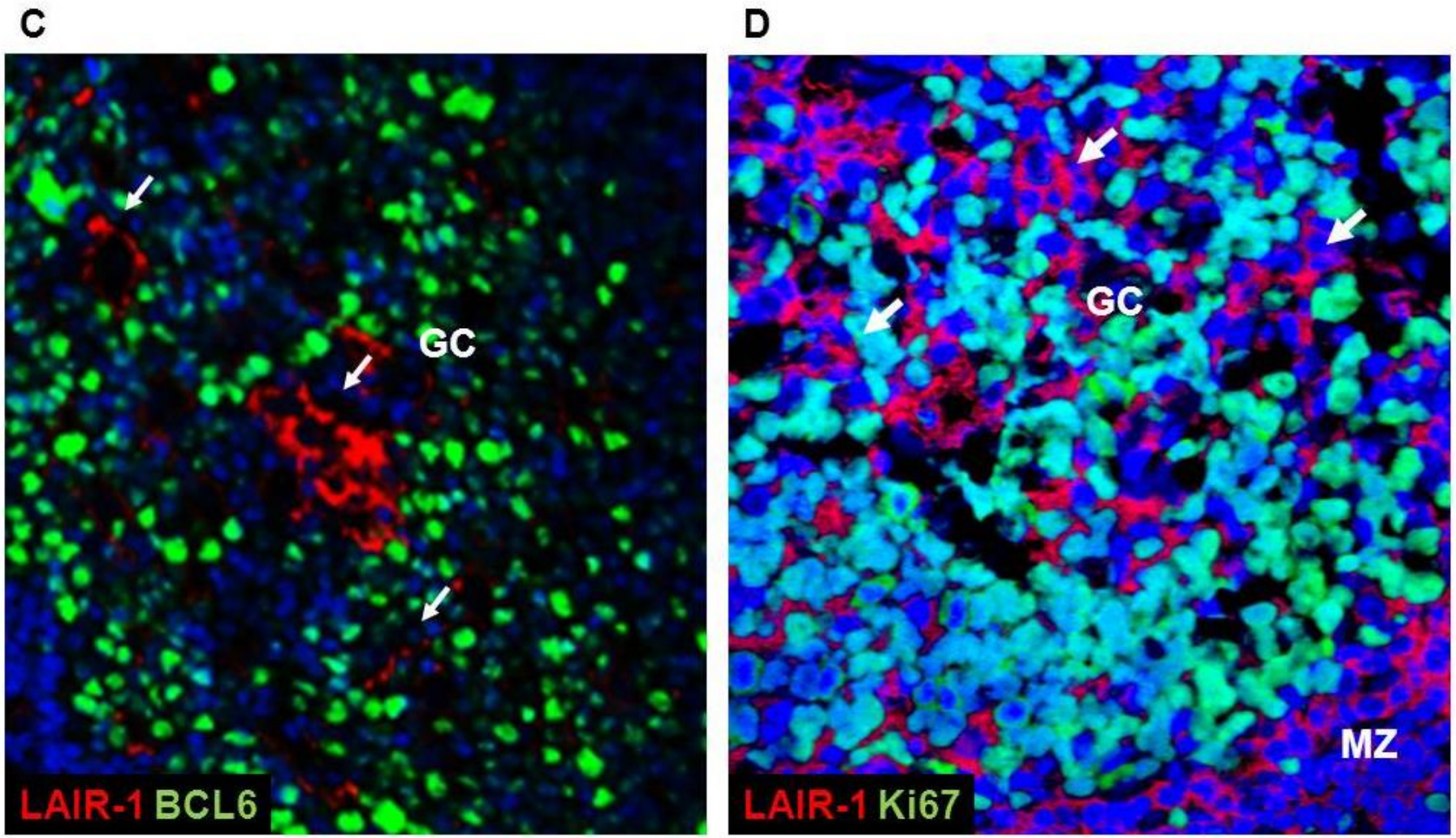
C
GC
LAIR-1 BCL6
D
GC
MZ
LAIR-1 Ki67

E

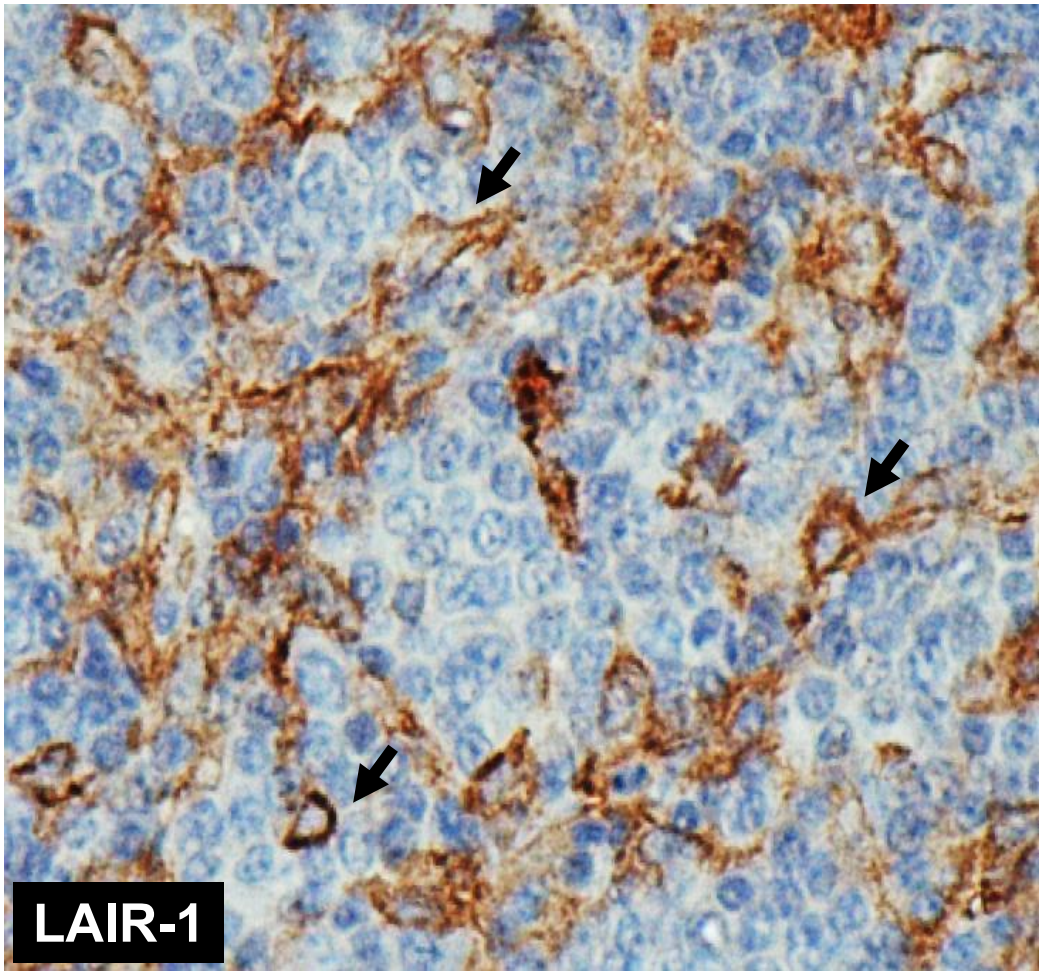

F

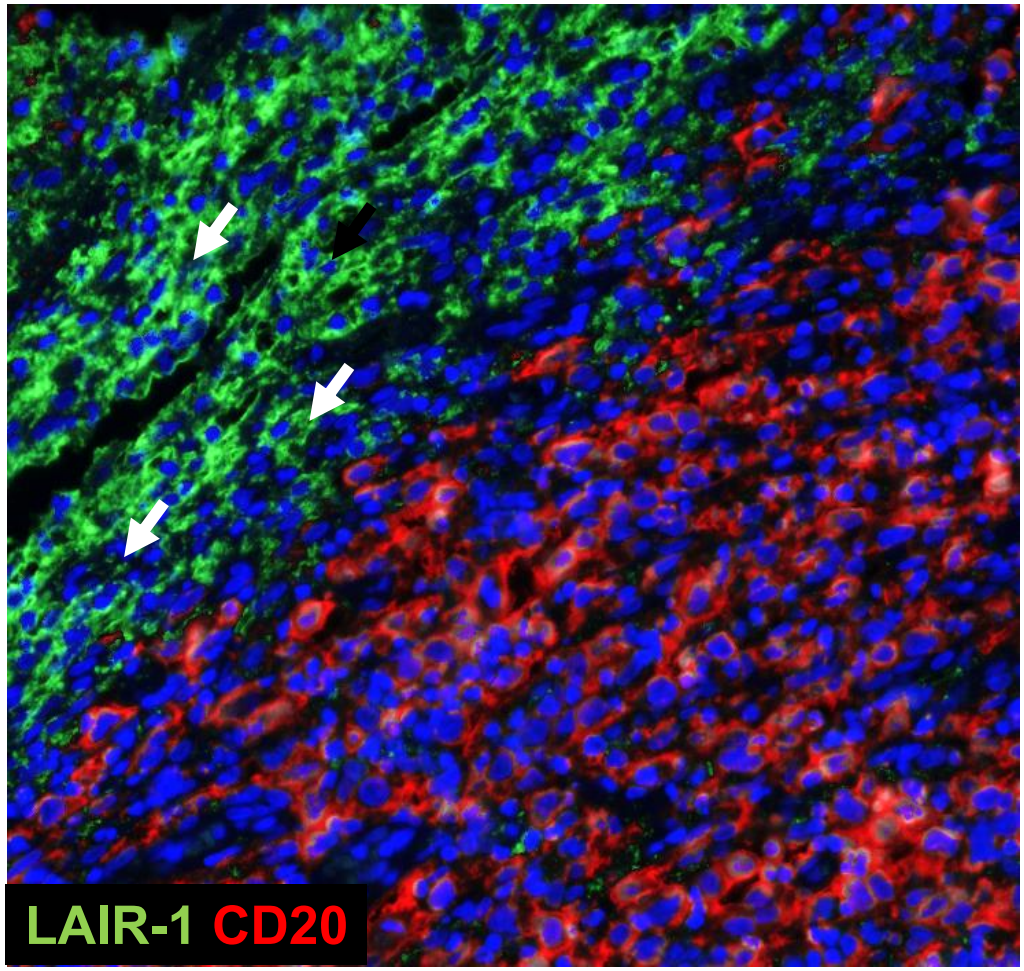

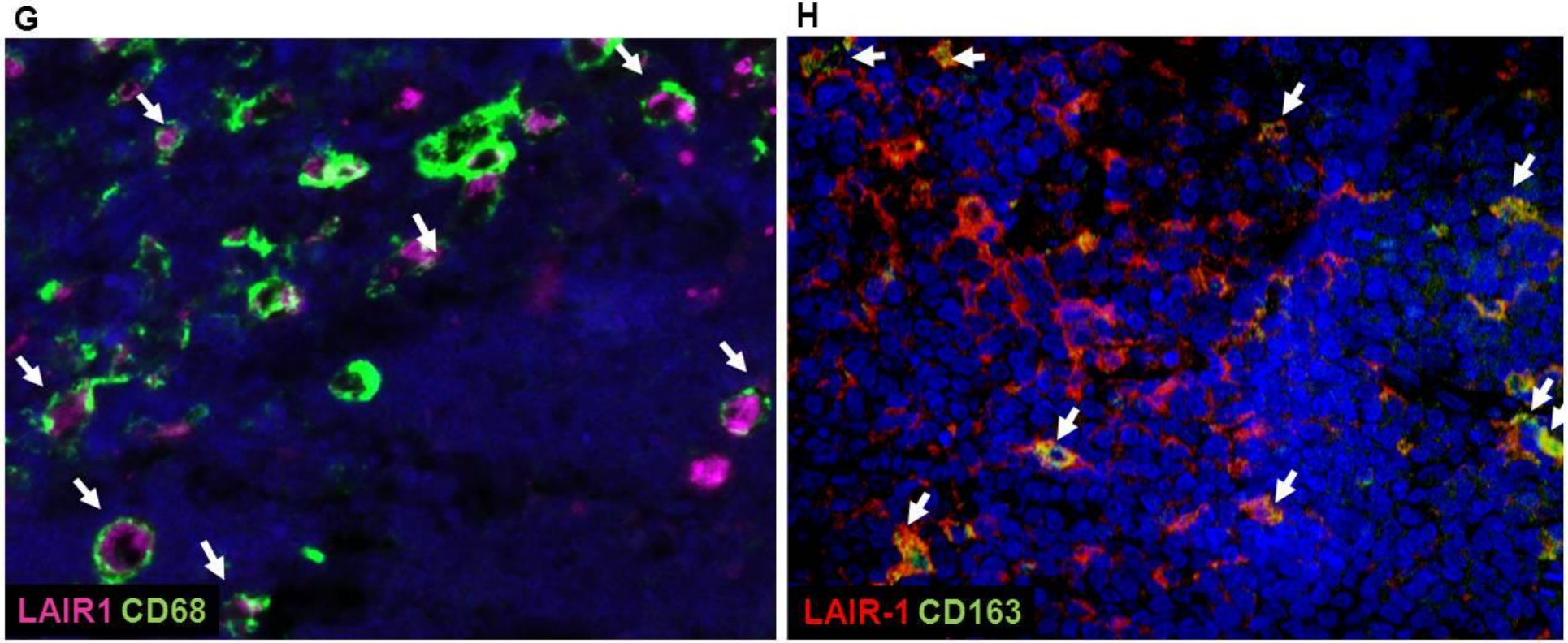
G
LAIR1 CD68
H
LAIR-1 CD163

I

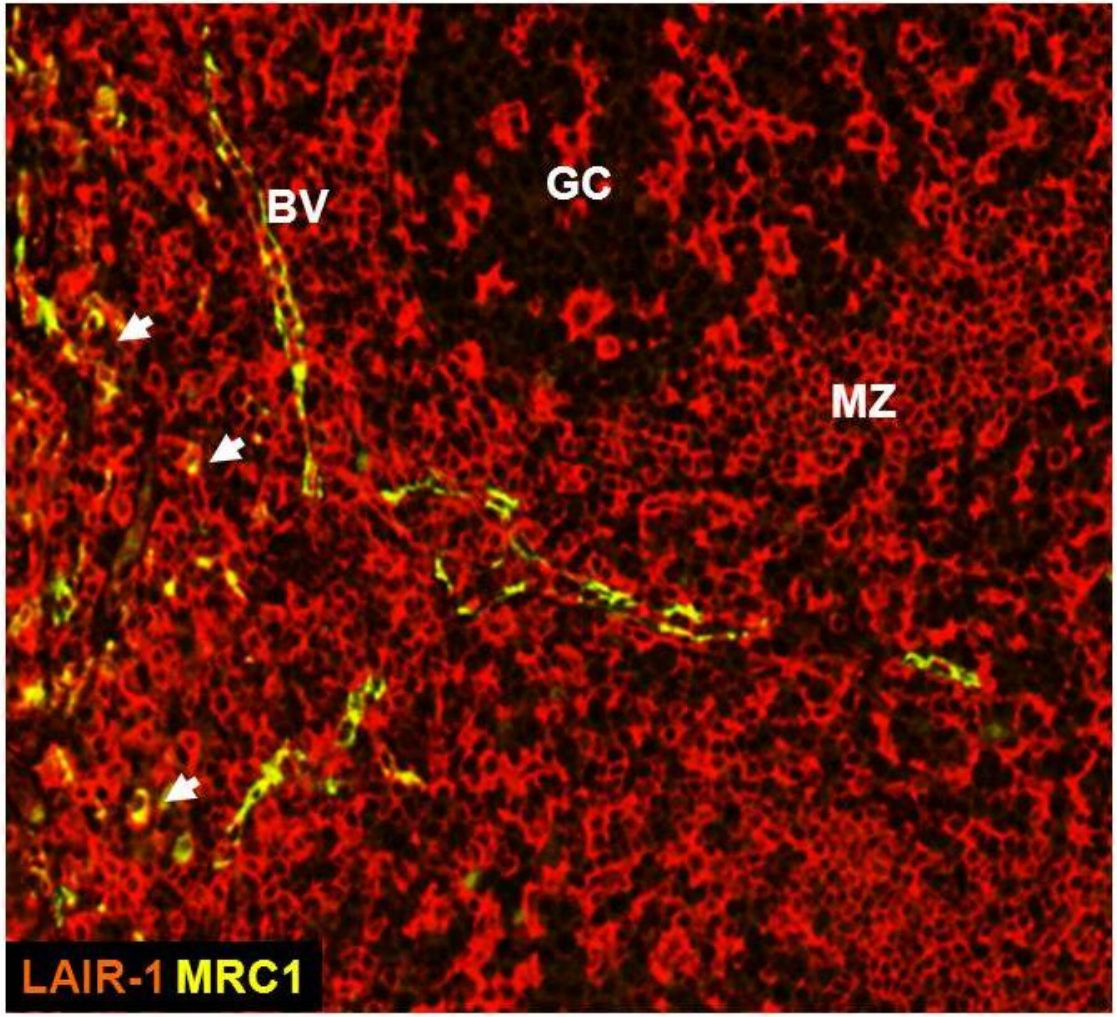

J

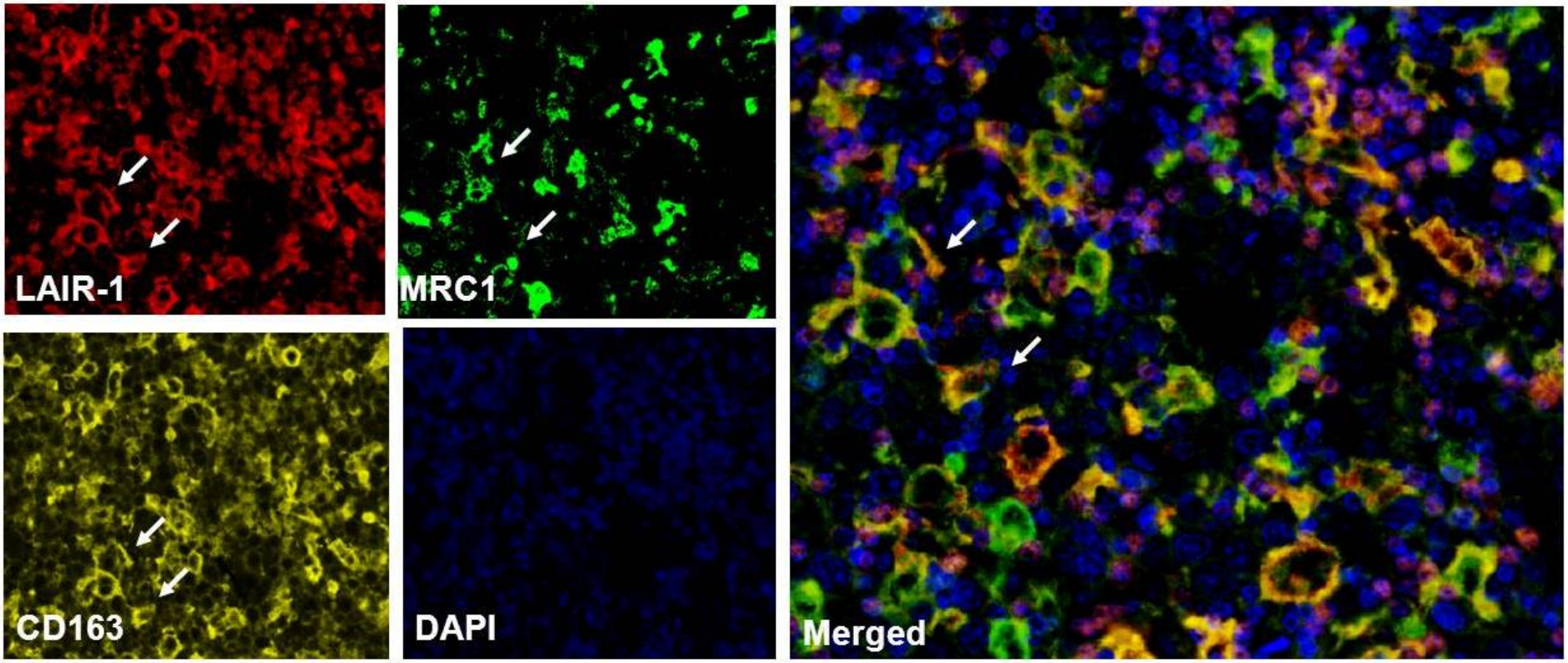

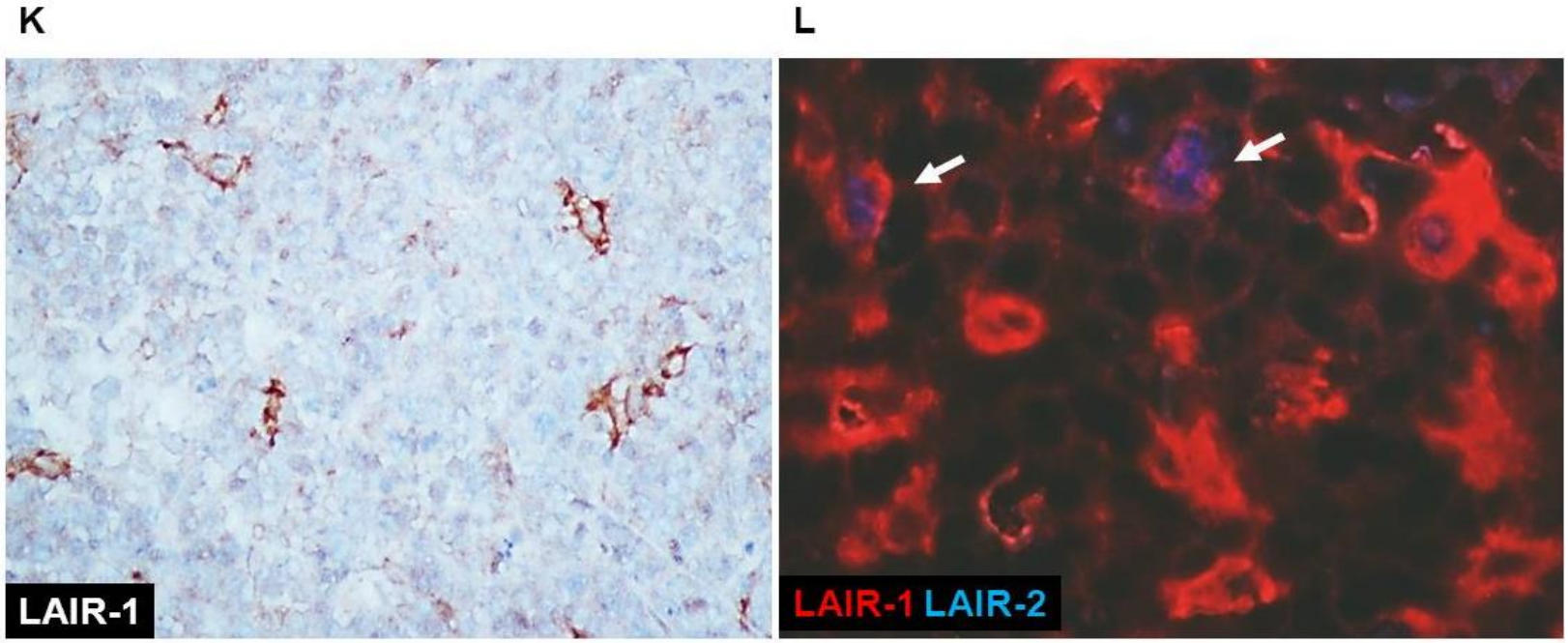

Figure 4.4: LAIR-1 expression in normal lymphoid tissues and in DLBCL

A) Low power photomicrograph showing IF for LAIR-1 (pink) located in GC cells 20X. B) Shows double labelling for LAIR-1 (pink) with CD68 (green) and confirm that LAIR-1-positive cells in the GC are macrophages (arrows) and in mantle zone lymphocytes, 40X C) IF shows that BCL6-expressing GC B cells (green) were LAIR-1 (red)-negative (arrows), 20X. D) IF shows that Ki67-expressing GC B cells (green) were also LAIR-1 (red)-negative (arrows),40X, E) IHC shows LAIR-1 expression in morphologically identifiable macrophages (brown), but not in tumour cells (blue nuclei) of DLBCL (arrows). F) IF confirms absence of LAIR-1 expression (green) in CD20-positive tumour cells (red) of DLBCL (arrows). G) IF confirms LAIR-1 expression (green) primarily located with tumour-associated macrophages (CD68; red) of DLBCL. H) IF shows that LAIR-1 (red) is present mostly within M2 macrophages expressing CD163 (green), arrows, 40X, I) IF tonsil shows that LAIR-1 (red) is present within M2 macrophages expressing MRC1 (yellow) outside GC (arrows), 20X J) IF shows that LAIR-1 (red) is present mostly within M2 macrophages expressing CD163 (green) and MRC1 (yellow) at the arrows, 20X, K) IHC shows recruitment of LAIR-1 positive cells with the morphology of macrophages in tumour microenvironment of A20 lymphoma mouse model, 40X L) IF of representative sample shows LAIR2 (blue) occasionally present in the microenvironment in contrast to abundance of LAIR-1 (red), 40X, IHC indicates immunohistochemistry, IF indicates immunofluorescence GC indicates germinal centre, MZ indicates mantle zone.

4.2.6 Low frequency of LAIR-1-expressing T cells in the microenvironment of DLBCL

Given that LAIR-1 has been reported to be expressed on most normal immune cells, including T cells, I next wanted to quantify numbers of LAIR-1-expressing T cells in the microenvironment of DLBCL, compared to those present in normal lymphoid tissues. To do this I co-stained 10 representative cases of DLBCL and normal lymphoid tissues for CD3 and LAIR-1. I observed that in all cases DLBCL had proportionally significantly fewer LAIR-1-expressing CD3 T cells than did normal lymphoid tissues (Figure 4.5A-B). In DLBCL, LAIR-1/CD3 double positive cells=0.36%, while in tonsil LAIR-1/CD3 double positive cells=13.84%, p value=0.01.

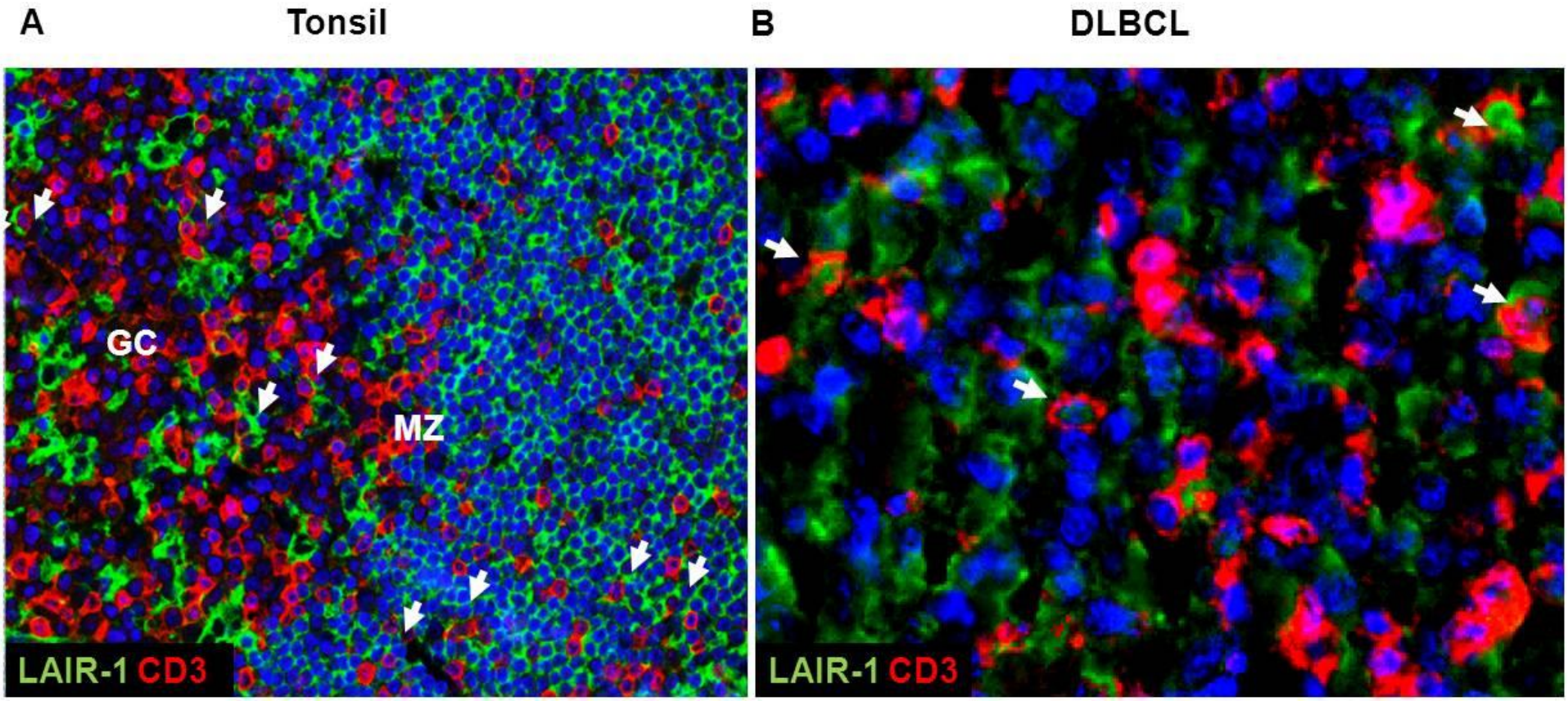

Figure 4.5: Lower frequency of T cells expressing LAIR-1 in DLBCL
A) IF Co-staining of normal lymphoid tissues (tonsil) and B) a representative case of DLBCL IF for CD3 (red) and LAIR-1 (green). In all cases DLBCL had proportionally fewer LAIR-1-expressing CD3 T cells than did normal lymphoid tissue, 20X, IF indicates immunofluorescence.

4.2.7 Effect of collagen and LAIR-1 expression on *in vitro* monocyte differentiation

Given that I had shown that LAIR-1 was highly expressed on M2 macrophages in DLBCL, I next explored the possibility that collagen might influence the differentiation of monocytes to macrophages. Before doing this I first wanted to measure the expression of LAIR-1 during the *in vitro* differentiation of peripheral blood derived monocytes using flow cytometry. These monocytes were differentiated with 5ng/ml of G-MCSF (for M1) 25ng/ml of MCSF for 10 days. In Figure 4.6, I show flow cytometry staining from monocytes polarized with GMCSF and MCSF on untreated or collagen coated plates for 10 days. There was no significant difference in LAIR-1 expression with or without collagen in M1, while in M2 it showed increase in levels of LAIR-1 while differentiating on collagen. Next, I used another method of collagen stimulation, post-differentiation of monocytes into macrophages (10 days) by adding soluble collagen. As seen in Figure 4.7, I show flow cytometry staining, there were no significant change in LAIR-1 expression following stimulation of differentiated M2 macrophages in collagen treated, acetic acid control and untreated cells. Next, I explored THP1 as a possible *in vitro* model for studying LAIR-1, using untreated and undifferentiated THP1 cells. In Figure 4.8, THP-1 showed baseline levels of expression of LAIR-1 (PE) and the monocyte marker CD14 (FITC) while there was expression of the M2 marker, CD163 (APC).

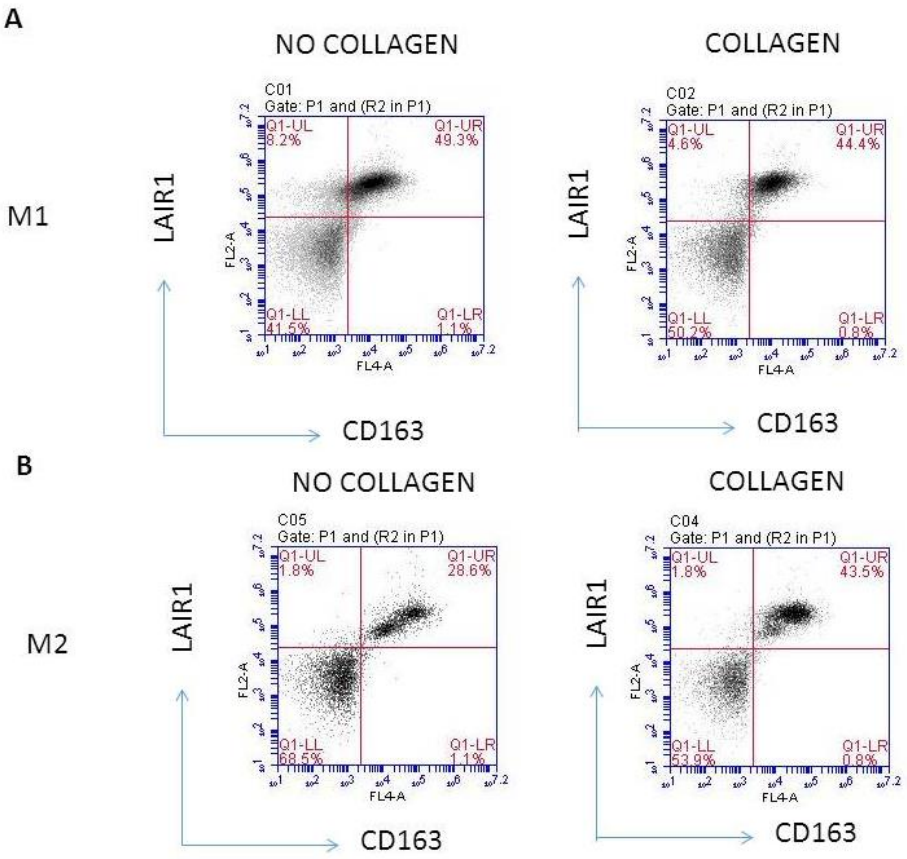

Figure 4.6 LAIR-1 increased in expression in M2 phenotype following differentiation on collagen coated plates

Primary monocytes isolated from PBMCs were cultured with GMCSF and MCSF for polarisation to M1 and M2 respectively +/- collagen type 1 coated plates. CD163 was used as a marker for M2 polarisation. After 10 days the cells were harvested and LAIR-1 expression was analysed by flow cytometry. I found LAIR-1 to be expressed on both stimulated and unstimulated M1 (panel A) and M2 macrophages (panel B), which showed to be increased on stimulated M2.

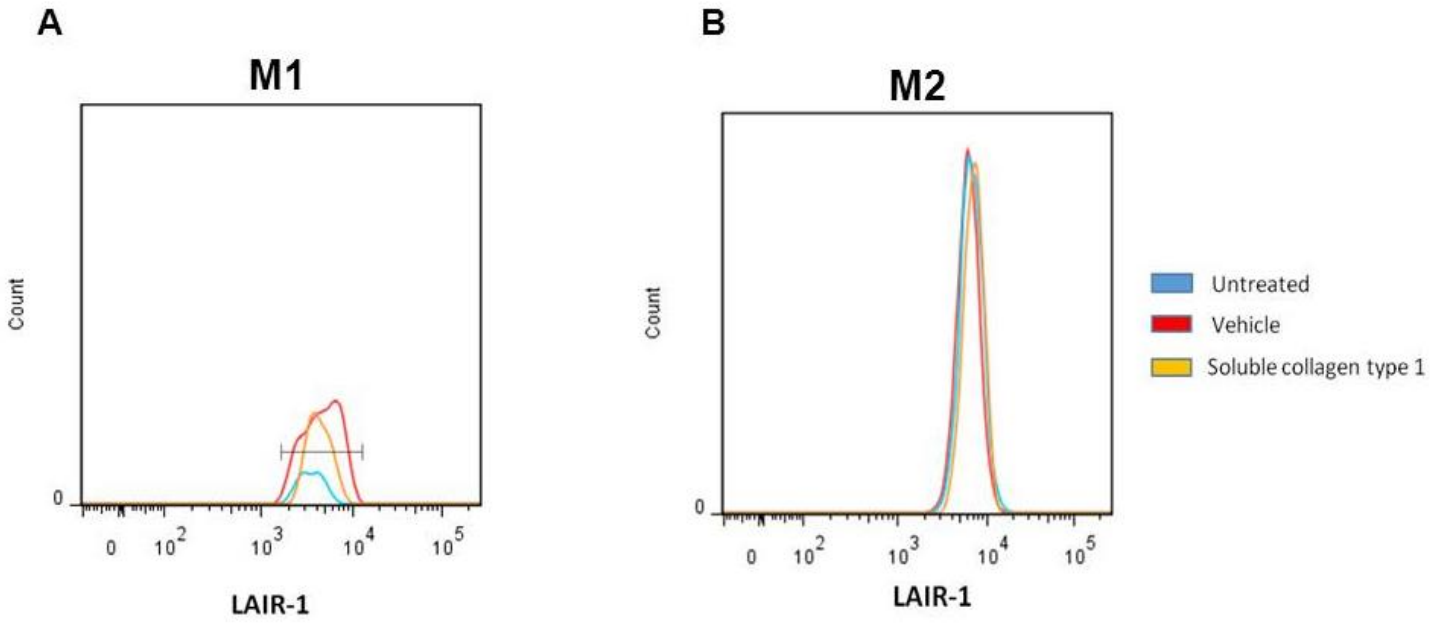

Figure 4.7 No significant difference in LAIR-1 expression in M1 and M2 phenotype post-differentiation in untreated, treated with acid and collagen in macrophages on FACS level

Primary monocytes isolated from PBMCs were cultured with GMCSF and MCSF for 10 days. The cells were harvested and then stimulated with soluble collagen for 24 hrs. Both M1 and M2 (the CD163+ population) was found to have no significant difference in level of expression of LAIR-1, PBMCs indicates peripheral blood mononuclear cell.

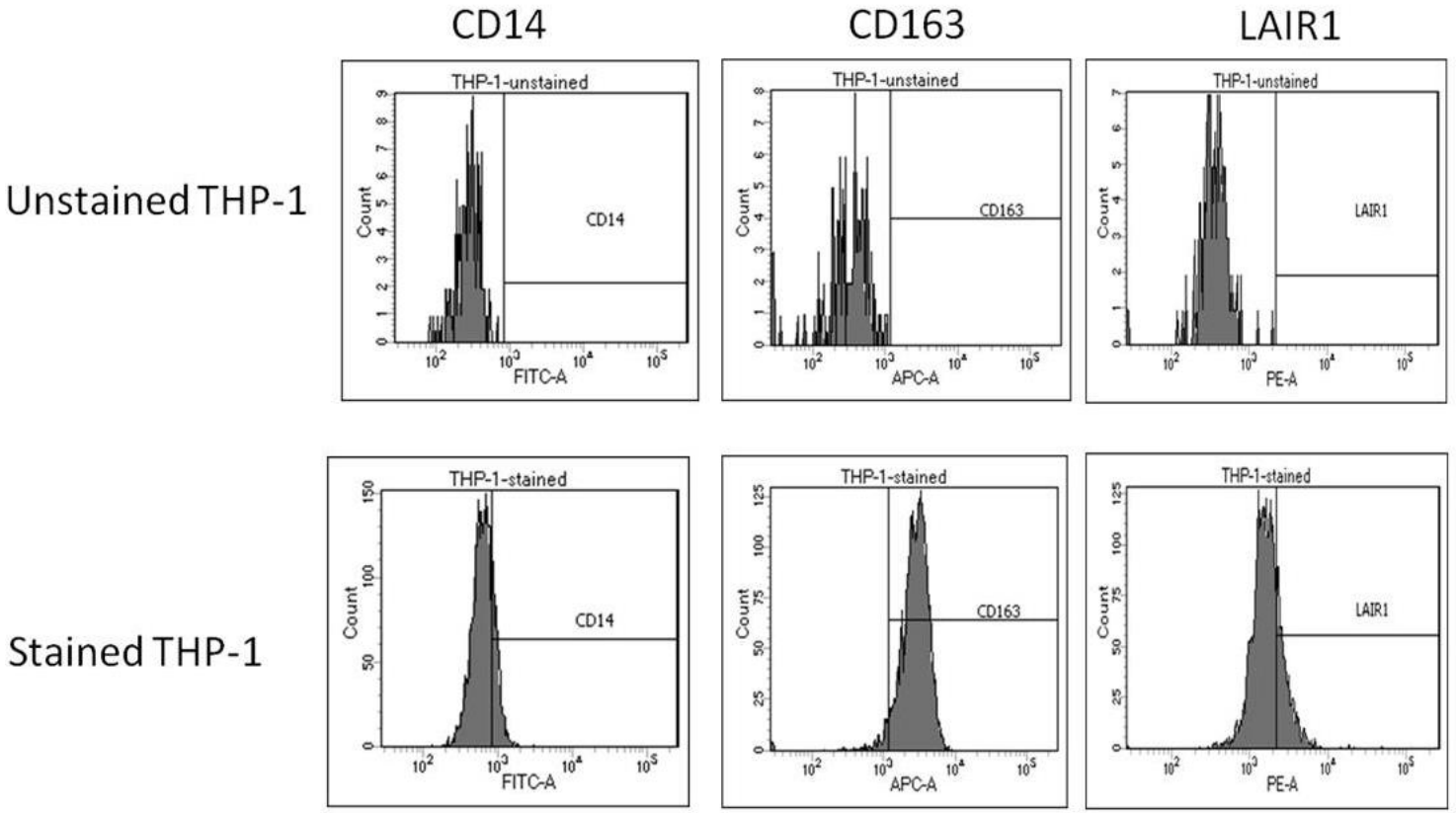

Figure 4.8 THP-1 was examined as a cell line model to study LAIR1. Determination of baseline levels of CD14, CD163 and LAIR-1 in THP-1.

Graphical representation of THP-1 baseline levels of CD14, CD163 and LAIR-1. THP-1 has low expression of the monocyte marker, CD14, a low expression of LAIR-1, and a high expression of the M2 marker, CD163.

4.2.8 Expression of LAIR-1 ligands, Type I and Type III collagen, in DLBCL

Next, I studied the protein expression of the two collagens, Type I and Type III, which are known ligands of LAIR-1. I selected these ligands because the re-analysis of the RNAseq data described above had shown the over-expression of collagen subunits, COL1A1, COL1A2, and COL3A1. Using IHC, I found that Type I collagen was present in the trabeculae/septa and vessels of the tonsil and absent from normal germinal centres (Figure 4.9A). Type III collagen was present in the capillaries and vessels in the mantle zone and the interfollicular regions, but was also absent from germinal centres (Figure 4.10A). Type I collagen was expressed in the stroma as fine fibres in 4/9 evaluable cases of DLBCL. In positive cases Type I collagen was not intimately associated with the tumour cell population but was rather located as a component of larger blood vessels and within surrounding connective tissues (Figure 4.9C-D). Type III Collagen was present in 4/8 evaluable cases of DLBCL (Figure 4.10B-D). Type III was observed in thick fibres around tumour cells, sometimes forming bands. Figure 4.10D shows the results of representative multiplex IHC confirming the close association between LAIR-1 expressing cells and Collagen III in 3/3 positive cases.

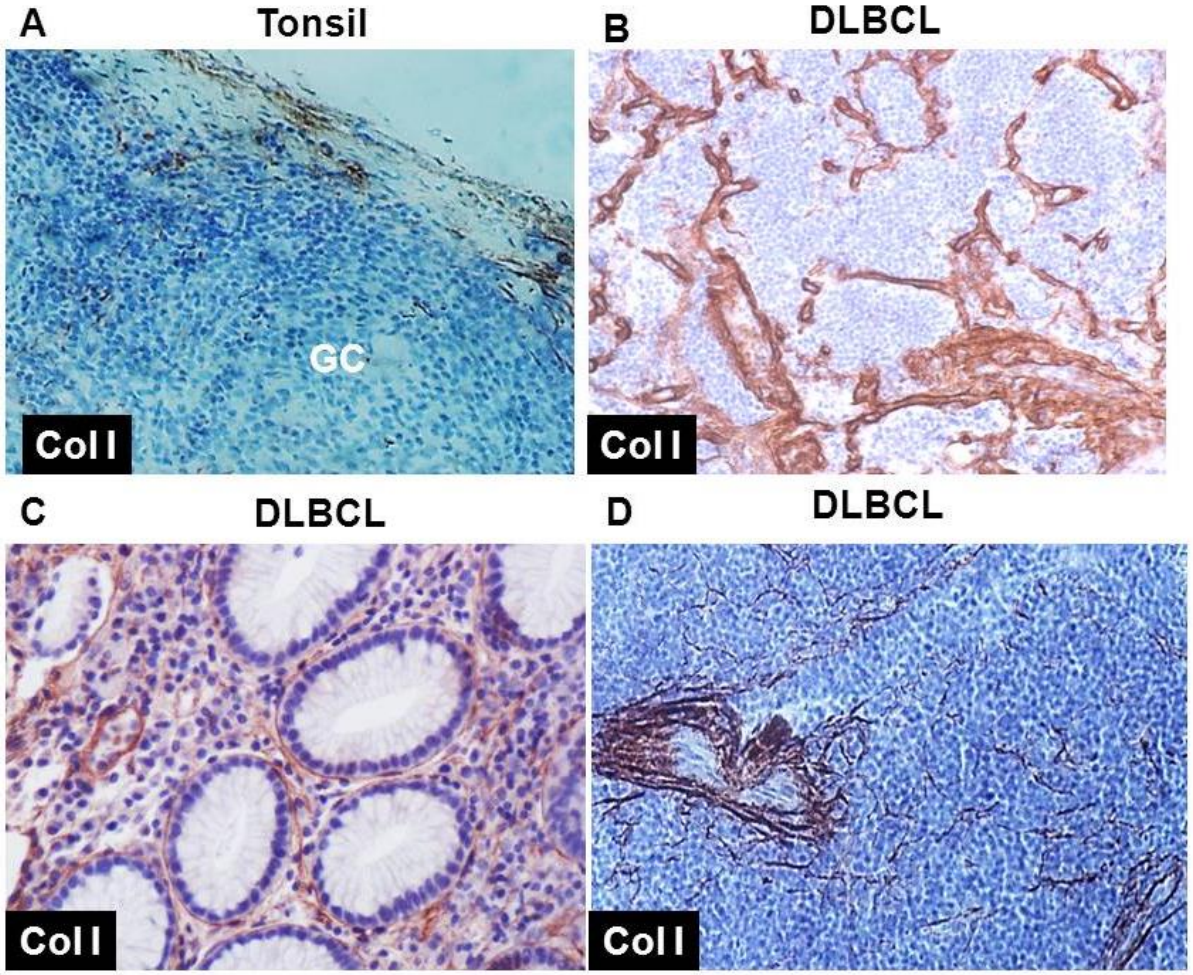

Figure 4.9: Expression of LAIR-1 ligand, Type I collagen in DLBCL Representative examples of IHC staining for Type I collagen (brown) showing it is absent in the GC A), 20x, In most cases Type I collagen was not intimately associated with the tumour cell population but was rather located as a component of larger blood vessels and within surrounding connective tissues as shown in these three examples, 40X, IHC indicates immunohistochemistry.

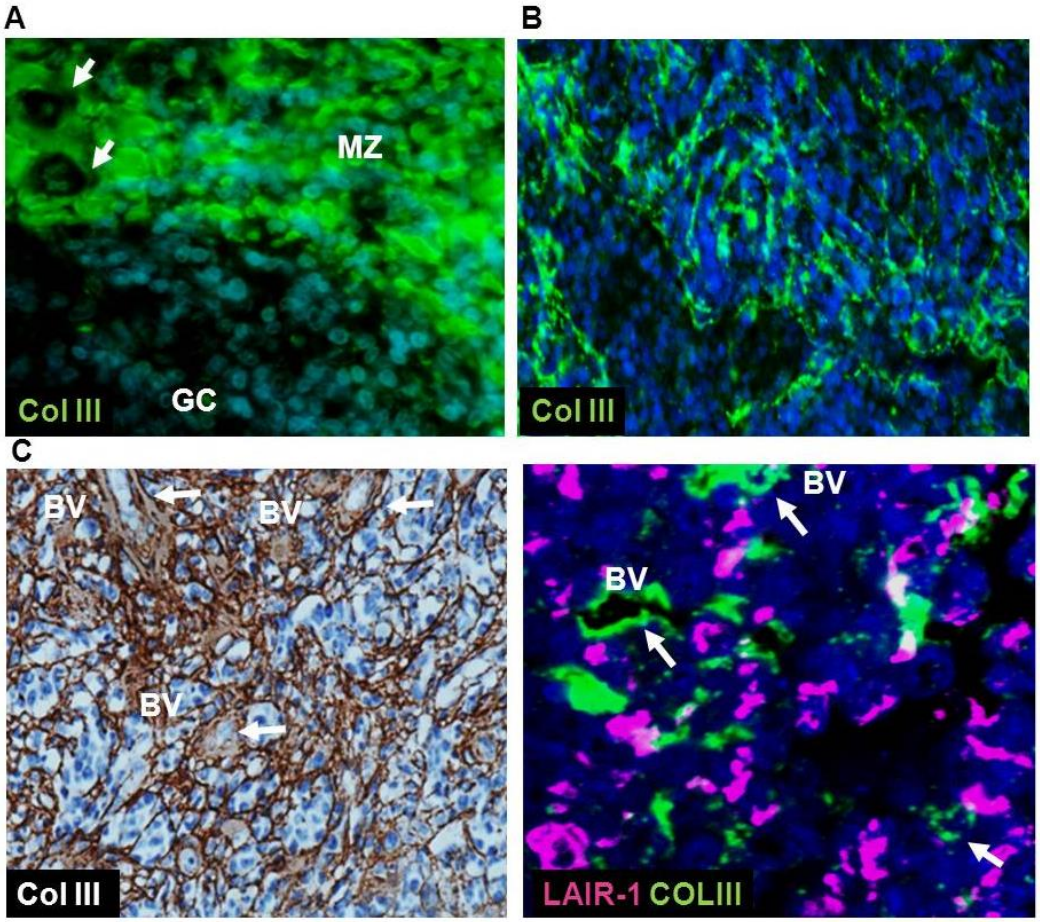

Figure 4.10: Expression of LAIR-1 ligand, Type III collagen in DLBCL. Representative examples of IHC and IF staining for Type III in DLBCL (brown and green, respectively). A) Collagen III is absent from germinal centres of tonsil but present in the vessels of the mantle zones, B-C) In most cases of DLBCL. Type III collagen was intimately associated with the tumour cell population as well as a component of blood vessels in the form of coarse intersecting bands in the tumour stroma (green and brown, respectively) D) shows the results of representative multiplex IHC showing a close association between LAIR-1 expressing cells (pink) and Collagen III (green), 40X, IHC indicates immunohistochemistry, IF indicate immunofluorescence, BV indicates blood vessel, GC indicates germinal centre, MZ indicates mantle zone.

4.2.9 Expression of C1q, an additional functional ligand of LAIR-1

I also studied the expression of C1q as a further known functional ligand of LAIR-1 and which has already described to cause the phosphorylation of LAIR-1 in monocytes **(Son et al., 2012)**. I used IHC in the TMA of DLBCL samples to show that C1q was expressed in the macrophages in 25/28 cases (Figure 4.11A-C).

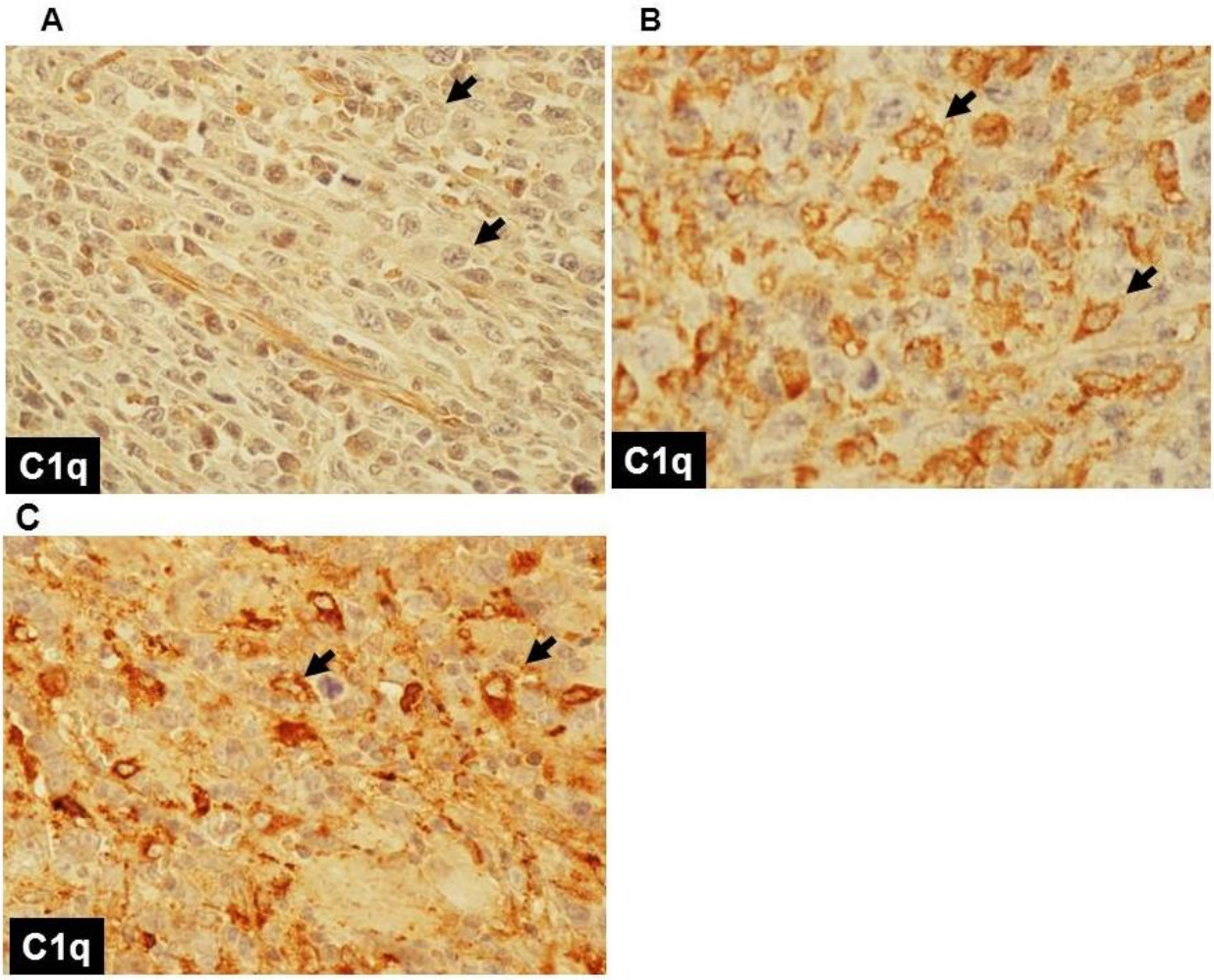

Figure 4.11: Expression of LAIR-1 ligand, C1q in DLBCL. An IHC of DLBCL, with only vessels positive for C1q (A). (B) and C) Representative examples of staining for C1q in DLBCL (brown staining). In most cases C1q was expressed in macrophages within microenvironment at the arrows, 40X, IHC indicates immunohistochemistry.

4.2.10 Over-expression of the collagen receptor, DDR-1 in a subset of DLBCL

Finally, I studied the expression of another collagen receptor, DDR-1, in DLBCL. Although the re-analysis of the datasets described in section 4.2.1 above did not reveal the over-expression of DDR-1 mRNA, this collagen receptor was of interest given that our group has already described its frequent over-expression in HL, a B cell malignancy related to DLBCL **(Cader et al., 2013)**. I first used IF to show that DDR-1 was expressed in the tumour cells of 3/9 cases of DLBCL samples, which was confirmed by co-staining with CD20 (Figure 4.12).

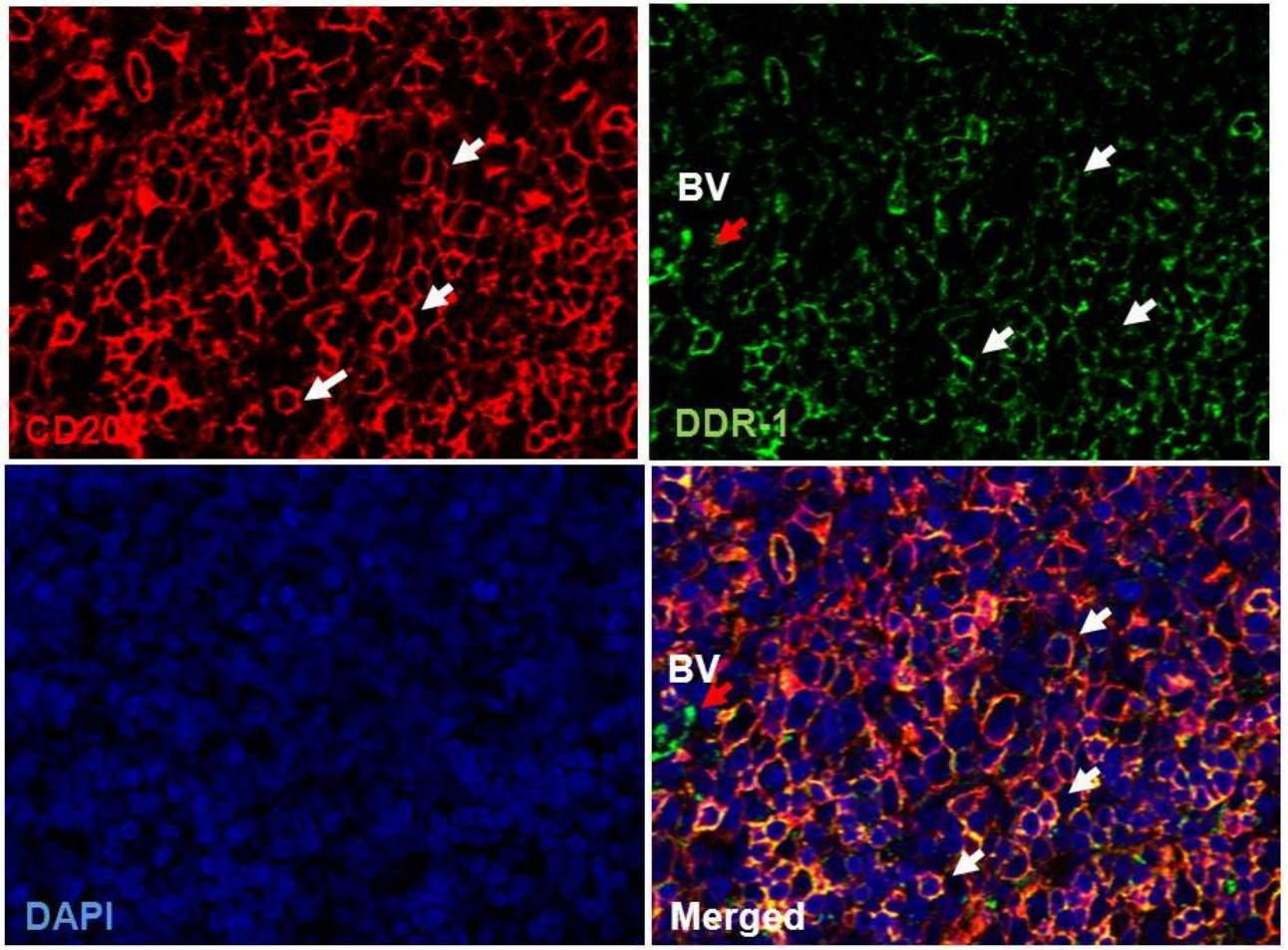

Figure 4.12: Expression of DDR-1 in DLBCL
Representative example of multiplex IF staining of DDR-1 and CD20 in DLBCL. DDR-1 was positive in the blood vessels (red arrow) and CD20-positive tumour cells (white arrows) 40X, IF indicate immunofluorescence.

4.2.11 Expression of DDR-1 ligands, Type IV and Type VI collagen, in DLBCL

Having shown that DDR-1 was over-expressed in primary DLBCL, I next studied the expression of two of its known ligands, collagens Type IV and Type VI. I selected these ligands because the re-analysis of the RNAseq data described above, had shown the over-expression of the collagen IV subunits, COL4A1, COL4A2, and COL4A5, as well as the collagen VI subunits COL6A1, COL6A2, COL6A3 and COL6A6. Using IHC, I found that Type IV collagen was absent in the normal germinal centres as highlighted by CD20 staining (Figure 4.14A). Type VI collagen was also largely absent from germinal centres, while present in the wall of blood vessels outside the germinal centre as highlighted by staining with B cell markers; CD19 and vessel marker; CD31. These collagen positive vessels were highlighted by staining of their endothelial cells with CD31 in normal tonsil (Figure 4.13 B and C respectively). Type VI collagen was observed in 24/25 evaluable cases of DLBCL. Type IV collagen was present in 4/6 evaluable cases of DLBCL (Figure 4.14B-D). In most cases Type IV collagen was deposited not only in the wall of the blood vessels, but also as fine branching fibres intimately associated with the tumour cell population and mainly emanating as a component of blood vessels, Type IV collagen was observed to be in close relation with LAIR-1 positive cells in an exploratory analysis of a small subset of DLBCL (Figure 4.14E). In contrast, Type VI was heterogeneously deposited as fine, or sometimes as coarse fibres intimately in contact with the tumour cells in addition to its presence in the wall of the blood vessels (Figure 4.13D-E). To confirm this, I used image J to measure the number of viable tumour cells in direct or close relation to Type VI collagen fibres. In all 6 cases studied (10 HPF (40x) per case), I found that >50% of tumour cells were intimately associated with Type VI collagen (Figure 4.13G).

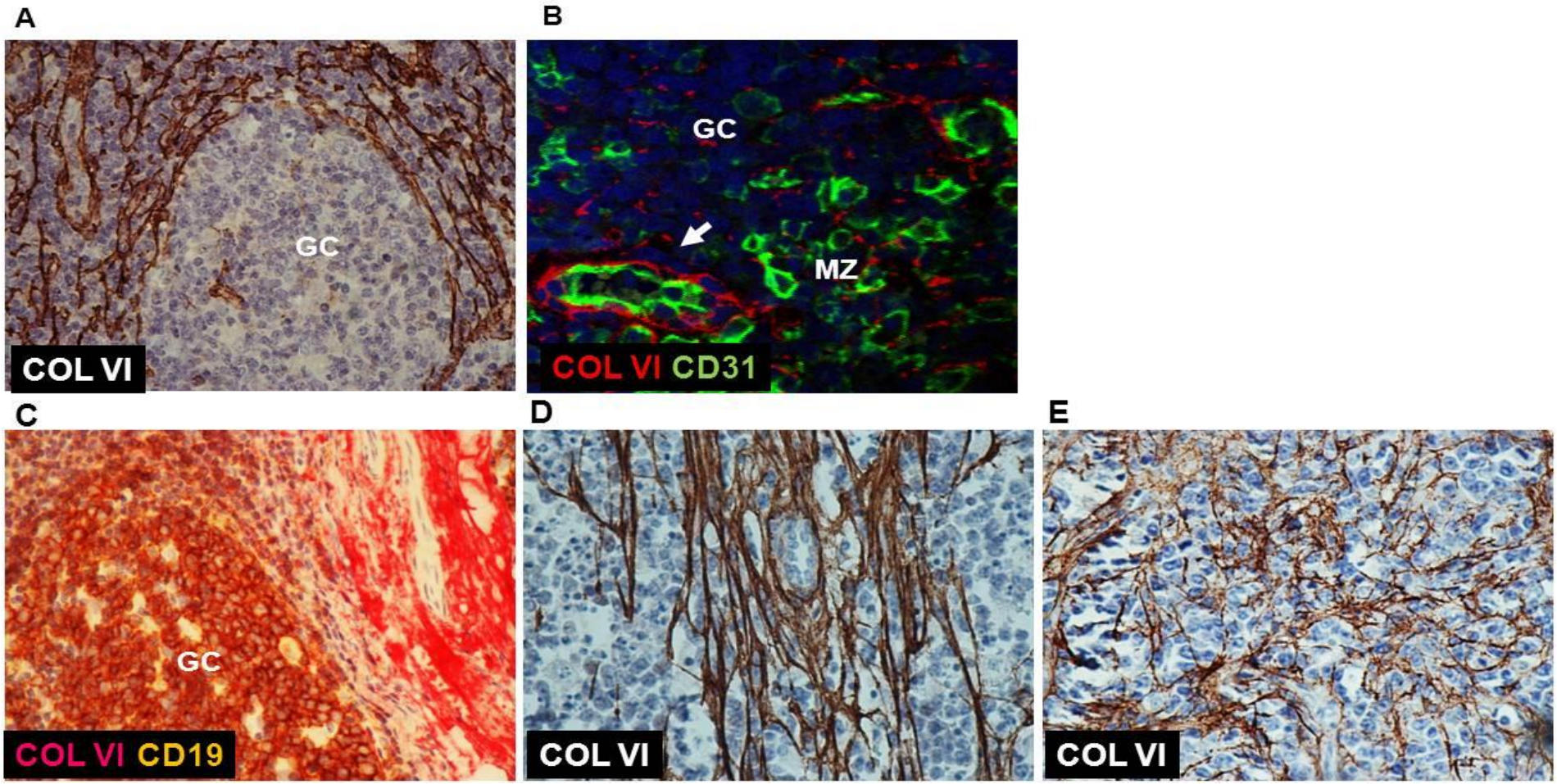

Figure 4.13: Expression of Type VI collagen in DLBCL
Representative examples of staining for Type VI in DLBCL. A) IHC shows the absence of Type VI collagen in GC of tonsil, but its presence in the vessels of the mantle and inter-follicular zones, 20X. B) Double IF showed co-expression of CD31 (green) and collagen VI (red) in tonsil, at the arrows 40X. C) Double IHC shows the absence of Type VI collagen (pink) in the germinal centre which is highlighted with CD19, a B cell marker (brown), 40X. D-E) IHC shows that in most cases Type VI collagen was intimately associated with the tumour cell population as well as a component of blood vessels, 40X, IHC indicates immunohistochemistry, IF indicates immunofluorescence.

F. Table 4.1 Results of quantification of COLVI DLBCL

Case Number	Viable tumour cells with contact or close contact collagen/10HPF		
	Mean total	**Range of total**	**%**
1	303.4	190-420	59.65
2	335.5	212-495	65.04
3	355.4	129-551	58.86
4	254.1	182-392	59.56
5	347	249-484	53.67
6	559.6	464-688	40.77
7	254.1	198-337	62.98
Total	2389.1	190-688	58.8

Table 4.1: Results of quantification using Image J for contact index for Type VI collagen by IHC with tumour cells. Tumour cells showed frequent relation, either direct or close to collagen fibres in the tumour stroma.

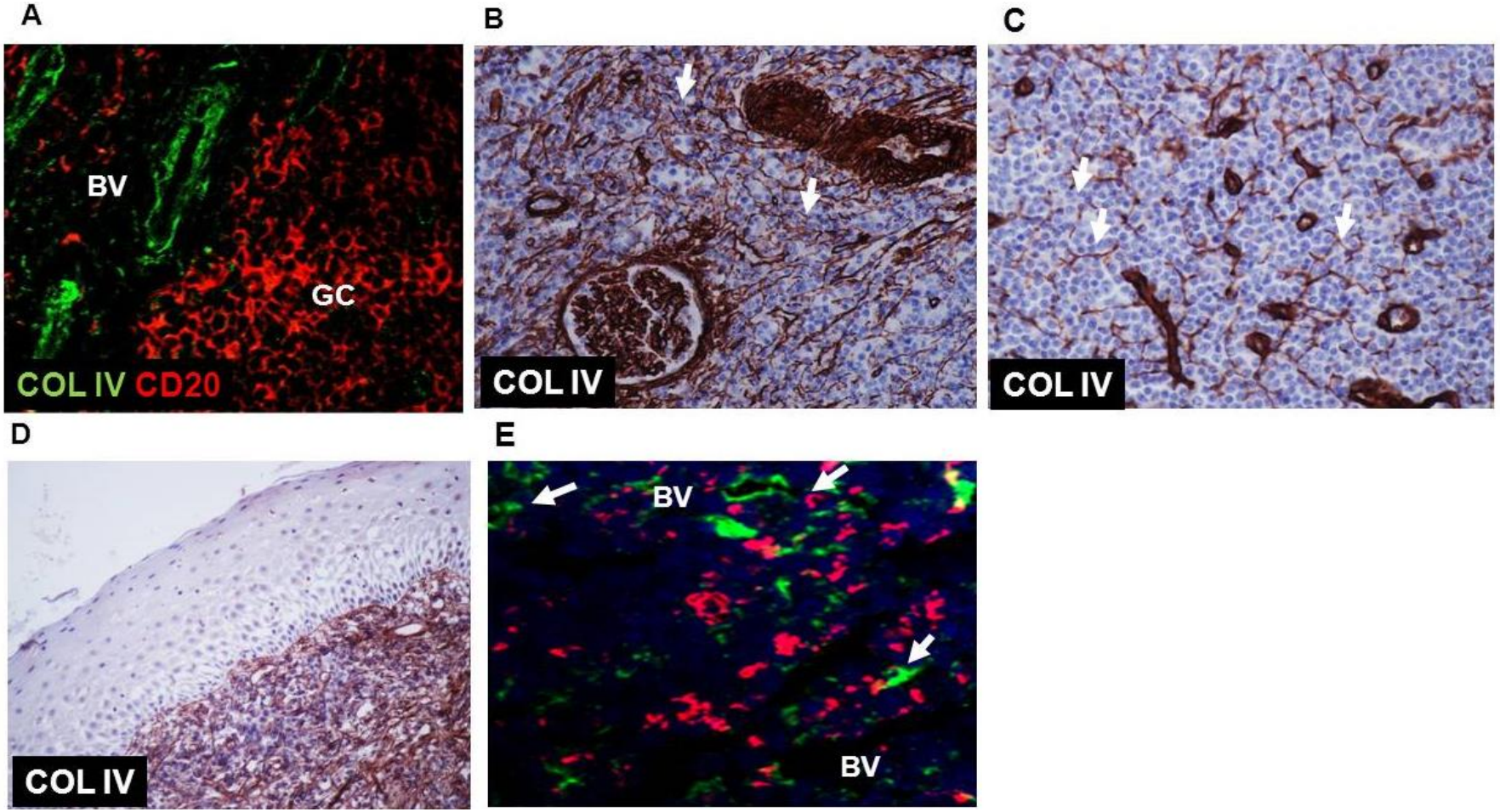

Figure 4.14: Expression of Type IV collagen in DLBCL
Representative examples of staining for Type IV in DLBCL. A) IF shows CD20-positive B cells of a germinal centre in normal tonsil (red) showed absence of collagen, Collagen IV is absent from germinal centres, but present in the vessels of the mantle and interfollicular zones (green). B-D) Renal, nodal and skin DLBCL showed positivity for collagen IV as thin branching fibres at the white arrows. E) Dual IF shows Type IV collagen (green) was intimately associated with the LAIR-1 positive population (red) in DLBCL, at the white arrows, IF indicates immunofluorescence

4.3 DISCUSSION

In this chapter I have shown that DLBCL is characterized by the overexpression of number of collagens and collagen receptors. One of the collagen receptor that was overexpressed in DLBCL was LAIR-1. LAIR-1 is a type I transmembrane glycoprotein which is a member of the Ig superfamily. It is a unique collagen receptor which is involved in various immune reactions, being expressed on the majority of human PBMCs, including NK, T, B, monocytes, and dendritic cells, and the majority of thymocytes. Cross-linking of LAIR-1 on human NK cells induces a potent inhibitory signal that is capable of decreasing target cell lysis by both resting and activated NK cells *in vitro*. It also acts as an inhibitory receptor on effector T cells **(Kridel et al., 2015)**. It is proposed that LAIR-1 signalling could be regulated via its expression because LAIR-1 levels are generally higher on less differentiated or naive cells, and lower on more activated or differentiated immune cells **(Leitinger, 2011)**.

In a previous study using microarray analysis, DLBCL was classified into three clusters, cluster-1, 2 and 3 which are responsible for ‘’oxidative phosphorylation, mitochondrial function and electron transport chain’’, ‘’Cell-cycle regulatory genes/DNA repair gene’’ and the ‘host response cluster’; LAIR-1 was overexpressed in DLBCL in the NK/T cell subcategory in the ‘host response cluster’ **(Monti et al., 2005)**, but little is known about it in the microenvironment of DLBCL. A meta-analysis performed in this chapter which included over 2000 DLBCL samples revealed that genes positively correlated with LAIR-1 were enriched for number of gene ontology terms which included regulation of nitric oxide (NO) biosynthetic process, regulation of macrophage activation during immune response and phagocytosis. Furthermore, genes positively correlated with LAIR-1 were

significantly enriched for genes present in a tumour macrophage signature **(Doig et al., 2013)**. This observation suggested that LAIR-1 expression might be localized mainly to tumour associated macrophages in DLBCL. This was confirmed by IHC, which revealed the co-expression of LAIR-1 with CD68, a pan-macrophage marker, and with CD163 and MRC1 which are both markers of M2 macrophages. This meta-analysis also revealed the significant enrichment of collagen genes among genes positively correlated with LAIR-1, including COL1A1 and COL3A1 which encode subunits of collagen type I and collagen type III, respectively. I used IHC to show that both collagen types are present in DLBCL. Significance of proteins expressed in vessel walls as in the vascular endothelium) may influence the tumour immune micro-environment, if such cells express collagens then these can potentially interact with tumour cells.

Co-localisation studies using proteins expressed in vessel walls (e.g. smooth muscle actin or vimentin) might be helpful to characterise this further. In some cases these collagens were intimately associated with macrophages. Taken together these observations suggest that LAIR-1 could be activated by its collagen ligands potentially leading to important signalling events in the tumour associated macrophages of DLBCL. I also found that C1q was expressed by tumour associated macrophages, but not in tumour cells, in DLBCL, providing a further means to activate LAIR-1 in the macrophages of DLBCL.

The expression of LAIR-1 was described before on monocytes and macrophages, but little is known about its function in these cells, except that LAIR-1 influenced the differentiation of monocytes to dendritic cells **(Son et al., 2012)** and that LAIR-1 expressing macrophages of LAIR-1-/- KO mouse show reduced expression of macrophage activation markers such as CD86 **(Tang et al., 2012)**.

During the course of these experiments I also observed that the expression of a naturally occurring functional antagonist of LAIR-1, LAIR-2, was expressed only at low levels on infiltrating macrophages.

Although compared with normal lymphoid tissues, I observed fewer CD3 positive cells expressing LAIR-1 in the microenvironment of DLBCL, it could be that LAIR-1 expression on tumour infiltrating T cells could have an immune checkpoint function mediated by collagen.

It is interesting to speculate that collagen binding to LAIR-1 could have an inhibitory impact on phagocytic functions, this could be important in DLBCL because rituximab is known to kill CD20-positive cells, through opsonization and macrophage phagocytosis **(Leidi et al., 2009)**.

DDR-1 is a receptor tyrosine kinase which has been shown to be over-expressed in a number of cancer types and which activates potentially oncogenic signals following its over-expression **(Valiathan et al., 2012)**. It has previously been shown that normal GC B cells express DDR-1 at very low levels, while in HL DDR-1 is more highly expressed. It has been shown that collagen type I can activate DDR-1 in HL cell lines. To compare these results, I have explored another EBV related B cell malignancy; DLBCL I explored the expression of DDR-1 in normal germinal centres and DLBCL tumours.

I show here for the first time, that DDR-1 is over-expressed at the protein level in a subset of DLBCL tissue samples (3/9 cases). As it has been shown that collagen can activate DDR-1 leading to the increased survival of lymphoma cells **(Cader et al., 2013)**. In this study, the expression of DDR ligands in DLBCL were examined. I found that collagens types III, IV and VI, are over-expressed in DLBCL, both at the RNA (re-analysis of published data) and also at the protein level. Biological functions

of DDRs can be targeted using small molecules inhibitors such as Bcr-Abl inhibitors **(Day et al., 2008)** and the B-Raf inhibitors, the VEGFR inhibitor and p38 MAPK inhibitor, which were found to inhibit both DDR-1 and DDR-2 **(Borza and Pozzi, 2014)**. Recently, few studies reported the identification of novel inhibitors, selected specifically for DDR-1 receptor, such as pyrozalopyrymidine, which has high affinity but not to others from 455 kinases tested, these can inhibit the proliferation of cancer cells highly expressing DDR-1 **(Gao et al., 2013)**. These preliminary observations suggest that DDR-1 and its ligands are aberrantly expressed in DLBCL and could be a potineal targets in DLBCL.

CHAPTER FIVE

S1PR1 DRIVES A FEED FORWARD SIGNALLING LOOP TO REGULATE THE OVER-EXPRESSION OF BATF3 IN HODGKIN LYMPHOMA CELLS

5.1 INTRODUCTION

Sphingosine-1-phosphate (S1P) is a small oncogenic lipid implicated in cancer growth, survival and invasion **(Moolenaar, 1999, Milstien and Spiegel, 2006)**. S1P molecule can be generated by the enzyme, sphingosine kinase 1 (SPHK1), which is over-expressed in different cancer types, including some non-HL **(Bayerl et al., 2008)**. Conversely, sphingosine-1-phosphate phosphatase (SGPP1), an enzyme which degrades S1P, is down-regulated during tumour development and progression **(Mandala et al., 2000, Le Stunff et al., 2007, Gao et al., 2015)**. Although the over-production of S1P is a characteristic of many cancers, the biological response to S1P is governed by the mix of different S1P receptors. There are five cell surface S1P receptors (S1PR1-5); each coupling to a different repertoire of G proteins. In B cells, S1PR1 mediates mitogenic/pro-survival and chemotactic S1P functions by coupling to Gi to activate Ras/ERK, PI3-K/Akt and Rac **(Takuwa et al., 2001, Takuwa, 2002, Takuwa et al., 2002)** whereas S1PR2 couples to G12/13 to inhibit PI3-K/Akt activity leading to reduced cell growth, survival and migration **(Arikawa et al., 2003, Inoki et al., 2006, Sanchez et al., 2005, Du et al., 2010)**. PI3-K is known to be aberrantly activated in many lymphomas where it provides one of the key survival signals **(Westin, 2014)**. PI3-K is known to be aberrantly activated in many lymphomas where it provides one of the key survival signals **(Westin, 2014)**. Multiple factors are such as loss of function of PTEN **(Wang et al., 2015)**, PIK3CA gene mutations, mTOR **(Westin, 2014)** which are known to activate this pathway. S1PR1 has previously been reported to be over-expressed in HRS cells and to promote their migration *in vitro* **(Kluk et al., 2013)**. In contrast, S1PR2 may be a tumour suppressor in B cell lymphomas; previous studies show

that S1PR2 is mutated in a subset of human DLBCL and that mice lacking S1PR2 expression develop DLBCL **(Cattoretti et al., 2009, Green and Cyster, 2012)**.

Previous studies from our group have shown that HRS cells over-express SPHK1. Basic leucine zipper transcription factor ATF-like (BATF) family is composed of BATF, BATF2 and BATF3, which originate from a bigger family of basic leucine zipper transcription factors **(Finn et al., 2009)**. BATF3 is normally expressed only in T helper type 1 cells and dendritic cells positive for CD8, while it is absent in T-reg and other hematopoietic cells **(Lee et al., 2017b)**. BATF3 is important in the function and development of dendritic cells **(Hildner et al., 2008, Murphy et al., 2013)**. BATF3 functions in the production of IL-12 in response to pathogens **(Hildner et al., 2008, Williams et al., 2001)**. Studies show that T lymphocyte differentiation into T-reg is inhibited by BATF3, as mediated by BATF3 inhibition of T-reg expression **(Lee et al., 2017b)**. It was recently reported that BATF3 is one of the oncogenic targets of the JAK/STAT oncogenic pathway, which is characteristic of the majority of HL and PMLBCL. BATF3 was reported to be overexpressed in CD30 positive lymphomas; HL (70%), CD30 positive DLBCL (75%), PMLBCL (88.8%) **(Lollies et al., 2018)**. BATF3 was shown to have an impact on the survival and growth of ALNHL and HL cell lines was associated with decreased cMYC expression in these cell lines, that BATF3 regulates cMYC functions mediated through binding to an AP1 site in cMYC gene **(Lollies et al., 2018)**. BATF3 has been reported to be expressed in the gene signature of ALNHL which is helpful in distinguishing this from another type of peripheral T cell NHL, with accuracy reaching 97% **(Piva et al., 2010)**. In this chapter I have used multiplex IF to study the expression of S1P receptors in HL, focusing mainly on S1PR1 and S1PR2, BATF3 as well as the expression and

activation of downstream signalling components. *Please note: Some data within this chapter is taken from our recent paper **(Vrzalikova et al., 2018)**.

5.2 RESULTS

5.2.1 Expression of S1P receptors in normal lymphoid tissue

I first studied the expression in HL, of S1PR1 and S1PR2; the major S1P receptors implicated in cancer pathogenesis. I first used conventional IHC and then multiplex IF with lymphoid markers, BCL6 and CD20, to show that normal GC B cells express S1PR2, but not S1PR1 (Figures 5.1 A and F) (Figures 5.1 B-E and G-L).

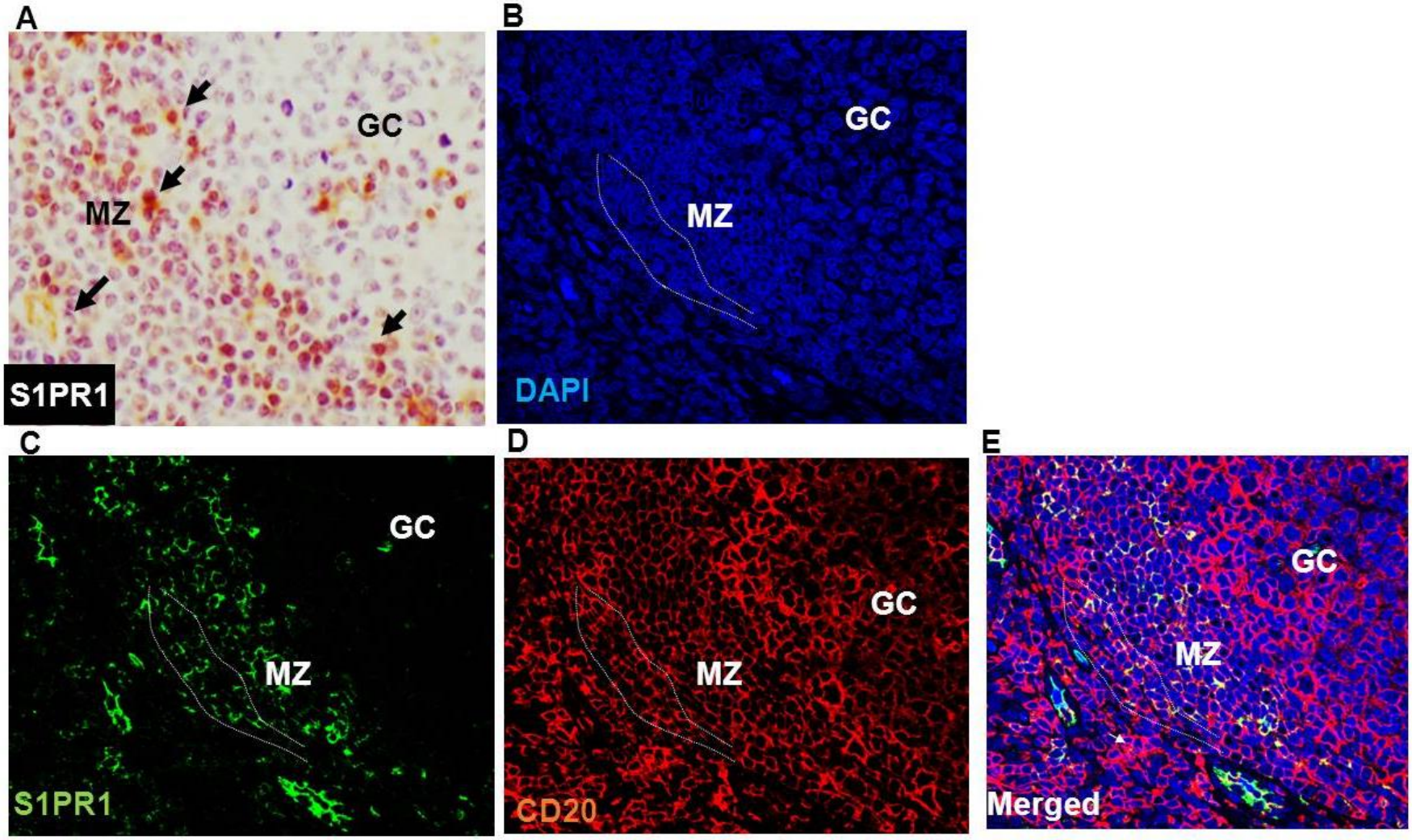

Figure 5.1: **Expression of S1PR1 and S1PR2 in normal lymphoid tissues** A-E) Normal tonsil IHC and multiplex IF: S1PR1 expression in MZ B cells and capillaries (white arrows) but not in normal GC B cells, confirmed by co-staining for CD20 (red) and S1PR1 (green).

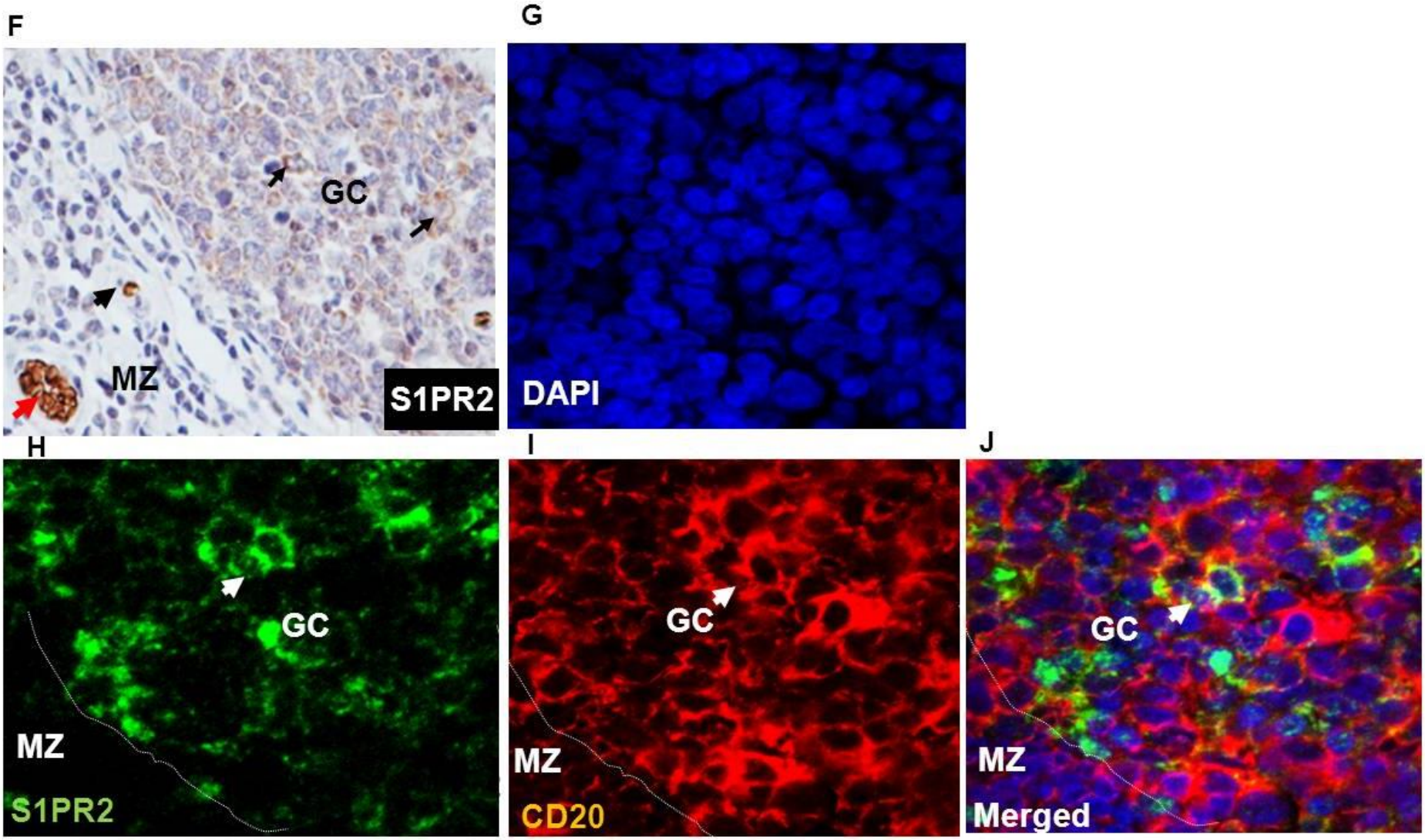

F-J) Normal tonsil IHC and multiplex IF: S1PR2 was weakly expressed in normal GC B cells and in red blood cells (black arrows), confirmed by co-staining with CD20 in red (white arrows).

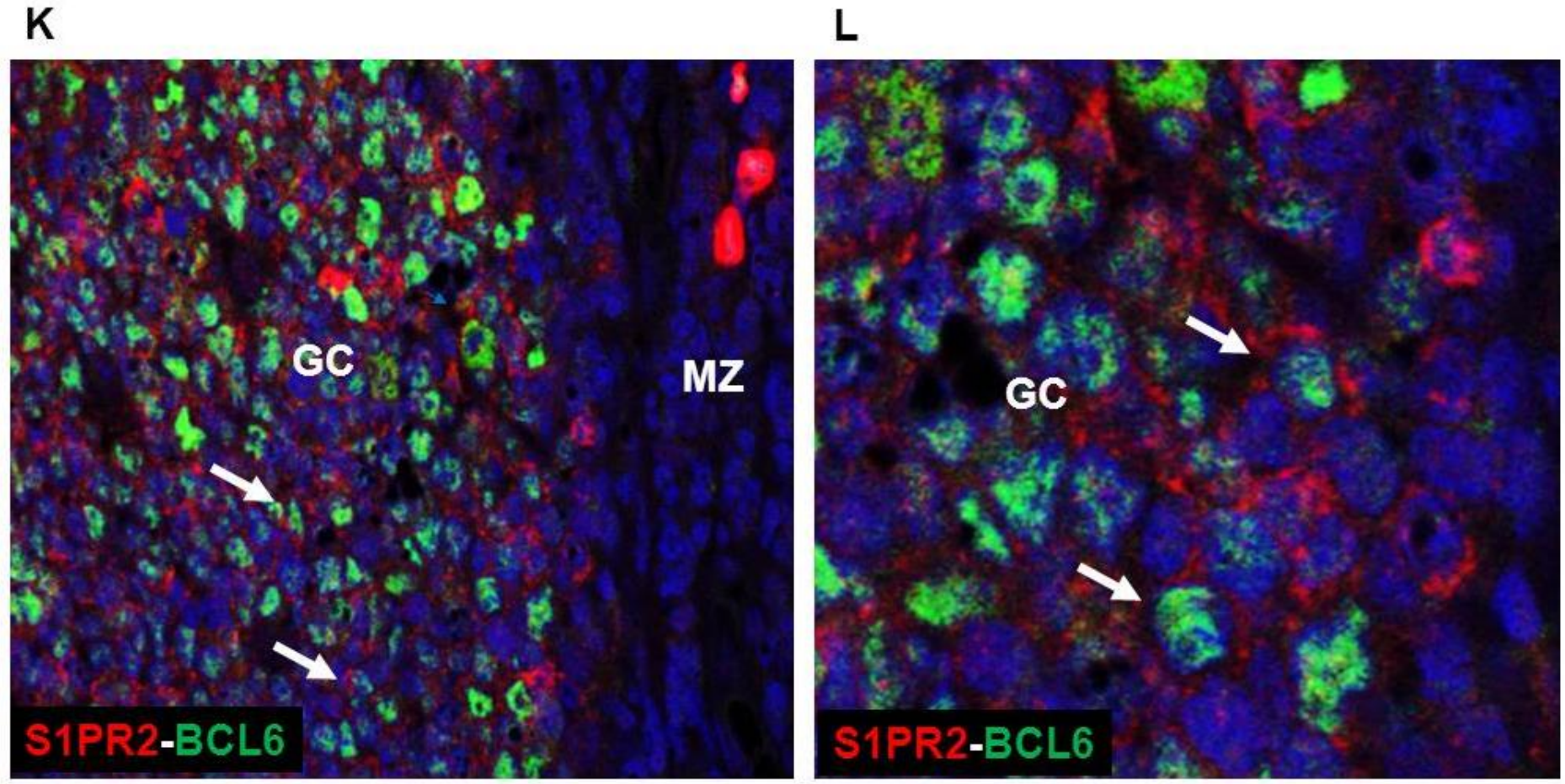

K-L) Co-staining with BCL6 (green) and S1PR2 (red) confirmed positivity for S1PR2 in GC B cells at the white arrows. A-K 40x magnification, L) zoomed.

5.2.2 Expression of S1P receptors in a cohort of HL

I studied the expression of S1PR1 and S1PR2 in a cohort of 61 cases. In 36/61 cases HRS cells expressed S1PR1 in the cytoplasm and/or membrane using a cut off whereby ≥25% of HRS cells had to be positive for the case to be scored positive. None of the 61 cases were positive for S1PR2. I confirmed these observations by multiplex staining with CD30 (Figure 5.2 A and B). I also found that HL cell lines including EBV positive (L591) and EBV negative (L428, L1236 and KMH2) lines showed expression of both receptors but in general levels of S1PR1 were higher (Figure 5.2 C). I concluded that in contrast to their normal counterparts, HRS cells in general express high levels of S1PR1 but lack expression of S1PR2.

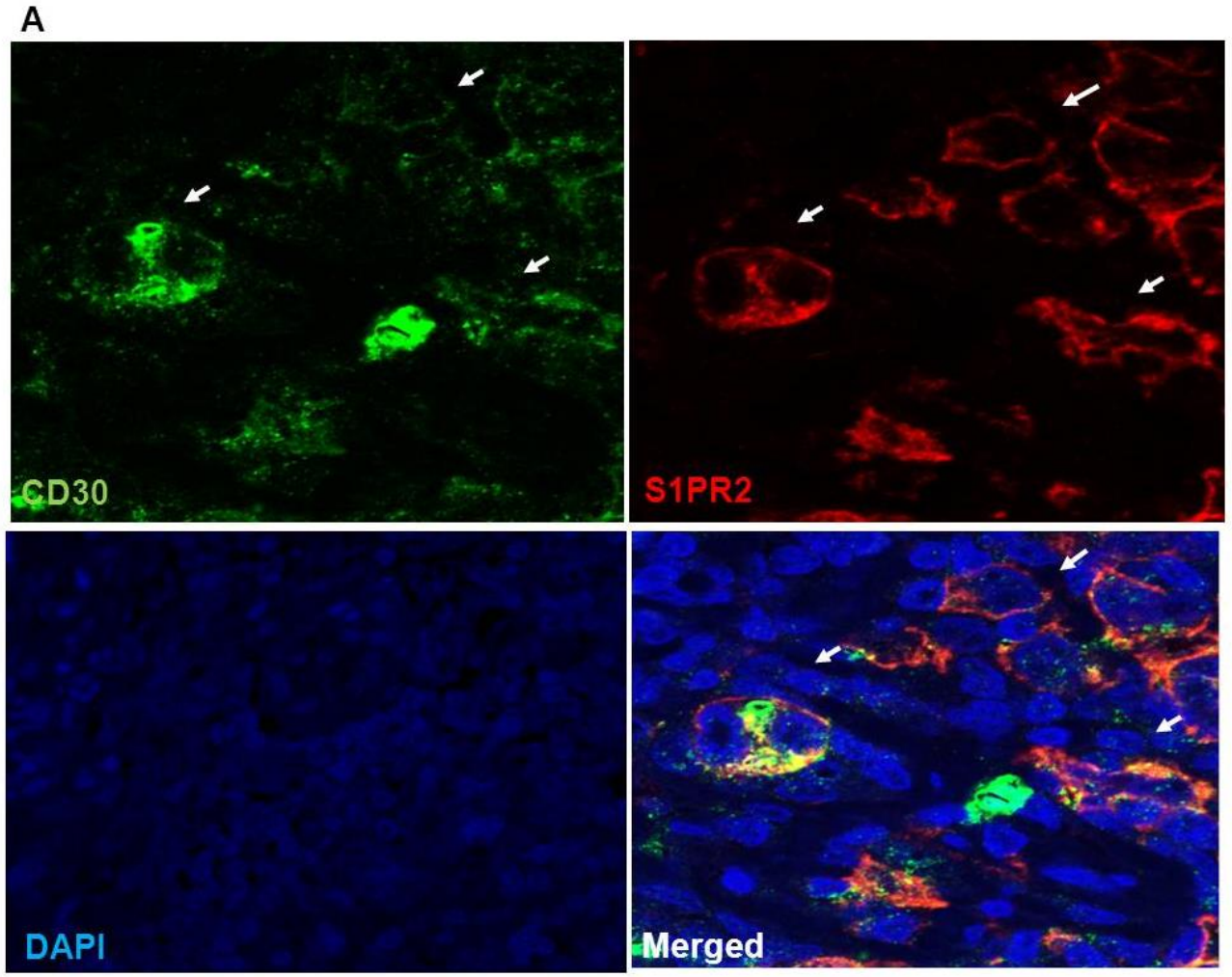
A
CD30
S1PR2
DAPI
Merged

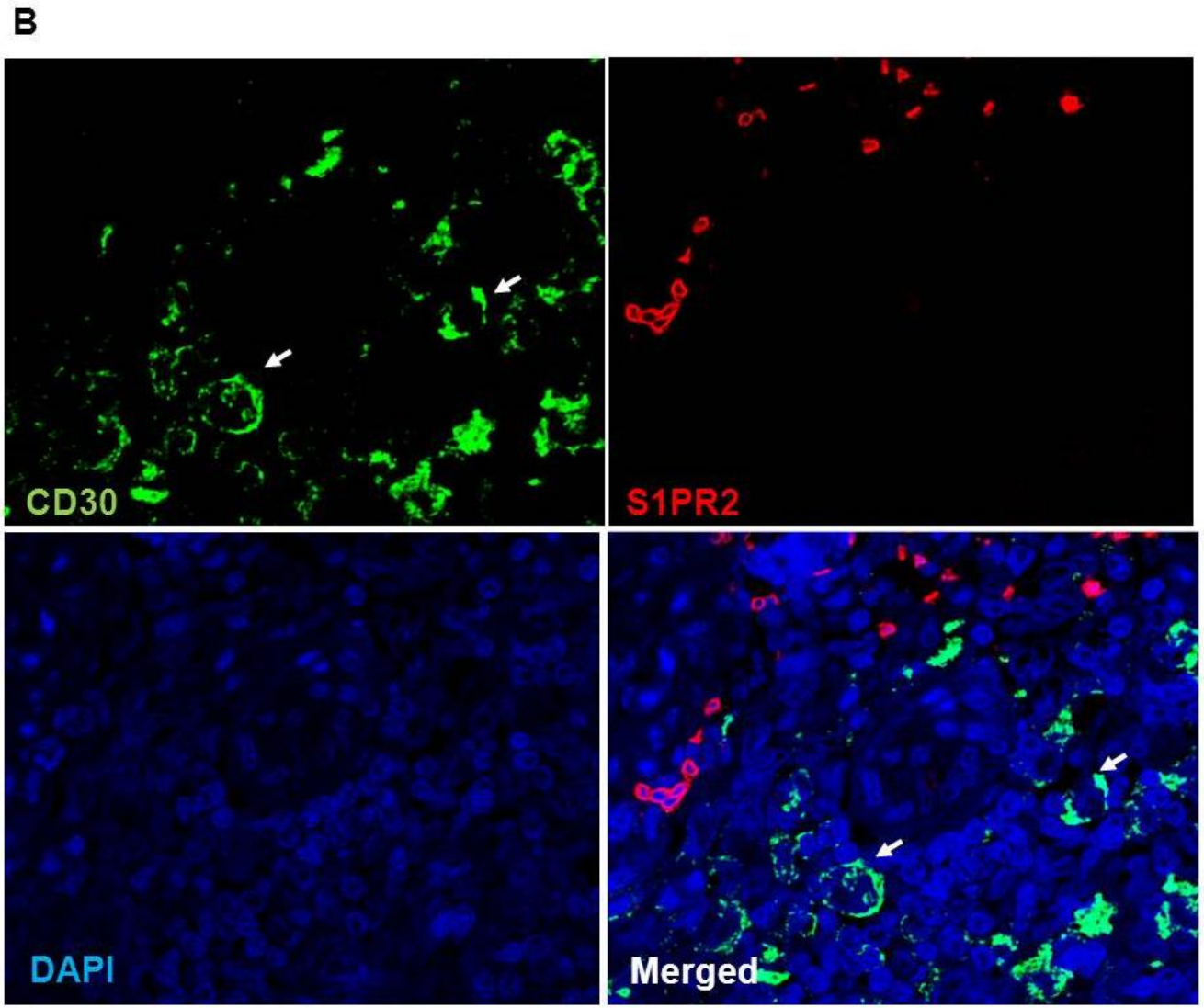

Figure 5.2: **Expression of S1PR1 and S1PR2 in HRS cells in clinical samples and HL cell lines**
A) and B): HRS cells expressed S1PR1 (green) in cytoplasmic and membranous pattern but not S1PR2 (red) (white arrows) confirmed by CD30 co-staining. Endothelial cells and red blood cells were strongly positive for S1PR1 and S1PR2, respectively.

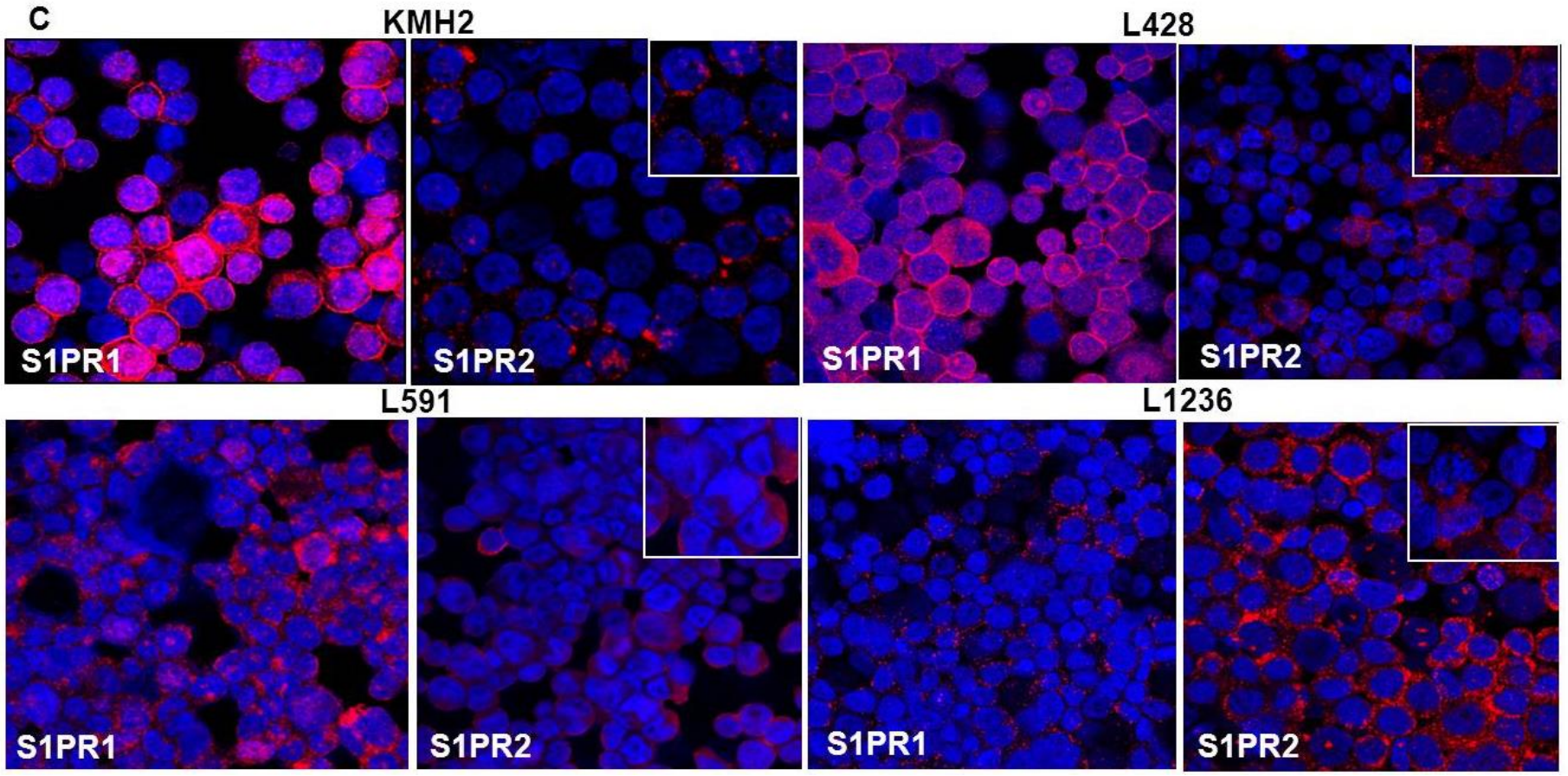

C) Expression of S1PR1 and S1PR2 in HL-derived cell lines: Immunohistochemical detection of S1PR1 (red) and S1PR2 (red) protein expression in HL cell lines, showing higher levels of S1PR1, 40x magnification.

5.2.3 S1P-induced PI3-K signalling in HRS cells is mediated by the differential expression of S1P receptors

I next studied the effects of S1P on PI3-K signalling in HRS cells using Akt phosphorylation as a read-out. L428 cells were treated with S1P and the phosphorylation of Akt in these cells studied using an antibody against the phosphorylated forms of Akt (Ser473). I found using IF followed by Vectra image analysis, that treatment of L428 cells with S1P increased the levels of pAkt in these cells compared to cells treated with BSA alone, used as a control. Time point was 24 Incubation following 24 hour treatment with S1P or BSA (Figure 5.3 A and B). However, I did not observe any increase in pAkt in L1236 cells which is reported to have constitutively high Akt **(Schwering et al., 2003a)** and which other members of our group have shown is resistant to the S1PR1 inhibitors, Siponimod and Ozanimod **(Vrzalikova et al., 2018)**. To study the effects of the individual receptors on pAkt, I stained L428 cells following transfection with an S1PR1 expression vector carrying a V5 tag and treatment with S1P. Time point was 15 min incubation following 24 hour treatment with S1P or BSA. I co-stained these cells for V5 and pAkt and found that in V5-positive cells were significantly more likely to also express pAkt than were un-transfected cells in the same population. This effect was seen with ($p<0.0001$) and without ($p<0.0001$) the addition of exogenous S1P (Figure 5.4 and table 5.1). To study the effect of S1PR2, which inhibits PI3-K/Akt activity, KMH2 cells were transfected with an S1PR2-HA expression vector, S1PR2 transfection experiments were performed in KMH2 cells because this is one of the lines that reacts to S1P at the early time points.

IF used to detect pAkt and the HA tag. I found that cells ectopically expressing S1PR2 were significantly more likely to be phospho-Akt negative than HA-negative cells in the same transfected population, an effect we observed with ($p<0.0001$) and without ($p<0.0001$) the addition of exogenous S1P (Figure 5.5 and Table 5.2). I conclude that S1PR1 expression, in the absence of S1PR2, can activate PI3-K signalling in HRS cells.

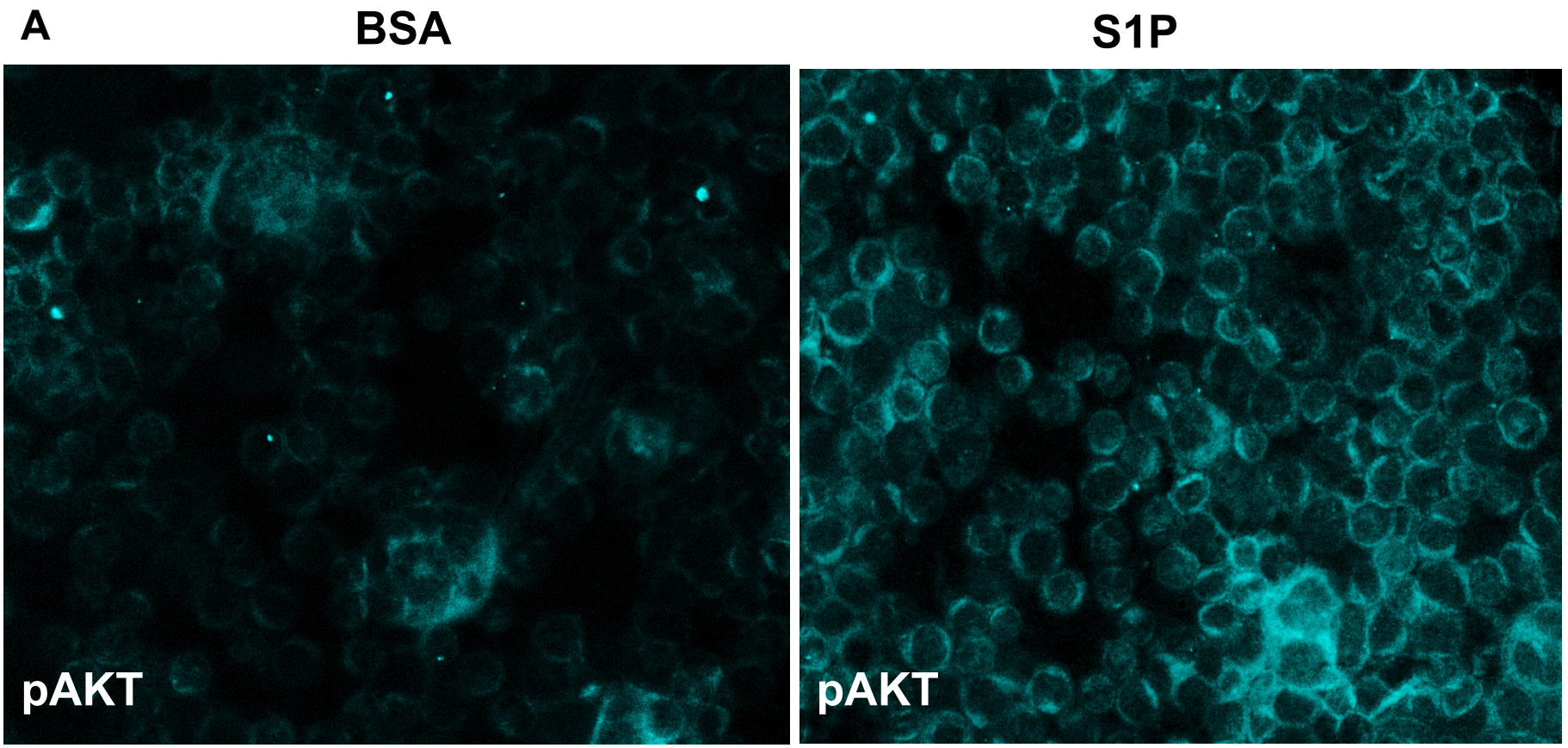
A
BSA
S1P
pAKT
pAKT

B

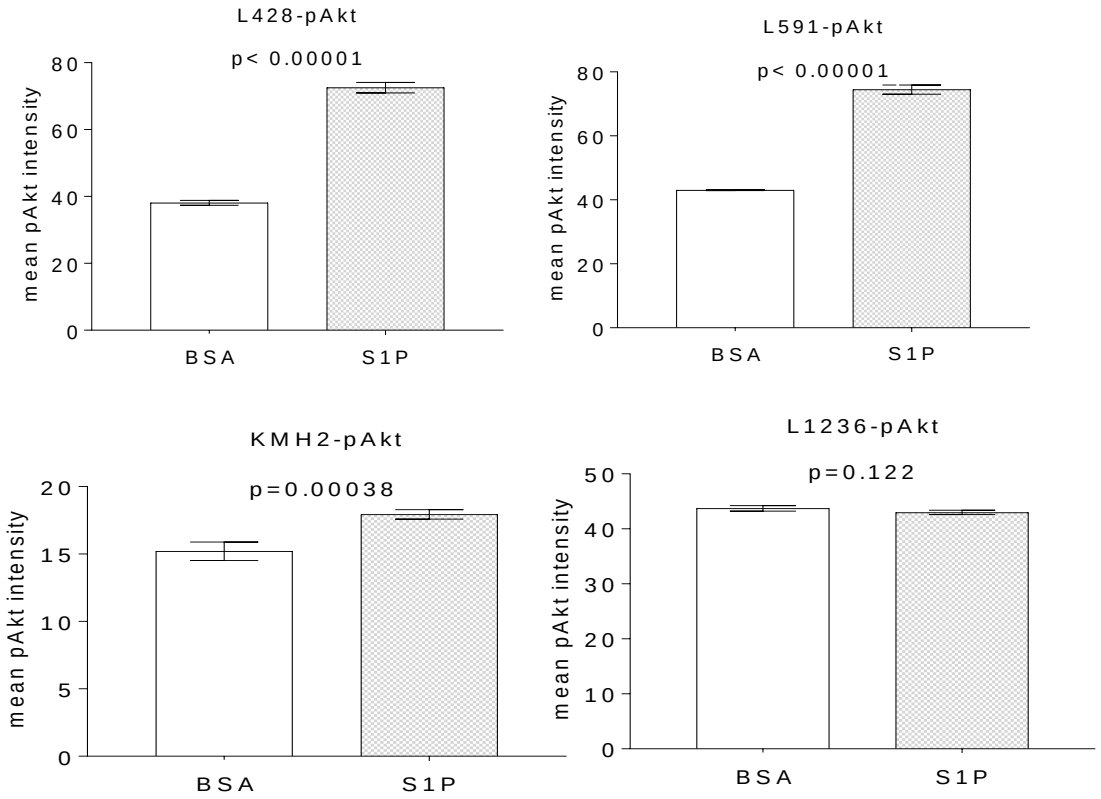

Figure 5.3: Regulation of Akt by S1P in L428 HL cell line A) SIP treatment correlated with the upregulation of the expression of Akt (yellow) in L428 cell line, 20x. B) Showed significant high levels of Akt in S1P treated L428, L591 and KMH2 but not L1236.

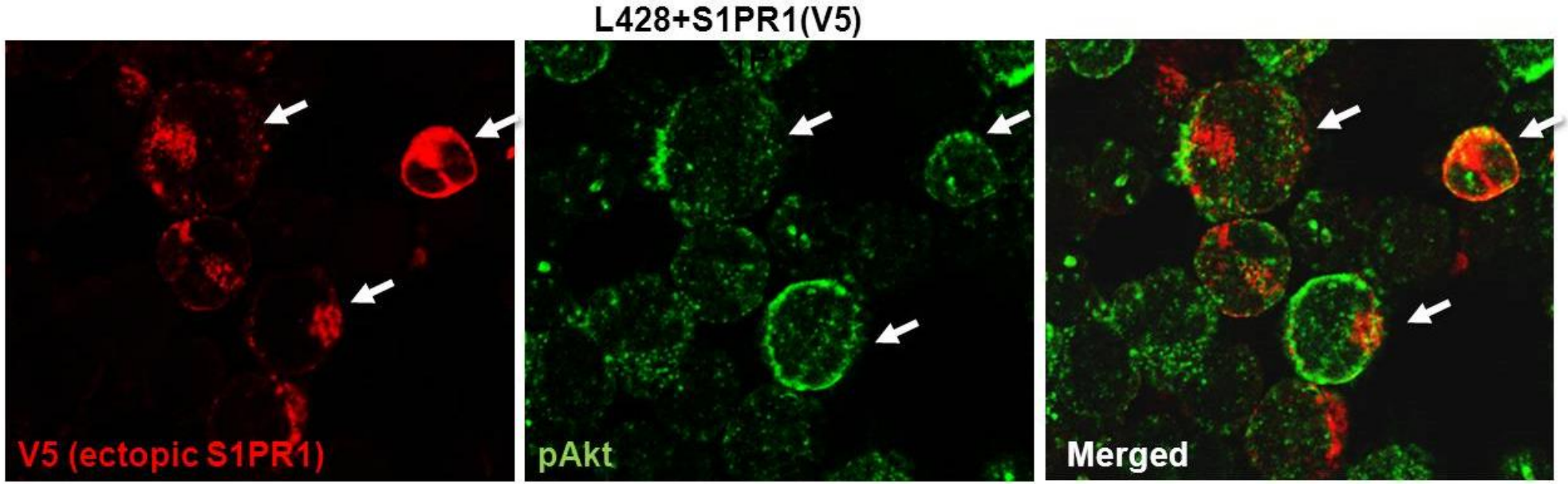

Figure 5.4: S1PR1 is correlated with overexpression of pAkt in S1P treated L428 cell line
IF for phospho-Akt and V5tag of the S1PR1 expression vector. White arrow showed transfected V5tag cells, double labelled with Akt, 40X.

Tables 5.1 showed the results of image analysis of phenotyping of V5 tag labelled L428 BSA and S1P treated cells.

L428+S1PR1(V5)+BSA

Cell phenotype	Number of cells	%
V5 single positive	70	1.65
pAkt single positive	2155	50.81
Double positive	659	15.54
Double negative	1357	32.00
Total	4241	100

Chi square=227.98, p<0.0001

L428+S1PR1(V5) +S1P

Cell phenotype	Number of cells	%
V5 single positive	265	18.49
pAkt single positive	297	20.73
Double positive	374	26.10
Double negative	497	34.68
Total	1433	100

Chi square= 63.50, p<0.0001

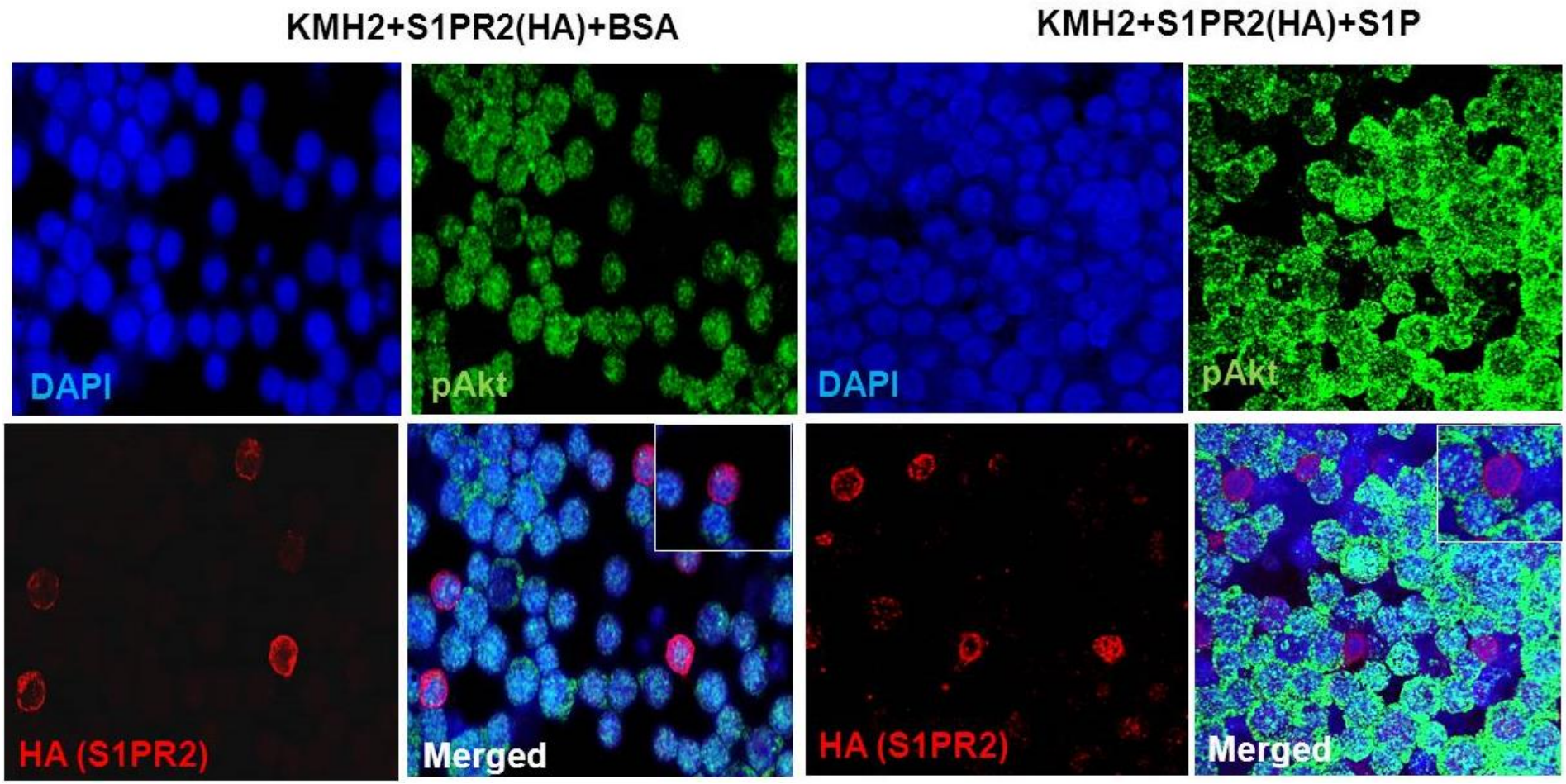

Figure 5.5: S1P-induced PI3-K signalling in KMH2 cell line is mediated by differential expression of S1P receptors
IF for phospho-Akt (green) and the HA tag of the S1PR2-HA expression vector (red), showing HA tag labelled cells ectopically expressing S1PR2, 40x.

Table 5.2: Results of image analysis of BSA and S1P treated KMH2 transfected with HA-tagged plasmid

BSA

Cell phenotype	Number of cells	%
pAkt single positive	1900	49.15
HA single positive	188	4.86
Double positive	22	0.57
Double negative	1756	45.42
Total	3866	100

Chi square=155.07, p<0.0001

S1P

Cell phenotype	Number of cells	%
pAkt single positive	1620	65.80
HA single positive	80	3.25
Double positive	34	1.38
Double negative	728	29.57
Total	2462	100

Chi square=68.60, p<0.0001

5.2.4 Expression of the transcription factor, BATF3, is regulated by PI3-K signalling in HRS cells

To identify the transcriptional targets of PI3-K signalling in HL cells, I took advantage of a microarray experiment that had been performed by a previous member of our group in which KMH2 cells were treated with the PI3-K inhibitor, LY294002 **(Jücker et al., 2002)**. A re-analysis of these data showed that the addition of LY294002 for 16 hours was followed by the up-regulation of 694 genes and the down-regulation of 330 genes. Re-analysis of Brune data set; GSE12453 **(Brune et al., 2008)** identified 743 genes up-regulated and 622 genes down-regulated in micro-dissected HRS cells compared with normal centrocytes. Genes up-regulated in HRS cells (OR=2.15; p<0.0001), but not those down-regulated in HRS cells (OR=1.00; p=0.96), were significantly enriched in genes down-regulated following PI3-K inhibition. Likewise, genes down-regulated in HRS cells (OR=2.95; p<0.0001), but not those up-regulated in HRS cells (OR=1.28; p=0.056), were significantly enriched in genes up-regulated after PI3-K inhibition. These data indicate that the activation of PI3-K signalling contributes to the transcriptional programme of HRS cells. I next wanted to establish if this was also the case for both the EBV-positive and EBV-negative forms of HL. To do this a third dataset was re-analysed from a published microarray by Steidl et al which compared gene expression in micro-dissected HRS cells with that in micro-dissected normal GCs and which had reported EBV status for a subset of cases **(Steidl et al., 2012)**. This revealed that the transcriptional targets of PI3-K signalling identified above were significantly enriched in those genes differentially expressed in both EBV-positive and EBV-negative HRS cells (not shown).

A gene ontology analysis revealed that genes regulated by PI3-K signalling in primary HRS cells were enriched for those with a function in ‘transcription initiation

from RNA polymerase II promoter', suggesting that PI3-K signalling might contribute to the aberrant expression of transcription factors observed in HRS cells (Figure 5.6 A). To identify relevant transcription factors targets genes regulated by PI3-K signalling in primary HRS cells were compared with a comprehensive set of transcription factors described by Vaquerizas et al **(Vaquerizas et al., 2009)** .This revealed the up-regulation of 12, and the down-regulation of 47 transcription factors by PI3-K signalling in HRS cells (Figure 5.6 B). They included the dendritic cell transcription factor, BATF3, which was previously reported to be over-expressed at the mRNA level in HRS cells **(Rosenwald, 2003, Schwering et al., 2003a)** and which was also the PI3-K regulated gene most highly up-regulated in the re-analysis of global gene expression in primary HRS cells described above **(Schwering et al., 2003b, Brune et al., 2008, Steidl et al., 2012)**.

To confirm that BATF3 was regulated by PI3-K signalling, I stained KMH2 cells transfected with a MYC-tagged plasmid containing either a constitutively active p110 gene or a constitutively active Akt1 gene, titrating the MYC antibody to detect only exogenous MYC. I found that cells ectopically expressing either p110 or Akt (Figure 5.7) were significantly more likely to be phospho-Akt-positive (both $p<10^{-4}$) and BATF3-positive (both $p<10^{-4}$) than were un-transfected cells (cells those that have not taken up the plasmid). These data show that PI3-K/Akt signalling leads to aberrant BATF3 expression in B cell lymphoma.

A

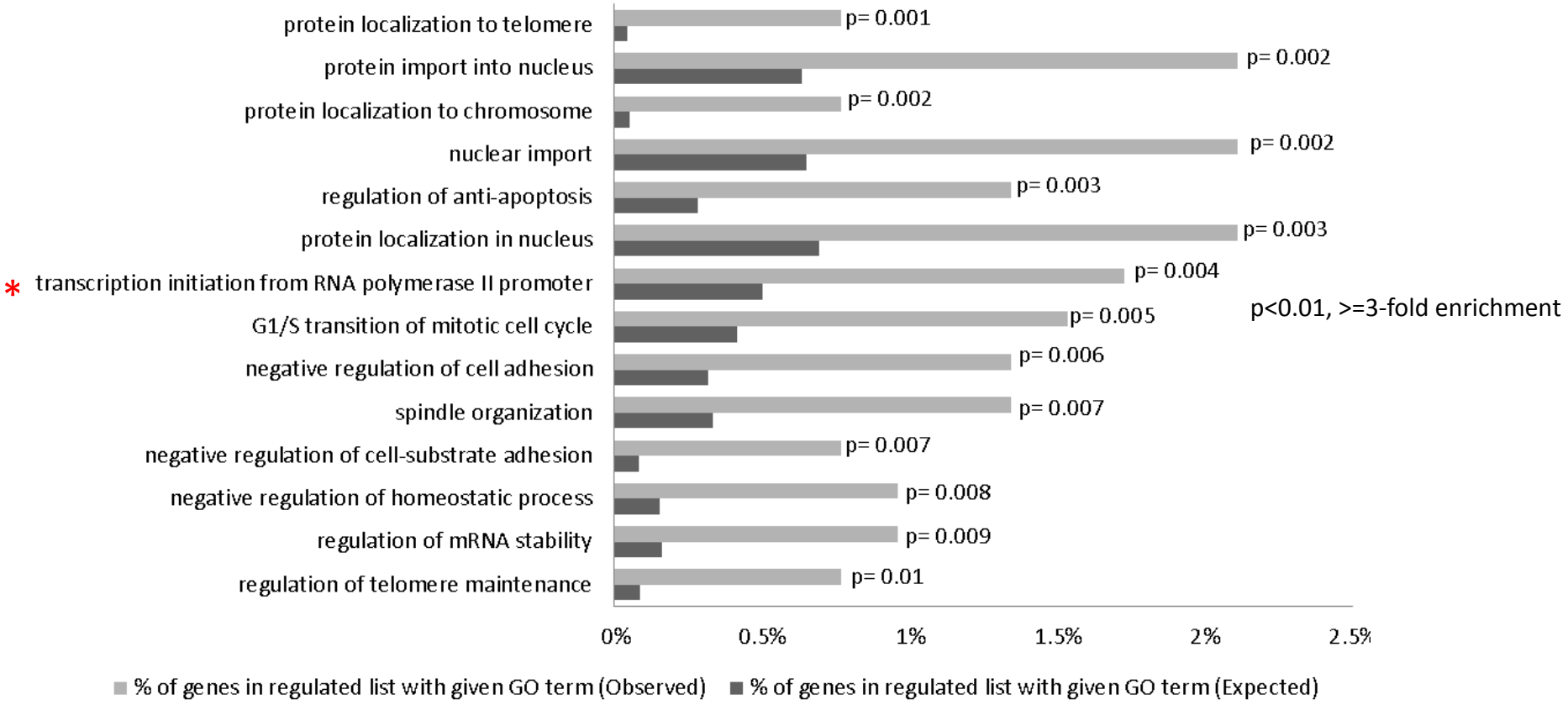
protein localization to telomere
protein import into nucleus
protein localization to chromosome
nuclear import
regulation of anti-apoptosis
protein localization in nucleus
* transcription initiation from RNA polymerase II promoter
G1/S transition of mitotic cell cycle
negative regulation of cell adhesion
spindle organization
negative regulation of cell-substrate adhesion
negative regulation of homeostatic process
regulation of mRNA stability
regulation of telomere maintenance
p= 0.001
p= 0.002
p= 0.002
p= 0.002
p= 0.003
p= 0.003
p= 0.004
p= 0.005
p= 0.006
p= 0.007
p= 0.007
p= 0.008
p= 0.009
p= 0.01
0%
0.5%
1%
1.5%
2%
2.5%
% of genes in regulated list with given GO term (Observed)
% of genes in regulated list with given GO term (Expected)
p<0.01, >=3-fold enrichment

B

Transcription factors up-regulated in HRS cells and by PI3K

ATF5
BATF
BAT3
CD36
DMRT1
GAT3
LHX2
MAZ
PRDM13
RXRA
SPIB
ZBTB32

Transcription factors on all arrays

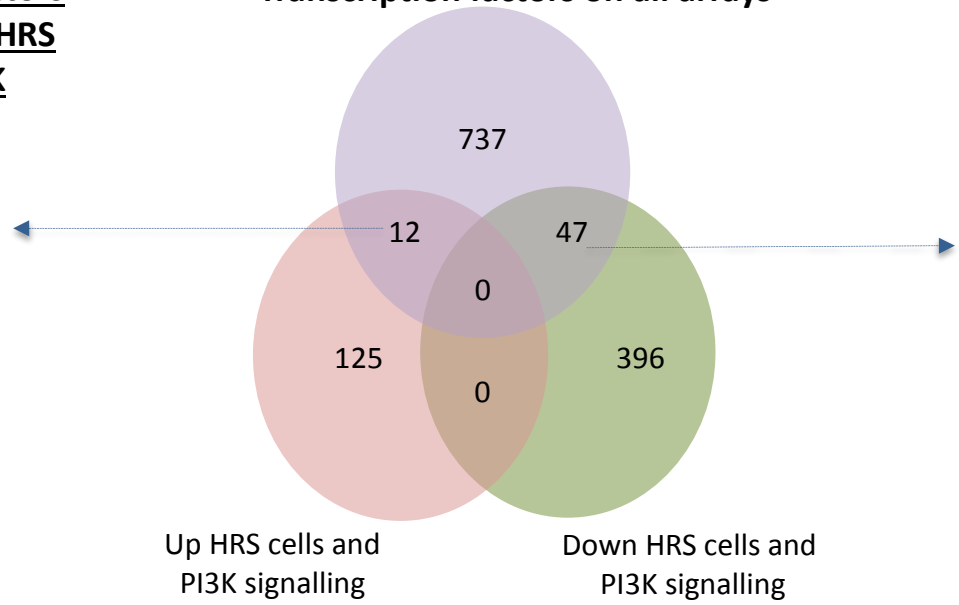

Transcription factors down-regulated in HRS cells and by PI3K

PRDM2	MBD2	NCOA1
GABPB1	BCL6	NR3C1
UBP1	TERF2	NFKB2
CUL3	KLF10	HMG20B
CDC5L	DUSP12	TGIF1
MBNL1	SLC30A9	H1FX
BACH1	ZFR	HIST1H1C
PRKRIR	MKRN1	
ZNF91	SMAD4	
COPS2	RERE	
RC3H2	CUL1	
ZBTB11	EDF1	
ZNF189	TERF2IP	
SP2	AKAP8L	
NFE2L2	HMGB3	
RBM6	ZNF267	
NFATC3	CREBL2	
MGMT	ZNF281	
RNF114	PRRX1	
TAX1BP1	ZFP36L2	

Figure 5.6: PI3-K signalling up-regulates BATF3 in HRS cells
A) Gene ontology analysis of genes regulated by PI3-K signaling in primary HRS cells (in at least one comparison; total of 137 up-regulated and 443 down-regulated genes) revealed enrichment of several functions including 'transcription initiation from RNA polymerase II promoter B) Comparison of genes regulated by PI3-K signalling in primary HRS cells with a comprehensive set of TF53 revealed the up-regulation of 12 TF and the down-regulation of 47 TF by PI3-K signalling in HRS cells.

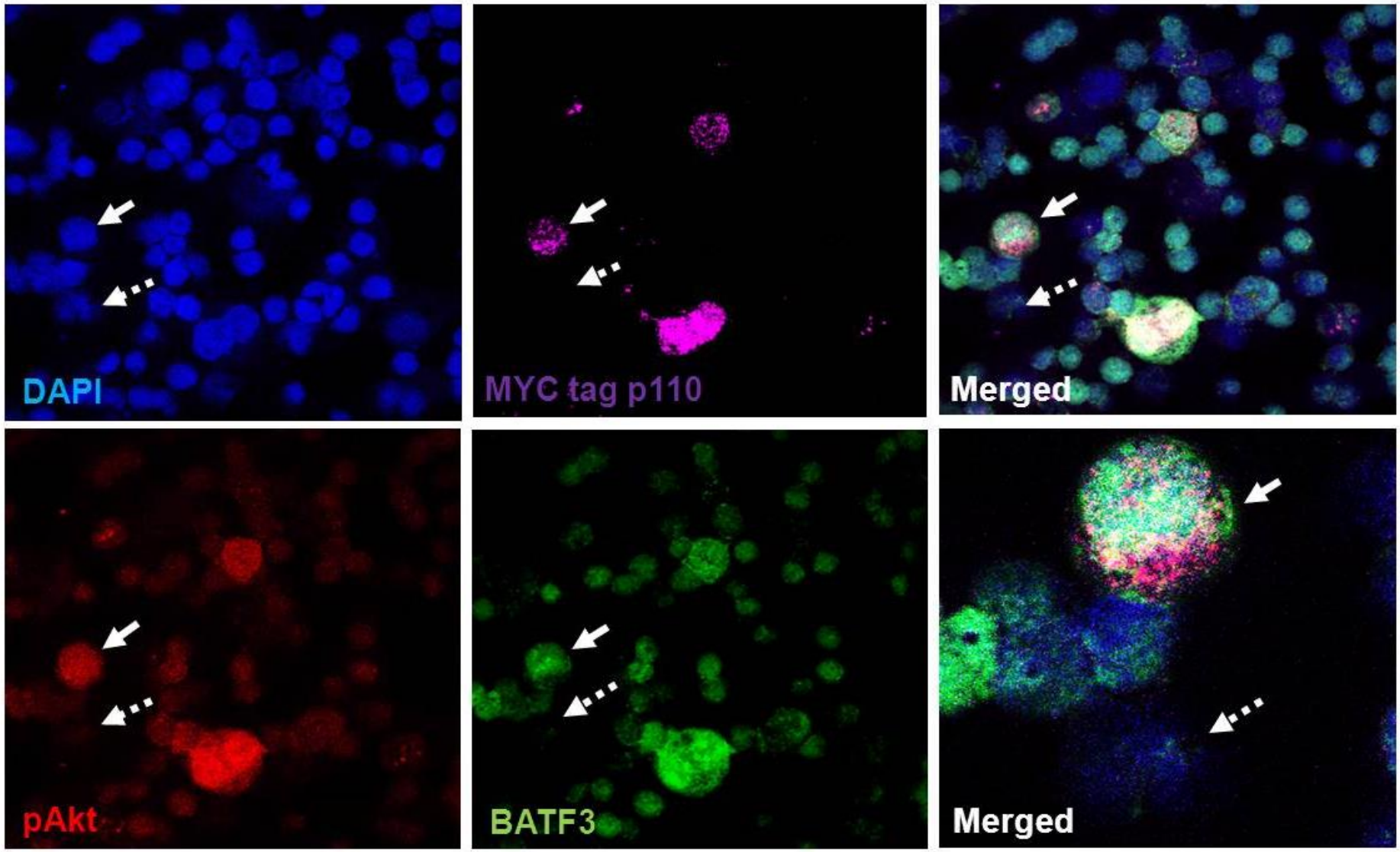
DAPI
MYC tag p110
Merged
pAkt
BATF3
Merged

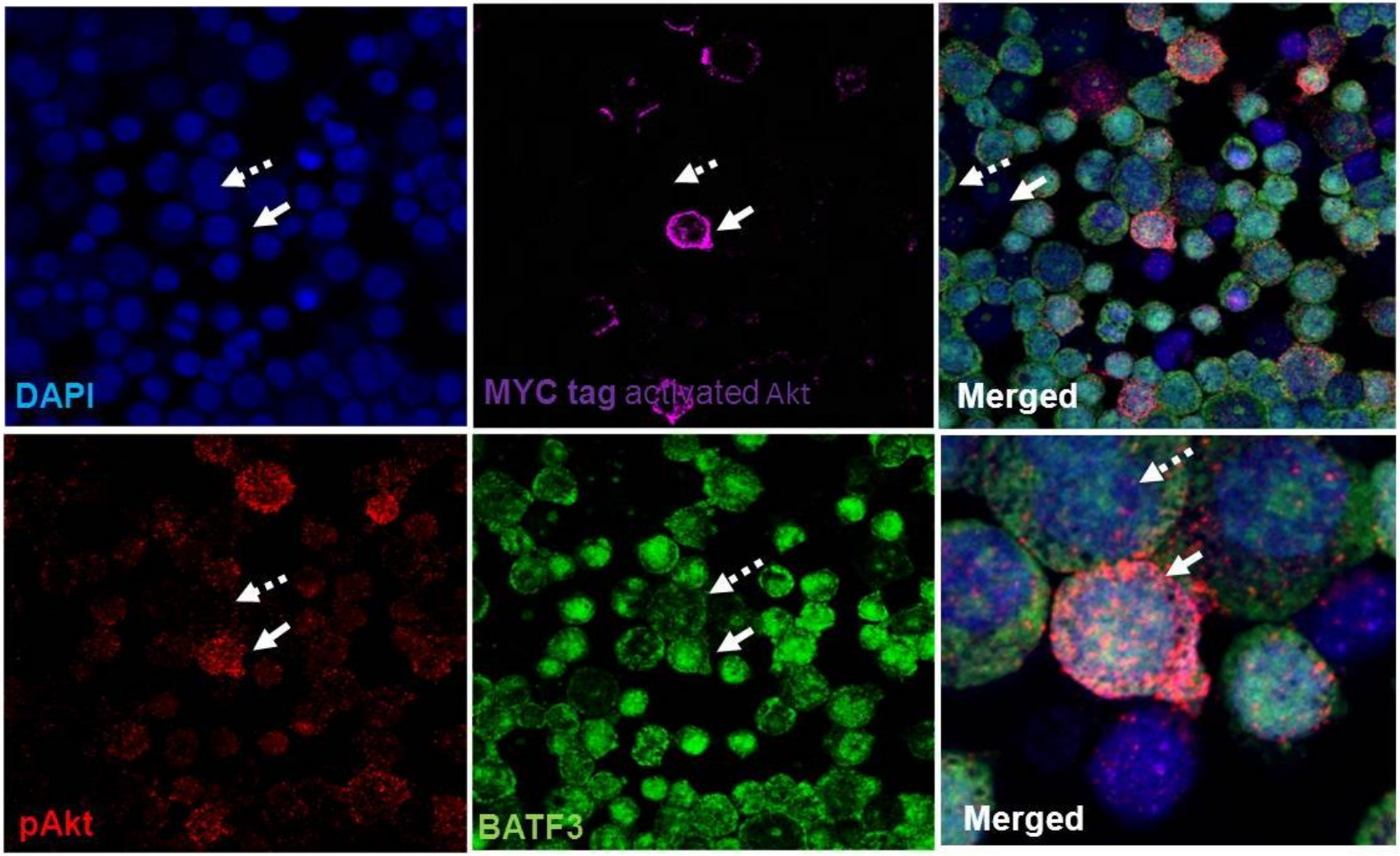

Figure 5.7: Regulation of BATF3 by Akt and p110 in KMH2 HL cell line. Multiplex IF following the transfection of KMH2 cells with a constitutively active p110 plasmid containing a MYC tag (top panel) and MYC tag activated Akt (bottom panel). Cells transfected with the plasmid were significantly more likely to stain with the phospho-Akt antibody (Chi square=80.46; $p<0.00001$) and to be BATF3-positive (Chi square=19.22; $p<0.00001$) (solid white arrows) compared with those cells in the same population that had not taken up the plasmid (broken white arrows), 40x.

5.2.5 BATF3 expression in normal lymphoid tissues

I next studied the expression of BATF3, a transcription factor that our group has shown in other preliminary experiments can be regulated by S1PR1 and which also regulates S1PR1, suggesting a feed-forward loop. A preliminary analysis performed in our group had also revealed that BATF3 mRNA was higher in HRS cells compared to all major B cell subsets. To verify this, I used IHC and IF for BATF3 and various lymphoid and non-lymphoid markers to describe BATF3 expression in normal lymphoid tissues (Figure 5.8). I showed that BATF3 protein was not detectable in most normal GC B cells (as shown by co-staining for BCL6) and only rarely in CD20-positive B cells outside the GC (which were mostly of immunoblast morphology). These cells were also CD30-positive. BATF3 was not expressed in 'tingible body' macrophages of the GC stained with CD68, or in CD123-positive plasmacytoid dendritic cells. BATF3 was only occasionally observed in CD3-positive cells in the interfollicular region and CD23-expressing follicular dendritic cells.

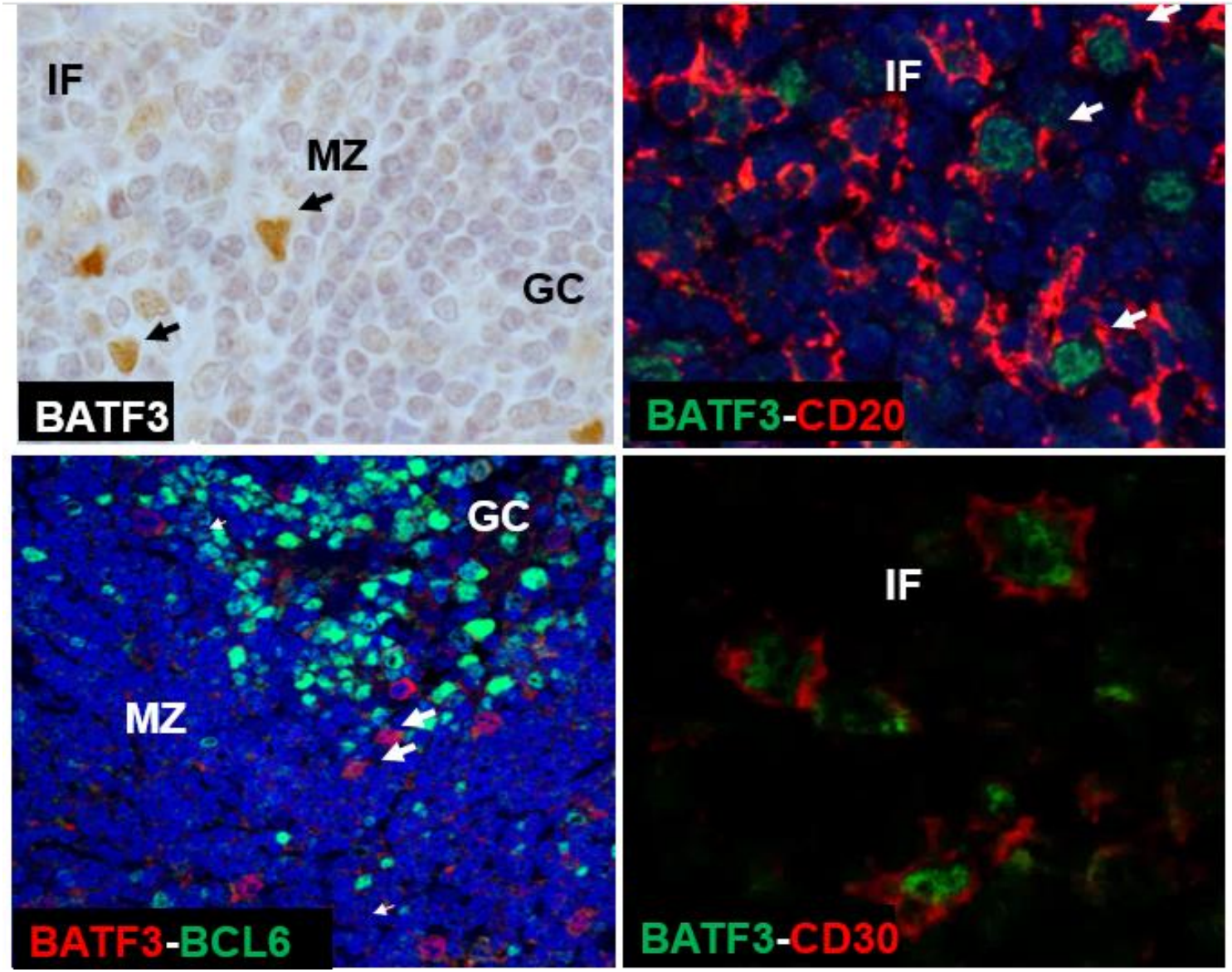
IF
MZ
GC
BATF3
IF
BATF3-CD20
GC
MZ
BATF3-BCL6
IF
BATF3-CD30

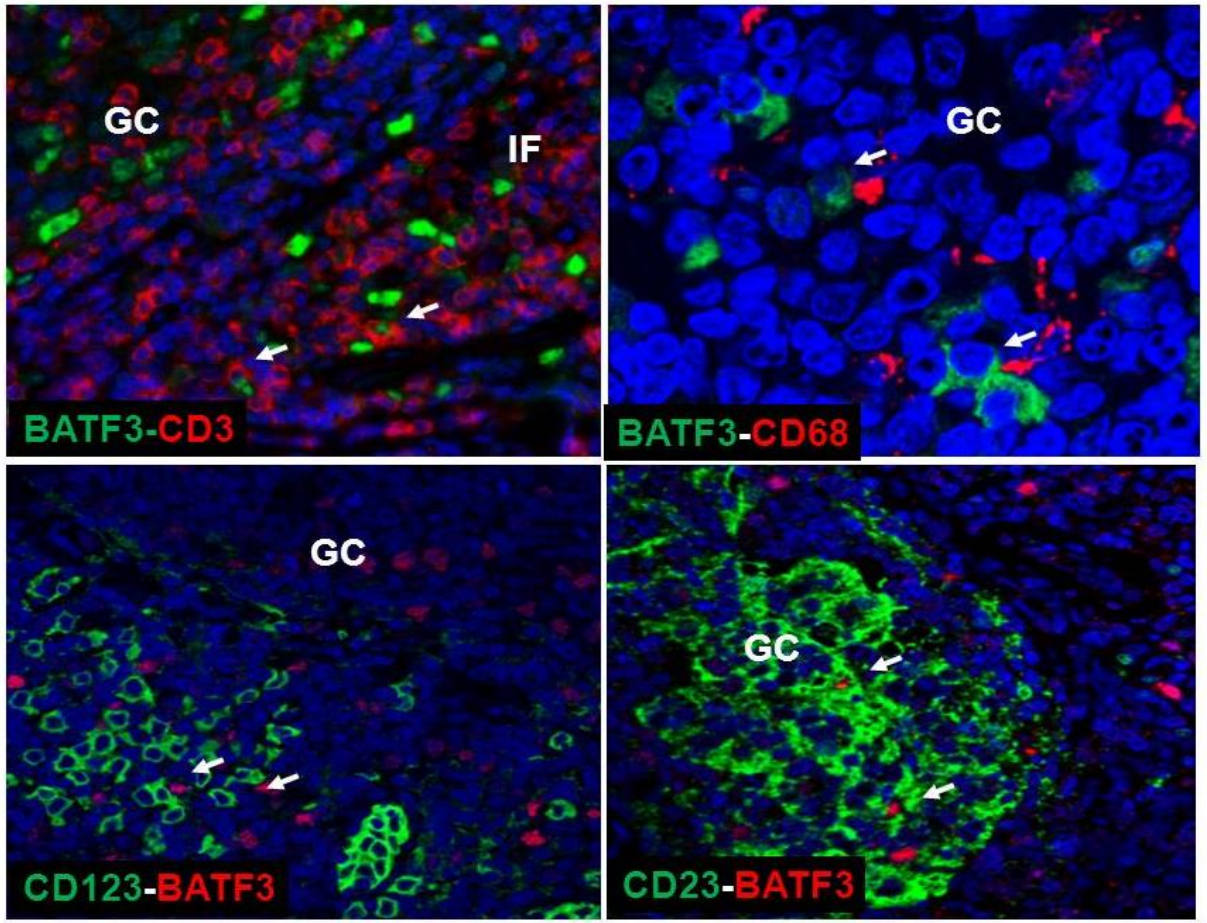

Figure 5.8: BATF3 expression in normal lymphoid tissues. Top four panels: IHC and IF of normal lymphoid tissue, BATF3-positive cells were mainly located outside the GC, some of which expressed CD20 (red) and CD30 (red) with immunoblast morphology in the interfollicular area but not BCL6 (green) in the GC (arrowed), 60X, 40X, 40X and 20X respectively .Bottom four panels: As expected BATF3 was not expressed in 'tingible body' macrophages of the GC stained with CD68 (red); arrowed and was only occasionally present in rare CD3-positive interfollicular T cells (red); arrowed but was not expressed in follicular T cells CD3-positive cells. BATF3 was occasionally detected in CD23 (green) while not present in CD123-positive follicular (green) plasmacytoid at the white arrows, dendritic cells, GC=germinal center, MZ=mantle zone, IF=interfollicular.

5.2.6 BATF3 overexpression in HL

Next, I studied BATF3 expression in HL. I found by IHC that BATF3 protein was strongly expressed in HRS cells, an observation that was confirmed by co-expression of BATF3 and CD30 in HRS cells shown by IF (Figure 5.9). BATF3 protein was strongly expressed in both EBV-positive (7/10) and EBV-negative (29/42) HRS cells and this was confirmed by CD30 co-staining and in HL cell lines. As IHC studies revealed LMP-1 expression is consistently positive in EBV associated HL **(Raab-Traub, 2002, Young and Rickinson, 2004, Deacon et al., 1993)**, so EBV status was determined by LMP-1 staining. This finding was consistent with our group's observation that EBV infection of peripheral blood and GC B cells was followed by the up-regulation of BATF3 mRNA expression and that ectopic expression of the EBV oncogene, LMP-1, increased BATF3 mRNA levels in primary human GC B cells. Therefore, there was no differences in BATF3 expression amongst according to EBV status in HL. As, PI3-K is also regulated by other non-viral mechanisms e.g PTEN loss **(Wang et al., 2015)**, therefore BATF3 would also be expected to be upregulated also in EBV negative cases. This observation was further supported by my finding that LMP-1-expressing L591 and Farage cells were significantly more likely to express BATF3 than were LMP-1-negative cells in the same culture (Chi square=552.5, $p<0.00001$ and Chi square=2621.11, $p<0.00001$, respectively). Furthermore, I also showed that LMP-1 transfection increased BATF3 protein expression in SUDHL4, a GC type DLBCL cell line (Chi square= 10.02; $p=0.0016$), as shown in Figure 5.10 and Table 5.3.

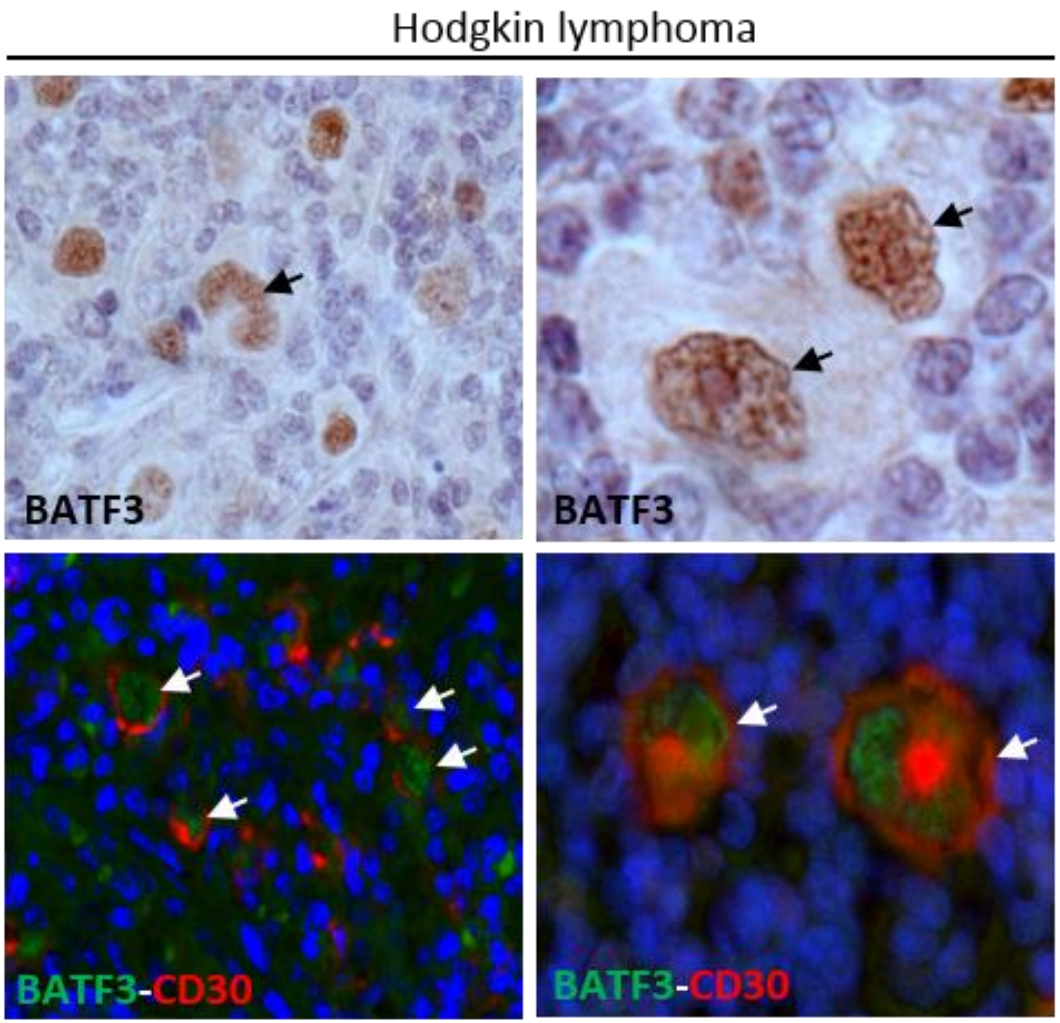

Figure 5.9 BATF3 is overexpressed in HL. Top left and right panels, IHC BATF3 expression in the nuclei of HRS cells by IHC (40X) and (60X) and bottom panels in same samples double stained for BATF3 (green) and CD30 (red) with low power (20X) and high power (40X) magnification.

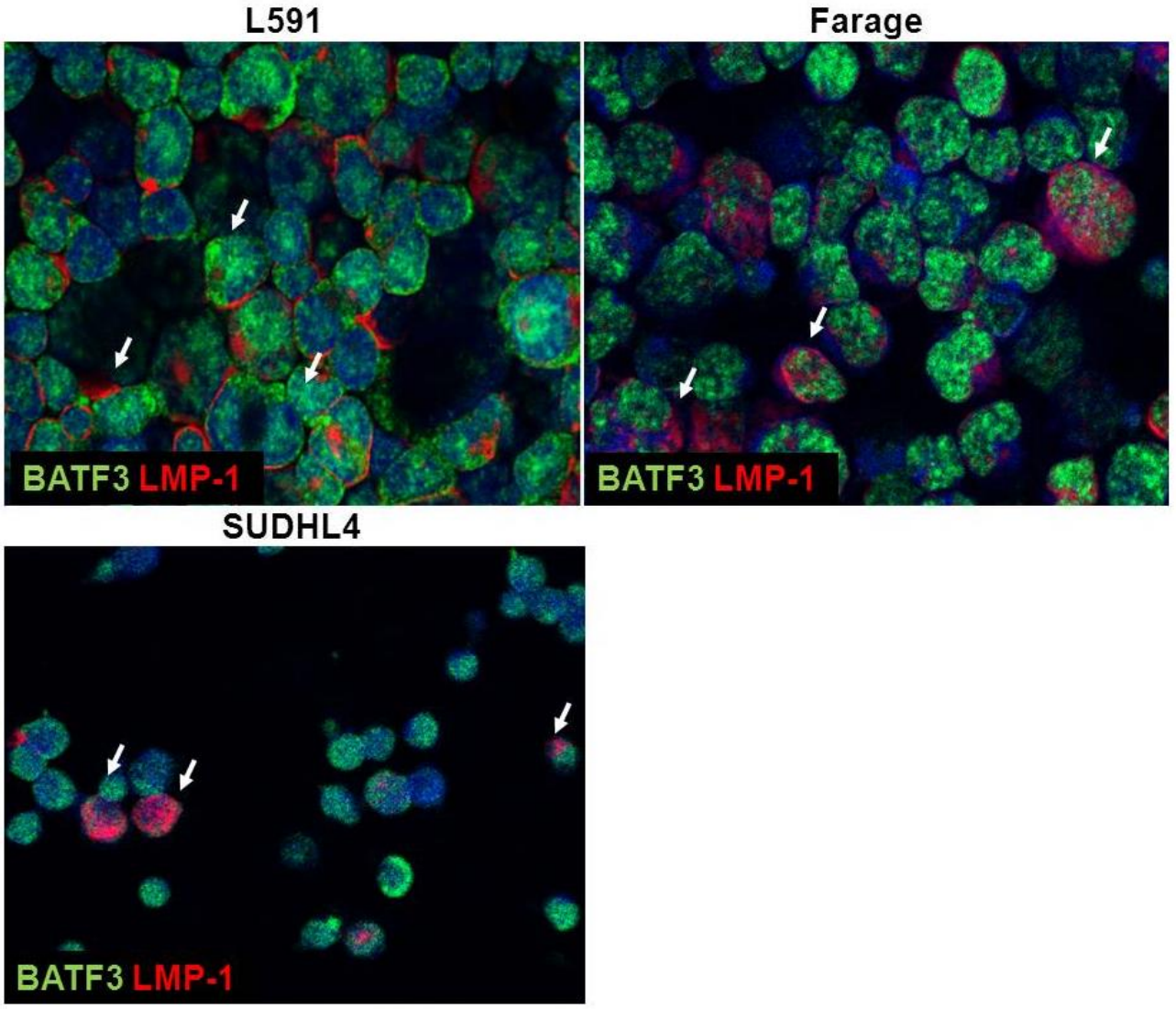

Figure 5.10 Co-expression of BATF3 and LMP-1 in B cell derived lymphoma cell lines
Double labelling showed that LMP-1-expressing L591, Farage and transfected SUDHL4 cells (red) were significantly more likely to express BATF3 (green) than were LMP-1-negative cells in the same culture, 40x.

Tables 5.3: Results of phenotyping of LMP-1 positive BATF3 cells in L591 HL cell line, transfected SUDHL4 and Farage DLBCL cell line

Phenotypes	L591 Counts	SUDHL4 cell line Counts	Farage cell line Counts
BATF3 LMP-1 double positive	2656	79	3672
LMP-1 single positive	1312	0	121
BATF3 single positive	288	489	643
Negative	779	63	1181
Total	5035	631	5617
Chi square	552.5	10.02	2621.1107
P-value	<0.00001	0.0016	<0.00001

Tables 5.3 show results of phenotyping of LMP-1 positive BATF3 in L591 HL cell line, SUDHL4 and Farage-EBV positive DLBCL cell line.

Expression of BATF3 and S1P receptors in primary DLBCL

I also studied the expression of BATF3 and S1P receptors in the tissues of TMA composed of 28 DLBCL patients that I classified into GCB and non-GCB types using the Hans algorithm **(Hans et al., 2004)**. Two cases showed drop out, so were excluded. 18/26 cases were positive for BATF3 (Figure 5.11 A-C) confirmed by double staining with CD20 (Figure 5.11 D). I also studied the relationship between BATF3, S1PR1 and S1PR2 expression in primary DLBCL. To do this, I used these same cases; 18 (69.23%) cases were positive for both BATF3 and S1PR1, 6 cases (23.07%) expressed only S1PR1, and 2 (7.69%) cases were negative for both and BATF3 single positive cases were absent. This represents a significant enrichment of S1PR1 positivity among BATF3-positive DLBCL (Chi-square=4.875, p=0.027). 7/27 cases of DLBCL did not express S1PR2. Although I did not observe a statistically significant association between the expression S1PR1 and S1PR2 in this small series, a meta-analysis of ten different DLBCL gene expression datasets **(Care et al., 2015)** revealed that the expression of S1PR1 was not only positively correlated with that of BATF3 ($r=0.17$, $p=0.013$), but was also negatively correlated with that of S1PR2 ($r=0.43$, $p<0.0001$).

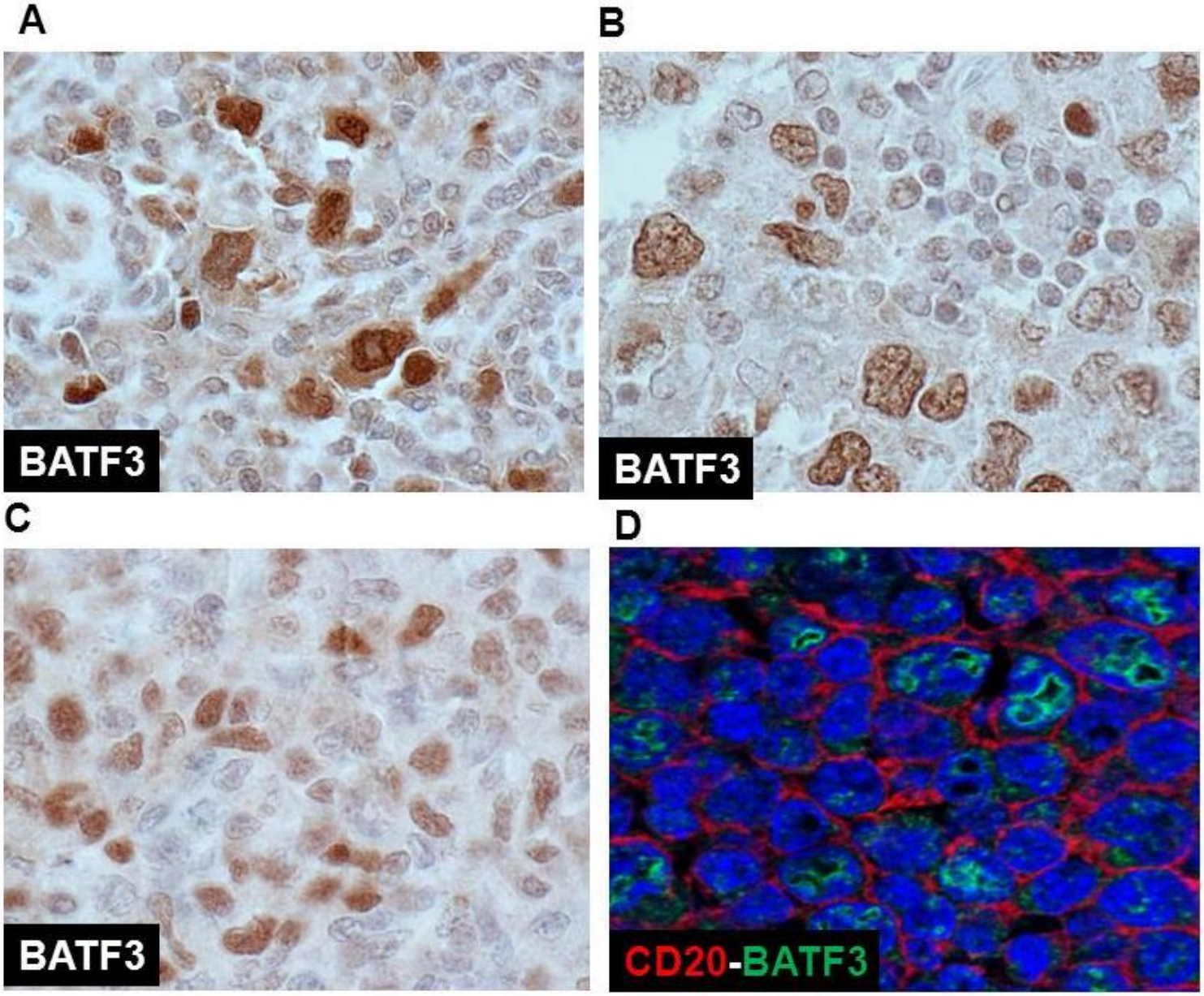
A
BATF3
B
BATF3
C
BATF3
D
CD20-BATF3

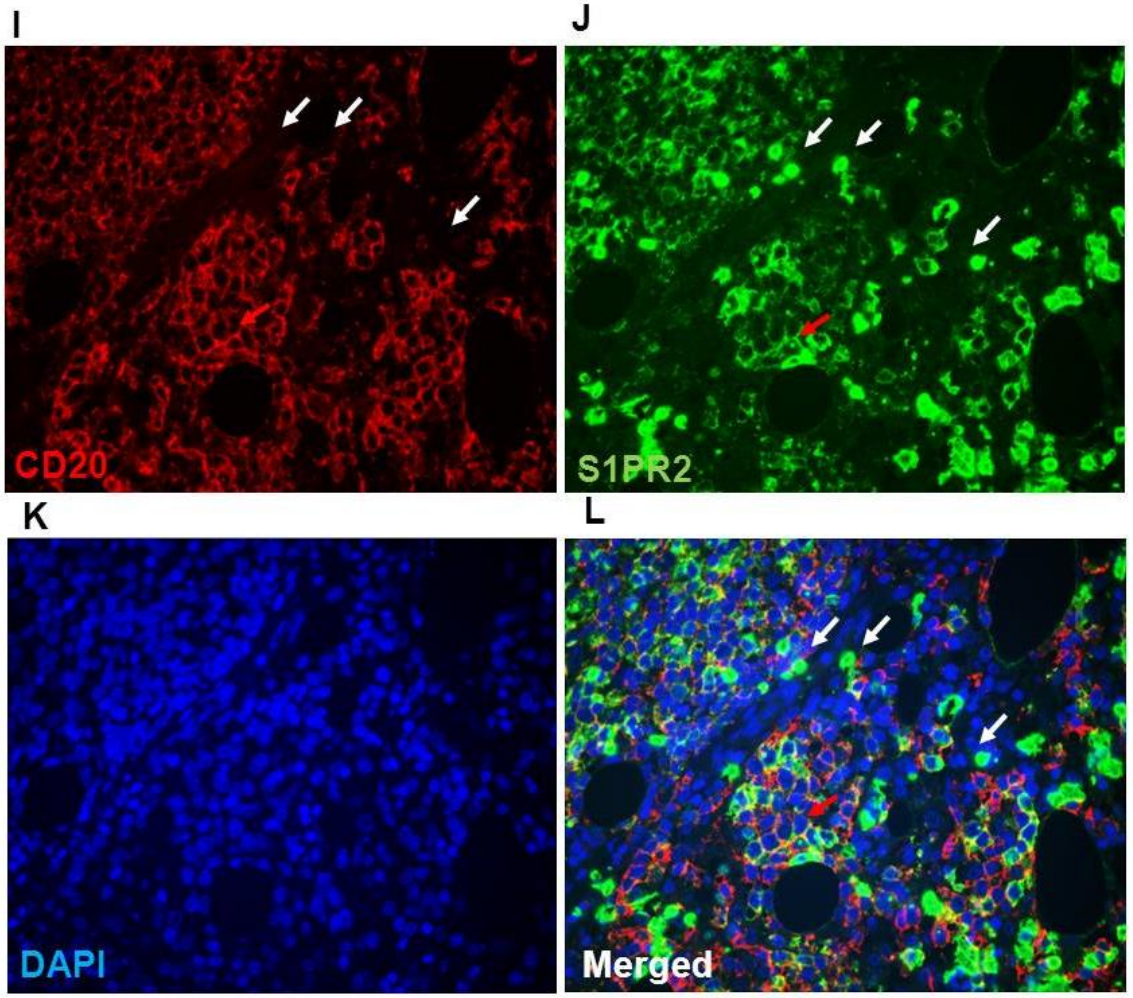

Figure 5.11 BATF3, S1PR1 and S1PR2 expression in DLBCL
A-C) Representative examples of immunostaining of DLBCL showing expression of BATF3 in the nuclei of tumour cells, 60X, D) IF of DLBCL confirms co-expression of BATF3 (green) and CD20 (red) in the tumour cells, E-H) IF of DLBCL confirms co-expression of S1PR1 (green) and CD20 (red) in the tumour cells, 40X, I-M) IF of DLBCL confirms co-expression of S1PR2 (green) and CD20 (red) in the tumour cells, S1PR2 is positive also in red blood cells (red arrows), 40X.

5.2.7 BATF3 up-regulates S1PR1 expression in HL

A microarray analysis following BATF3 knockdown in L428 cells performed by Dr Vrzalikova in our group had revealed that BATF3 increased S1PR1 mRNA (not shown). Next, I sought to show that BATF3 regulated S1PR1 at the protein level. To do this I stained HL cell lines (L1236, L428 and KMH2) treated with either BATF3 siRNA or non-targeting siRNA as a control. L428 cell line was selected amongst other HL cell lines for BATF3 knockdown because it was the least difficult in transfection and shown to give the most efficient BATF3 knockdown.

Multiplex IF revealed that compared to controls, the mean intensity per cell expression of BATF3 and S1PR1 protein was significantly lower in both L428 (Figure 5.12 A) and L1236 cells (both $p<0.0001$; not shown). I did find significantly decreased numbers of BATF3-positive and S1PR1-positive cells in siRNA-transfected L428 with the mean intensity of BATF3 and S1PR1 positive cells 3526/7479 [47.15%] of cells positive for BATF3 and S1PR1) compared with control cells (=2045/2401 [85.17%] and 1955/2401 (81.42%) of cells positive for BATF3 and S1PR1, respectively; not shown) (Chi square for the difference in proportions of BATF3 positive and S1PR1-positive cells=1077.82 and 864.64, respectively; $p<0.0001$ for both comparisons); (Figure 5.12 B). Finally, I co-stained untreated HL cell lines for both BATF3 and S1PR1. Furthermore I showed that, S1P treatment of HL cell lines, not only increase pAKT but also the protein expression of BATF3 and S1PR1, which is in keeping with the data in L428 cells. Time point was 24 hours incubation following 24 hour treatment with S1P or BSA, I found that S1P treatment increased the level of pAkt in both KMH2 and L591 cells, but while L1236 showed no change upon treatment. This analysis revealed that the expression of S1PR1 and BATF3 were significantly positively correlated in all cell lines (Figure 5.13 A-B).

Co-expression of BATF3 and S1PR1 in normal lymphoid tissues

Next, I performed a quantitative analysis of BATF3 in normal lymphoid tissue using multiplex IF. An illustration of the phenotyping of cells is shown in Figure 5.14. This analysis revealed the frequent co-expression of BATF3 and S1PR1 in cells of the extra-follicular regions of tonsil rather than in the GC (Figure 5.15 and Table 5.4).

Co-expression of BATF3 and S1PR1 in primary HL samples

Finally, I found that BATF3-positive primary HL were significantly more likely to be S1PR1-positive than BATF3-negative HL ($p<0.0001$; Figure 5.16 left panel). Next, I performed image analysis on representative cases of HL to ascertain the relationship between BATF3 and S1PR1 expression in HRS cells at the single cell level. In all the cases examined, using multiplex IF for BATF3-S1PR1-CD30, I found that BATF3-expressing CD30-positive HRS cells were significantly more likely to be S1PR1-positive than were BATF3-negative CD30-positive cells (Figure 5.16 right panel and Table 5.5). Taken together these data identify a feed forward S1P signalling loop that drives constitutive BATF3 expression in HRS cells.

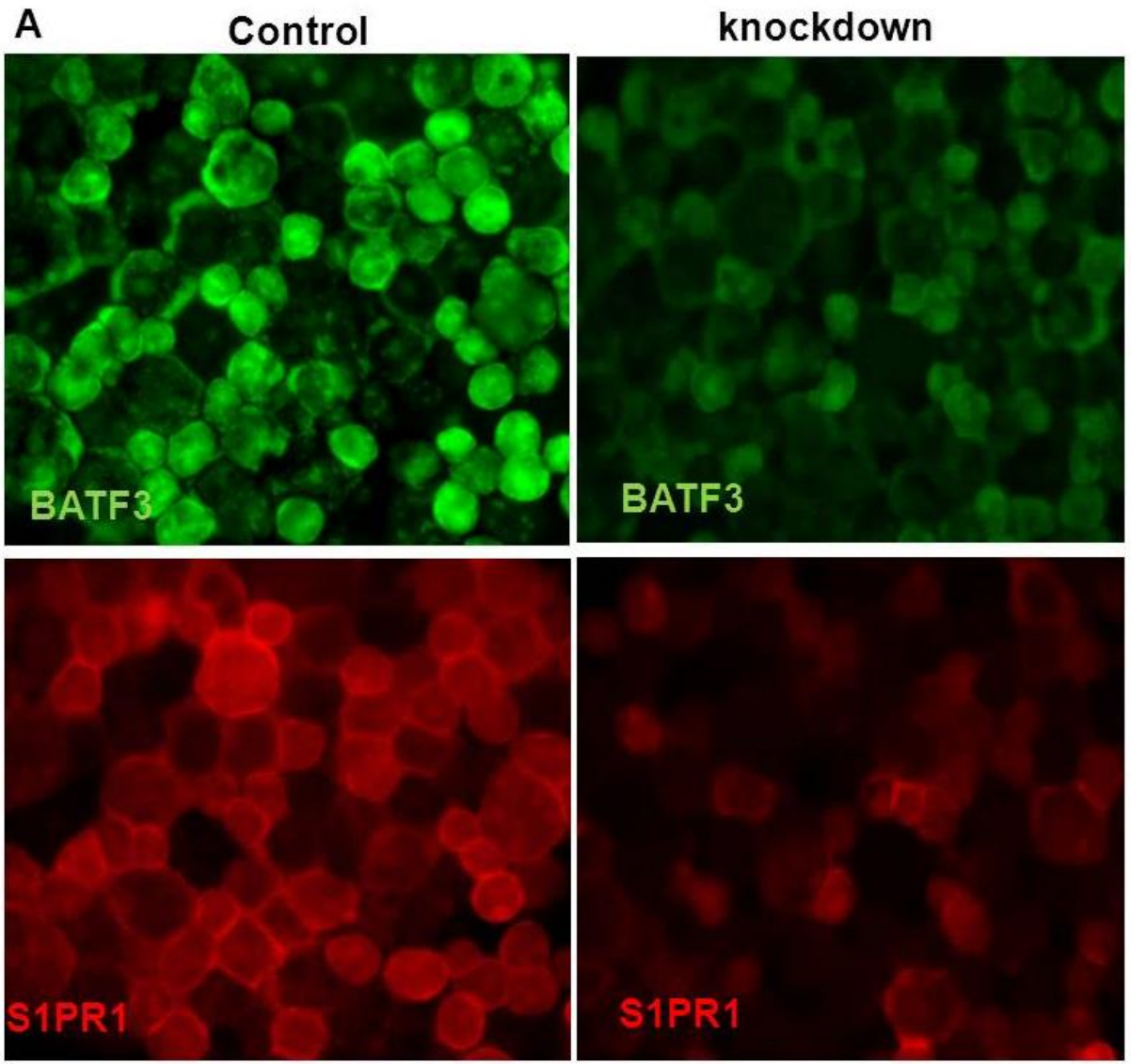
A
Control
knockdown
BATF3
BATF3
S1PR1
S1PR1

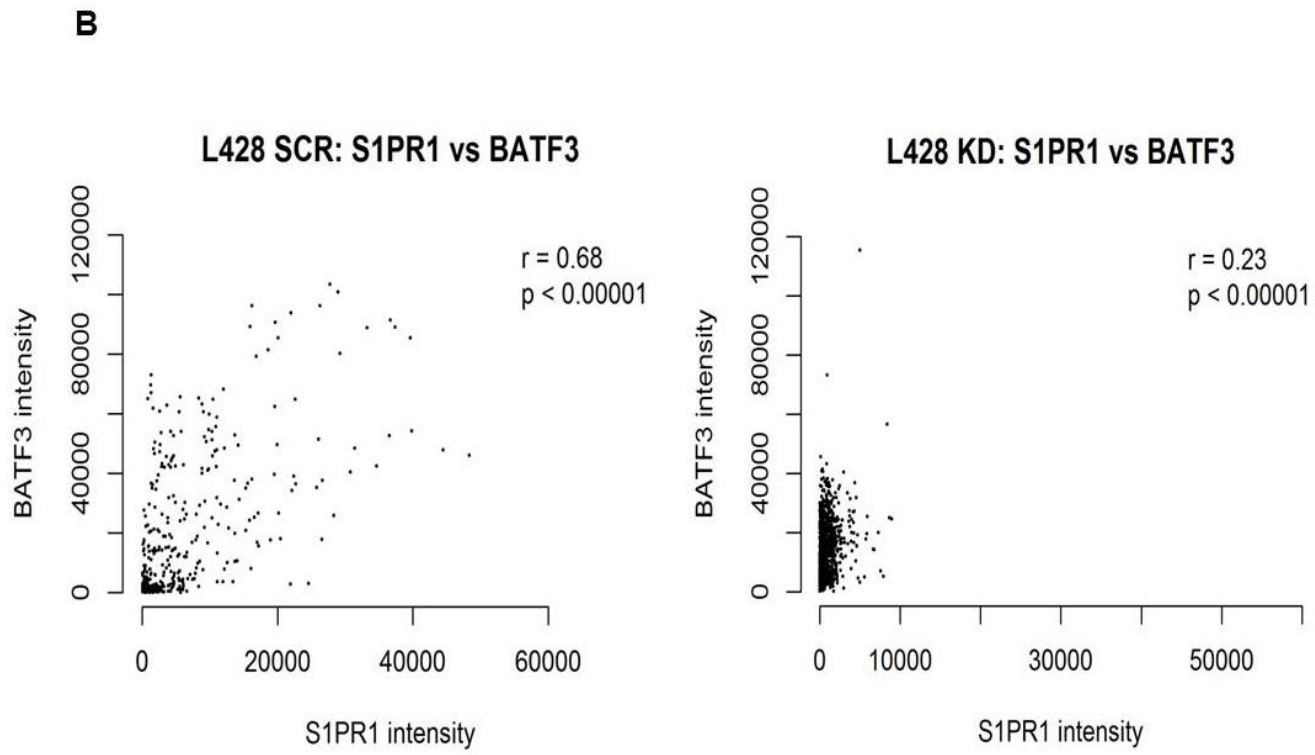

Figure 5.12 knock-down of BATF3 decreases S1PR1 protein expression in L428 cells

A) Top right panels: Multiplex IF showed that the L428 cells transfected with BATF3 specific siRNA expressed lower levels of BATF3 and S1PR1 proteins than did control cells (left panels), 20X. B) This analysis revealed a significant reduction in the mean staining intensity in knockdown cells compared to controls for both BATF3 (L428 cells: control mean = 22301.81; knock-down mean = 14496.72; t-test p-value <0.0001) and S1PR1 (L428 cells: control mean = 7033.26; knock-down mean =797.02; t test p-value <0.0001). Right panels: The levels of BATF3 and S1PR1 were significantly positively correlated at the single cell level in both siRNA-treated and control cell.

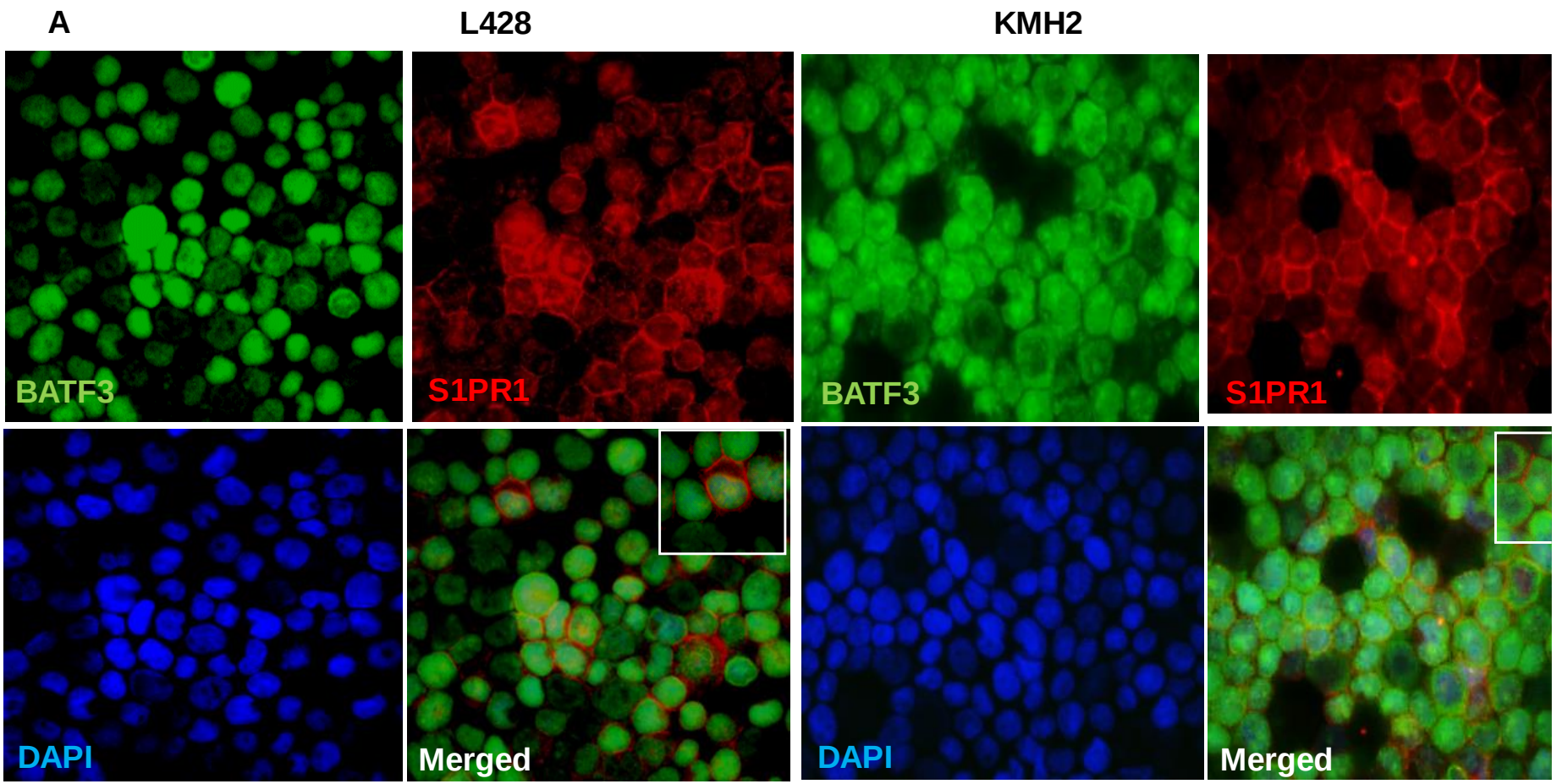

1

A continued

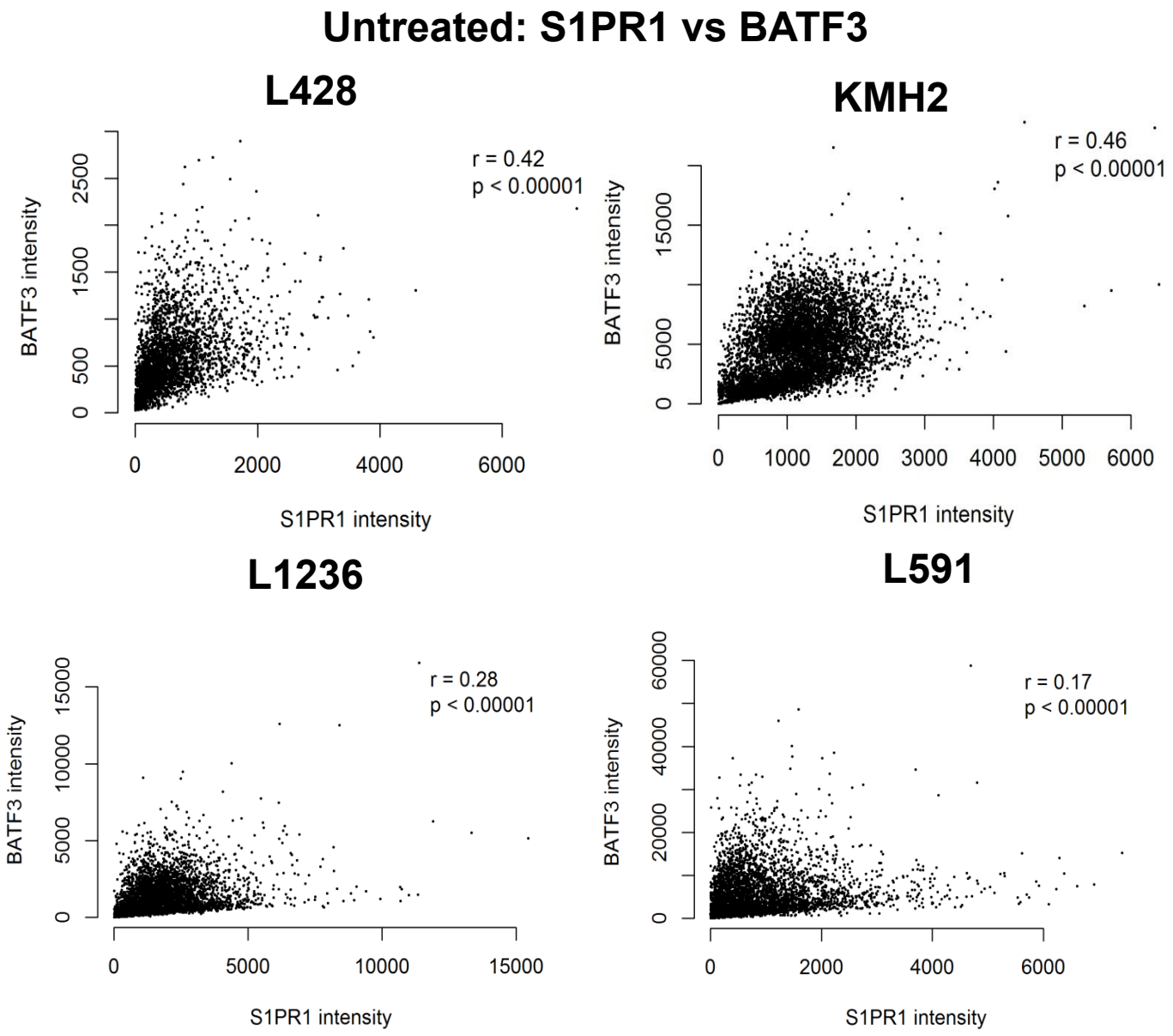
Untreated: S1PR1 vs BATF3
L428
r = 0.42
p < 0.00001
BATF3 intensity
0
500
1500
2500
0
2000
4000
6000
S1PR1 intensity
KMH2
r = 0.46
p < 0.00001
BATF3 intensity
0
5000
15000
0
1000
2000
3000
4000
5000
6000
S1PR1 intensity
L1236
r = 0.28
p < 0.00001
BATF3 intensity
0
5000
10000
15000
0
5000
10000
15000
S1PR1 intensity
L591
r = 0.17
p < 0.00001
BATF3 intensity
0
20000
40000
60000
0
2000
4000
6000
S1PR1 intensity

Untreated: AKT vs BATF3

L428

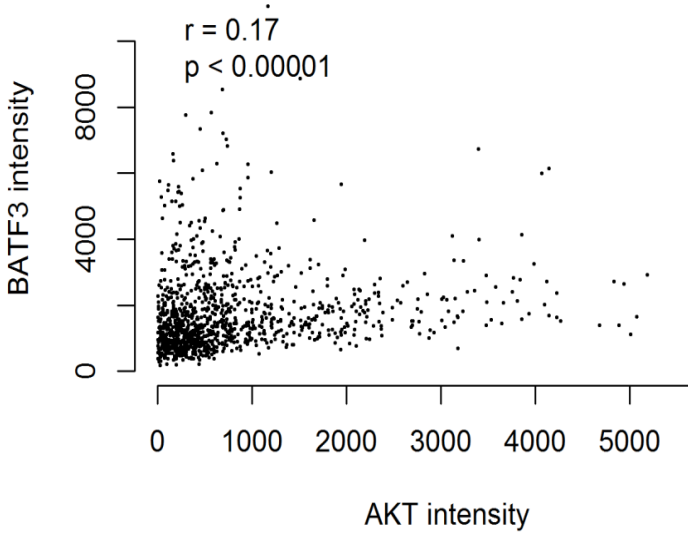

KMH2

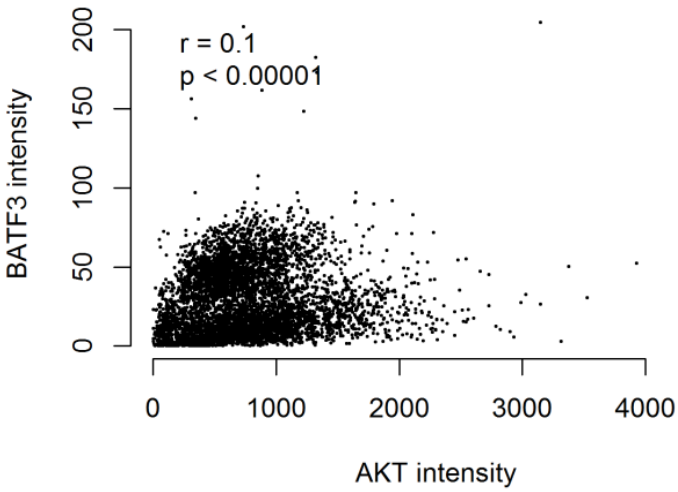

L1236

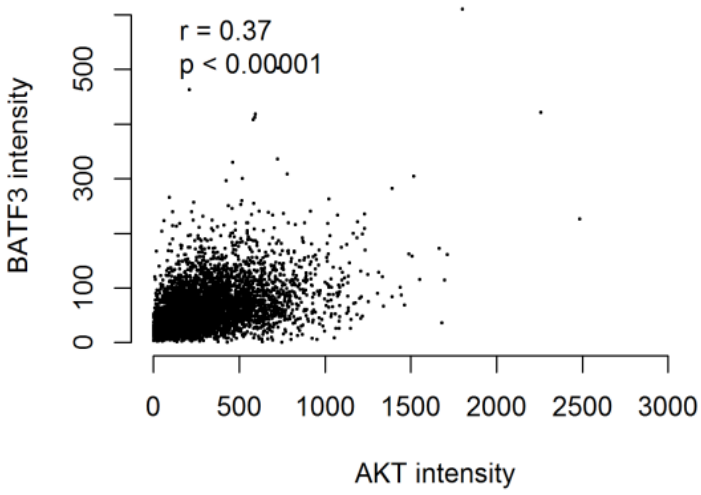

L591

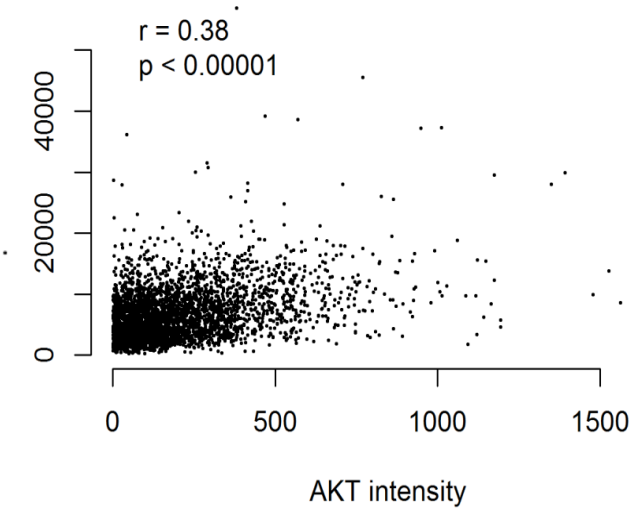

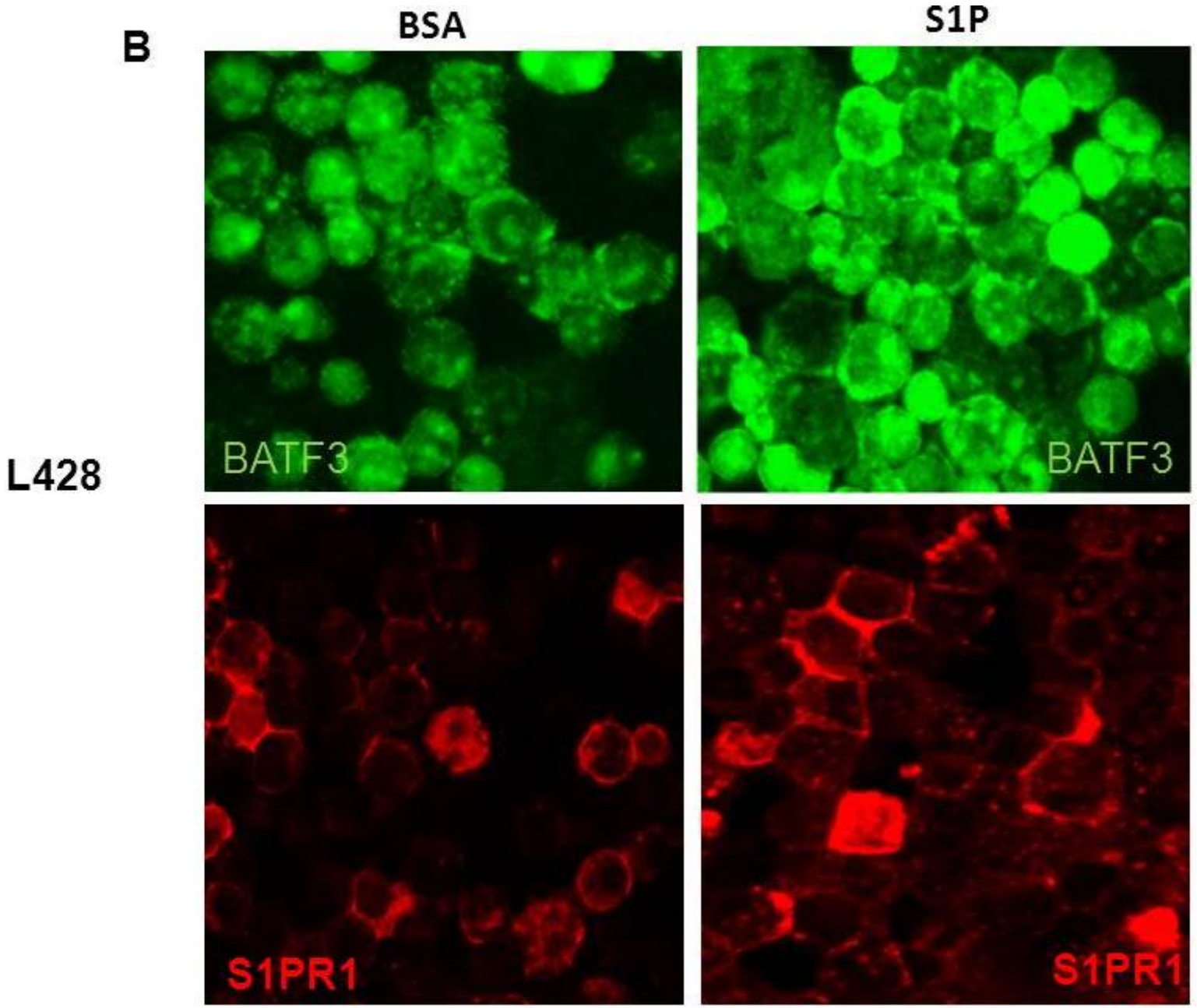
B
BSA
S1P
L428
BATF3
BATF3
S1PR1
S1PR1

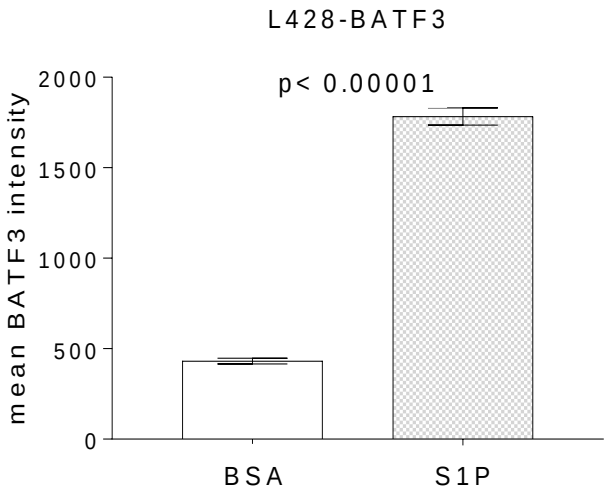
L428-BATF3
p< 0.00001
mean BATF3 intensity
2000
1500
1000
500
0
BSA
S1P

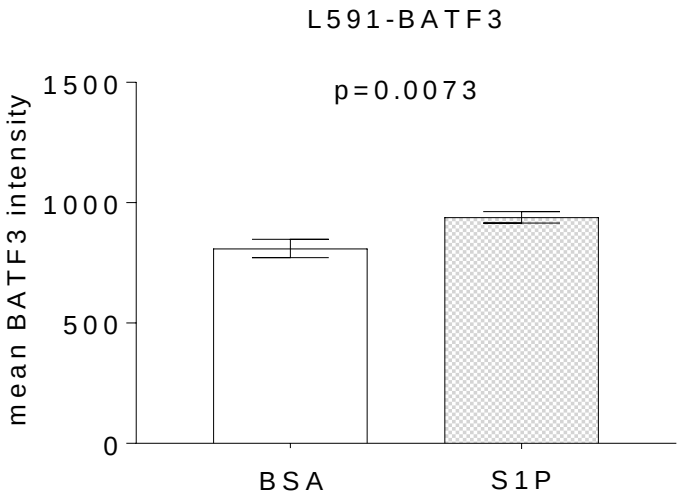
L591-BATF3
p=0.0073
mean BATF3 intensity
1500
1000
500
0
BSA
S1P

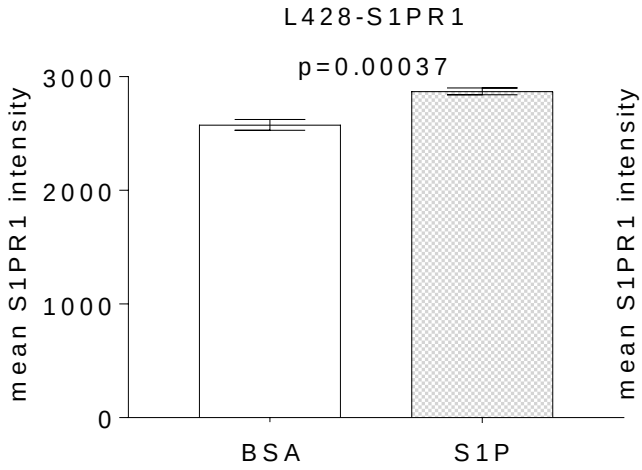
L428-S1PR1
p=0.00037
mean S1PR1 intensity
3000
2000
1000
0
BSA
S1P

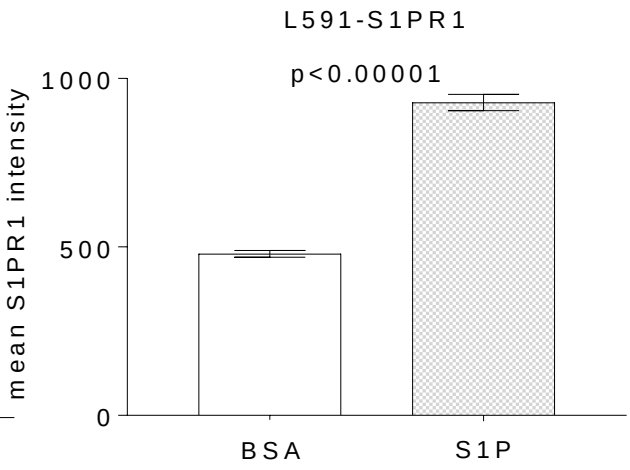
L591-S1PR1
p<0.00001
mean S1PR1 intensity
1000
500
0
BSA
S1P

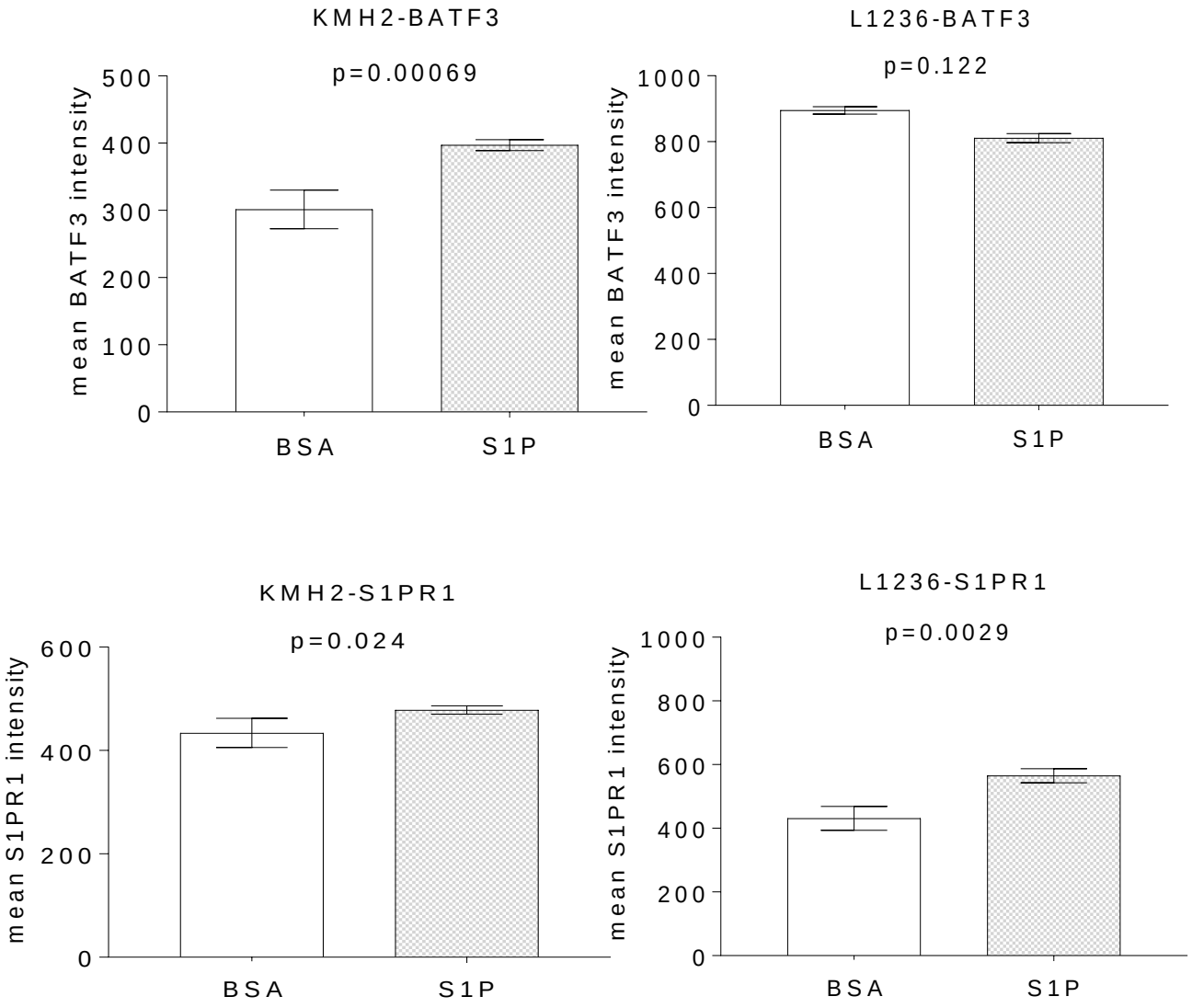

Figure 5.13 BATF3 expression correlates with S1PR1 expression in untreated, BSA and S1P treated HL cell lines

A) Double staining shows that BATF3 positive cells (Top panels) were significantly more likely to also express S1PR1. Shown are representative images of the staining of the untreated L428 and KMH2 lines, 40X. Correlations between BATF3 and S1PR1 expression in all HL cell lines are shown in the lower panels with $p<0.0001$ (Bottom panels).

B) Top panel: Representative images of S1P and BSA treated L428, showed BATF3 and S1PR1 co-localization in both conditions, 40X. C). Bottom panel showed Image analysis of single cells following the treatment of HL cell lines with S1P shows significantly increased levels of BATF3 and S1PR1 protein levels in L428, L591 and KMH2 cells measured by mean fluorescence intensity on IF.

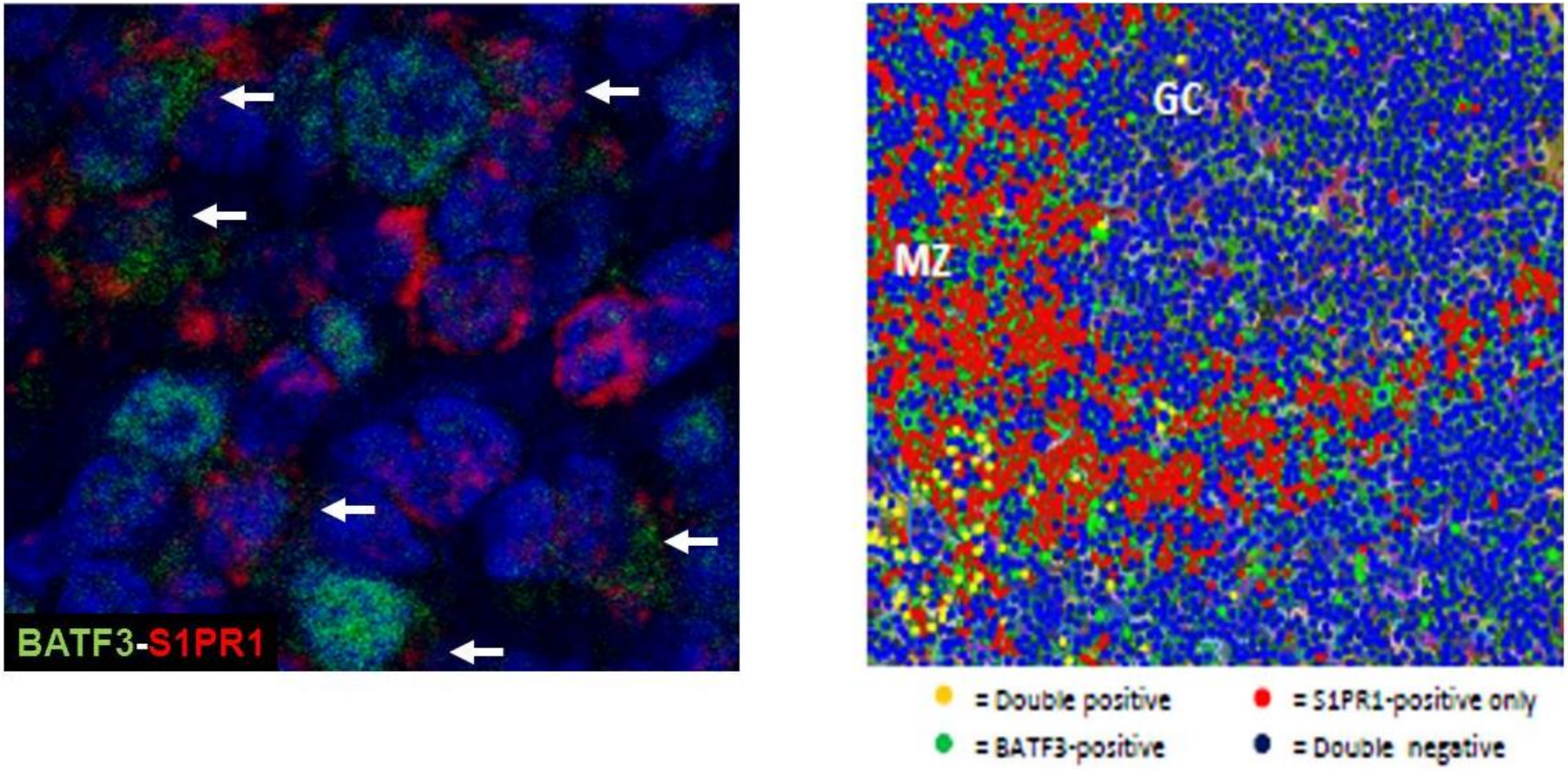

Figure 5.14: BATF3 and S1PR1 co-expression and quantification in normal lymphoid tissue
Top left panel shows the detection of S1PR1 (red) in a single BATF3-expressing lymphocyte (green) in the interfollicular region of a normal tonsil. Most of the S1PR1-positive cells in normal lymphoid tissues did not express BATF3, 40x. Top right panel is a phenotyping map showing that cells co-expressing BATF3 and S1PR1 are mainly located outside germinal centres.

Table 5.4: Phenotyping results of BATF3 expressing S1PR1 lymphoid cells in different anatomic localization in normal lymphoid tissue

Anatomic distribution	Phenotype			
	BATF3 single positive	S1PR1 single positive	BATF3-S1PR1 double positive	Negative
Follicular (Germinal centre+Mantle zone)	112	6443	89	18148
Non follicular (Interfollicular+Paracortical)	260	477	62	3916
Total	372	6920	151	22064

Table 5.4 shows the results of single cell image analysis using Inform software indicating the proportions of cells co-expressing BATF3 and S1PR1 in different anatomic locations.

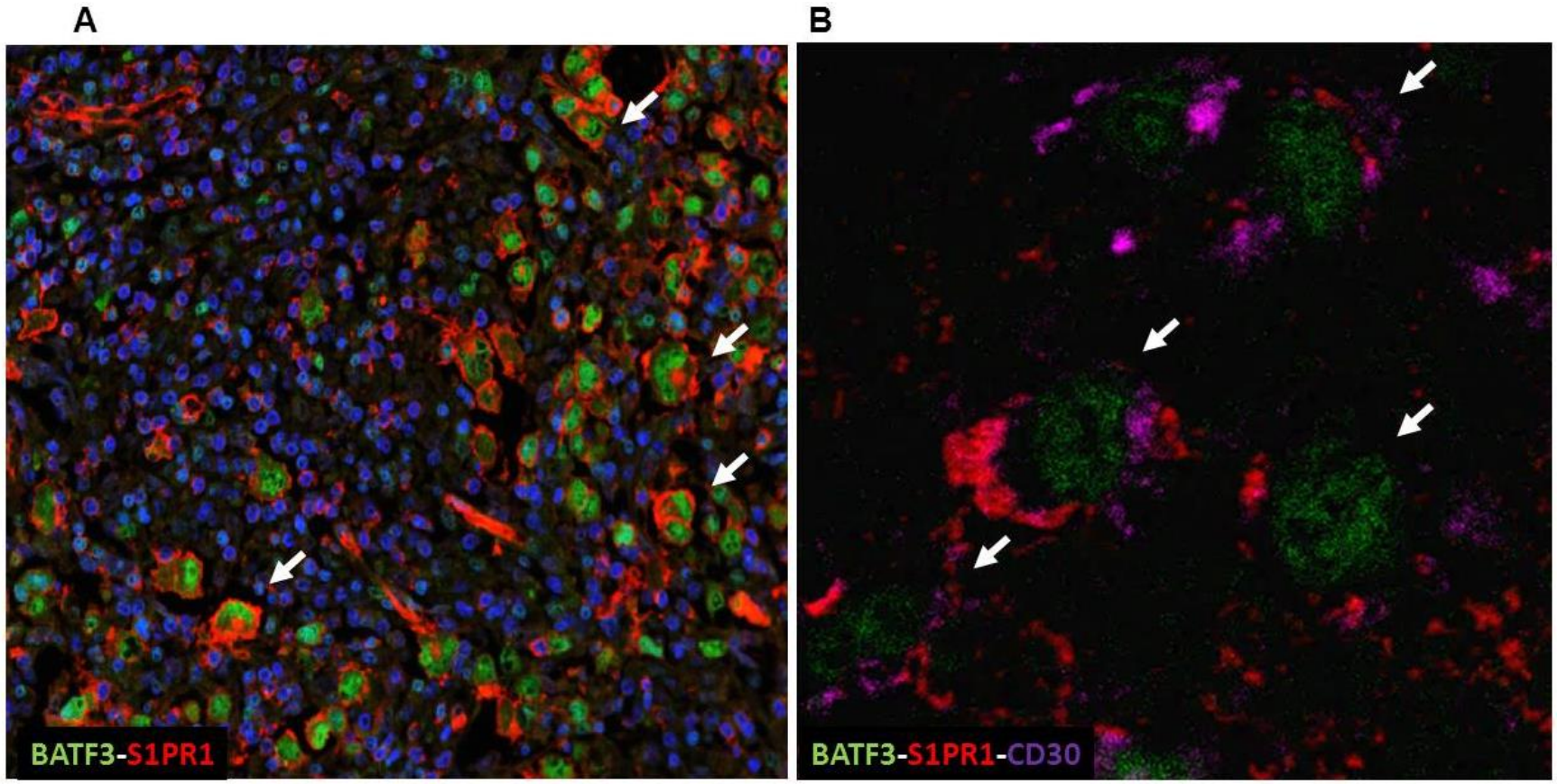

Figure 5.15: Correlation of BATF3 and S1PR1 HL, and single cell analysis of BATF3 and S1PR1 expression in CD30-positive cells of HL. Left panel, photomicrograph of co-staining for BATF3, and S1PR1 in HL, with the majority of cases having co-expression of BATF3 and S1PR1 in HL, 40x. Right Panel, photomicrograph of co-staining for BATF3, S1PR1 and CD30 in HRS cells, 40x.

Table 5.5 single cell image analysis of BATF3 and S1PR1 in CD30 – positive cells of HL

Phenotype	Case 1	Case 2	Case 3	Case 4	Case 5	Case 6
BATF3 single	1	22	29	1	2	3
S1PR1 single	0	0	0	0	0	0
BATF3-S1PR1 double positive	51	131	89	448	215	217
Negative	40	6	209	220	5	15
Total	92	159	327	669	222	235
Chi-square	84.105	23.569	212.790	659.990	126.340	179.470
p-value	<0.00001	<0.00001	<0.00001	<0.00001	<0.00001	<0.00001

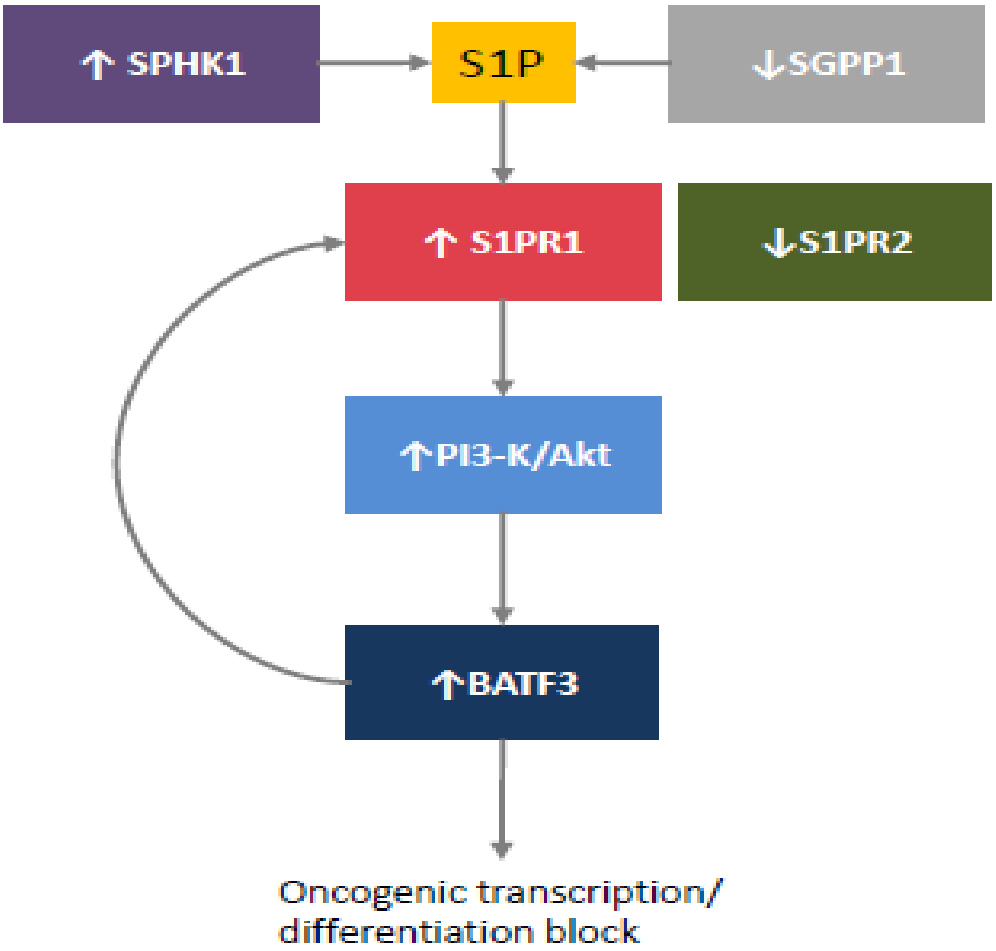

Figure 5.16: Proposed model for the regulation of BATF3 by S1P signalling in HRS cells. S1P availability is regulated by SPHK1, which is upregulated in HRS cells and which catalyses S1P production, and SGPP1, which is down-regulated in HRS cells and which degrades S1P. S1P acts on the S1P receptor, S1PR1; in the absence of S1PR2 this drives PI3-K/Akt signalling leading to increased BATF3 expression. S1PR1 expression is increased by BATF3 leading to a feed-forward loop to sustain S1P signalling and constitutive BATF3 transcription.

5.3 DISCUSSION

In this chapter I have shown that HRS cells express BATF3, a transcription factor that is important for the development of CD8α+ classical dendritic cells **(Hildner et al., 2008)** and related non-lymphoid CD103+CD11b- dendritic cells **(Edelson et al., 2010)**. Re-analysis of existing global expression datasets and IHC showed that BATF3 expression was significantly higher in primary HRS cells compared with normal B cells. My data also show that BATF3 is regulated by PI3-K/Akt signalling, a pathway that is known to be constitutively activated in HRS cells **(Jücker et al., 2002, Dutton et al., 2005, De and Brown, 2010)**.

I showed that PI3-K/Akt signalling is regulated by S1P in HRS cells and that this is dependent upon the increased expression of S1PR1 together with the decreased expression of S1PR2. The up-regulation of S1PR1 in HRS cells has been reported before, albeit in only 7/57 cases, a considerable lower proportion than I have reported here **(Kluk et al., 2013)**; despite the fact that I used the same cut-off employed by Kluk et al. The observation that BATF3 induces the expression of S1PR1 identifies a feed-forward loop which leads to constitutive S1P signalling, PI3-K/Akt activation and sustained BATF3 transcriptional activity (Figure 5.16). The major source of the S1P necessary to sustain this loop is likely to be the HRS cells, since they express SPHK1 in the absence of the S1P phosphatase, SGPP1 **(Vrzalikova et al., 2018)**. The feed-forward loop described here could be important for the pathogenesis of HL since it has been shown that the knockdown of BATF3 significantly reduces the survival of HL cell lines **(Lollies et al., 2018)** and that BATF3 can induce B cell lymphomas in a murine model (Weiser *et al*, personal communication)

.Both EBV-positive and EBV-negative HRS cells displayed high levels of BATF3. This was consistent with our unpublished observation that BATF3 expression was increased following either EBV infection or LMP-1 expression in B cells. Given that EBV and LMP-1 are alone sufficient to induce PI3-K/Akt signalling in B cells **(Dawson et al., 2003, Wlodarski et al., 2005)** the regulation of BATF3 by EBV is likely to be mediated by PI3-K/Akt signalling. Because the EBV lytic cycle has been shown to be induced upon terminal B cell differentiation **(Laichalk and Thorley-Lawson, 2005)** leading to viral replication and cell death, the increased BATF3 expression observed in EBV-infected tumour cells could be important for suppression of the lytic cycle, in turn preventing replication-induced cell death.

These data also suggest that the therapeutic blockade of S1P signalling could inhibit the oncogenic effects of BATF3. Studies using S1PR1 inhibitor and evaluation of BATF3 RNA and protein levels might be helpful to characterise downstream effect of S1PR1 on BATF3 in HL cell lines.

The two functional antagonists of S1PR1, Ozanimod and Siponimod, which our group has shown can block the S1P-mediated activation of Akt, are already in phase II and III clinical trials of patients with inflammatory and autoimmune diseases. These and other S1PR1 modulators should be investigated for their therapeutic potential in HL.

CHAPTER SIX
GENERAL DISCUSSION

6. General discussion

I have shown for the first time that PD-L1 over-expression in NPC could be broadly separated into two types; marginal and diffuse with different pathogenic mechanisms; adaptive (induced) and constitutive (intrinsic) mechanisms respectively. These data suggest that NPC tumours can intrinsically up-regulate PD-L1 in the tumour cells (Intrinsic type), while T cells infiltrating NPC can up-regulate PD-L1 in the marginal/cytokine induced type. These differences are important because they are associated with distinct effects on outcome **(Heeren et al., 2016)**. This finding is of interest since it will help to develop immunotherapeutic strategies for PD-L1 positive NPC, although it will require information on larger patient cohort. I employed a new method of digital analysis of multiplexed stained tissue sections using Vectra and Inform software to study the differential expression of these markers in NPC as well as their relationship to T cells distribution in the same tumour in different tumour locations (tumour and tumour stroma). For the first time, I have shown that PD-L1 expressing tumour in the marginal type, were focally associated with T cell depleted/poor areas in the same tumour group expressing PD-L1 at the border. It will be of interest to determine if other immune cells in addition to T cells e.g. plasma cells, natural killer cells, myeloid-derived cell populations; dendritic cells and macrophages also expressing PD-L1 in the tumour microenvironment **(Giuliani et al., 2017, Tang et al., 2018)**.

I have shown that LMP-1 was not associated with up-regulation of PD-L1 using a re-analysis of published RNA-seq data. This suggests the possibility that non-viral molecular pathways are involved in up-regulating PD-L1. PD-L1 expression can be upregulated by other oncogenic signalling pathways such as NF-κb **(Fang et al., 2014)**. Recent genomic reports showed that LMP-1 expression and mutations

affecting negative regulators of NF-κB expression (found in 41% of cases) are mutually exclusive in NPC, suggesting both viral (LMP-1) and non-viral (genetic) events can lead to PD-L1 expression in NPC **(Li et al., 2017)**.

I also discovered for the first time that multiple immune checkpoints can be co-expressed in the same NPC tumours. These preliminary observations suggest that it is important to consider existence of these, in relation to their expression in patients, who do not respond to PD1/PD-L1 blockade, or in those who eventually develop resistance to these treatments. To determine if this is the case will necessitate further study and validation on larger patient cohorts. These possibilities are supported by the observation that PD1 inhibitors have shown modest response in NPC patients in clinical trial of advanced stage NPC **(Hsu et al., 2017)**; however poor-response to single immunotherapy as PD1 blockade has been reported in subset of patients in one of those trials **(Hsu et al., 2017)**. The rationale behind targeting multiple checkpoints is that some receptors can inhibit T cell function by regulating different immune mechanisms, such as CTLA-4 and PD1 where blocking both receptors has been to improve tumour responses in a murine model **(Curran et al., 2010)**. In addition, targeting CTLA4 and PD1 using combined Nivolumab and Ipilimumab showed a response rate of 60% compared to 11% using monotherapy (Ipilimumab) in melanoma patients **(Li et al., 2016)**, although the high rate of immunosuppressive side effects were not encouraging **(Callahan, 2016)**. Thus, I discovered other immune checkpoints apart from CTLA4 which were co-expressed in the re-analysis of NPC published data such as LAG3 which was co-expressed in same samples with PD-L1, which necessitates to be confirmed in NPC, but my finding was consistent with other reports which showed co-expression and positive correlation of PD1 and LAG3 in colorectal cancer **(Lal et al., 2015)**. Current clinical

trial for melanoma patients showed good response for combined immunotherapy for LAG-3 and PD1. Furthermore other recent combination immune checkpoint therapy trials reported promising results including those that combine inhibitors of PD-1 with LAG-3, TIM3 or CTLA4 **(O'Donnell et al., 2017)**.

I have shown that T-regs positive for FOXP3 are frequent in NPC samples, which is consistent with previous reports **(Lau et al., 2007, Yip et al., 2009)**. Clinical trials used anti-T-reg therapies such as the anti-CD25 antibody, daclizumab, reported successful depletion of T-regs **(Rech and Vonderheide, 2009)**. In addition anti-CD25 drug, denileukin diftitox resulted in the depletion of T-regs in NPC, which were supressing the CD8 specific immune response against EBNA-1 and LMP-2-expressing positive tumour cells **(Fogg et al., 2013)**.

This study took the advantage of the benefits of multiplex IHC technologies. During the course of my studies, I optimized multiple panels which included collagen markers, immune cells of different types and specific LMP-1 target genes in three EBV related tumors. This approach was useful not only characterizing the microenvironment of DLBCL and NPC but also in studying LMP-1 related signalling pathways including PI3-K and another oncogenic pathways such as S1P signalling. In these studies, I characterized the expression of a novel transcription factor BATF3 and was able to identify that it was not only over-expressed in HL, but also expressed by a subset of normal cells in normal lymphoid tissue including a subset of CD30 positive cells. In HL, I described its co-expression with S1PR1 in HRS cells, and studied its regulation by a constitutively active PI3-K mediated through signalling pathway pAKT. I also showed that the S1PR1 receptor is overexpressed in HRS cells in clinical samples which is consistent with previous reports **(Kluk et al., 2013)**. I also showed that for the first time that S1PR1 but not S1PR2, is able to

activate AKT in HL, this was done using *in vitro* transfected EBV positive and negative HL cell lines and quantifying levels of downstream signalling proteins. This approach has the advantage over immunoblotting as it can quantify changes at the single cell level *in vitro* eliminating problems associated with poor efficiency of transient transfection. Furthermore, it enables assessment of relative levels of surrounding partners in primary tissue. Although the majority of HL patients respond to treatment, a subset (25%–30%) have refractory disease or will relapse following first-line therapy **(Canellos et al., 2014)**, it is possible that targeting aberrant S1P signalling pathway could provide an alternative therapeutic approach for these patients which can block S1P signalling e.g. using Sphingomab antibody can benefit those patients. Sphingomab has showed clinical responses in resistant renal cell carcinoma with improved survival approaching 20 months **(Pal et al., 2017)**. These data may suggest resistant HL patients may benefit from this drug.

CHAPTER SEVEN
CONCLUSIONS AND FUTURE WOK

7. Conclusions and future work

In this thesis I have focused partly on the contribution of the microenvironment to the pathogens of DLBCL; by exploring both the expression of collagens and collagen receptors. My data revealed that LAIR-1 is highly expressed by tumour-associated macrophages. Many studies have shown that the presence of M2 macrophages is associated with poor outcomes in both DLBCL and HL. However, future work should include a study of the impact of tumour-associated macrophages expressing LAIR-1 on survival in DLBCL. KO LAIR-1-/- mice are available and provide an opportunity to study how LAIR-1 could influence macrophage function relevant to the pathogenesis of DLBCL. Moreover, recent studies have shown that M2 macrophages influence the therapeutic response to rituximab and so future studies could investigate how collagen ligation of LAIR-1 affects Rituximab-mediated phagocytosis of tumour cells. LAIR-1 was also expressed on a minor subset of T cells in DLBCL and this warrants further study, as this could mediate an important immune checkpoint in DLBCL.

I also explored the expression of immune checkpoints, including PD1/PD-L1 in NPC and I described that PD-L1 is present in the diffuse type in around 50% of patients which suggest the constitutive mechanism of resistance is present in some cases. I found also that the diffuse type of PD-L1 expression, unlike published data was present diffusely within some groups of tumour cells. The remaining half of patients displayed a marginal type expression. Further studies are required to determine the clinical impact of these different phenotypes after therapy using drugs including block PD1 effects. PD-L1 expression is significantly positively correlated with expression of PD-L2 and also with other immune checkpoints such as like BTLA, CTLA and IDO1. Further studies are required to establish which cell types express

these checkpoints molecules in NPC, and to explore simultaneous blockade of multiple immune checkpoints in animal models and eventually in NPC patients.

As we have access to NPC samples with their clinic-pathological data with our collaborators in University of Malaysia, it will be interesting to explore the expression of other immune checkpoints protein and correlate them with outcome.

Finally, I studied the S1P-S1PR1-AKT signalling pathway in HL and found that a signalling loop involving S1PR1 and BATF3 pathway. This pathway would seem to be important for the pathogenesis of HL, since it has previously been shown to be important for HRS cells survival. Further studies could explore if targeting S1P signalling, either using S1P neutralizing antibodies, such as sphingomab, or S1PR1 inhibitor could be useful in blocking this pathway, both *in vitro*, and eventually in animal models.

APPENDICES

Appendix 1: Clinical and pathological details of NPC samples

Case number	Gender	Ethnicity	Age at diagnosis (years)	Histopathology
1	Male	White	34	Non keratinizing Undifferentiated nasopharyngeal carcinoma
2	Female	Asian	40	Undifferentiated nasopharyngeal carcinoma
4	Male	White	51	Poorly differentiated/undifferentiated nasopharyngeal carcinoma
6	Male	White	78	Poorly differentiated nasopharyngeal carcinoma
7	Male	White	60	Keratinizing squamous cell carcinoma
8	Male	Chinese	79	Nasopharyngeal carcinoma ‘’NOS’’
9	Female	Mixed	28	Undifferentiated nasopharyngeal carcinoma ‘’Non keratinizing type’’
10	Male	White	21	Undifferentiated nasopharyngeal carcinoma
11	Male	White	78	Poorly differentiated nasopharyngeal carcinoma
12	Male	White	59	Non keratinizing nasopharyngeal carcinoma
14	Male	White	19	Undifferentiated nasopharyngeal carcinoma
15	Male	White	71	Non keratinizing Undifferentiated nasopharyngeal carcinoma
16	Female	White	56	Non keratinizing Undifferentiated nasopharyngeal carcinoma with spindle cell component
17	Female	Other: Filipino/Latin	37	Not available
18	Male	Chinese	47	Non keratinizing Undifferentiated nasopharyngeal carcinoma with
20	Male	White	38	Poorly differentiated nasopharyngeal carcinoma
21	Male	White	45	Nasopharyngeal carcinoma ‘’unclassified’’

22	Male	White	61	Poorly differentiated nasopharyngeal carcinoma

Appendix 2: Immune related and immune checkpoint genes

Gene list class	Name of the gene
Immune checkpoint receptors	PDCD1 CTLA4 TIGIT BTLA HAVCR2 LGALS9
Immune checkpoint ligands	CD274 PDCD1LG2 LAG3
Costimulatory Receptors	CD28 CD40 ICOS
Costimulatory Ligands (B7 family)	CD80 CD86 CD40L VTCN1 CD276
TNF family	TNFSF9 TNFRSF4 TNFSF4 TNFRSF18 TNFSF18 TNFSF14 TNFRSF14 TNFSF11 TNFRSF11A TNFRSF8 LTBR CD27 TNFRSF9
Adhesion	PVR CD226 CEACAM1 NECTIN2 CD2
Secreted enzymes	IDO1 GZMB ARG1 IDO1

KIRs (NK Cell)	KIR3DL1 KIR2DL4 KIR2DL3
Interleukin	IL2RB IL10 IL1A IL6 IL12B IL18
Transcription factor	TBX21 (T-bet)
Leukocyte Ig-like family	LILRB2 LILRB1 LILRA2 LILRA3
Unclassified	CD160 CD70 CD47 SIRPA ADORA2A SLAMF1 LAIR1 LAIR2 NCR3 TMIGD2

Appendix 3: Co-ordinate Immune Response Cluster (CIRC) signature genes

Gene list class	Name of the gene
MHC class I-related	HLA-A HLA-B HLA-C MICB ULBP1 ULBP2 ULBP3
MHC class II-related	HLA-DMA HLA-DMB HLA-DOA HLA-DOB HLA-DPA1 HLA-DPB1 HLA-DQA1 HLA-DQA2 HLA-DRA HLA-DRB5
Chemokines/Receptors	CCL11 CCL2 CCL5 CX3CL1 CXCL10 CXCL9
Cytokines/Receptors	IFNγ IL12RB2 IL17A IL18RAP IL7R
Transcription Factors	STAT1

	STAT3 TBX21 IRF1
TNF Family	TNFRSF14 TNFSF4
B7 family	CD80 CD86 CD276 VTCN1
Immune checkpoint ligands	PDCD1LG2 CD274 LAG3
Immune checkpoint receptors	PDCD1 CTLA4 HAVCR2
Scaffold	ACTB
CD3/TCR related	CD247 CD3D CD3E CD3G CD4 CD8B
Secreted Enzyme	GNLY GZMB

References

ABRAMSON, J. S. & SHIPP, M. A. 2005. Advances in the biology and therapy of diffuse large B-cell lymphoma: moving toward a molecularly targeted approach. *Blood,* 106**,** 1164-1174.

AKAO, Y., BANNO, Y., NAKAGAWA, Y., HASEGAWA, N., KIM, T.-J., MURATE, T., IGARASHI, Y. & NOZAWA, Y. 2006. High expression of sphingosine kinase 1 and S1P receptors in chemotherapy-resistant prostate cancer PC3 cells and their camptothecin-induced up-regulation. *Biochemical and biophysical research communications,* 342**,** 1284-1290.

ALDINUCCI, D., GLOGHINI, A., PINTO, A., DE FILIPPI, R. & CARBONE, A. 2010. The classical Hodgkin's lymphoma microenvironment and its role in promoting tumour growth and immune escape. *The Journal of pathology,* 221**,** 248-263.

ALDINUCCI, D., POLETTO, D., GLOGHINI, A., NANNI, P., DEGAN, M., PERIN, T., CEOLIN, P., ROSSI, F. M., GATTEI, V. & CARBONE, A. 2002. Expression of functional interleukin-3 receptors on Hodgkin and Reed-Sternberg cells. *The American journal of pathology,* 160**,** 585-596.

ALIZADEH, A. A., EISEN, M. B., DAVIS, R. E., MA, C., LOSSOS, I. S., ROSENWALD, A., BOLDRICK, J. C., SABET, H., TRAN, T. & YU, X. 2000. Distinct types of diffuse large B-cell lymphoma identified by gene expression profiling. *Nature,* 403**,** 503.

ALVAREZ, S. E., HARIKUMAR, K. B., HAIT, N. C., ALLEGOOD, J., STRUB, G. M., KIM, E. Y., MACEYKA, M., JIANG, H., LUO, C. & KORDULA, T. 2010. Sphingosine-1-phosphate is a missing cofactor for the E3 ubiquitin ligase TRAF2. *Nature,* 465**,** 1084.

ALVES, F., VOGEL, W., MOSSIE, K., MILLAUER, B., HÖFLER, H. & ULLRICH, A. 1995. Distinct structural characteristics of discoidin I subfamily receptor tyrosine kinases and complementary expression in human cancer. *Oncogene,* 10**,** 609-618.

ANDERSON, L. J. & LONGNECKER, R. 2009. Epstein-Barr virus latent membrane protein 2A exploits Notch1 to alter B-cell identity in vivo. *Blood,* 113**,** 108-116.

ANDERTON, E., YEE, J., SMITH, P., CROOK, T., WHITE, R. & ALLDAY, M. 2008. Two Epstein–Barr virus (EBV) oncoproteins cooperate to repress expression of the proapoptotic tumour-suppressor Bim: clues to the pathogenesis of Burkitt's lymphoma. *Oncogene,* 27**,** 421.

ANSELL, S. M., LESOKHIN, A. M., BORRELLO, I., HALWANI, A., SCOTT, E. C., GUTIERREZ, M., SCHUSTER, S. J., MILLENSON, M. M., CATTRY, D. & FREEMAN, G. J. 2015. PD-1 blockade with nivolumab in relapsed or refractory Hodgkin's lymphoma. *New England Journal of Medicine,* 372**,** 311-319.

ARIKAWA, K., TAKUWA, N., YAMAGUCHI, H., SUGIMOTO, N., KITAYAMA, J., NAGAWA, H., TAKEHARA, K. & TAKUWA, Y. 2003. Ligand-dependent inhibition of B16 melanoma cell migration and invasion via endogenous S1P2 G protein-coupled receptor requirement of inhibition of cellular Rac activity. *Journal of Biological Chemistry,* 278**,** 32841-32851.

ASCIERTO, P. A., CAPONE, M., URBA, W. J., BIFULCO, C. B., BOTTI, G., LUGLI, A., MARINCOLA, F. M., CILIBERTO, G., GALON, J. & FOX, B. A. 2013. The additional facet of immunoscore: immunoprofiling as a possible predictive tool for cancer treatment. BioMed Central.

AUST, S., FELIX, S., AUER, K., BACHMAYR-HEYDA, A., KENNER, L., DEKAN, S., MEIER, S. M., GERNER, C., GRIMM, C. & PILS, D. 2017. Absence of PD-L1 on tumor cells is associated with reduced MHC I expression and PD-L1 expression increases in recurrent serous ovarian cancer. *Scientific reports,* 7**,** 42929.

AVERY, K., AVERY, S., SHEPHERD, J., HEATH, P. R. & MOORE, H. 2008. Sphingosine-1-phosphate mediates transcriptional regulation of key targets associated with

survival, proliferation, and pluripotency in human embryonic stem cells. *Stem cells and development,* 17**,** 1195-1206.
BABCOCK, G. J., DECKER, L. L., VOLK, M. & THORLEY-LAWSON, D. A. 1998. EBV persistence in memory B cells in vivo. *Immunity,* 9**,** 395-404.
BABCOCK, G. J., HOCHBERG, D. & THORLEY-LAWSON, D. A. 2000. The expression pattern of Epstein-Barr virus latent genes in vivo is dependent upon the differentiation stage of the infected B cell. *Immunity,* 13**,** 497-506.
BAER, R., BANKIER, A., BIGGIN, M., DEININGER, P., FARRELL, P., GIBSON, T., HATFULL, G., HUDSON, G., SATCHWELL, S. & SEGUIN, C. 1984. DNA sequence and expression of the B95-8 Epstein—Barr virus genome. *Nature,* 310**,** 207.
BANYARD, J., BAO, L. & ZETTER, B. R. 2003. Type XXIII collagen, a new transmembrane collagen identified in metastatic tumor cells. *Journal of Biological Chemistry,* 278**,** 20989-20994.
BARAN, Y., SALAS, A., SENKAL, C. E., GUNDUZ, U., BIELAWSKI, J., OBEID, L. M. & OGRETMEN, B. 2007. Alterations of ceramide/sphingosine 1-phosphate rheostat involved in the regulation of resistance to imatinib-induced apoptosis in K562 human chronic myeloid leukemia cells. *Journal of Biological Chemistry,* 282**,** 10922-10934.
BARBER, D. L., WHERRY, E. J., MASOPUST, D., ZHU, B., ALLISON, J. P., SHARPE, A. H., FREEMAN, G. J. & AHMED, R. 2006. Restoring function in exhausted CD8 T cells during chronic viral infection. *Nature,* 439**,** 682.
BARGOU, R., LENG, C., KRAPPMANN, D., EMMERICH, F., MAPARA, M., BOMMERT, K., ROYER, H., SCHEIDEREIT, C. & DORKEN, B. 1996. High-level nuclear NF-kappa B and Oct-2 is a common feature of cultured Hodgkin/Reed-Sternberg cells. *Blood,* 87**,** 4340-4347.
BARGOU, R. C., EMMERICH, F., KRAPPMANN, D., BOMMERT, K., MAPARA, M. Y., ARNOLD, W., ROYER, H. D., GRINSTEIN, E., GREINER, A. & SCHEIDEREIT, C. 1997. Constitutive nuclear factor-kappaB-RelA activation is required for proliferation and survival of Hodgkin's disease tumor cells. *The Journal of clinical investigation,* 100**,** 2961-2969.
BARNES, L. 2005. *Pathology and genetics of head and neck tumours*, IARC.
BARTH, T. F., MARTIN-SUBERO, J. I., JOOS, S., MENZ, C. K., HASEL, C., MECHTERSHEIMER, G., PARWARESCH, R. M., LICHTER, P., SIEBERT, R. & MÖLLER, P. 2003. Gains of 2p involving the REL locus correlate with nuclear c-Rel protein accumulation in neoplastic cells of classical Hodgkin lymphoma. *Blood,* 101**,** 3681-3686.
BAUMFORTH, K. R., BIRGERSDOTTER, A., REYNOLDS, G. M., WEI, W., KAPATAI, G., FLAVELL, J. R., KALK, E., PIPER, K., LEE, S. & MACHADO, L. 2008. Expression of the Epstein-Barr virus-encoded Epstein-Barr virus nuclear antigen 1 in Hodgkin's lymphoma cells mediates Up-regulation of CCL20 and the migration of regulatory T cells. *The American journal of pathology,* 173**,** 195-204.
BAYERL, M. G., BRUGGEMAN, R. D., CONROY, E. J., HENGST, J. A., KING, T. S., JIMENEZ, M., CLAXTON, D. F. & YUN, J. K. 2008. Sphingosine kinase 1 protein and mRNA are overexpressed in non-Hodgkin lymphomas and are attractive targets for novel pharmacological interventions. *Leukemia & lymphoma,* 49**,** 948-954.
BECHTEL, D., KURTH, J., UNKEL, C. & KÜPPERS, R. 2005. Transformation of BCR-deficient germinal-center B cells by EBV supports a major role of the virus in the pathogenesis of Hodgkin and posttransplantation lymphomas. *Blood,* 106**,** 4345-4350.
BÉGUELIN, W., POPOVIC, R., TEATER, M., JIANG, Y., BUNTING, K. L., ROSEN, M., SHEN, H., YANG, S. N., WANG, L. & EZPONDA, T. 2013. EZH2 is required for germinal center formation and somatic EZH2 mutations promote lymphoid transformation. *Cancer cell,* 23**,** 677-692.
BI, X.-W., WANG, H., ZHANG, W.-W., WANG, J.-H., LIU, W.-J., XIA, Z.-J., HUANG, H.-Q., JIANG, W.-Q., ZHANG, Y.-J. & WANG, L. 2016. PD-L1 is upregulated by EBV-

driven LMP1 through NF-κB pathway and correlates with poor prognosis in natural killer/T-cell lymphoma. *Journal of hematology & oncology,* 9**,** 109.

BLANK, C., KUBALL, J., VOELKL, S., WIENDL, H., BECKER, B., WALTER, B., MAJDIC, O., GAJEWSKI, T. F., THEOBALD, M. & ANDREESEN, R. 2006. Blockade of PD-L1 (B7-H1) augments human tumor-specific T cell responses in vitro. *International journal of cancer,* 119**,** 317-327.

BOHERS, E., MARESCHAL, S., BOUZELFEN, A., MARCHAND, V., RUMINY, P., MAINGONNAT, C., MÉNARD, A. L., ETANCELIN, P., BERTRAND, P. & DUBOIS, S. 2014. Targetable activating mutations are very frequent in GCB and ABC diffuse large B-cell lymphoma. *Genes, Chromosomes and Cancer,* 53**,** 144-153.

BOHLE, V., DÖRING, C., HANSMANN, M. & KÜPPERS, R. 2013. Role of early B-cell factor 1 (EBF1) in Hodgkin lymphoma. *Leukemia,* 27**,** 671.

BORZA, C. M. & POZZI, A. 2014. Discoidin domain receptors in disease. *Matrix Biology,* 34**,** 185-192.

BOSE, S., YAP, L. F., FUNG, M., STARZCYNSKI, J., SALEH, A., MORGAN, S., DAWSON, C., CHUKWUMA, M. B., MAINA, E. & BUETTNER, M. 2009. The ATM tumour suppressor gene is down-regulated in EBV-associated nasopharyngeal carcinoma. *The Journal of pathology,* 217**,** 345-352.

BOUR-JORDAN, H., ESENSTEN, J. H., MARTINEZ-LLORDELLA, M., PENARANDA, C., STUMPF, M. & BLUESTONE, J. A. 2011. Intrinsic and extrinsic control of peripheral T-cell tolerance by costimulatory molecules of the CD28/B7 family. *Immunological reviews,* 241**,** 180-205.

BRÄUNINGER, A., SCHMITZ, R., BECHTEL, D., RENNÉ, C., HANSMANN, M. L. & KÜPPERS, R. 2006. Molecular biology of Hodgkin's and Reed/Sternberg cells in Hodgkin's lymphoma. *International journal of cancer,* 118**,** 1853-1861.

BRINKMANN, V. 2007. Sphingosine 1-phosphate receptors in health and disease: mechanistic insights from gene deletion studies and reverse pharmacology. *Pharmacology & therapeutics,* 115**,** 84-105.

BRUNE, V., TIACCI, E., PFEIL, I., DÖRING, C., ECKERLE, S., VAN NOESEL, C. J., KLAPPER, W., FALINI, B., VON HEYDEBRECK, A. & METZLER, D. 2008. Origin and pathogenesis of nodular lymphocyte–predominant Hodgkin lymphoma as revealed by global gene expression analysis. *Journal of Experimental Medicine,* 205**,** 2251-2268.

BRYAN, L. J. & GORDON, L. I. 2015. Blocking tumor escape in hematologic malignancies: the anti-PD-1 strategy. *Blood reviews,* 29**,** 25-32.

BUSSON, P. 2013. *Nasopharyngeal carcinoma: keys for translational medicine and biology*, Springer Science & Business Media.

BUSSON, P., GANEM, G., FLORES, P., MUGNERET, F., CLAUSSE, B., CAILLOU, B., BRAHAM, K., WAKASUGI, H., LIPINSKI, M. & TURSZ, T. 1988. Establishment and characterization of three transplantable EBV - containing nasopharyngeal carcinomas. *International journal of cancer,* 42**,** 599-606.

CABANNES, E., KHAN, G., AILLET, F., JARRETT, R. F. & HAY, R. T. 1999. Mutations in the IkBa gene in Hodgkin's disease suggest a tumour suppressor role for IκBα. *Oncogene,* 18**,** 3063.

CADER, F. Z., VOCKERODT, M., BOSE, S., NAGY, E., BRUNDLER, M.-A., KEARNS, P. & MURRAY, P. G. 2013. The EBV oncogene LMP1 protects lymphoma cells from cell death through the collagen-mediated activation of DDR1. *Blood,* 122**,** 4237-4245.

CAHIR-MCFARLAND, E. D., CARTER, K., ROSENWALD, A., GILTNANE, J. M., HENRICKSON, S. E., STAUDT, L. M. & KIEFF, E. 2004. Role of NF-κB in cell

survival and transcription of latent membrane protein 1-expressing or Epstein-Barr virus latency III-infected cells. *Journal of virology,* 78**,** 4108-4119.
CALDWELL, R. G., WILSON, J. B., ANDERSON, S. J. & LONGNECKER, R. 1998. Epstein-Barr virus LMP2A drives B cell development and survival in the absence of normal B cell receptor signals. *Immunity,* 9**,** 405-411.
CALLAHAN, M. K. 2016. Immune checkpoint therapy in melanoma. *The Cancer Journal,* 22**,** 73-80.
CALLAHAN, M. K., POSTOW, M. A. & WOLCHOK, J. D. 2016. Targeting T cell co-receptors for cancer therapy. *Immunity,* 44**,** 1069-1078.
CANELLOS, G. P., ROSENBERG, S. A., FRIEDBERG, J. W., LISTER, T. A. & DEVITA, V. T. 2014. Treatment of Hodgkin lymphoma: a 50-year perspective. *Journal of Clinical Oncology,* 32**,** 163-168.
CARBONE, A., GLOGHINI, A., GATTEI, V., ALDINUCCI, D., DEGAN, M., DE PAOLI, P., ZAGONEL, V. & PINTO, A. 1995. Expression of functional CD40 antigen on Reed-Sternberg cells and Hodgkin's disease cell lines. *Blood,* 85**,** 780-789.
CARE, M. A., WESTHEAD, D. R. & TOOZE, R. M. 2015. Gene expression meta-analysis reveals immune response convergence on the IFNγ-STAT1-IRF1 axis and adaptive immune resistance mechanisms in lymphoma. *Genome medicine,* 7**,** 96.
CATTARUZZA, L., GLOGHINI, A., OLIVO, K., DI FRANCIA, R., LORENZON, D., DE FILIPPI, R., CARBONE, A., COLOMBATTI, A., PINTO, A. & ALDINUCCI, D. 2009. Functional coexpression of Interleukin (IL)-7 and its receptor (IL-7R) on Hodgkin and Reed - Sternberg cells: Involvement of IL - 7 in tumor cell growth and microenvironmental interactions of Hodgkin's lymphoma. *International journal of cancer,* 125**,** 1092-1101.
CATTORETTI, G., MANDELBAUM, J., LEE, N., CHAVES, A. H., MAHLER, A. M., CHADBURN, A., DALLA-FAVERA, R., PASQUALUCCI, L. & MACLENNAN, A. J. 2009. Targeted disruption of the S1P2 sphingosine 1-phosphate receptor gene leads to diffuse large B-cell lymphoma formation. *Cancer research,* 69**,** 8686-8692.
CHAGANTI, S., BELL, A. I., PASTOR, N. B., MILNER, A. E., DRAYSON, M., GORDON, J. & RICKINSON, A. B. 2005. Epstein-Barr virus infection in vitro can rescue germinal center B cells with inactivated immunoglobulin genes. *Blood,* 106**,** 4249-4252.
CHAN, A. S. C., TO, K. F., LO, K. W., DING, M., LI, X., JOHNSON, P. & HUANG, D. P. 2002. Frequent chromosome 9p losses in histologically normal nasopharyngeal epithelia from southern Chinese. *International journal of cancer,* 102**,** 300-303.
CHAN, A. S. C., TO, K. F., LO, K. W., MAK, K. F., PAK, W., CHIU, B., GARY, M., DING, M., LI, X. & LEE, J. C. K. 2000. High frequency of chromosome 3p deletion in histologically normal nasopharyngeal epithelia from southern Chinese. *Cancer research,* 60**,** 5365-5370.
CHAN, W. C. 2013. CD30, another useful predictor of survival in DLBCL? *Blood,* 121**,** 2582-2583.
CHANG, R. A., MILLER, S. D. & LONGNECKER, R. 2012. Epstein-Barr virus latent membrane protein 2A exacerbates experimental autoimmune encephalomyelitis and enhances antigen presentation function. *Scientific reports,* 2**,** 353.
CHEN, B. J., CHAPUY, B., OUYANG, J., SUN, H. H., ROEMER, M. G., XU, M. L., YU, H., FLETCHER, C. D., FREEMAN, G. J. & SHIPP, M. A. 2013. PD-L1 expression is characteristic of a subset of aggressive B-cell lymphomas and virus-associated malignancies. *Clinical cancer research,* 19**,** 3462-3473.
CHEN, T.-C., CHEN, C.-H., WANG, C.-P., LIN, P.-H., YANG, T.-L., LOU, P.-J., KO, J.-Y., WU, C.-T. & CHANG, Y.-L. 2017. The immunologic advantage of recurrent nasopharyngeal carcinoma from the viewpoint of Galectin-9/Tim-3-related changes in the tumour microenvironment. *Scientific reports,* 7**,** 10349.
CHIBA, K., YANAGAWA, Y., MASUBUCHI, Y., KATAOKA, H., KAWAGUCHI, T., OHTSUKI, M. & HOSHINO, Y. 1998. FTY720, a novel immunosuppressant, induces sequestration of circulating mature lymphocytes by acceleration of lymphocyte

homing in rats. I. FTY720 selectively decreases the number of circulating mature lymphocytes by acceleration of lymphocyte homing. *The Journal of Immunology,* 160**,** 5037-5044.

CHIU, A., XU, W., HE, B., DILLON, S. R., GROSS, J. A., SIEVERS, E., QIAO, X., SANTINI, P., HYJEK, E. & LEE, J.-W. 2007. Hodgkin lymphoma cells express TACI and BCMA receptors and generate survival and proliferation signals in response to BAFF and APRIL. *Blood,* 109**,** 729-739.

CHOI, W. W., WEISENBURGER, D. D., GREINER, T. C., PIRIS, M. A., BANHAM, A. H., DELABIE, J., BRAZIEL, R. M., GENG, H., IQBAL, J. & LENZ, G. 2009. A new immunostain algorithm classifies diffuse large B-cell lymphoma into molecular subtypes with high accuracy. *Clinical cancer research,* 15**,** 5494-5502.

CHOU, C.-C., CHOU, M.-J. & TZEN, C.-Y. 2009. PIK3CA mutation occurs in nasopharyngeal carcinoma but does not significantly influence the disease-specific survival. *Medical Oncology,* 26**,** 322.

CHUN, J. 2013. *Lysophospholipid Receptors: Signaling and Biochemistry*, John Wiley & Sons.

CHUN, J., HLA, T., LYNCH, K. R., SPIEGEL, S. & MOOLENAAR, W. H. 2010. International union of basic and clinical pharmacology. LXXVIII. Lysophospholipid receptor nomenclature. *Pharmacological reviews,* 62**,** 579-587.

CHUNG, G. T. Y., LOU, W. P. K., CHOW, C., TO, K. F., CHOY, K. W., LEUNG, A. W. C., TONG, C. Y. K., YUEN, J. W. F., KO, C. W. & YIP, T. T. C. 2013. Constitutive activation of distinct NF-κB signals in EBV-associated nasopharyngeal carcinoma. *The Journal of pathology,* 231**,** 311-322.

COHEN, J. I., MOCARSKI, E. S., RAAB-TRAUB, N., COREY, L. & NABEL, G. J. 2013. The need and challenges for development of an Epstein-Barr virus vaccine. *Vaccine,* 31**,** B194-B196.

COHEN, M., VISTAROP, A. G., HUAMAN, F., NARBAITZ, M., METREBIAN, F., DE MATTEO, E., PRECIADO, M. V. & CHABAY, P. A. 2017. Cytotoxic response against Epstein Barr virus coexists with diffuse large B-cell lymphoma tolerogenic microenvironment: clinical features and survival impact. *Scientific Reports,* 7**,** 10813.

CONDEELIS, J. & POLLARD, J. W. 2006. Macrophages: obligate partners for tumor cell migration, invasion, and metastasis. *Cell,* 124**,** 263-266.

COUTINHO, R., CLEAR, A. J., MAZZOLA, E., OWEN, A., GREAVES, P., WILSON, A., MATTHEWS, J., LEE, A., ALVAREZ, R. & DA SILVA, M. G. 2015. Revisiting the immune microenvironment of diffuse large B-cell lymphoma using a tissue microarray and immunohistochemistry: robust semi-automated analysis reveals CD3 and FoxP3 as potential predictors of response to R-CHOP. *Haematologica,* 100**,** 363-369.

CROMME, F., MEIJER, C., SNIJDERS, P., UYTERLINDE, A., KENEMANS, P., HELMERHORST, T., STERN, P., VAN DEN BRULE, A. & WALBOOMERS, J. 1993. Analysis of MHC class I and II expression in relation to presence of HPV genotypes in premalignant and malignant cervical lesions. *British journal of cancer,* 67**,** 1372.

CURRAN, M. A., MONTALVO, W., YAGITA, H. & ALLISON, J. P. 2010. PD-1 and CTLA-4 combination blockade expands infiltrating T cells and reduces regulatory T and myeloid cells within B16 melanoma tumors. *Proceedings of the National Academy of Sciences,* 107**,** 4275-4280.

CUVILLIER, O., ADER, I., BOUQUEREL, P., BRIZUELA, L., MALAVAUD, B., MAZEROLLES, C. & RISCHMANN, P. 2010. Activation of sphingosine kinase-1 in cancer: implications for therapeutic targeting. *Current molecular pharmacology,* 3**,** 53-65.

CUVILLIER, O., PIRIANOV, G., KLEUSER, B., VANEK, P. G., COSO, O. A., GUTKIND, J. S. & SPIEGEL, S. 1996. Suppression of ceramide-mediated programmed cell death by sphingosine-1-phosphate. *Nature,* 381**,** 800.

CYSTER, J. G. 2005. Chemokines, sphingosine-1-phosphate, and cell migration in secondary lymphoid organs. *Annu. Rev. Immunol.,* 23**,** 127-159.

DAS, S., ONGUSAHA, P. P., YANG, Y. S., PARK, J.-M., AARONSON, S. A. & LEE, S. W. 2006. Discoidin domain receptor 1 receptor tyrosine kinase induces cyclooxygenase-2 and promotes chemoresistance through nuclear factor-κB pathway activation. *Cancer Research,* 66**,** 8123-8130.

DAWSON, C. W., PORT, R. J. & YOUNG, L. S. The role of the EBV-encoded latent membrane proteins LMP1 and LMP2 in the pathogenesis of nasopharyngeal carcinoma (NPC). Seminars in cancer biology, 2012. Elsevier, 144-153.

DAWSON, C. W., RICKINSON, A. B. & YOUNG, L. S. 1990. Epstein–Barr virus latent membrane protein inhibits human epithelial cell differentiation. *Nature,* 344**,** 777.

DAWSON, C. W., TRAMOUNTANIS, G., ELIOPOULOS, A. G. & YOUNG, L. S. 2003. Epstein-Barr virus latent membrane protein 1 (LMP1) activates the phosphatidylinositol 3-kinase/Akt pathway to promote cell survival and induce actin filament remodeling. *Journal of Biological Chemistry,* 278**,** 3694-3704.

DAY, E., WATERS, B., SPIEGEL, K., ALNADAF, T., MANLEY, P. W., BUCHDUNGER, E., WALKER, C. & JARAI, G. 2008. Inhibition of collagen-induced discoidin domain receptor 1 and 2 activation by imatinib, nilotinib and dasatinib. *European journal of pharmacology,* 599**,** 44-53.

DE, J. & BROWN, R. E. 2010. Tissue-microarray based immunohistochemical analysis of survival pathways in nodular sclerosing classical Hodgkin lymphoma as compared with Non-Hodgkin's lymphoma. *International journal of clinical and experimental medicine,* 3**,** 55.

DEACON, E., PALLESEN, G., NIEDOBITEK, G., CROCKER, J., BROOKS, L., RICKINSON, A. & YOUNG, L. 1993. Epstein-Barr virus and Hodgkin's disease: transcriptional analysis of virus latency in the malignant cells. *Journal of Experimental Medicine,* 177**,** 339-349.

DENNIS, G., SHERMAN, B. T., HOSACK, D. A., YANG, J., GAO, W., LANE, H. C. & LEMPICKI, R. A. 2003. DAVID: database for annotation, visualization, and integrated discovery. *Genome biology,* 4**,** R60.

DOERR, J. R., MALONE, C. S., FIKE, F. M., GORDON, M. S., SOGHOMONIAN, S. V., THOMAS, R. K., TAO, Q., MURRAY, P. G., DIEHL, V. & TEITELL, M. A. 2005. Patterned CpG methylation of silenced B cell gene promoters in classical Hodgkin lymphoma-derived and primary effusion lymphoma cell lines. *Journal of molecular biology,* 350**,** 631-640.

DOIG, T. N., HUME, D. A., THEOCHARIDIS, T., GOODLAD, J. R., GREGORY, C. D. & FREEMAN, T. C. 2013. Coexpression analysis of large cancer datasets provides insight into the cellular phenotypes of the tumour microenvironment. *BMC genomics,* 14**,** 469.

DONG H, T. L., XIE M, ZHOU L, JI Q. 2016. RNASeq identified human transcriptome alterations in Chinese Nasopharyngeal Carcinoma [internet]. *Available from: https://www.ncbi.nlm.nih.gov/geo/query/acc.cgi?acc=GSE68799*.

DU, W., TAKUWA, N., YOSHIOKA, K., OKAMOTO, Y., GONDA, K., SUGIHARA, K., FUKAMIZU, A., ASANO, M. & TAKUWA, Y. 2010. S1P2, the G protein–coupled receptor for sphingosine-1-phosphate, negatively regulates tumor angiogenesis and tumor growth in vivo in mice. *Cancer research,* 70**,** 772-781.

DUTTON, A., REYNOLDS, G. M., DAWSON, C. W., YOUNG, L. S. & MURRAY, P. G. 2005. Constitutive activation of phosphatidyl-inositide 3 kinase contributes to the survival of Hodgkin's lymphoma cells through a mechanism involving Akt kinase and mTOR. *The Journal of pathology,* 205**,** 498-506.

EDELSON, B. T., WUMESH, K., JUANG, R., KOHYAMA, M., BENOIT, L. A., KLEKOTKA, P. A., MOON, C., ALBRING, J. C., ISE, W. & MICHAEL, D. G. 2010. Peripheral CD103+ dendritic cells form a unified subset developmentally related to CD8α+ conventional dendritic cells. *Journal of Experimental Medicine,* 207**,** 823-836.

EMMERICH, F., MEISER, M., HUMMEL, M., DEMEL, G., FOSS, H.-D., JUNDT, F., MATHAS, S., KRAPPMANN, D., SCHEIDEREIT, C. & STEIN, H. 1999. Overexpression of I kappa B alpha without inhibition of NF-κB activity and mutations in the I kappa B alpha gene in Reed-Sternberg cells. *Blood,* 94**,** 3129-3134.

EMMERICH, F., THEURICH, S., HUMMEL, M., HAEFFKER, A., VRY, M. S., DÖHNER, K., BOMMERT, K., STEIN, H. & DÖRKEN, B. 2003. Inactivating I kappa B epsilon mutations in Hodgkin/Reed–Sternberg cells. *The Journal of pathology,* 201**,** 413-420.

ENDO, K., IGARASHI, Y., NISAR, M., ZHOU, Q. & HAKOMORI, S.-I. 1991. Cell membrane signaling as target in cancer therapy: inhibitory effect of N, N-dimethyl and N, N, N-trimethyl sphingosine derivatives on in vitro and in vivo growth of human tumor cells in nude mice. *Cancer research,* 51**,** 1613-1618.

ENGEL, J. & BÄCHINGER, H. P. 2005. Structure, stability and folding of the collagen triple helix. *Collagen.* Springer.

ESTRADA, R., ZENG, Q., LU, H., SAROJINI, H., LEE, J.-F., MATHIS, S. P., SANCHEZ, T., WANG, E., KONTOS, C. D. & LIN, C.-Y. 2008. Up-regulating sphingosine 1-phosphate receptor-2 signaling impairs chemotactic, wound-healing, and morphogenetic responses in senescent endothelial cells. *Journal of Biological Chemistry,* 283**,** 30363-30375.

FANG, W., ZHANG, J., HONG, S., ZHAN, J., CHEN, N., QIN, T., TANG, Y., ZHANG, Y., KANG, S. & ZHOU, T. 2014. EBV-driven LMP1 and IFN-γ up-regulate PD-L1 in nasopharyngeal carcinoma: Implications for oncotargeted therapy. *Oncotarget,* 5**,** 12189.

FINN, R. D., MISTRY, J., TATE, J., COGGILL, P., HEGER, A., POLLINGTON, J. E., GAVIN, O. L., GUNASEKARAN, P., CERIC, G. & FORSLUND, K. 2009. The Pfam protein families database. *Nucleic acids research,* 38**,** D211-D222.

FIUMARA, P., SNELL, V., LI, Y., MUKHOPADHYAY, A., YOUNES, M., GILLENWATER, A. M., CABANILLAS, F., AGGARWAL, B. B. & YOUNES, A. 2001. Functional expression of receptor activator of nuclear factor κB in Hodgkin disease cell lines. *Blood,* 98**,** 2784-2790.

FLAVELL, J. R., BAUMFORTH, K. R., WOOD, V. H., DAVIES, G. L., WEI, W., REYNOLDS, G. M., MORGAN, S., BOYCE, A., KELLY, G. L. & YOUNG, L. S. 2008. Down-regulation of the TGF-beta target gene, PTPRK, by the Epstein-Barr virus–encoded EBNA1 contributes to the growth and survival of Hodgkin lymphoma cells. *Blood,* 111**,** 292-301.

FLIES, D. B., SANDLER, B. J., SZNOL, M. & CHEN, L. 2011. Blockade of the B7-H1/PD-1 pathway for cancer immunotherapy. *The Yale journal of biology and medicine,* 84**,** 409.

FOGG, M., MURPHY, J. R., LORCH, J., POSNER, M. & WANG, F. 2013. Therapeutic targeting of regulatory T cells enhances tumor-specific CD8+ T cell responses in Epstein–Barr virus associated nasopharyngeal carcinoma. *Virology,* 441**,** 107-113.

FRAPPIER, L. 2012a. Contributions of Epstein–Barr nuclear antigen 1 (EBNA1) to cell immortalization and survival. *Viruses,* 4**,** 1537-1547.

FRAPPIER, L. 2012b. EBNA1 and host factors in Epstein–Barr virus latent DNA replication. *Current opinion in virology,* 2**,** 733-739.

FRAPPIER, L. Role of EBNA1 in NPC tumourigenesis. Seminars in cancer biology, 2012c. Elsevier, 154-161.

FRENCH, K. J., SCHRECENGOST, R. S., LEE, B. D., ZHUANG, Y., SMITH, S. N., EBERLY, J. L., YUN, J. K. & SMITH, C. D. 2003. Discovery and evaluation of inhibitors of human sphingosine kinase. *Cancer research,* 63**,** 5962-5969.

FUKUDA, M. & LONGNECKER, R. 2007. Epstein-Barr virus latent membrane protein 2A mediates transformation through constitutive activation of the Ras/PI3-K/Akt Pathway. *Journal of virology,* 81**,** 9299-9306.

GAO, M., DUAN, L., LUO, J., ZHANG, L., LU, X., ZHANG, Y., ZHANG, Z., TU, Z., XU, Y. & REN, X. 2013. Discovery and optimization of 3-(2-(Pyrazolo [1, 5-a] pyrimidin-6-yl)

ethynyl) benzamides as novel selective and orally bioavailable discoidin domain receptor 1 (DDR1) inhibitors. *Journal of medicinal chemistry,* 56**,** 3281-3295.

GAO, X. Y., LI, L., WANG, X. H., WEN, X. Z., JI, K., YE, L., CAI, J., JIANG, W. G. & JI, J. F. 2015. Inhibition of sphingosine-1-phosphate phosphatase 1 promotes cancer cells migration in gastric cancer: clinical implications. *Oncology reports,* 34**,** 1977-1987.

GARRIDO, F., RUIZ-CABELLO, F. & APTSIAURI, N. 2017. Rejection versus escape: the tumor MHC dilemma. *Cancer Immunology, Immunotherapy,* 66**,** 259-271.

GAUDIO, F., INGRAVALLO, G., PERRONE, T., DABBICCO, D., RUGGIERI, S., TAMMA, R., LADDAGA, F., GAGLIARDI, V., DE CANDIA, M. & RIBATTI, D. 2017. Microenvironment expression in diffuse large B-cell lymphomas. *Hematological Oncology,* 35**,** 296-297.

GEORGAKIS, G. V., LI, Y., RASSIDAKIS, G. Z., MEDEIROS, L. J., MILLS, G. B. & YOUNES, A. 2006. Inhibition of the phosphatidylinositol-3 kinase/Akt promotes G1 cell cycle arrest and apoptosis in Hodgkin lymphoma. *British journal of haematology,* 132**,** 503-511.

GIRES, O., ZIMBER-STROBL, U., GONNELLA, R., UEFFING, M., MARSCHALL, G., ZEIDLER, R., PICH, D. & HAMMERSCHMIDT, W. 1997. Latent membrane protein 1 of Epstein–Barr virus mimics a constitutively active receptor molecule. *The EMBO journal,* 16**,** 6131-6140.

GIULIANI, M., JANJI, B. & BERCHEM, G. 2017. Activation of NK cells and disruption of PD-L1/PD-1 axis: two different ways for lenalidomide to block myeloma progression. *Oncotarget,* 8**,** 24031.

GOETZL, E. J., WANG, W., MCGIFFERT, C., HUANG, M. C. & GRÄLER, M. H. 2004. Sphingosine 1-phosphate and its G protein-coupled receptors constitute a multifunctional immunoregulatory system. *Journal of cellular biochemistry,* 92**,** 1104-1114.

GOWRISHANKAR, K., GUNATILAKE, D., GALLAGHER, S. J., TIFFEN, J., RIZOS, H. & HERSEY, P. 2015. Inducible but not constitutive expression of PD-L1 in human melanoma cells is dependent on activation of NF-κB. *PloS one,* 10**,** e0123410.

GREAVES, P., CLEAR, A., OWEN, A., IQBAL, S., LEE, A., MATTHEWS, J., WILSON, A., CALAMINICI, M. & GRIBBEN, J. G. 2013. Defining characteristics of classical Hodgkin lymphoma microenvironment T-helper cells. *Blood,* 122**,** 2856-2863.

GREEN, J. A. & CYSTER, J. G. 2012. S1PR2 links germinal center confinement and growth regulation. *Immunological reviews,* 247**,** 36-51.

GREEN, M. R., RODIG, S., JUSZCZYNSKI, P., OUYANG, J., SINHA, P., O'DONNELL, E., NEUBERG, D. & SHIPP, M. A. 2012a. Constitutive AP-1 activity and EBV infection induce PD-L1 in Hodgkin lymphomas and posttransplant lymphoproliferative disorders: implications for targeted therapy. *Clinical cancer research,* 18**,** 1611-1618.

GREEN, T. M., YOUNG, K. H., VISCO, C., XU-MONETTE, Z. Y., ORAZI, A., GO, R. S., NIELSEN, O., GADEBERG, O. V., MOURITS-ANDERSEN, T. & FREDERIKSEN, M. 2012b. Immunohistochemical double-hit score is a strong predictor of outcome in patients with diffuse large B-cell lymphoma treated with rituximab plus cyclophosphamide, doxorubicin, vincristine, and prednisone. *Journal of clinical oncology,* 30**,** 3460-3467.

GUILLERMET-GUIBERT, J., DAVENNE, L., PCHEJETSKI, D., SAINT-LAURENT, N., BRIZUELA, L., GUILBEAU-FRUGIER, C., DELISLE, M.-B., CUVILLIER, O., SUSINI, C. & BOUSQUET, C. 2009. Targeting the sphingolipid metabolism to defeat pancreatic cancer cell resistance to the chemotherapeutic gemcitabine drug. *Molecular cancer therapeutics,* 8**,** 809-820.

GUILLOTON, F., CARON, G., MÉNARD, C., PANGAULT, C., AMÉ-THOMAS, P., DULONG, J., DE VOS, J., ROSSILLE, D., HENRY, C. & LAMY, T. 2012.

Mesenchymal stromal cells orchestrate follicular lymphoma cell niche through the CCL2-dependent recruitment and polarization of monocytes. *Blood,* 119**,** 2556-2567.

GUNAWARDANA, J., CHAN, F. C., TELENIUS, A., WOOLCOCK, B., KRIDEL, R., TAN, K. L., BEN-NERIAH, S., MOTTOK, A., LIM, R. S. & BOYLE, M. 2014. Recurrent somatic mutations of PTPN1 in primary mediastinal B cell lymphoma and Hodgkin lymphoma. *Nature genetics,* 46**,** 329.

GUTIÉRREZ-GARCÍA, G., CARDESA-SALZMANN, T., CLIMENT, F., GONZÁLEZ-BARCA, E., MERCADAL, S., MATE, J. L., SANCHO, J. M., ARENILLAS, L., SERRANO, S. & ESCODA, L. 2011. Gene-expression profiling and not immunophenotypic algorithms predicts prognosis in patients with diffuse large B-cell lymphoma treated with immunochemotherapy. *Blood,* 117**,** 4836-4843.

HANS, C. P., WEISENBURGER, D. D., GREINER, T. C., GASCOYNE, R. D., DELABIE, J., OTT, G., MÜLLER-HERMELINK, H. K., CAMPO, E., BRAZIEL, R. M. & JAFFE, E. S. 2004. Confirmation of the molecular classification of diffuse large B-cell lymphoma by immunohistochemistry using a tissue microarray. *Blood,* 103**,** 275-282.

HARIWIYANTO, B., SASTROWIYOTO, S., MUBARIKA, S. & SALUGU, M. 2010. LMP1 and LMP2 may be prognostic factors for outcome of therapy in nasopharyngeal cancers in Indonesia. *Asian Pac J Cancer Prev,* 11**,** 763-766.

HAY, E. D. 2013. *Cell biology of extracellular matrix*, Springer Science & Business Media.

HE, X., CHEN, Z., FU, T., JIN, X., YU, T., LIANG, Y., ZHAO, X. & HUANG, L. 2014. Ki-67 is a valuable prognostic predictor of lymphoma but its utility varies in lymphoma subtypes: evidence from a systematic meta-analysis. *BMC cancer,* 14**,** 153.

HEATH, E., BEGUE-PASTOR, N., CHAGANTI, S., CROOM-CARTER, D., SHANNON-LOWE, C., KUBE, D., FEEDERLE, R., DELECLUSE, H.-J., RICKINSON, A. B. & BELL, A. I. 2012. Epstein-Barr virus infection of naive B cells in vitro frequently selects clones with mutated immunoglobulin genotypes: implications for virus biology. *PLoS pathogens,* 8**,** e1002697.

HEEREN, A. M., PUNT, S., BLEEKER, M. C., GAARENSTROOM, K. N., VAN DER VELDEN, J., KENTER, G. G., DE GRUIJL, T. D. & JORDANOVA, E. S. 2016. Prognostic effect of different PD-L1 expression patterns in squamous cell carcinoma and adenocarcinoma of the cervix. *Modern Pathology,* 29**,** 753.

HEFFERNAN-STROUD, L. A., HELKE, K. L., JENKINS, R. W., DE COSTA, A.-M., HANNUN, Y. A. & OBEID, L. M. 2012. Defining a role for sphingosine kinase 1 in p53-dependent tumors. *Oncogene,* 31**,** 1166.

HENDERSON, S., ROWE, M., GREGORY, C., CROOM-CARTER, D., WANG, F., LONGNECKER, R., KIEFF, E. & RICKINSON, A. 1991. Induction of bcl-2 expression by Epstein-Barr virus latent membrane protein 1 protects infected B cells from programmed cell death. *Cell,* 65**,** 1107-1115.

HERSEY, P. & GOWRISHANKAR, K. 2015. Pembrolizumab joins the anti-PD-1 armamentarium in the treatment of melanoma. *Future Oncology,* 11**,** 133-140.

HERTEL, C. B., ZHOU, X.-G., HAMILTON-DUTOIT, S. J. & JUNKER, S. 2002. Loss of B cell identity correlates with loss of B cell-specific transcription factors in Hodgkin/Reed-Sternberg cells of classical Hodgkin lymphoma. *Oncogene,* 21**,** 4908.

HILDNER, K., EDELSON, B. T., PURTHA, W. E., DIAMOND, M., MATSUSHITA, H., KOHYAMA, M., CALDERON, B., SCHRAML, B. U., UNANUE, E. R. & DIAMOND, M. S. 2008. Batf3 deficiency reveals a critical role for CD8α+ dendritic cells in cytotoxic T cell immunity. *Science,* 322**,** 1097-1100.

HINZ, M., LEMKE, P., ANAGNOSTOPOULOS, I., HACKER, C., KRAPPMANN, D., MATHAS, S., DÖRKEN, B., ZENKE, M., STEIN, H. & SCHEIDEREIT, C. 2002. Nuclear factor κB–dependent gene expression profiling of Hodgkin's disease tumor cells, pathogenetic significance, and link to constitutive signal transducer and

activator of transcription 5a activity. *Journal of Experimental Medicine,* 196**,** 605-617.

HISANO, N., YATOMI, Y., SATOH, K., AKIMOTO, S., MITSUMATA, M., FUJINO, M. A. & OZAKI, Y. 1999. Induction and suppression of endothelial cell apoptosis by sphingolipids: a possible in vitro model for cell-cell interactions between platelets and endothelial cells. *Blood,* 93**,** 4293-4299.

HLA, T. & MACIAG, T. 1990. An abundant transcript induced in differentiating human endothelial cells encodes a polypeptide with structural similarities to G-protein-coupled receptors. *Journal of Biological Chemistry,* 265**,** 9308-9313.

HORIE, R., WATANABE, T., MORISHITA, Y., ITO, K., ISHIDA, T., KANEGAE, Y., SAITO, I., HIGASHIHARA, M., MORI, S. & KADIN, M. E. 2002. Ligand-independent signaling by overexpressed CD30 drives NF-κB activation in Hodgkin–Reed-Sternberg cells. *Oncogene,* 21**,** 2493.

HSU, C., LEE, S.-H., EJADI, S., EVEN, C., COHEN, R., LE TOURNEAU, C., MEHNERT, J., ALGAZI, A., VAN BRUMMELEN, E. & YUAN, S. 2015. Antitumor activity and safety of pembrolizumab in patients with PD-L1-positive nasopharyngeal carcinoma: interim results from a phase 1b study. *Ann Oncol,* 26**,** 93-102.

HSU, C., LEE, S.-H., EJADI, S., EVEN, C., COHEN, R. B., LE TOURNEAU, C., MEHNERT, J. M., ALGAZI, A., VAN BRUMMELEN, E. M. & SARAF, S. 2017. Safety and Antitumor Activity of Pembrolizumab in Patients With Programmed Death-Ligand 1–Positive Nasopharyngeal Carcinoma: Results of the KEYNOTE-028 Study. *Journal of Clinical Oncology,* 35**,** 4050-4056.

HSU, W.-L., TSE, K.-P., LIANG, S., CHIEN, Y.-C., SU, W.-H., KELLY, J. Y., CHENG, Y.-J., TSANG, N.-M., HSU, M.-M. & CHANG, K.-P. 2012. Evaluation of human leukocyte antigen-A (HLA-A), other non-HLA markers on chromosome 6p21 and risk of nasopharyngeal carcinoma. *PloS one,* 7**,** e42767.

HUANG, R.-Y., EPPOLITO, C., LELE, S., SHRIKANT, P., MATSUZAKI, J. & ODUNSI, K. 2015. LAG3 and PD1 co-inhibitory molecules collaborate to limit CD8+ T cell signaling and dampen antitumor immunity in a murine ovarian cancer model. *Oncotarget,* 6**,** 27359.

HUDNALL, S. D. & KÜPPERS, R. 2018. *Precision Molecular Pathology of Hodgkin Lymphoma*, Springer.

HUI, E. P., TAYLOR, G. S., JIA, H., MA, B. B., CHAN, S. L., HO, R., WONG, W.-L., WILSON, S., JOHNSON, B. F. & EDWARDS, C. 2013. Phase I trial of recombinant modified vaccinia ankara encoding Epstein–Barr viral tumor antigens in nasopharyngeal carcinoma patients. *Cancer research,* 73**,** 1676-1688.

INOKI, I., TAKUWA, N., SUGIMOTO, N., YOSHIOKA, K., TAKATA, S., KANEKO, S. & TAKUWA, Y. 2006. Negative regulation of endothelial morphogenesis and angiogenesis by S1P 2 receptor. *Biochemical and biophysical research communications,* 346**,** 293-300.

ISHII, I., FUKUSHIMA, N., YE, X. & CHUN, J. 2004. Lysophospholipid receptors: signaling and biology. *Annual review of biochemistry,* 73**,** 321-354.

IWAI, Y., ISHIDA, M., TANAKA, Y., OKAZAKI, T., HONJO, T. & MINATO, N. 2002. Involvement of PD-L1 on tumor cells in the escape from host immune system and tumor immunotherapy by PD-L1 blockade. *Proceedings of the National Academy of Sciences,* 99**,** 12293-12297.

IZBAN, K. F., ERGIN, M., HUANG, Q., QIN, J.-Z., MARTINEZ, R. L., SCHNITZER, B., NI, H., NICKOLOFF, B. J. & ALKAN, S. 2001. Characterization of NF-κB expression in Hodgkin's disease: inhibition of constitutively expressed NF-κB results in spontaneous caspase-independent apoptosis in Hodgkin and Reed-Sternberg cells. *Modern Pathology,* 14**,** 297.

JAFFE, E. S., HARRIS, N. L., VARDIMAN, J., ARBER, D. A. & CAMPO, E. 2010. *Hematopathology E-Book*, Elsevier Health Sciences.

JOHNSON, J. D., EDMAN, J. C. & RUTTER, W. J. 1993. A receptor tyrosine kinase found in breast carcinoma cells has an extracellular discoidin I-like domain. *Proceedings of the National Academy of Sciences,* 90**,** 5677-5681.

JOOS, S., GRANZOW, M., HOLTGREVE-GREZ, H., SIEBERT, R., HARDER, L., MARTÍN-SUBERO, J. I., WOLF, J., ADAMOWICZ, M., BARTH, T. F. & LICHTER, P. 2003. Hodgkin's lymphoma cell lines are characterized by frequent aberrations on chromosomes 2p and 9p including REL and JAK2. *International journal of cancer,* 103**,** 489-495.

JOOS, S., KÜPPER, M., OHL, S., VON BONIN, F., MECHTERSHEIMER, G., BENTZ, M., MARYNEN, P., MÖLLER, P., PFREUNDSCHUH, M. & TRÜMPER, L. 2000. Genomic imbalances including amplification of the tyrosine kinase gene JAK2 in CD30+ Hodgkin cells. *Cancer research,* 60**,** 549-552.

JÜCKER, M., SÜDEL, K., HORN, S., SICKEL, M., WEGNER, W., FIEDLER, W. & FELDMAN, R. 2002. Expression of a mutated form of the p85α regulatory subunit of phosphatidylinositol 3-kinase in a Hodgkin's lymphoma-derived cell line (CO). *Leukemia,* 16**,** 894.

JUNDT, F., ACIKGÖZ, Ö., KWON, S., SCHWARZER, R., ANAGNOSTOPOULOS, I., WIESNER, B., MATHAS, S., HUMMEL, M., STEIN, H. & REICHARDT, H. 2008. Aberrant expression of Notch1 interferes with the B-lymphoid phenotype of neoplastic B cells in classical Hodgkin lymphoma. *Leukemia,* 22**,** 1587.

JUNDT, F., ANAGNOSTOPOULOS, I., FÖRSTER, R., MATHAS, S., STEIN, H. & DÖRKEN, B. 2002a. Activated Notch1 signaling promotes tumor cell proliferation and survival in Hodgkin and anaplastic large cell lymphoma. *Blood,* 99**,** 3398-3403.

JUNDT, F., KLEY, K., ANAGNOSTOPOULOS, I., PRÖBSTING, K. S., GREINER, A., MATHAS, S., SCHEIDEREIT, C., WIRTH, T., STEIN, H. & DÖRKEN, B. 2002b. Loss of PU. 1 expression is associated with defective immunoglobulin transcription in Hodgkin and Reed-Sternberg cells of classical Hodgkin disease. *Blood,* 99**,** 3060-3062.

JUNGNICKEL, B., STARATSCHEK-JOX, A., BRÄUNINGER, A., SPIEKER, T., WOLF, J., DIEHL, V., HANSMANN, M.-L., RAJEWSKY, K. & KÜPPERS, R. 2000. Clonal deleterious mutations in the IκBα gene in the malignant cells in Hodgkin's lymphoma. *Journal of Experimental Medicine,* 191**,** 395-402.

KANG, X., LU, Z., CUI, C., DENG, M., FAN, Y., DONG, B., HAN, X., XIE, F., TYNER, J. W. & COLIGAN, J. E. 2015. The ITIM-containing receptor LAIR1 is essential for acute myeloid leukaemia development. *Nature cell biology,* 17**,** 665.

KANZLER, H., KÜPPERS, R., HANSMANN, M.-L. & RAJEWSKY, K. 1996. Hodgkin and Reed-Sternberg cells in Hodgkin's disease represent the outgrowth of a dominant tumor clone derived from (crippled) germinal center B cells. *Journal of Experimental Medicine,* 184**,** 1495-1505.

KAPATAI, G. & MURRAY, P. 2007. Contribution of the Epstein–Barr virus to the molecular pathogenesis of Hodgkin lymphoma. *Journal of clinical pathology,* 60**,** 1342-1349.

KAPITONOV, D., ALLEGOOD, J. C., MITCHELL, C., HAIT, N. C., ALMENARA, J. A., ADAMS, J. K., ZIPKIN, R. E., DENT, P., KORDULA, T. & MILSTIEN, S. 2009. Targeting sphingosine kinase 1 inhibits Akt signaling, induces apoptosis, and suppresses growth of human glioblastoma cells and xenografts. *Cancer research,* 69**,** 6915-6923.

KAPP, U., YEH, W.-C., PATTERSON, B., ELIA, A. J., KÄGI, D., HO, A., HESSEL, A., TIPSWORD, M., WILLIAMS, A. & MIRTSOS, C. 1999. Interleukin 13 is secreted by and stimulates the growth of Hodgkin and Reed-Sternberg cells. *Journal of Experimental Medicine,* 189**,** 1939-1946.

KAUPPILA, S., STENBÄCK, F., RISTELI, J., JUKKOLA, A. & RISTELI, L. 1998. Aberrant type I and type III collagen gene expression in human breast cancer in vivo. *The Journal of pathology,* 186**,** 262-268.

KERR, B., LEAR, A., ROWE, M., CROOM-CARTER, D., YOUNG, L., ROOKES, S., GALLIMORE, P. & RICKINSON, A. 1992. Three transcriptionally distinct forms of Epstein-Barr virus latency in somatic cell hybrids: cell phenotype dependence of virus promoter usage. *Virology,* 187**,** 189-201.

KHABIR, A., KARRAY, H., RODRIGUEZ, S., ROSÉ, M., DAOUD, J., FRIKHA, M., BOUDAWARA, T., MIDDELDORP, J., JLIDI, R. & BUSSON, P. 2005. EBV latent membrane protein 1 abundance correlates with patient age but not with metastatic behavior in north African nasopharyngeal carcinomas. *Virology journal,* 2**,** 39.

KIM, H.-G., HWANG, S.-Y., AARONSON, S. A., MANDINOVA, A. & LEE, S. W. 2011. DDR1 receptor tyrosine kinase promotes prosurvival pathway through Notch1 activation. *Journal of Biological Chemistry,* 286**,** 17672-17681.

KIM, H. R., HA, S.-J., HONG, M. H., HEO, S. J., KOH, Y. W., CHOI, E. C., KIM, E. K., PYO, K. H., JUNG, I. & SEO, D. 2016. PD-L1 expression on immune cells, but not on tumor cells, is a favorable prognostic factor for head and neck cancer patients. *Scientific reports,* 6**,** 36956.

KLUK, M. J., RYAN, K. P., WANG, B., ZHANG, G., RODIG, S. J. & SANCHEZ, T. 2013. Sphingosine-1-phosphate receptor 1 in classical Hodgkin lymphoma: assessment of expression and role in cell migration. *Laboratory investigation,* 93**,** 462.

KÖCHERT, K., ULLRICH, K., KREHER, S., ASTER, J., KITAGAWA, M., JÖHRENS, K., ANAGNOSTOPOULOS, I., JUNDT, F., LAMPRECHT, B. & ZIMBER-STROBL, U. 2011. High-level expression of Mastermind-like 2 contributes to aberrant activation of the NOTCH signaling pathway in human lymphomas. *Oncogene,* 30**,** 1831.

KOUVIDOU, C., RONTOGIANNI, D., TZARDI, M., DATSERIS, G., PANAYIOTIDES, I., DARIVIANAKI, K., KARIDI, E., DELIDES, G. & KANAVAROS, P. 1995. β2-Microglobulin and HLA-DR Expression in Relation to the Presence of Epstein-Barr Virus in Nasopharyngeal Carcinomas. *Pathobiology,* 63**,** 320-327.

KRIDEL, R., STEIDL, C. & GASCOYNE, R. D. 2015. Tumor-associated macrophages in diffuse large B-cell lymphoma. Haematologica.

KUBE, D., HOLTICK, U., VOCKERODT, M., AHMADI, T., HAIER, B., BEHRMANN, I., HEINRICH, P. C., DIEHL, V. & TESCH, H. 2001. STAT3 is constitutively activated in Hodgkin cell lines. *Blood,* 98**,** 762-770.

KULWICHIT, W., EDWARDS, R. H., DAVENPORT, E. M., BASKAR, J. F., GODFREY, V. & RAAB-TRAUB, N. 1998. Expression of the Epstein–Barr virus latent membrane protein 1 induces B cell lymphoma in transgenic mice. *Proceedings of the National Academy of Sciences,* 95**,** 11963-11968.

KÜPPERS, R. 2009. The biology of Hodgkin's lymphoma. *Nature Reviews Cancer,* 9**,** 15.

KÜPPERS, R., KLEIN, U., SCHWERING, I., DISTLER, V., BRÄUNINGER, A., CATTORETTI, G., TU, Y., STOLOVITZKY, G. A., CALIFANO, A. & HANSMANN, M.-L. 2003. Identification of Hodgkin and Reed-Sternberg cell-specific genes by gene expression profiling. *The Journal of clinical investigation,* 111**,** 529-537.

KÜPPERS, R., RAJEWSKY, K., ZHAO, M., SIMONS, G., LAUMANN, R., FISCHER, R. & HANSMANN, M.-L. 1994. Hodgkin disease: Hodgkin and Reed-Sternberg cells picked from histological sections show clonal immunoglobulin gene rearrangements and appear to be derived from B cells at various stages of development. *Proceedings of the National Academy of Sciences,* 91**,** 10962-10966.

L'HÔTE, C. G., THOMAS, P. H. & GANESAN, T. S. 2002. Functional analysis of discoidin domain receptor 1: effect of adhesion on DDR1 phosphorylation. *The FASEB Journal,* 16**,** 234-236.

LAICHALK, L. L. & THORLEY-LAWSON, D. A. 2005. Terminal differentiation into plasma cells initiates the replicative cycle of Epstein-Barr virus in vivo. *Journal of virology,* 79**,** 1296-1307.

LAJOIE, V., LEMIEUX, B., SAWAN, B., LICHTENSZTEJN, D., LICHTENSZTEJN, Z., WELLINGER, R., MAI, S. & KNECHT, H. 2015. LMP1 mediates multinuclearity through downregulation of shelterin proteins and formation of telomeric aggregates. *Blood,* 125**,** 2101-2110.

LAKE, A., SHIELD, L. A., CORDANO, P., CHUI, D. T., OSBORNE, J., CRAE, S., WILSON, K. S., TOSI, S., KNIGHT, S. J. & GESK, S. 2009. Mutations of NFKBIA, encoding IκBα, are a recurrent finding in classical Hodgkin lymphoma but are not a unifying feature of non-EBV-associated cases. *International journal of cancer,* 125**,** 1334-1342.

LAL, N., BEGGS, A. D., WILLCOX, B. E. & MIDDLETON, G. W. 2015. An immunogenomic stratification of colorectal cancer: implications for development of targeted immunotherapy. *Oncoimmunology,* 4**,** e976052.

LAM, N. & SUGDEN, B. 2003. CD40 and its viral mimic, LMP1: similar means to different ends. *Cellular signalling,* 15**,** 9-16.

LARKIN, J., CHIARION-SILENI, V., GONZALEZ, R., GROB, J. J., COWEY, C. L., LAO, C. D., SCHADENDORF, D., DUMMER, R., SMYLIE, M. & RUTKOWSKI, P. 2015. Combined nivolumab and ipilimumab or monotherapy in untreated melanoma. *New England Journal of Medicine,* 373**,** 23-34.

LAU, K., CHENG, S., LO, K., LEE, S., WOO, J., VAN HASSELT, C., LEE, S., RICKINSON, A. & NG, M. 2007. Increase in circulating Foxp3+ CD4+ CD25 high regulatory T cells in nasopharyngeal carcinoma patients. *British journal of cancer,* 96**,** 617.

LE STUNFF, H., GIUSSANI, P., MACEYKA, M., LÉPINE, S., MILSTIEN, S. & SPIEGEL, S. 2007. Recycling of sphingosine is regulated by the concerted actions of sphingosine-1-phosphate phosphohydrolase 1 and sphingosine kinase 2. *Journal of Biological Chemistry,* 282**,** 34372-34380.

LEBBINK, R. J., DE RUITER, T., ADELMEIJER, J., BRENKMAN, A. B., VAN HELVOORT, J. M., KOCH, M., FARNDALE, R. W., LISMAN, T., SONNENBERG, A. & LENTING, P. J. 2006. Collagens are functional, high affinity ligands for the inhibitory immune receptor LAIR-1. *Journal of Experimental Medicine,* 203**,** 1419-1425.

LEE, H., DENG, J., KUJAWSKI, M., YANG, C., LIU, Y., HERRMANN, A., KORTYLEWSKI, M., HORNE, D., SOMLO, G. & FORMAN, S. 2010. STAT3-induced S1PR1 expression is crucial for persistent STAT3 activation in tumors. *Nature medicine,* 16**,** 1421.

LEE, H. M., LO, K. W., WEI, W., TSAO, S. W., CHUNG, G. T. Y., IBRAHIM, M. H., DAWSON, C. W., MURRAY, P. G., PATERSON, I. C. & YAP, L. F. 2017a. Oncogenic S1P signalling in EBV-associated nasopharyngeal carcinoma activates AKT and promotes cell migration through S1P receptor 3. *The Journal of pathology,* 242**,** 62-72.

LEE, V. H., LO, A. W., LEUNG, C.-Y., SHEK, W.-H., KWONG, D. L., LAM, K.-O., TONG, C.-C., SZE, C.-K. & LEUNG, T.-W. 2016. Correlation of PD-L1 expression of tumor cells with survival outcomes after radical intensity-modulated radiation therapy for non-metastatic nasopharyngeal carcinoma. *PloS one,* 11**,** e0157969.

LEE, W., KIM, H. S., HWANG, S. S. & LEE, G. R. 2017b. The transcription factor Batf3 inhibits the differentiation of regulatory T cells in the periphery. *Experimental & molecular medicine,* 49**,** e393.

LEIDI, M., GOTTI, E., BOLOGNA, L., MIRANDA, E., RIMOLDI, M., SICA, A., RONCALLI, M., PALUMBO, G. A., INTRONA, M. & GOLAY, J. 2009. M2 macrophages phagocytose rituximab-opsonized leukemic targets more efficiently than m1 cells in vitro. *The Journal of Immunology,* 182**,** 4415-4422.

LEITINGER, B. 2003. Molecular analysis of collagen binding by the human discoidin domain receptors, DDR1 and DDR2 identification of collagen binding sites in DDR2. *Journal of Biological Chemistry,* 278**,** 16761-16769.

LEITINGER, B. 2011. Transmembrane collagen receptors. *Annual review of cell and developmental biology,* 27**,** 265-290.

LENZ, G., WRIGHT, G., DAVE, S., XIAO, W., POWELL, J., ZHAO, H., XU, W., TAN, B., GOLDSCHMIDT, N. & IQBAL, J. 2008. Stromal gene signatures in large-B-cell lymphomas. *New England Journal of Medicine,* 359**,** 2313-2323.

LI, J., ZHANG, X.-S., XIE, D., DENG, H.-X., GAO, Y.-F., CHEN, Q.-Y., HUANG, W.-L., MASUCCI, M. G. & ZENG, Y.-X. 2007. Expression of immune-related molecules in primary EBV positive Chinese nasopharyngeal carcinoma: associated with latent membrane protein 1 (LMP1) expression. *Cancer biology & therapy,* 6**,** 1997-2004.

LI, Q.-F., WU, C.-T., GUO, Q., WANG, H. & WANG, L.-S. 2008. Sphingosine 1-phosphate induces Mcl-1 upregulation and protects multiple myeloma cells against apoptosis. *Biochemical and biophysical research communications,* 371**,** 159-162.

LI, X., FASANO, R., WANG, E., YAO, K.-T. & MARINCOLA, F. M. 2009. HLA associations with nasopharyngeal carcinoma. *Current molecular medicine,* 9**,** 751-765.

LI, Y., LI, F., JIANG, F., LV, X., ZHANG, R., LU, A. & ZHANG, G. 2016. A mini-review for cancer immunotherapy: molecular understanding of PD-1/PD-L1 pathway & translational blockade of immune checkpoints. *International journal of molecular sciences,* 17**,** 1151.

LI, Y. Y., CHUNG, G. T., LUI, V. W., TO, K.-F., MA, B. B., CHOW, C., JOHN, K., WOO, S., YIP, K. Y. & SEO, J. 2017. Exome and genome sequencing of nasopharynx cancer identifies NF-κB pathway activating mutations. *Nature communications,* 8**,** 14121.

LIAO, Y., SMYTH, G. K. & SHI, W. 2013. The Subread aligner: fast, accurate and scalable read mapping by seed-and-vote. *Nucleic acids research,* 41**,** e108-e108.

LIN, D.-C., MENG, X., HAZAWA, M., NAGATA, Y., VARELA, A. M., XU, L., SATO, Y., LIU, L.-Z., DING, L.-W. & SHARMA, A. 2014. The genomic landscape of nasopharyngeal carcinoma. *Nature genetics,* 46**,** 866.

LIU, P., XIE, B.-L., CAI, S.-H., HE, Y.-W., ZHANG, G., YI, Y.-M. & DU, J. 2009. Expression of indoleamine 2, 3-dioxygenase in nasopharyngeal carcinoma impairs the cytolytic function of peripheral blood lymphocytes. *BMC cancer,* 9**,** 416.

LIU, Y., DENG, J., WANG, L., LEE, H., ARMSTRONG, B., SCUTO, A., KOWOLIK, C., WEISS, L. M., FORMAN, S. & YU, H. 2012. S1PR1 is an effective target to block STAT3 signaling in activated B cell–like diffuse large B-cell lymphoma. *Blood,* 120**,** 1458-1465.

LO, K.-W., CHUNG, G. T.-Y. & TO, K.-F. Deciphering the molecular genetic basis of NPC through molecular, cytogenetic, and epigenetic approaches. Seminars in cancer biology, 2012. Elsevier, 79-86.

LO, K. W., TO, K. F. & HUANG, D. P. 2004. Focus on nasopharyngeal carcinoma. *Cancer cell,* 5**,** 423-428.

LOLLIES, A., HARTMANN, S., SCHNEIDER, M., BRACHT, T., WEIß, A., ARNOLDS, J., KLEIN-HITPASS, L., SITEK, B., HANSMANN, M. & KÜPPERS, R. 2018. An oncogenic axis of STAT-mediated BATF3 upregulation causing MYC activity in classical Hodgkin lymphoma and anaplastic large cell lymphoma. *Leukemia,* 32**,** 92.

LUN, S. W. M., CHEUNG, C. C. M., CHOW, C., CHUNG, G. T. Y. & LO, K. W. 2013. Molecular Genetics of Nasopharyngeal Carcinoma. *eLS*.

LUNG, H. L., CHEUNG, A. K. L., KO, J. M. Y., CHENG, Y., STANBRIDGE, E. J. & LUNG, M. L. Deciphering the molecular genetic basis of NPC through functional approaches. Seminars in cancer biology, 2012. Elsevier, 87-95.

MA, B., GOH, B., LIM, W., LO, K., HUI, E. & RIESS, J. 2017. Multicenter phase II study of nivolumab in previously treated patients with recurrent and metastatic non-keratinizing nasopharyngeal carcinoma—Mayo Clinic Phase 2 Consortium P2C-MN026, NCI9742, NCT02339558. *Cancer Res,* 77.

MA, X.-B., ZHENG, Y., YUAN, H.-P., JIANG, J. & WANG, Y.-P. 2015. CD43 expression in diffuse large B-cell lymphoma, not otherwise specified: CD43 is a marker of adverse prognosis. *Human pathology,* 46**,** 593-599.

MANCAO, C., ALTMANN, M., JUNGNICKEL, B. & HAMMERSCHMIDT, W. 2005. Rescue of “crippled” germinal center B cells from apoptosis by Epstein-Barr virus. *Blood,* 106**,** 4339-4344.

MANDALA, S., HAJDU, R., BERGSTROM, J., QUACKENBUSH, E., XIE, J., MILLIGAN, J., THORNTON, R., SHEI, G.-J., CARD, D. & KEOHANE, C. 2002. Alteration of

lymphocyte trafficking by sphingosine-1-phosphate receptor agonists. *Science,* 296**,** 346-349.

MANDALA, S. M., THORNTON, R., GALVE-ROPERH, I., POULTON, S., PETERSON, C., OLIVERA, A., BERGSTROM, J., KURTZ, M. B. & SPIEGEL, S. 2000. Molecular cloning and characterization of a lipid phosphohydrolase that degrades sphingosine-1-phosphate and induces cell death. *Proceedings of the National Academy of Sciences,* 97**,** 7859-7864.

MANDELBAUM, J., BHAGAT, G., TANG, H., MO, T., BRAHMACHARY, M., SHEN, Q., CHADBURN, A., RAJEWSKY, K., TARAKHOVSKY, A. & PASQUALUCCI, L. 2010. BLIMP1 is a tumor suppressor gene frequently disrupted in activated B cell-like diffuse large B cell lymphoma. *Cancer cell,* 18**,** 568-579.

MANI, H. & JAFFE, E. S. 2009. Hodgkin lymphoma: an update on its biology with new insights into classification. *Clinical Lymphoma and Myeloma,* 9**,** 206-216.

MANSO, B., WENZL, K., ASMANN, Y., MAURER, M., MANSKE, M., YANG, Z., SLAGER, S., NOWAKOWSKI, G., ANSELL, S. & WITZIG, T. 2017. Whole-exome analysis reveals novel somatic genomic alterations associated with cell of origin in diffuse large B-cell lymphoma. *Blood cancer journal,* 7**,** e553.

MANTOVANI, A., ALLAVENA, P. & SICA, A. 2004. Tumour-associated macrophages as a prototypic type II polarised phagocyte population: role in tumour progression. *European journal of cancer,* 40**,** 1660-1667.

MARAFIOTI, T., HUMMEL, M., FOSS, H.-D., LAUMEN, H., KORBJUHN, P., ANAGNOSTOPOULOS, I., LAMMERT, H., DEMEL, G., THEIL, J. & WIRTH, T. 2000. Hodgkin and Reed-Sternberg cells represent an expansion of a single clone originating from a germinal center B-cell with functional immunoglobulin gene rearrangements but defective immunoglobulin transcription. *Blood,* 95**,** 1443-1450.

MARCHESI, F., CIRILLO, M., BIANCHI, A., GATELY, M., OLIMPIERI, O. M., CERCHIARA, E., RENZI, D., MICERA, A., BALZAMINO, B. O. & BONINI, S. 2015. High density of CD68+/CD163+ tumour - associated macrophages (M2 - TAM) at diagnosis is significantly correlated to unfavorable prognostic factors and to poor clinical outcomes in patients with diffuse large B-cell lymphoma. *Hematological oncology,* 33**,** 110-112.

MARTíN-SUBERO, J. I., GESK, S., HARDER, L., SONOKI, T., TUCKER, P. W., SCHLEGELBERGER, B., GROTE, W., NOVO, F. J., CALASANZ, M. J. & HANSMANN, M. L. 2002. Recurrent involvement of the REL and BCL11Aloci in classical Hodgkin lymphoma. *Blood,* 99**,** 1474-1477.

MARTIN-SUBERO, J. I., WLODARSKA, I., BASTARD, C., PICQUENOT, J.-M., HÖPPNER, J., GIEFING, M., KLAPPER, W. & SIEBERT, R. 2006. Chromosomal rearrangements involving the BCL3 locus are recurrent in classical Hodgkin and peripheral T-cell lymphoma. *Blood,* 108**,** 401-403.

MARTIN, K. A., LUPEY, L. N. & TEMPERA, I. 2016. Epstein-Barr virus oncoprotein LMP1 mediates epigenetic changes in host gene expression through PARP1. *Journal of virology,* 90**,** 8520-8530.

MARUO, S., ZHAO, B., JOHANNSEN, E., KIEFF, E., ZOU, J. & TAKADA, K. 2011. Epstein-Barr virus nuclear antigens 3C and 3A maintain lymphoblastoid cell growth by repressing p16INK4A and p14ARF expression. *Proceedings of the National Academy of Sciences,* 108**,** 1919-1924.

MASSARI, F., SANTONI, M., CICCARESE, C., SANTINI, D., ALFIERI, S., MARTIGNONI, G., BRUNELLI, M., PIVA, F., BERARDI, R. & MONTIRONI, R. 2015. PD-1 blockade therapy in renal cell carcinoma: current studies and future promises. *Cancer treatment reviews,* 41**,** 114-121.

MASSINI, G., SIEMER, D. & HOHAUS, S. 2009. EBV in Hodgkin lymphoma. *Mediterranean journal of hematology and infectious diseases,* 1.

MATHAS, S., JANZ, M., HUMMEL, F., HUMMEL, M., WOLLERT-WULF, B., LUSATIS, S., ANAGNOSTOPOULOS, I., LIETZ, A., SIGVARDSSON, M. & JUNDT, F. 2006.

Intrinsic inhibition of transcription factor E2A by HLH proteins ABF-1 and Id2 mediates reprogramming of neoplastic B cells in Hodgkin lymphoma. *Nature immunology,* 7**,** 207.

MATHAS, S., JÖHRENS, K., JOOS, S., LIETZ, A., HUMMEL, F., JANZ, M., JUNDT, F., ANAGNOSTOPOULOS, I., BOMMERT, K. & LICHTER, P. 2005. Elevated NF-κB p50 complex formation and Bcl-3 expression in classical Hodgkin, anaplastic large-cell, and other peripheral T-cell lymphomas. *Blood,* 106**,** 4287-4293.

MATLOUBIAN, M., LO, C. G., CINAMON, G., LESNESKI, M. J., XU, Y., BRINKMANN, V., ALLENDE, M. L., PROIA, R. L. & CYSTER, J. G. 2004. Lymphocyte egress from thymus and peripheral lymphoid organs is dependent on S1P receptor 1. *Nature,* 427**,** 355.

MCCARTY, J. K., MILLER, L., COX, E., KONRATH, J. & MCCARTY, S. K. 1985. Estrogen receptor analyses. Correlation of biochemical and immunohistochemical methods using monoclonal antireceptor antibodies. *Archives of pathology & laboratory medicine,* 109**,** 716-721.

MCCURLEY, T. L., GAY, R. E., GAY, S., GLICK, A. D., HARALSON, M. A. & COLLINS, R. D. 1986. The extracellular matrix in "sclerosing" follicular center cell lymphomas: An immunohistochemical and ultrastructural study. *Human pathology,* 17**,** 930-938.

MEDINA, P. J. & ADAMS, V. R. 2016. PD-1 Pathway Inhibitors: Immuno-Oncology Agents for Restoring Antitumor Immune Responses. *Pharmacotherapy: The Journal of Human Pharmacology and Drug Therapy,* 36**,** 317-334.

MENTER, T., BODMER-HAECKI, A., DIRNHOFER, S. & TZANKOV, A. 2016. Evaluation of the diagnostic and prognostic value of PDL1 expression in Hodgkin and B-cell lymphomas. *Human pathology,* 54**,** 17-24.

MERCHANT, M., SWART, R., KATZMAN, R. B., IKEDA, M., IKEDA, A., LONGNECKER, R., DYKSTRA, M. L. & PIERCE, S. K. 2001. The effects of the Epstein-Barr virus latent membrane protein 2A on B cell function. *International reviews of immunology,* 20**,** 805-835.

MEYAARD, L. 1999. LAIR-1, a widely distributed human ITIM-bearing receptor on hematopoietic cells. *Immunoreceptor Tyrosine-based Inhibition Motifs.* Springer.

MEYAARD, L. 2008. The inhibitory collagen receptor LAIR-1 (CD305). *Journal of leukocyte biology,* 83**,** 799-803.

MEYAARD, L., ADEMA, G. J., CHANG, C., WOOLLATT, E., SUTHERLAND, G. R., LANIER, L. L. & PHILLIPS, J. H. 1997. LAIR-1, a novel inhibitory receptor expressed on human mononuclear leukocytes. *Immunity,* 7**,** 283-290.

MEYER, P. N., FU, K., GREINER, T. C., SMITH, L. M., DELABIE, J., GASCOYNE, R. D., OTT, G., ROSENWALD, A., BRAZIEL, R. M. & CAMPO, E. 2010. Immunohistochemical methods for predicting cell of origin and survival in patients with diffuse large B-cell lymphoma treated with rituximab. *Journal of clinical oncology,* 29**,** 200-207.

MILSTIEN, S. & SPIEGEL, S. 2006. Targeting sphingosine-1-phosphate: a novel avenue for cancer therapeutics. *Cancer cell,* 9**,** 148-150.

MITRA, P., OSKERITZIAN, C. A., PAYNE, S. G., BEAVEN, M. A., MILSTIEN, S. & SPIEGEL, S. 2006. Role of ABCC1 in export of sphingosine-1-phosphate from mast cells. *Proceedings of the national academy of sciences,* 103**,** 16394-16399.

MOMTAZ, P. & POSTOW, M. A. 2014. Immunologic checkpoints in cancer therapy: focus on the programmed death-1 (PD-1) receptor pathway. *Pharmacogenomics and personalized medicine,* 7**,** 357.

Cader MONTOTO, S. & FITZGIBBON, J. 2011. Transformation of indolent B-cell lymphomas. *Journal of clinical oncology,* 29**,** 1827-1834.

MOOLENAAR, W. H. 1999. Bioactive lysophospholipids and their G protein-coupled receptors. *Experimental cell research,* 253**,** 230-238.

MORIN, R. D., MENDEZ-LAGO, M., MUNGALL, A. J., GOYA, R., MUNGALL, K. L., CORBETT, R. D., JOHNSON, N. A., SEVERSON, T. M., CHIU, R. & FIELD, M.

2011. Frequent mutation of histone-modifying genes in non-Hodgkin lymphoma. *Nature,* 476**,** 298.
MOTSCH, N., PFUHL, T., MRAZEK, J., BARTH, S. & GRÄSSER, F. A. 2007. Epstein-Barr virus-encoded latent membrane protein 1 (LMP1) induces the expression of the cellular microRNA miR-146a. *RNA biology,* 4**,** 131-137.
MUENST, S., HOELLER, S., DIRNHOFER, S. & TZANKOV, A. 2009. Increased programmed death-1+ tumor-infiltrating lymphocytes in classical Hodgkin lymphoma substantiate reduced overall survival. *Human pathology,* 40**,** 1715-1722.
MULTHAUPT, H. A., LEITINGER, B., GULLBERG, D. & COUCHMAN, J. R. 2016. Extracellular matrix component signaling in cancer. *Advanced drug delivery reviews,* 97**,** 28-40.
MURPHY, T. L., TUSSIWAND, R. & MURPHY, K. M. 2013. Specificity through cooperation: BATF–IRF interactions control immune-regulatory networks. *Nature reviews immunology,* 13**,** 499.
MURRAY, P. & BELL, A. 2015. Contribution of the Epstein-Barr Virus to the pathogenesis of Hodgkin lymphoma. *Epstein Barr Virus Volume 1.* Springer.
NEMA, R., VISHWAKARMA, S., AGARWAL, R., PANDAY, R. K. & KUMAR, A. 2016. Emerging role of sphingosine-1-phosphate signaling in head and neck squamous cell carcinoma. *OncoTargets and therapy,* 9**,** 3269.
NETWORK, C. G. A. 2015. Comprehensive genomic characterization of head and neck squamous cell carcinomas. *Nature,* 517**,** 576.
NETWORK, C. G. A. R. 2014. Comprehensive molecular characterization of gastric adenocarcinoma. *Nature,* 513**,** 202.
NUTT, S. L. & KEE, B. L. 2007. The transcriptional regulation of B cell lineage commitment. *Immunity,* 26**,** 715-725.
O'BRIEN, N., JONES, S. T., WILLIAMS, D. G., CUNNINGHAM, H. B., MORENO, K., VISENTIN, B., GENTILE, A., VEKICH, J., SHESTOWSKY, W. & HIRAIWA, M. 2009. Production and characterization of monoclonal anti-sphingosine-1-phosphate antibodies. *Journal of lipid research,* 50**,** 2245-2257.
O'DONNELL, J. S., LONG, G. V., SCOLYER, R. A., TENG, M. W. & SMYTH, M. J. 2017. Resistance to PD1/PDL1 checkpoint inhibition. *Cancer treatment reviews,* 52**,** 71-81.
OGRETMEN, B. & HANNUN, Y. A. 2001. Updates on functions of ceramide in chemotherapy-induced cell death and in multidrug resistance. *Drug Resistance Updates,* 4**,** 368-377.
OKAMOTO, H., TAKUWA, N., YATOMI, Y., GONDA, K., SHIGEMATSU, H. & TAKUWA, Y. 1999. EDG3 is a functional receptor specific for sphingosine 1-phosphate and sphingosylphosphorylcholine with signaling characteristics distinct from EDG1 and AGR16. *Biochemical and biophysical research communications,* 260**,** 203-208.
OKAMOTO, H., TAKUWA, N., YOKOMIZO, T., SUGIMOTO, N., SAKURADA, S., SHIGEMATSU, H. & TAKUWA, Y. 2000. Inhibitory regulation of Rac activation, membrane ruffling, and cell migration by the G protein-coupled sphingosine-1-phosphate receptor EDG5 but not EDG1 or EDG3. *Molecular and Cellular Biology,* 20**,** 9247-9261.
OKOSHI, H., HAKOMORI, S.-I., NISAR, M., ZHOU, Q., KIMURA, S., TASHIRO, K. & IGARASHI, Y. 1991. Cell membrane signaling as target in cancer therapy II: Inhibitory effect of N, N, N-trimethylsphingosine on metastatic potential of murine B16 melanoma cell line through blocking of tumor cell-dependent platelet aggregation. *Cancer research,* 51**,** 6019-6024.
OMAR, Z. A., ALI, Z. M. & TAMIN, N. S. I. 2006. Malaysian Cancer Statistics-Data and Figure, Peninsular Malaysia 2006. *National cancer registry, ministry of health Malaysia*.
OOFT, M. L., VAN IPENBURG, J. A., SANDERS, M. E., KRANENDONK, M., HOFLAND, I., DE BREE, R., KOLJENOVIĆ, S. & WILLEMS, S. M. 2017. Prognostic role of tumour-associated macrophages and regulatory T cells in EBV-positive and EBV-

negative nasopharyngeal carcinoma. *Journal of clinical pathology*, jclinpath-2017-204664.

OTT, P. A. & HODI, F. S. 2012. The B7-H1/PD-1 pathway in cancers associated with infections and inflammation: opportunities for therapeutic intervention. *Chinese clinical oncology,* 2.

OYAMA, T., ICHIMURA, K., SUZUKI, R., SUZUMIYA, J., OHSHIMA, K., YATABE, Y., YOKOI, T., KOJIMA, M., KAMIYA, Y. & TAJI, H. 2003. Senile EBV+ B-cell lymphoproliferative disorders: a clinicopathologic study of 22 patients. *The American journal of surgical pathology,* 27**,** 16-26.

OYAMA, T., YAMAMOTO, K., ASANO, N., OSHIRO, A., SUZUKI, R., KAGAMI, Y., MORISHIMA, Y., TAKEUCHI, K., IZUMO, T. & MORI, S. 2007. Age-related EBV-associated B-cell lymphoproliferative disorders constitute a distinct clinicopathologic group: a study of 96 patients. *Clinical Cancer Research,* 13**,** 5124-5132.

PAGES, F., KIRILOVSKY, A., MLECNIK, B., ASSLABER, M., TOSOLINI, M., BINDEA, G., LAGORCE, C., WIND, P., MARLIOT, F. & BRUNEVAL, P. 2009. In situ cytotoxic and memory T cells predict outcome in patients with early-stage colorectal cancer. *Journal of Clinical Oncology,* 27**,** 5944-5951.

PAL, S. K., DRABKIN, H. A., REEVES, J. A., HAINSWORTH, J. D., HAZEL, S. E., PAGGIARINO, D. A., WOJCIAK, J., WOODNUTT, G. & BHATT, R. S. 2017. A phase 2 study of the sphingosine-1-phosphate antibody sonepcizumab in patients with metastatic renal cell carcinoma. *Cancer,* 123**,** 576-582.

PARDOLL, D. M. 2012. The blockade of immune checkpoints in cancer immunotherapy. *Nature Reviews Cancer,* 12**,** 252.

PARIKKA, M., KAINULAINEN, T., TASANEN, K., VÄÄNÄNEN, A., BRUCKNER-TUDERMAN, L. & SALO, T. 2003. Alterations of collagen XVII expression during transformation of oral epithelium to dysplasia and carcinoma. *Journal of Histochemistry & Cytochemistry,* 51**,** 921-929.

PARSA, A. T., WALDRON, J. S., PANNER, A., CRANE, C. A., PARNEY, I. F., BARRY, J. J., CACHOLA, K. E., MURRAY, J. C., TIHAN, T. & JENSEN, M. C. 2007. Loss of tumor suppressor PTEN function increases B7-H1 expression and immunoresistance in glioma. *Nature medicine,* 13**,** 84.

PASQUALUCCI, L., COMPAGNO, M., HOULDSWORTH, J., MONTI, S., GRUNN, A., NANDULA, S. V., ASTER, J. C., MURTY, V. V., SHIPP, M. A. & DALLA-FAVERA, R. 2006. Inactivation of the PRDM1/BLIMP1 gene in diffuse large B cell lymphoma. *Journal of Experimental Medicine,* 203**,** 311-317.

PASQUALUCCI, L. & DALLA-FAVERA, R. The genetic landscape of diffuse large B-cell lymphoma. Seminars in hematology, 2015. Elsevier, 67-76.

PATHMANATHAN, R., PRASAD, U., CHANDRIKA, G., SADLER, R., FLYNN, K. & RAAB-TRAUB, N. 1995a. Undifferentiated, nonkeratinizing, and squamous cell carcinoma of the nasopharynx. Variants of Epstein-Barr virus-infected neoplasia. *The American journal of pathology,* 146**,** 1355.

PATHMANATHAN, R., PRASAD, U., SADLER, R., FLYNN, K. & RAAB-TRAUB, N. 1995b. Clonal proliferations of cells infected with Epstein–Barr virus in preinvasive lesions related to nasopharyngeal carcinoma. *New England Journal of Medicine,* 333**,** 693-698.

PCHEJETSKI, D., GOLZIO, M., BONHOURE, E., CALVET, C., DOUMERC, N., GARCIA, V., MAZEROLLES, C., RISCHMANN, P., TEISSIÉ, J. & MALAVAUD, B. 2005. Sphingosine kinase-1 as a chemotherapy sensor in prostate adenocarcinoma cell and mouse models. *Cancer research,* 65**,** 11667-11675.

PENG, H., CHEN, Y., GONG, P., CAI, L., LYU, X., JIANG, Q., WANG, J., LU, J., YAO, K. & LIU, K. 2016. Higher methylation intensity induced by EBV LMP1 via NF-κB/DNMT3b signaling contributes to silencing of PTEN gene. *Oncotarget,* 7**,** 40025.

PEREZ-DIEZ, A., JONCKER, N. T., CHOI, K., CHAN, W. F., ANDERSON, C. C., LANTZ, O. & MATZINGER, P. 2007. CD4 cells can be more efficient at tumor rejection than CD8 cells. *Blood,* 109**,** 5346-5354.

PFEFFER, S., ZAVOLAN, M., GRÄSSER, F. A., CHIEN, M., RUSSO, J. J., JU, J., JOHN, B., ENRIGHT, A. J., MARKS, D. & SANDER, C. 2004. Identification of virus-encoded microRNAs. *Science,* 304**,** 734-736.

PINTO, A., ALDINUCCI, D., GLOGHINI, A., ZAGONEL, A., DEGAN, M., PERIN, V., TODESCO, M., DE IULIIS, A., IMPROTA, S. & SACCO, C. 1997. The role of eosinophils in the pathobiology of Hodgkin's disease. *Annals of oncology,* 8**,** S89-S96.

PIVA, R., AGNELLI, L., PELLEGRINO, E., TODOERTI, K., GROSSO, V., TAMAGNO, I., FORNARI, A., MARTINOGLIO, B., MEDICO, E. & ZAMO, A. 2010. Gene expression profiling uncovers molecular classifiers for the recognition of anaplastic large-cell lymphoma within peripheral T-cell neoplasms. *Journal of clinical oncology,* 28**,** 1583-1590.

PON, J. R. & MARRA, M. A. 2016. Clinical impact of molecular features in diffuse large B-cell lymphoma and follicular lymphoma. *Blood,* 127**,** 181-186.

PORTIS, T., DYCK, P. & LONGNECKER, R. 2003. Epstein-Barr Virus (EBV) LMP2A induces alterations in gene transcription similar to those observed in Reed-Sternberg cells of Hodgkin lymphoma. *Blood,* 102**,** 4166-4178.

PORTIS, T. & LONGNECKER, R. 2004. Epstein–Barr virus (EBV) LMP2A alters normal transcriptional regulation following B-cell receptor activation. *Virology,* 318**,** 524-533.

QIAN, B.-Z. & POLLARD, J. W. 2010. Macrophage diversity enhances tumor progression and metastasis. *Cell,* 141**,** 39-51.

QUAN, L., CHEN, X., LIU, A., ZHANG, Y., GUO, X., YAN, S. & LIU, Y. 2015. PD-1 blockade can restore functions of T-cells in Epstein-Barr virus-positive diffuse large B-cell lymphoma in vitro. *PLoS One,* 10**,** e0136476.

QUEZADA, S. A., SIMPSON, T. R., PEGGS, K. S., MERGHOUB, T., VIDER, J., FAN, X., BLASBERG, R., YAGITA, H., MURANSKI, P. & ANTONY, P. A. 2010. Tumor-reactive CD4+ T cells develop cytotoxic activity and eradicate large established melanoma after transfer into lymphopenic hosts. *Journal of Experimental Medicine,* 207**,** 637-650.

RAAB-TRAUB, N. Epstein–Barr virus in the pathogenesis of NPC. Seminars in cancer biology, 2002. Elsevier, 431-441.

RAAB-TRAUB, N. & FLYNN, K. 1986. The structure of the termini of the Epstein-Barr virus as a marker of clonal cellular proliferation. *Cell,* 47**,** 883-889.

RAJENDRA, S., ACKROYD, R., KARIM, N., MOHAN, C., HO, J. J. & KUTTY, M. 2006. Loss of human leucocyte antigen class I and gain of class II expression are early events in carcinogenesis: clues from a study of Barrett's oesophagus. *Journal of clinical pathology,* 59**,** 952-957.

RAMMAL, H., SABY, C., MAGNIEN, K., VAN-GULICK, L., GARNOTEL, R., BUACHE, E., EL BTAOURI, H., JEANNESSON, P. & MORJANI, H. 2016. Discoidin domain receptors: potential actors and targets in cancer. *Frontiers in pharmacology,* 7**,** 55.

RE, D., MÜSCHEN, M., AHMADI, T., WICKENHAUSER, C., STARATSCHEK-JOX, A., HOLTICK, U., DIEHL, V. & WOLF, J. 2001. Oct-2 and Bob-1 deficiency in Hodgkin and Reed Sternberg cells. *Cancer research,* 61**,** 2080-2084.

RECH, A. J. & VONDERHEIDE, R. H. 2009. Clinical use of anti-CD25 antibody daclizumab to enhance immune responses to tumor antigen vaccination by targeting regulatory T cells. *Annals of the New York Academy of Sciences,* 1174**,** 99-106.

REICHEL, J., CHADBURN, A., RUBINSTEIN, P. G., GIULINO-ROTH, L., TAM, W., LIU, Y., GAIOLLA, R., ENG, K., BRODY, J. & INGHIRAMI, G. 2015. Flow sorting and exome sequencing reveal the oncogenome of primary Hodgkin and Reed-Sternberg cells. *Blood,* 125**,** 1061-1072.

REN, R., TYRYSHKIN, K., GRAHAM, C. H., KOTI, M. & SIEMENS, D. R. 2017. Comprehensive immune transcriptomic analysis in bladder cancer reveals subtype specific immune gene expression patterns of prognostic relevance. *Oncotarget,* 8**,** 70982.

RENNÉ, C., HINSCH, N., WILLENBROCK, K., FUCHS, M., KLAPPER, W., ENGERT, A., KÜPPERS, R., HANSMANN, M. L. & BRÄUNINGER, A. 2007. The aberrant coexpression of several receptor tyrosine kinases is largely restricted to EBV-negative cases of classical Hodgkin's lymphoma. *International journal of cancer,* 120**,** 2504-2509.

RENNÉ, C., MARTIN-SUBERO, J. I., EICKERNJÄGER, M., HANSMANN, M.-L., KÜPPERS, R., SIEBERT, R. & BRÄUNINGER, A. 2006. Aberrant expression of ID2, a suppressor of B-cell-specific gene expression, in Hodgkin's lymphoma. *The American journal of pathology,* 169**,** 655-664.

RENNÉ, C., WILLENBROCK, K., KÜPPERS, R., HANSMANN, M.-L. & BRÄUNINGER, A. 2005. Autocrine-and paracrine-activated receptor tyrosine kinases in classic Hodgkin lymphoma. *Blood,* 105**,** 4051-4059.

REUSCH, J. A., NAWANDAR, D. M., WRIGHT, K. L., KENNEY, S. C. & MERTZ, J. E. 2015. Cellular differentiation regulator BLIMP1 induces Epstein-Barr virus lytic reactivation in epithelial and B cells by activating transcription from both the R and Z promoters. *Journal of virology,* 89**,** 1731-1743.

RICKINSON, A., ROWE, M., HART, I., YAO, Q., HENDERSON, L., RABIN, H. & EPSTEIN, M. 1984. T-cell-mediated regression of “spontaneous” and of Epstein-Barr virus-induced B-cell transformation in vitro: studies with cyclosporin A. *Cellular immunology,* 87**,** 646-658.

ROBINSON, M. D., MCCARTHY, D. J. & SMYTH, G. K. 2010. edgeR: a Bioconductor package for differential expression analysis of digital gene expression data. *Bioinformatics,* 26**,** 139-140.

ROEMER, M. G., ADVANI, R. H., REDD, R. A., PINKUS, G. S., NATKUNAM, Y., LIGON, A. H., CONNELLY, C. F., PAK, C. J., CAREY, C. D. & DAADI, S. E. 2016. Classical Hodgkin lymphoma with reduced β2M/MHC class I expression is associated with inferior outcome independent of 9p24. 1 status. *Cancer immunology research,* 4**,** 910-916.

ROSAI, J. 2011. *Rosai and Ackerman's surgical pathology e-book*, Elsevier Health Sciences.

ROSENWALD, A. 2003. DNA microarrays in lymphoid malignancies. *Oncology (Williston Park, NY),* 17**,** 1743-8; discussion 1750, 1755, 1758-9 passim.

ROSENWALD, A., WRIGHT, G., CHAN, W. C., CONNORS, J. M., CAMPO, E., FISHER, R. I., GASCOYNE, R. D., MULLER-HERMELINK, H. K., SMELAND, E. B. & GILTNANE, J. M. 2002. The use of molecular profiling to predict survival after chemotherapy for diffuse large-B-cell lymphoma. *New England Journal of Medicine,* 346**,** 1937-1947.

ROSENWALD, A., WRIGHT, G., LEROY, K., YU, X., GAULARD, P., GASCOYNE, R. D., CHAN, W. C., ZHAO, T., HAIOUN, C. & GREINER, T. C. 2003. Molecular diagnosis of primary mediastinal B cell lymphoma identifies a clinically favorable subgroup of diffuse large B cell lymphoma related to Hodgkin lymphoma. *Journal of Experimental Medicine,* 198**,** 851-862.

ROWE, M., FITZSIMMONS, L. & BELL, A. I. 2014. Epstein-Barr virus and Burkitt lymphoma. *Chinese journal of cancer,* 33**,** 609.

ROZALI, E. N., HATO, S. V., ROBINSON, B. W., LAKE, R. A. & LESTERHUIS, W. J. 2012. Programmed death ligand 2 in cancer-induced immune suppression. *Clinical and Developmental Immunology,* 2012.

RUCKHÄBERLE, E., RODY, A., ENGELS, K., GAETJE, R., VON MINCKWITZ, G., SCHIFFMANN, S., GRÖSCH, S., GEISSLINGER, G., HOLTRICH, U. & KARN, T. 2008. Microarray analysis of altered sphingolipid metabolism reveals prognostic

significance of sphingosine kinase 1 in breast cancer. *Breast cancer research and treatment,* 112**,** 41-52.
SANCHEZ, T., ESTRADA-HERNANDEZ, T., PAIK, J.-H., WU, M.-T., VENKATARAMAN, K., BRINKMANN, V., CLAFFEY, K. & HLA, T. 2003. Phosphorylation and action of the immunomodulator FTY720 inhibits vascular endothelial cell growth factor-induced vascular permeability. *Journal of Biological Chemistry,* 278**,** 47281-47290.
SANCHEZ, T. & HLA, T. 2004. Structural and functional characteristics of S1P receptors. *Journal of cellular biochemistry,* 92**,** 913-922.
SANCHEZ, T., THANGADA, S., WU, M.-T., KONTOS, C. D., WU, D., WU, H. & HLA, T. 2005. PTEN as an effector in the signaling of antimigratory G protein-coupled receptor. *Proceedings of the National Academy of Sciences of the United States of America,* 102**,** 4312-4317.
SANTALA, M., SIMOJOKI, M., RISTELI, J., RISTELI, L. & KAUPPILA, A. 1999. Type I and type III collagen metabolites as predictors of clinical outcome in epithelial ovarian cancer. *Clinical cancer research,* 5**,** 4091-4096.
SATO, K., MALCHINKHUU, E., HORIUCHI, Y., MOGI, C., TOMURA, H., TOSAKA, M., YOSHIMOTO, Y., KUWABARA, A. & OKAJIMA, F. 2007. Critical role of ABCA1 transporter in sphingosine 1 - phosphate release from astrocytes. *Journal of neurochemistry,* 103**,** 2610-2619.
SAUER, B., GONSKA, H., MANGGAU, M., KIM, D., SCHRAUT, C., SCHÄFER-KORTING, M. & KLEUSER, B. 2005. Sphingosine 1-phosphate is involved in cytoprotective actions of calcitriol in human fibroblasts and enhances the intracellular Bcl-2/Bax rheostat. *Die Pharmazie-An International Journal of Pharmaceutical Sciences,* 60**,** 298-304.
SCHLÖßER, H. A., THEURICH, S., SHIMABUKURO-VORNHAGEN, A., HOLTICK, U., STIPPEL, D. L. & BERGWELT-BAILDON, M. V. 2014. Overcoming tumor-mediated immunosuppression. *Immunotherapy,* 6**,** 973-988.
SCHMITZ, R., HANSMANN, M.-L., BOHLE, V., MARTIN-SUBERO, J. I., HARTMANN, S., MECHTERSHEIMER, G., KLAPPER, W., VATER, I., GIEFING, M. & GESK, S. 2009. TNFAIP3 (A20) is a tumor suppressor gene in Hodgkin lymphoma and primary mediastinal B cell lymphoma. *Journal of Experimental Medicine,* 206**,** 981-989.
SCHREIBER, R. D., OLD, L. J. & SMYTH, M. J. 2011. Cancer immunoediting: integrating immunity's roles in cancer suppression and promotion. *Science,* 331**,** 1565-1570.
SCHÜPPEL, M., KÜRSCHNER, U., KLEUSER, U., SCHÄFER-KORTING, M. & KLEUSER, B. 2008. Sphingosine 1-phosphate restrains insulin-mediated keratinocyte proliferation via inhibition of Akt through the S1P2 receptor subtype. *Journal of Investigative Dermatology,* 128**,** 1747-1756.
SCHWARTZ, M., ZHANG, Y. & ROSENBLATT, J. D. 2016. B cell regulation of the anti-tumor response and role in carcinogenesis. *Journal for immunotherapy of cancer,* 4**,** 40.
SCHWERING, I., BRÄUNINGER, A., DISTLER, V., JESDINSKY, J., DIEHL, V., HANSMANN, M.-L., RAJEWSKY, K. & KÜPPERS, R. 2003a. Profiling of Hodgkin's lymphoma cell line L1236 and germinal center B cells: identification of Hodgkin's lymphoma–specific genes. *Molecular Medicine,* 9**,** 85.
SCHWERING, I., BRÄUNINGER, A., KLEIN, U., JUNGNICKEL, B., TINGUELY, M., DIEHL, V., HANSMANN, M.-L., DALLA-FAVERA, R., RAJEWSKY, K. & KÜPPERS, R. 2003b. Loss of the B-lineage–specific gene expression program in Hodgkin and Reed-Sternberg cells of Hodgkin lymphoma. *Blood,* 101**,** 1505-1512.
SCOGNAMIGLIO, G., DE CHIARA, A., DI BONITO, M., TATANGELO, F., LOSITO, N. S., ANNICIELLO, A., DE CECIO, R., D'ALTERIO, C., SCALA, S. & CANTILE, M. 2016. Variability in immunohistochemical detection of programmed death ligand 1 (PD-L1) in cancer tissue types. *International journal of molecular sciences,* 17**,** 790.
SCOTT, F., CLEMONS, B., BROOKS, J., BRAHMACHARY, E., POWELL, R., DEDMAN, H., DESALE, H., TIMONY, G., MARTINBOROUGH, E. & ROSEN, H. 2016.

Ozanimod (RPC1063) is a potent sphingosine-1-phosphate receptor-1 (S1P1) and receptor-5 (S1P5) agonist with autoimmune disease-modifying activity. *British journal of pharmacology,* 173**,** 1778-1792.

SENGUPTA, S., DEN BOON, J. A., CHEN, I.-H., NEWTON, M. A., DAHL, D. B., CHEN, M., CHENG, Y.-J., WESTRA, W. H., CHEN, C.-J. & HILDESHEIM, A. 2006. Genome-wide expression profiling reveals EBV-associated inhibition of MHC class I expression in nasopharyngeal carcinoma. *Cancer research,* 66**,** 7999-8006.

SHANG, B., LIU, Y., JIANG, S.-J. & LIU, Y. 2015. Prognostic value of tumor-infiltrating FoxP3+ regulatory T cells in cancers: a systematic review and meta-analysis. *Scientific reports,* 5**,** 15179.

SHANMUGARATNAM, K. 1978. Histological typing of nasopharyngeal carcinoma. *IARC scientific publications***,** 3-12.

SHEN, L., LI, H., SHI, Y., WANG, D., GONG, J., XUN, J., ZHOU, S., XIANG, R. & TAN, X. 2016. M2 tumour-associated macrophages contribute to tumour progression via legumain remodelling the extracellular matrix in diffuse large B cell lymphoma. *Scientific reports,* 6**,** 30347.

SHOULDERS, M. D. & RAINES, R. T. 2009. Collagen structure and stability. *Annual review of biochemistry,* 78**,** 929-958.

SHRIVASTAVA, A., RADZIEJEWSKI, C., CAMPBELL, E., KOVAC, L., MCGLYNN, M., RYAN, T. E., DAVIS, S., GOLDFARB, M. P., GLASS, D. J. & LEMKE, G. 1997. An orphan receptor tyrosine kinase family whose members serve as nonintegrin collagen receptors. *Molecular cell,* 1**,** 25-34.

SKALSKA, L., WHITE, R. E., FRANZ, M., RUHMANN, M. & ALLDAY, M. J. 2010. Epigenetic repression of p16INK4A by Latent Epstein-Barr Virus requires the interaction of EBNA3A and EBNA3C with CtBP. *PLoS pathogens,* 6**,** e1000951.

SKINNIDER, B. F., ELIA, A. J., GASCOYNE, R. D., PATTERSON, B., TRUMPER, L., KAPP, U. & MAK, T. W. 2002. Signal transducer and activator of transcription 6 is frequently activated in Hodgkin and Reed-Sternberg cells of Hodgkin lymphoma. *Blood,* 99**,** 618-626.

SKINNIDER, B. F., ELIA, A. J., GASCOYNE, R. D., TRÜMPER, L. H., VON BONIN, F., KAPP, U., PATTERSON, B., SNOW, B. E. & MAK, T. W. 2001. Interleukin 13 and interleukin 13 receptor are frequently expressed by Hodgkin and Reed-Sternberg cells of Hodgkin lymphoma. *Blood,* 97**,** 250-255.

ŠMAHEL, M. 2017. PD-1/PD-L1 Blockade Therapy for Tumors with Downregulated MHC Class I Expression. *International journal of molecular sciences,* 18**,** 1331.

SMITH, D. W. & SUGDEN, B. 2013. Potential cellular functions of Epstein-Barr nuclear antigen 1 (EBNA1) of Epstein-Barr virus. *Viruses,* 5**,** 226-240.

SMITH, E. M., ÅKERBLAD, P., KADESCH, T., AXELSON, H. & SIGVARDSSON, M. 2005. Inhibition of EBF function by active Notch signaling reveals a novel regulatory pathway in early B-cell development. *Blood,* 106**,** 1995-2001.

SMITH, S. M. 2017. Aggressive B-cell lymphoma: the double-hit and double-expressor phenotypes. *Clinical advances in hematology & oncology: H&O,* 15**,** 40-42.

SOBUE, S., MURAKAMI, M., BANNO, Y., ITO, H., KIMURA, A., GAO, S., FURUHATA, A., TAKAGI, A., KOJIMA, T. & SUZUKI, M. 2008a. v-Src oncogene product increases sphingosine kinase 1 expression through mRNA stabilization: alteration of AU-rich element-binding proteins. *Oncogene,* 27**,** 6023.

SOBUE, S., NEMOTO, S., MURAKAMI, M., ITO, H., KIMURA, A., GAO, S., FURUHATA, A., TAKAGI, A., KOJIMA, T. & NAKAMURA, M. 2008b. Implications of sphingosine kinase 1 expression level for the cellular sphingolipid rheostat: relevance as a marker for daunorubicin sensitivity of leukemia cells. *International journal of hematology,* 87**,** 266-275.

SON, M., SANTIAGO-SCHWARZ, F., AL-ABED, Y. & DIAMOND, B. 2012. C1q limits dendritic cell differentiation and activation by engaging LAIR-1. *Proceedings of the National Academy of Sciences,* 109**,** E3160-E3167.

SONG, M., CHEN, D., LU, B., WANG, C., ZHANG, J., HUANG, L., WANG, X., TIMMONS, C. L., HU, J. & LIU, B. 2013. PTEN loss increases PD-L1 protein expression and affects the correlation between PD-L1 expression and clinical parameters in colorectal cancer. *PloS one,* 8**,** e65821.

SONI, V., CAHIR-MCFARLAND, E. & KIEFF, E. 2007. LMP1 TRAFficking activates growth and survival pathways. *TNF Receptor Associated Factors (TRAFs).* Springer.

SPIEGEL, S. & MILSTIEN, S. 2003. Sphingosine-1-phosphate: an enigmatic signalling lipid. *Nature reviews Molecular cell biology,* 4**,** 397.

SPRINGER, S. 2015. Transport and quality control of MHC class I molecules in the early secretory pathway. *Current opinion in immunology,* 34**,** 83-90.

STEIDL, C., DIEPSTRA, A., LEE, T., CHAN, F. C., FARINHA, P., TAN, K., TELENIUS, A., BARCLAY, L., SHAH, S. P. & CONNORS, J. M. 2012. Gene expression profiling of microdissected Hodgkin Reed-Sternberg cells correlates with treatment outcome in classical Hodgkin lymphoma. *Blood,* 120**,** 3530-3540.

STEIDL, C., SHAH, S. P., WOOLCOCK, B. W., RUI, L., KAWAHARA, M., FARINHA, P., JOHNSON, N. A., ZHAO, Y., TELENIUS, A. & NERIAH, S. B. 2011. MHC class II transactivator CIITA is a recurrent gene fusion partner in lymphoid cancers. *Nature,* 471**,** 377.

STEIN, H., MARAFIOTI, T., FOSS, H.-D., LAUMEN, H., HUMMEL, M., ANAGNOSTOPOULOS, I., WIRTH, T., DEMEL, G. & FALINI, B. 2001. Down-regulation of BOB. 1/OBF. 1 and Oct2 in classical Hodgkin disease but not in lymphocyte predominant Hodgkin disease correlates with immunoglobulin transcription. *Blood,* 97**,** 496-501.

SWERDLOW, S. H., CAMPO, E., HARRIS, N., JAFFE, E., PILERI, S., STEIN, H., THIELE, J. & VARDIMAN, J. 2008. World Health Organization classification of tumours. *Pathology and genetics of tumours of haematopoietic and lymphoid tissues***,** 2008.

SWERDLOW, S. H., CAMPO, E., PILERI, S. A., HARRIS, N. L., STEIN, H., SIEBERT, R., ADVANI, R., GHIELMINI, M., SALLES, G. A. & ZELENETZ, A. D. 2016. The 2016 revision of the World Health Organization classification of lymphoid neoplasms. *Blood,* 127**,** 2375-2390.

SZYLBERG, Ł., KARBOWNIK, D. & MARSZAŁEK, A. 2016. The role of FOXP3 in human cancers. *Anticancer research,* 36**,** 3789-3794.

TAHA, T. A., KITATANI, K., EL-ALWANI, M., BIELAWSKI, J., HANNUN, Y. A. & OBEID, L. M. 2006. Loss of sphingosine kinase-1 activates the intrinsic pathway of programmed cell death: modulation of sphingolipid levels and the induction of apoptosis. *The FASEB journal,* 20**,** 482-484.

TAKUWA, Y. 2002. Subtype-specific differential regulation of Rho family G proteins and cell migration by the Edg family sphingosine-1-phosphate receptors. *Biochimica et Biophysica Acta (BBA)-Molecular and Cell Biology of Lipids,* 1582**,** 112-120.

TAKUWA, Y., OKAMOTO, H., TAKUWA, N., GONDA, K., SUGIMOTO, N. & SAKURADA, S. 2001. Subtype-specific, differential activities of the EDG family receptors for sphingosine-1-phosphate, a novel lysophospholipid mediator. *Molecular and cellular endocrinology,* 177**,** 3-11.

TAKUWA, Y., TAKUWA, N. & SUGIMOTO, N. 2002. The Edg Family G Protein-Coupled Receptors for Lysophospholipids: Their Signaling Properties and Biologicla Activities. *The Journal of Biochemistry,* 131**,** 767-771.

TANG, H., LIANG, Y., ANDERS, R. A., TAUBE, J. M., QIU, X., MULGAONKAR, A., LIU, X., HARRINGTON, S. M., GUO, J. & XIN, Y. 2018. PD-L1 on host cells is essential for PD-L1 blockade–mediated tumor regression. *The Journal of clinical investigation,* 128.

TANG, X., TIAN, L., ESTESO, G., CHOI, S.-C., BARROW, A. D., COLONNA, M., BORREGO, F. & COLIGAN, J. E. 2012. Leukocyte-associated Ig-like receptor-1–deficient mice have an altered immune cell phenotype. *The Journal of Immunology,* 188**,** 548-558.

TAUBE, J. M., ANDERS, R. A., YOUNG, G. D., XU, H., SHARMA, R., MCMILLER, T. L., CHEN, S., KLEIN, A. P., PARDOLL, D. M. & TOPALIAN, S. L. 2012. Colocalization of inflammatory response with B7-h1 expression in human melanocytic lesions supports an adaptive resistance mechanism of immune escape. *Science translational medicine,* 4**,** 127ra37-127ra37.

TAYLOR, G. S. & STEVEN, N. M. 2016. Therapeutic vaccination strategies to treat nasopharyngeal carcinoma. *Chinese clinical oncology,* 5.

TERAI, K., SOGA, T., TAKAHASHI, M., KAMOHARA, M., OHNO, K., YATSUGI, S., OKADA, M. & YAMAGUCHI, T. 2003. Edg-8 receptors are preferentially expressed in oligodendrocyte lineage cells of the rat CNS. *Neuroscience,* 116**,** 1053-1062.

TESTONI, M., ZUCCA, E., YOUNG, K. & BERTONI, F. 2015. Genetic lesions in diffuse large B-cell lymphomas. *Annals of Oncology,* 26**,** 1069-1080.

THAVENTHIRAN, J. E., FEARON, D. T. & GATTINONI, L. 2013. Transcriptional regulation of effector and memory CD8+ T cell fates. *Current opinion in immunology,* 25**,** 321-328.

THEIL, J., LAUMEN, H., MARAFIOTI, T., HUMMEL, M., LENZ, G., WIRTH, T. & STEIN, H. 2001. Defective octamer-dependent transcription is responsible for silenced immunoglobulin transcription in Reed-Sternberg cells. *Blood,* 97**,** 3191-3196.

THOMPSON, L. D. 2006. *Head and neck pathology*, Churchill Livingstone.

THOREAU, M., PENNY, H. L., TAN, K., REGNIER, F., WEISS, J. M., LEE, B., JOHANNES, L., DRANSART, E., LE BON, A. & ABASTADO, J.-P. 2015. Vaccine-induced tumor regression requires a dynamic cooperation between T cells and myeloid cells at the tumor site. *Oncotarget,* 6**,** 27832.

TIACCI, E., DÖRING, C., BRUNE, V., VAN NOESEL, C. J., KLAPPER, W., MECHTERSHEIMER, G., FALINI, B., KÜPPERS, R. & HANSMANN, M.-L. 2012. Analyzing primary Hodgkin and Reed-Sternberg cells to capture the molecular and cellular pathogenesis of classical Hodgkin lymphoma. *Blood,* 120**,** 4609-4620.

TILLY, H., GOMES DA SILVA, M., VITOLO, U., JACK, A., MEIGNAN, M., LOPEZ-GUILLERMO, A., WALEWSKI, J., ANDRÉ, M., JOHNSON, P. & PFREUNDSCHUH, M. 2015. Diffuse large B-cell lymphoma (DLBCL): ESMO Clinical Practice Guidelines for diagnosis, treatment and follow-up. *Annals of oncology,* 26**,** v116-v125.

TOPALIAN, S. L., DRAKE, C. G. & PARDOLL, D. M. 2015. Immune checkpoint blockade: a common denominator approach to cancer therapy. *Cancer cell,* 27**,** 450-461.

TOPALIAN, S. L., TAUBE, J. M., ANDERS, R. A. & PARDOLL, D. M. 2016. Mechanism-driven biomarkers to guide immune checkpoint blockade in cancer therapy. *Nature Reviews Cancer,* 16**,** 275.

TORLAKOVIC, E., TIERENS, A., DANG, H. D. & DELABIE, J. 2001. The transcription factor PU. 1, necessary for B-cell development is expressed in lymphocyte predominance, but not classical Hodgkin's disease. *The American journal of pathology,* 159**,** 1807-1814.

TOTH, Z. E. & MEZEY, E. 2007. Simultaneous visualization of multiple antigens with tyramide signal amplification using antibodies from the same species. *Journal of Histochemistry & Cytochemistry,* 55**,** 545-554.

TSANG, W., CHAN, J., TANG, S., TSE, C. & CHEUNG, M. 1992. Large cell lymphoma with fibrillary matrix. *Histopathology,* 20**,** 80-82.

TSE, C., CHAN, J., YUEN, R. & NG, C. 1991. Malignant lymphoma with myxoid stroma: a new pattern in need of recognition. *Histopathology,* 18**,** 31-35.

TSUJIKAWA, T., KUMAR, S., BORKAR, R. N., AZIMI, V., THIBAULT, G., CHANG, Y. H., BALTER, A., KAWASHIMA, R., CHOE, G. & SAUER, D. 2017. Quantitative multiplex immunohistochemistry reveals myeloid-inflamed tumor-immune complexity associated with poor prognosis. *Cell reports,* 19**,** 203-217.

TUMEH, P. C., HARVIEW, C. L., YEARLEY, J. H., SHINTAKU, I. P., TAYLOR, E. J., ROBERT, L., CHMIELOWSKI, B., SPASIC, M., HENRY, G. & CIOBANU, V. 2014.

PD-1 blockade induces responses by inhibiting adaptive immune resistance. *Nature,* 515**,** 568.

USHMOROV, A., RITZ, O., HUMMEL, M., LEITHÄUSER, F., MÖLLER, P., STEIN, H. & WIRTH, T. 2004. Epigenetic silencing of the immunoglobulin heavy-chain gene in classical Hodgkin lymphoma-derived cell lines contributes to the loss of immunoglobulin expression. *Blood,* 104**,** 3326-3334.

VADAS, M., XIA, P., MCCAUGHAN, G. & GAMBLE, J. 2008. The role of sphingosine kinase 1 in cancer: oncogene or non-oncogene addiction? *Biochimica et Biophysica Acta (BBA)-Molecular and Cell Biology of Lipids,* 1781**,** 442-447.

VÄISÄNEN, T., VÄISÄNEN, M. R., AUTIO-HARMAINEN, H. & PIHLAJANIEMI, T. 2005. Type XIII collagen expression is induced during malignant transformation in various epithelial and mesenchymal tumours. *The Journal of pathology,* 207**,** 324-335.

VALIATHAN, R. R., MARCO, M., LEITINGER, B., KLEER, C. G. & FRIDMAN, R. 2012. Discoidin domain receptor tyrosine kinases: new players in cancer progression. *Cancer and Metastasis Reviews,* 31**,** 295-321.

VAN WAES, C. & MUSBAHI, O. 2017. Genomics and advances towards precision medicine for head and neck squamous cell carcinoma. *Laryngoscope investigative otolaryngology,* 2**,** 310-319.

VAQUERIZAS, J. M., KUMMERFELD, S. K., TEICHMANN, S. A. & LUSCOMBE, N. M. 2009. A census of human transcription factors: function, expression and evolution. *Nature Reviews Genetics,* 10**,** 252.

VICARI, A. P. & TRINCHIERI, G. 2004. Interleukin-10 in viral diseases and cancer: exiting the labyrinth? *Immunological reviews,* 202**,** 223-236.

VILLOUTREIX, B. O. & MITEVA, M. A. 2016. Discoidin domains as emerging therapeutic targets. *Trends in pharmacological sciences,* 37**,** 641-659.

VISENTIN, B., VEKICH, J. A., SIBBALD, B. J., CAVALLI, A. L., MORENO, K. M., MATTEO, R. G., GARLAND, W. A., LU, Y., YU, S. & HALL, H. S. 2006. Validation of an anti-sphingosine-1-phosphate antibody as a potential therapeutic in reducing growth, invasion, and angiogenesis in multiple tumor lineages. *Cancer cell,* 9**,** 225-238.

VITOLO, U., CHIAPPELLA, A., FERRERI, A. J., MARTELLI, M., BALDI, I., BALZAROTTI, M., BOTTELLI, C., CONCONI, A., GOMEZ, H. & LOPEZ-GUILLERMO, A. 2011. First-line treatment for primary testicular diffuse large B-cell lymphoma with rituximab-CHOP, CNS prophylaxis, and contralateral testis irradiation: final results of an international phase II trial. *Journal of Clinical Oncology,* 29**,** 2766-2772.

VOCKERODT, M., MORGAN, S., KUO, M., WEI, W., CHUKWUMA, M., ARRAND, J., KUBE, D., GORDON, J., YOUNG, L. & WOODMAN, C. 2008. The Epstein–Barr virus oncoprotein, latent membrane protein-1, reprograms germinal centre B cells towards a Hodgkin's Reed–Sternberg-like phenotype. *The Journal of pathology,* 216**,** 83-92.

VOCKERODT, M., WEI, W., NAGY, E., PROUZOVA, Z., SCHRADER, A., KUBE, D., ROWE, M., WOODMAN, C. B. & MURRAY, P. G. 2013. Suppression of the LMP2A target gene, EGR-1, protects Hodgkin's lymphoma cells from entry to the EBV lytic cycle. *The Journal of pathology,* 230**,** 399-409.

VOGEL, W., GISH, G. D., ALVES, F. & PAWSON, T. 1997. The discoidin domain receptor tyrosine kinases are activated by collagen. *Molecular cell,* 1**,** 13-23.

VRAZO, A. C., CHAUCHARD, M., RAAB-TRAUB, N. & LONGNECKER, R. 2012. Epstein-Barr virus LMP2A reduces hyperactivation induced by LMP1 to restore normal B cell phenotype in transgenic mice. *PLoS pathogens,* 8**,** e1002662.

VRZALIKOVA, K., IBRAHIM, M., VOCKERODT, M., PERRY, T., MARGIELEWSKA, S., LUPINO, L., NAGY, E., SOILLEUX, E., LIEBELT, D. & HOLLOWS, R. 2018. S1PR1 drives a feedforward signalling loop to regulate BATF3 and the transcriptional programme of Hodgkin lymphoma cells. *Leukemia,* 32**,** 214.

VRZALIKOVA, K., LEONARD, S., FAN, Y., BELL, A., VOCKERODT, M., FLODR, P., WRIGHT, K. L., ROWE, M., TAO, Q. & MURRAY, P. G. 2012. Hypomethylation and over-expression of the beta isoform of BLIMP1 is induced by Epstein-Barr virus infection of B cells; potential implications for the pathogenesis of EBV-associated lymphomas. *Pathogens,* 1**,** 83-101.

VRZALIKOVA, K., VOCKERODT, M., LEONARD, S., BELL, A., WEI, W., SCHRADER, A., WRIGHT, K. L., KUBE, D., ROWE, M. & WOODMAN, C. B. 2011. Down-regulation of BLIMP1α by the EBV oncogene, LMP-1, disrupts the plasma cell differentiation program and prevents viral replication in B cells: implications for the pathogenesis of EBV-associated B-cell lymphomas. *Blood,* 117**,** 5907-5917.

WADA, N., ZAKI, M. A., HORI, Y., HASHIMOTO, K., TSUKAGUCHI, M., TATSUMI, Y., ISHIKAWA, J., TOMINAGA, N., SAKODA, H. & TAKE, H. 2012. Tumour-associated macrophages in diffuse large B-cell lymphoma: a study of the Osaka Lymphoma Study Group. *Histopathology,* 60**,** 313-319.

WANG, J., ZHOU, M., XU, J.-Y., CHEN, B. & OUYANG, J. 2015. Combination of BCL-2 and MYC protein expression improves high-risk stratification in diffuse large B-cell lymphoma. *OncoTargets and therapy,* 8**,** 2645.

WANG, S., MEDEIROS, L. J., XU-MONETTE, Z. Y., ZHANG, S., O'MALLEY, D. P., ORAZI, A., ZUO, Z., BUESO-RAMOS, C. E., YIN, C. C. & LIU, Z. 2014. Epstein-Barr virus–positive nodular lymphocyte predominant Hodgkin lymphoma. *Annals of diagnostic pathology,* 18**,** 203-209.

WEBB, T., KIMBALL, A. & SUN, W. 2015. Mantle cell lymphoma associated sphingosine-1 phosphate inhibits natural killer T cell mediated antitumor responses (TUM2P. 1042). Am Assoc Immnol.

WENIGER, M., MELZNER, I., MENZ, C., WEGENER, S., BUCUR, A., DORSCH, K., MATTFELDT, T., BARTH, T. & MÖLLER, P. 2006. Mutations of the tumor suppressor gene SOCS-1 in classical Hodgkin lymphoma are frequent and associated with nuclear phospho-STAT5 accumulation. *Oncogene,* 25**,** 2679.

WESTIN, J. R. 2014. Status of PI3K/Akt/mTOR pathway inhibitors in lymphoma. *Clinical Lymphoma, Myeloma and Leukemia,* 14**,** 335-342.

WHERRY, E. J. & AHMED, R. 2004. Memory CD8 T-cell differentiation during viral infection. *Journal of virology,* 78**,** 5535-5545.

WHITE, R. E., RÄMER, P. C., NARESH, K. N., MEIXLSPERGER, S., PINAUD, L., ROONEY, C., SAVOLDO, B., COUTINHO, R., BÖDÖR, C. & GRIBBEN, J. 2012. EBNA3B-deficient EBV promotes B cell lymphomagenesis in humanized mice and is found in human tumors. *The Journal of clinical investigation,* 122.

WILLIAMS, K. L., NANDA, I., LYONS, G. E., KUO, C. T., SCHMID, M., LEIDEN, J. M., KAPLAN, M. H. & TAPAROWSKY, E. J. 2001. Characterization of murine BATF: a negative regulator of activator protein-1 activity in the thymus. *European journal of immunology,* 31**,** 1620-1627.

WINDH, R. T., LEE, M.-J., HLA, T., AN, S., BARR, A. J. & MANNING, D. R. 1999. Differential coupling of the sphingosine 1-phosphate receptors Edg-1, Edg-3, and H218/Edg-5 to the Gi, Gq, and G12 families of heterotrimeric G proteins. *Journal of Biological Chemistry,* 274**,** 27351-27358.

WLODARSKI, P., KASPRZYCKA, M., LIU, X., MARZEC, M., ROBERTSON, E. S., SLUPIANEK, A. & WASIK, M. A. 2005. Activation of mammalian target of rapamycin in transformed B lymphocytes is nutrient dependent but independent of Akt, mitogen-activated protein kinase/extracellular signal-regulated kinase kinase, insulin growth factor-I, and serum. *Cancer research,* 65**,** 7800-7808.

WOLCHOK, J. D., KLUGER, H., CALLAHAN, M. K., POSTOW, M. A., RIZVI, N. A., LESOKHIN, A. M., SEGAL, N. H., ARIYAN, C. E., GORDON, R.-A. & REED, K. 2013. Nivolumab plus ipilimumab in advanced melanoma. *New England Journal of Medicine,* 369**,** 122-133.

WOOD, V., O'NEIL, J., WEI, W., STEWART, S., DAWSON, C. & YOUNG, L. 2007. Epstein–Barr virus-encoded EBNA1 regulates cellular gene transcription and modulates the STAT1 and TGFβ signaling pathways. *Oncogene,* 26**,** 4135.

XIA, P., GAMBLE, J. R., WANG, L., PITSON, S. M., MORETTI, P. A., WATTENBERG, B. W., D'ANDREA, R. J. & VADAS, M. A. 2000. An oncogenic role of sphingosine kinase. *Current Biology,* 10**,** 1527-1530.

YAGI, H., KAMBA, R., CHIBA, K., SOGA, H., YAGUCHI, K., NAKAMURA, M. & ITOH, T. 2000. Immunosuppressant FTY720 inhibits thymocyte emigration. *European journal of immunology,* 30**,** 1435-1444.

YAMAMOTO, R., NISHIKORI, M., KITAWAKI, T., SAKAI, T., HISHIZAWA, M., TASHIMA, M., KONDO, T., OHMORI, K., KURATA, M. & HAYASHI, T. 2008. PD-1–PD-1 ligand interaction contributes to immunosuppressive microenvironment of Hodgkin lymphoma. *Blood,* 111**,** 3220-3224.

YAN, H., HOU, X., LI, T., ZHAO, L., YUAN, X., FU, H. & ZHU, R. 2016. CD4+ T cell-mediated cytotoxicity eliminates primary tumor cells in metastatic melanoma through high MHC class II expression and can be enhanced by inhibitory receptor blockade. *Tumor Biology,* 37**,** 15949-15958.

YAO, Y., MINTER, H. A., CHEN, X., REYNOLDS, G. M., BROMLEY, M. & ARRAND, J. R. 2000. Heterogeneity of HLA and EBER expression in epstein-barr virus-associated nasopharyngeal carcinoma. *International journal of cancer,* 88**,** 949-955.

YIN, L., LIAO, W., DENG, X., TANG, M., GU, H., LI, X., YI, W. & CAO, Y. 2001. LMP1 activates NF-kappa B via degradation of I kappa B alpha in nasopharyngeal carcinoma cells. *Chinese medical journal,* 114**,** 718-722.

YIP, W., ABDULLAH, M., YUSOFF, S. & SEOW, H.-F. 2009. Increase in tumour-infiltrating lymphocytes with regulatory T cell immunophenotypes and reduced ζ-chain expression in nasopharyngeal carcinoma patients. *Clinical & Experimental Immunology,* 155**,** 412-422.

YOUNG, L. S. & DAWSON, C. W. 2014. Epstein-Barr virus and nasopharyngeal carcinoma. *Chinese journal of cancer,* 33**,** 581.

YOUNG, L. S. & RICKINSON, A. B. 2004. Epstein–Barr virus: 40 years on. *Nature Reviews Cancer,* 4**,** 757.

YOUNG, L. S., YAP, L. F. & MURRAY, P. G. 2016. Epstein–Barr virus: more than 50 years old and still providing surprises. *Nature Reviews Cancer,* 16**,** 789.

ZHANG, B., KRACKER, S., YASUDA, T., CASOLA, S., VANNEMAN, M., HÖMIG-HÖLZEL, C., WANG, Z., DERUDDER, E., LI, S. & CHAKRABORTY, T. 2012. Immune surveillance and therapy of lymphomas driven by Epstein-Barr virus protein LMP1 in a mouse model. *Cell,* 148**,** 739-751.

ZHANG, H., DESAI, N. N., OLIVERA, A., SEKI, T., BROOKER, G. & SPIEGEL, S. 1991. Sphingosine-1-phosphate, a novel lipid, involved in cellular proliferation. *The Journal of cell biology,* 114**,** 155-167.

ZHANG, J., FANG, W., QIN, T., YANG, Y., HONG, S., LIANG, W., MA, Y., ZHAO, H., HUANG, Y. & XUE, C. 2015. Co-expression of PD-1 and PD-L1 predicts poor outcome in nasopharyngeal carcinoma. *Medical oncology,* 32**,** 86.

ZHANG, Y.-L., LI, J., MO, H.-Y., QIU, F., ZHENG, L.-M., QIAN, C.-N. & ZENG, Y.-X. 2010. Different subsets of tumor infiltrating lymphocytes correlate with NPC progression in different ways. *Molecular cancer,* 9**,** 4.

ZHAO, S., LI, F., LEAK, R. K., CHEN, J. & HU, X. 2014. Regulation of neuroinflammation through programed death-1/programed death ligand signaling in neurological disorders. *Frontiers in cellular neuroscience,* 8**,** 271.

ZHAO, Y., WANG, Y., ZENG, S. & HU, X. 2012. LMP1 expression is positively associated with metastasis of nasopharyngeal carcinoma: evidence from a meta-analysis. *Journal of clinical pathology,* 65**,** 41-45.

ZHENG, L., CAO, C., CHENG, G., HU, Q. & CHEN, X. 2017. Cytomembranic PD-L1 expression in locoregionally advanced nasopharyngeal carcinoma. *OncoTargets and therapy,* 10**,** 5483.

ZHOU, Y., MIAO, J., WU, H., TANG, H., KUANG, J., ZHOU, X., PENG, Y., HU, D., SHI, D. & DENG, W. 2017a. PD-1 and PD-L1 expression in 132 recurrent nasopharyngeal carcinoma: the correlation with anemia and outcomes. *Oncotarget,* 8**,** 51210.

ZHOU, Y., SHI, D., MIAO, J., WU, H., CHEN, J., ZHOU, X., HU, D., ZHAO, C., DENG, W. AND XIE, C., 2017b. PD-L1 predicts poor prognosis for nasopharyngeal carcinoma irrespective of PD-1 and EBV-DNA load. Scientific reports, 7, p.43627.

ZHU, Q., CAI, M.-Y., CHEN, C.-L., HU, H., LIN, H.-X., LI, M., WENG, D.-S., ZHAO, J.-J., GUO, L. & XIA, J.-C. 2017. Tumor cells PD-L1 expression as a favorable prognosis factor in nasopharyngeal carcinoma patients with pre-existing intratumor-infiltrating lymphocytes. *OncoImmunology,* 6**,** e1312240.

ZOU, W. & CHEN, L. 2008. Inhibitory B7-family molecules in the tumour microenvironment. *Nature Reviews Immunology,* 8**,** 467.

ZUCCA, E., CONCONI, A., MUGHAL, T. I., SARRIS, A., SEYMOUR, J., VITOLO, U., KLASA, R., OZSAHIN, M., MEAD, G. M. & GIANNI, M. 2003. Patterns of outcome and prognostic factors in primary large-cell lymphoma of the testis in a survey by the International Extranodal Lymphoma Study Group. *Journal of Clinical Oncology,* 21**,** 20-27.

ZUO, J., CURRIN, A., GRIFFIN, B. D., SHANNON-LOWE, C., THOMAS, W. A., RESSING, M. E., WIERTZ, E. J. & ROWE, M. 2009. The Epstein-Barr virus G-protein-coupled receptor contributes to immune evasion by targeting MHC class I molecules for degradation. *PLoS pathogens,* 5**,** e1000255.